

**Impact of complement regulator factor H on
thrombin's role in fibrin clot formation and the
anticoagulant protein C pathway**

Doctor of Philosophy (PhD)

April 2021

Genevieve McCluskey

School of Pharmacy and Pharmaceutical Sciences,

Redwood Building

King Edward VII Avenue

CF10 3NB

Cardiff

United Kingdom

Acknowledgements

I would first like to thank my supervisor Dr Meike Heurich, for all her support, guidance, and immense participation throughout the three years of my PhD. She showed me how to always persevere and not give up.

I would also like to thank Andrea Brancale, my second supervisor for his input and guidance with the molecular modelling.

I would also like to thank Pr. Paul Morgan for all the feedback in the project, and for inviting me to participate in the Complement Biology Group meetings which allowed me to present my work to colleagues.

I would like to thank Dr P Vince Jenkins for also giving important feedback and support to the project and for allowing me to perform experiments in the Haemostasis Lab. Thank you also to Pr. Peter Collins for his critical feedback and help with the work.

Thank you to Dr Roger Preston and his research group at the Royal College of Surgeons Ireland, for welcoming me into his lab during my first year and teaching me essential lab skills.

I must acknowledge the advice and support of Dr Emma Kidd, my advisor, and Dr Chris Thomas, who were also huge supports during my PhD and helped me through.

Dedication

I would like to dedicate this thesis to my incredible brothers, Maximilian, Axel and Felix.

Summary

Complement is part of innate immunity in blood plasma and contributes to eliminating pathogens and cellular debris from the host system. Coagulation is involved in haemostasis, enabling clotting after injury to a blood vessel. Both pathways are evolutionarily linked and composed of effector proteins called zymogens and regulators. Recently, increasing evidence has demonstrated the molecular interactions, or crosstalk, between complement and coagulation. Understanding the importance of the molecular crosstalk is key to further determine the impact of its dysregulation in diseases.

A key step in the coagulation system is the generation of the enzyme thrombin which further enhances the pathway, and cleaves fibrinogen into fibrin to form a clot, preventing fluid loss. Thrombin is also tightly regulated to prevent excess thrombi formation, for instance through its interaction with endothelial membrane bound cofactor thrombomodulin, enabling protein C activation which downregulates upstream coagulation factors. Complement factor H, a key regulator of the alternative pathway in complement activation in the fluid phase and on cell surfaces, has been shown to interact with thrombomodulin, as well as other coagulation components such as factor XII, factor XIII, von Willebrand factor and platelets. However, the role and involvement of factor H in coagulation activation and regulation remains poorly understood.

The aim of this work was to analyse the impact of factor H on thrombin's anticoagulant role in protein C activation, in the presence and absence of thrombomodulin, as well as on its procoagulant role, in the cleavage of fibrinogen into fibrin. Therefore, I developed biochemical assays to assess activated protein C generation, and thrombin-mediated fibrin clot generation in a pure protein system and in plasma, in the presence of factor H. Finally, I investigated the binding sites on factor H using SPR and binding assays supported by computational modelling.

Factor H enhanced protein C activation by the thrombin/thrombomodulin complex but also by thrombin alone. It also enhanced the rate of fibrin clot formation and altered the structure of the clot. Absence of factor H in plasma increased clotting time and restoration of physiological levels decreased it significantly. Importantly, it was determined that thrombomodulin, and primarily thrombin, are ligands for factor H, and these interactions mediated these functional effects. It was also showed that the C-terminal domain of factor H is one binding site involved in the interaction with thrombin. To conclude, factor H could be a potential novel ligand for thrombomodulin and thrombin, regulating its pro and anticoagulant roles. This is relevant in

diseases such as atypical hemolytic uremic syndrome (aHUS) where complement and coagulation are dysregulated due to mutations in factor H.

Abbreviations

aHUS: atypical hemolytic uremic syndrome

AMD: age-related macular degeneration

AP: alternative pathway

APC: activated protein C

APS: antiphospholipid syndrome

aPTT: activated partial thromboplastin time

AT: antithrombin

C1INH: C1 inhibitor

C3^{-/-} mice: *complement C3* knock out mice

C3(H₂O)Bb: fluid phase C3 convertase

C3bBbC3b: C5 convertase

C3bBb: alternative pathway convertase

C3G: C3 glomerulopathy

C3GN: C3 glomerulonephritis

C4bC2bC3b: classical or lectin pathway convertase

C4bC2b: classical and lectin pathway convertase

C4BP: C4 binding protein

CaCl₂: calcium chloride

CFD: complement fixation diluent

CFDNA: circulating free DNA

CFH^{-/-} mice: *complement factor H* knockout mice

CFI: complement factor I

CP: classical pathway

CR1: complement receptor 1

CRP: C-reactive protein

CS: chondroitin sulphate moiety

Da: Dalton

DAF: decay accelerating factor

DDD, or MPGN2: dense deposit disease or membranoproliferative glomerulonephritis 2

DNA: deoxyribonucleic acid

DIC: disseminated intravascular coagulation

EC50: concentration at which 50% substrate is produced

ECL: Enhanced chemiluminescence

EGF1-6: endothelial growth factor domains 1 to 6

EGF456: thrombomodulin recombinant construct EGF456

ELISA: enzyme-linked immunosorbent assay

EPCR: endothelial protein C receptor

FB depleted: factor B depleted plasma

FB: factor B

FBS: foetal bovine serum

FD: factor D

FH depleted: factor H depleted plasma

FH/FB depleted: factor H and factor B depleted plasma

FH: factor H

FI: factor I, or fibrinogen

FIa: active factor I, or fibrin

FII: factor II, or prothrombin

FIIa: active factor II, or thrombin

FIXa: active factor IX

FpA: fibrinopeptide A

FpB: fibrinopeptide B

FVa: active factor V

FVIIa: active factor VII

FVIIIa: active factor FVIII

FVIIIa: active factor VIII

FXa: active factor X

FXIa: active factor XI

FXIa: active factor XI

FXIIa: active factor XII
FXIIIa: active factor XIII
g: gram
GAGs: glycosaminoglycans
GP1 α : glycoprotein I α
HA: hereditary angioedema
HEPES: 4-(2-hydroxyethyl)-1-piperazineethanesulfonic acid
HMGB1: high mobility group box 1
HRP: horse radish peroxidase
HS: heparan sulfate
HUS: haemolytic uremic syndrome
IC50: concentration at which 50% substrate is inhibited
IgG: Immunoglobulin G
IgM: Immunoglobulin M
IL6: interleukin 6
k : kilo (10^6)
 K_D : affinity constant
kd: dissociation constant
L : litres
LLD: lectin like domain
LP: lectin pathway
mm: millimetre (10^{-3})
M: molar
MASP: mannose binding lectin associated protease
MAC, or C5b-9: membrane attack complex
MCP: membrane cofactor protein
MCS: multiple cloning site
MEME: minimum essential medium eagle
MES: 2-(N-morpholino)ethanesulfonic acid
MOE: molecular operating environment

n: nano (10^{-9})

NaCl: sodium chloride

NETs: neutrophil extracellular traps

NHP: normal human plasma

NHS/EDC coupling kit: 1-ethyl-3-(3-dimethylaminopropyl) carbodiimide hydrochloride (EDC), N-hydroxysuccinimide (NHS)

NHS: normal human serum

NMR: nuclear magnetic resonance

OPD substrate: o-phenylenediamine dihydrochloride

P/S: penicillin and streptomycin

PAMPs: pathogen associated molecular patterns

PAR: protease activated receptors

PBS: Phosphate Buffered Saline

PBST 0.1%: Phosphate buffered saline with tween 0.1% (v/v)

PC: protein C

PDB: protein database bank

PNH: paroxysmal nocturnal haemoglobinuria

PPACK thrombin: active site of thrombin inhibited by short peptide sequence PPACK

PPP:

PS: protein S

PT: prothrombin time

PVDF: PolyVinylidene Fluoride

RBCs: red blood cells

ROTEM: rotational thromboelastometry

RU: resonance units

S/T: serine/threonine rich domain

SCR: short consensus repeats

SDS-PAGE: sodium dodecyl sulphate-polyacrylamide gel electrophoresis

sEGF456-S/T: soluble thrombomodulin construct EGF456 and serine/threonine rich domain

SLE: systemic lupus erythematosus

sLLD: soluble thrombomodulin construct lectin like domain

SPR: surface plasmon resonance

sTM: soluble thrombomodulin construct full length

TAFIa: active thrombin activated fibrinolysis inhibitor

TF: tissue factor

TGA: thrombin generation assay

TM: thrombomodulin

TNF: tumour necrotic factor

TTP: thrombotic thrombocytopenic purpura

UK: United Kingdom

VWD: von Willebrand disease

vWF: von Willebrand factor

μ: micro (10^{-6})

Contents

Chapter 1: Introduction	1
1.1. The complement system.....	2
1.1.1. Complement activation.....	2
1.1.2. The alternative pathway and terminal pathway.....	3
1.1.3. Complement regulators	4
1.1.4. Complement regulator factor H.....	5
1.1.5. Factor H deficiency and dysregulation in disease.....	7
1.2. The coagulation system	10
1.2.1. The extrinsic and intrinsic pathway	10
1.2.2. The central role of thrombin.....	12
1.2.3. Fibrin formation and structure	16
1.2.4. The anticoagulant protein C pathway.....	18
1.2.5. Thrombomodulin	19
1.3. Coagulation and complement crosstalk	21
1.3.1 Complement and coagulation crosstalk.....	21
1.3.2 Factor H interactions with several coagulation factors	24
1.4. Homology modelling of proteins	26
1.5. Research question and Hypothesis.....	28
1.5.1. Functional analysis of thrombin binding to factor H shows no significant effect on complement activity.	28
1.5.2. Research question.....	29
1.5.3. Hypothesis.....	29
1.5.4. Aims and objectives	29
Chapter 2: Materials and methods.....	31
2.1. Materials	31
2.2. Methods.....	41
2.2.1. Complement haemolysis assay to measure complement activation and regulation in serum	41
2.2.2. Mouse plasma preparation.....	42
2.2.3. Human plasma and serum isolation.....	43
2.2.4. Affinity depletion of complement factors from citrated human plasma.....	43
2.2.5. Complement factor H purification from human citrate plasma or serum.....	45
2.2.6. Activated partial thromboplastin time (aPTT) and prothrombin time (PT) in human normal plasma and complement depleted plasma.....	46
2.2.7. Turbidity assays monitoring fibrin clot formation in pure protein system in the presence or absence of factor H.....	49

2.2.8. Turbidity assays in normal plasma and factor H depleted plasma	51
2.2.9. Fluorescent microscopy of a fibrin clot in the presence or absence of factor H	52
2.2.10. Activated protein C generation assay	53
2.2.11. Thrombomodulin EGF456-ST domain plasmid vector design	55
2.2.12. Coomassie staining	58
2.2.13. Western blotting of recombinant thrombomodulin constructs.....	59
2.2.14. Enzyme-linked immunosorbent assay for thrombomodulin-factor H complex detection	60
2.2.15. Surface Plasmon Resonance (SPR) binding interaction and affinity analysis	61
2.2.16. Molecular modelling	64
2.2.17. Statistical methods.....	69
Chapter 3: Factor H effect on fibrin clot generation in plasma-based turbidity assays	70
3.1. Absence of factor H and complement C3 increase levels of soluble thrombomodulin in mice	71
3.2. Restoration of factor H decreases activated partial thromboplastin time in human factor H- depleted plasma	73
3.3. Anti-factor H antibodies against SCR1-3 and SCR19-20 decreased activated partial thromboplastin time in human plasma	79
3.3.1. Factor H depleted plasma has increased time to clot compared to factor H and factor B depleted plasma.....	81
3.3.2. Restoration of factor H to factor H/factor B depleted plasma moderately affects fibrin clot formation in plasma.....	83
Chapter 4: Factor H effect on fibrin clot generation in pure protein turbidity assays	86
4.1 Fibrin generation depends on thrombin concentration, and is enhanced by factor H	86
4.2. Factor H affects fibrin clot formation in a dose dependent manner	88
4.3. Factor H affects fibrin clot formation in a dose dependent manner also in the absence of von Willebrand factor	90
4.4. Factor H affects fibrin clot formation in a dose dependent manner by specific domains	92
4.5. Factor H influences the fibrin clot structure by affecting fibre thickness, increasing pore size and number, and decreasing fibre density	94
4.5.1. Factor H impacts fibrin clot structure	94
4.5.2. Factor H impacts fibrin clot structure when formed with vWF-depleted fibrinogen.....	96
Chapter 5: Factor H impact on thrombin's anticoagulant role.....	99
5.1. Impact of factor H on protein C activation	99
5.1.1. Factor H enhances protein C activation in a protein C concentration dependent manner by the thrombin-thrombomodulin complex and thrombin alone.....	99
5.1.2. Factor H enhances protein C activation in a concentration dependent manner	103
5.1.3. Factor H enhances the thrombomodulin-thrombin-mediated protein C activation with purified rabbit thrombomodulin.....	104

5.2. In house soluble recombinant full length thrombomodulin and EGF456-ST domains enhance protein C activation.....	107
Chapter 6: Binding of factor H with thrombomodulin, thrombin and fibrinogen	110
6.1. Analysis of binding between factor H and thrombomodulin.....	110
6.1.1. Domain specific anti-thrombomodulin capture antibodies influence thrombomodulin-factor H binding in solid phase binding assays	110
6.1.2. Binding interaction analysis of factor H domains interaction with domain specific antibody-captured thrombomodulin using surface plasmon resonance	112
6.2. Binding analysis of factor H with thrombin	117
6.2.1. Binding affinity of factor H with thrombin.....	117
6.2.2. Binding of factor H SCR domains with thrombin	118
6.3. Binding of factor H with fibrinogen	120
6.3.1. Binding of factor H with fibrinogen using a solid phase binding assay.....	120
6.3.2. Binding of factor H with fibrinogen.....	121
6.4. <i>In silico</i> analysis of binding interactions of thrombin and factor H	122
6.4.1. Building the full- length factor H homology model	123
6.4.2. Modelling the binding interaction between factor H SCR19-20 and full-length, and thrombin	128
6.4.3. Modelling the binding interaction between factor H and thrombomodulin	132
6.4.4. Modelling the binding interaction between the thrombin-thrombomodulin complex and factor H SCR19-20	136
Chapter 7. Discussion.....	139
7.1. Soluble thrombomodulin is increased in <i>CFH</i> ^{-/-} mice, with normal thrombin-antithrombin levels	139
7.2. Absence of factor H in human plasma increases clotting time via activated partial thromboplastin time and prothrombin time.	142
7.3. Factor H enhances fibrin clot formation by decreasing lag time, and increasing velocity and maximal turbidity, and alters fibrin clot structure.....	143
7.4. Factor H enhances thrombin's anticoagulant role by increasing protein C activation by the thrombin-thrombomodulin complex and by thrombin alone	147
7.5. Factor H interacts with EGF1-2 and EGF6 of thrombomodulin and exosite II of thrombin, via SCR6-8 and SCR18-20.....	149
7.6. Factor H deficiency and dysregulation in disease states	151
7.7. Future perspectives:	157
7.8. Limitations of the study	159
References	161
Appendices.....	179

List of figures

Figure 1.1. The complement cascade.

Figure 1.2. Factor H regulates complement through different mechanisms in the alternative pathway.

Figure 1.3. Factor H regulates complement through 3 key regions.

Figure 1.4. The coagulation cascade.

Figure 1.5. Thrombin is a serine protease with several domains enabling its diversity and specificity.

Figure 1.6. Representation of thrombin and its inhibitors and ligands.

Figure 1.7. Fibrinogen is cleaved by thrombin to yield an insoluble fibrin clot.

Figure 1.8. Thrombin binding and cleavage of protein C in presence and absence of thrombomodulin.

Figure 1.9. Thrombomodulin contains 5 domains.

Figure 1.10. Selected crosstalk between complement and coagulation.

Figure 1.11. Involvement of factor H with clotting and coagulation factors and the effect of the interaction.

Figure 2.1. Set up and preparation of complement factor B and factor H-depleted normal human plasma using affinity chromatography.

Figure 2.2. Detection of contaminants in factor H purification from human plasma.

Figure 2.3. Visual representation of activated partial thromboplastin time assay (aPTT).

Figure 2.4. Typical representation of a turbidity assay graph.

Figure 2.5. Representation of the set up for fluorescent microscopy.

Figure 2.6. Plasmid pcDNA3.1+6HIS design used as a vector for transport and transfection of the thrombomodulin constructs.

Figure 2.7. Factor H fragments flowed over thrombomodulin captured via monoclonal domain-specific antibodies.

Figure 2.8. Factor H or thrombin flowed over thrombin and fibrinogen to determine binding affinity.

Figure 3.1. Thrombin does not impact complement haemolysis regulation by factor H in serum.

Figure 3.2. Quantification of murine plasma soluble thrombomodulin, thrombin-antithrombin complex and activated protein C in CFH^{-/-} and C3^{-/-} mice.

Figure 3.3. Detection of factor B in normal, FH depleted, FB depleted and FH/FB depleted plasmas.

Figure 3.4. Verification of factor H depletion in normal pre-depletion, FH depleted, FB depleted and FH/FB depleted plasmas.

Figure 3.5. Δ FB/ Δ FH, and Δ FH plasmas have significantly increased activated partial thromboplastin time and prothrombin time compared to normal plasma.

Figure 3.6. Restoration of physiological concentration of factor H decreases aPTT in Δ FB/ Δ FH plasma.

Figure 3.7. Factor H decreases activated partial thromboplastin time in factor H depleted plasma in a dose dependent manner

Figure 3.8. Diagram representing the binding sites of the anti-factor H monoclonal antibodies.

Figure 3.9. Factor H antibodies against SCR1-3 and SCR20 decrease activated partial thromboplastin time.

Figure 3.10. FH depleted plasma has a lower velocity and maximal turbidity compared to FH/FB depleted and FB depleted plasmas

Figure 3.11. Factor H moderately affects the lag time and velocity in Δ FH plasma.

Figure 3.12. Factor H moderately affects the velocity in Δ FB/ Δ FH depleted plasma.

Figure 4.1. Fibrin clot formation depends on thrombin concentration and is enhanced in the presence of factor H by decreasing lag time and increasing velocity and maximal turbidity.

Figure 4.2. Factor H enhances fibrin clot formation in a dose dependent manner by decreasing lag time and increasing velocity and maximal turbidity.

Figure 4.3. Factor H enhances fibrin clot formation in a dose dependent manner by decreasing lag time and increasing velocity and maximal turbidity with vWF-depleted plasma.

Figure 4.4. Impact of factor H fragments on lag time, velocity and maximal turbidity in fibrin clot formation.

Figure 4.5. Factor H binds with the fibrin network, decreases fibre density and affects structure.

Figure 4.6. Factor H binds with the fibrin network, decreases fibre density and affects structure with vWF-depleted fibrinogen.

Figure 5.1. Factor H enhances thrombin-mediated protein C activation in presence and absence of thrombomodulin.

Figure 5.2. Commercial factor H enhances protein C activation in presence and absence of thrombomodulin.

Figure 5.3. Factor H increases thrombin-thrombomodulin and thrombin-only mediated protein C activation in a dose dependent manner.

Figure 5.4. Factor H enhances protein C activation in the presence of the soluble rabbit form of thrombomodulin and EGF456.

Figure 5.5. Recombinant thrombomodulin constructs soluble full length and 456-S/T generate activated protein C at a low level.

Figure 6.1. Thrombin binds EGF5 and EGF6 of thrombomodulin, and factor H binds EGF6 of thrombomodulin.

Figure 6.2. Factor H constructs SCR1-5, SCR6-8 and SCR18-20 bind C3b.

Figure 6.3. Factor H domains SCR6-8 and SCR18-20 bind thrombomodulin independent of capture antibody.

Figure 6.4. Factor H SCR6-8 binds thrombomodulin.

Figure 6.5. Factor H constructs 18-20 bind thrombomodulin.

Figure 6.6. Factor H binds with nanomolar affinity to immobilised PPACK-thrombin.

Figure 6.7. Factor H SCR1-4, SCR6-8 and SCR18-20 bind thrombin.

Figure 6.8. Factor H binds fibrinogen in a concentration dependent manner.

Figure 6.9. Thrombin binds with micromolar affinity to immobilised fibrinogen.

Figure 6.10. Factor H binds with nanomolar affinity to immobilised fibrinogen.

Figure 6.11. Homology model of SCR14 of factor H.

Figure 6.12. Homology model of SCR17 of factor H.

Figure 6.13. Model of full-length factor H.

Figure 6.14. Binding interaction between SCR19-20 (PDB ID 2G7I) of factor H and thrombin (PDB ID 1YPG).

Figure 6.15. Binding interaction between full-length factor H and thrombin.

Figure 6.16. Binding interaction between SCR19-20 of factor H (PDB ID 2G7I) and thrombomodulin EGF456 (PDB ID 1DX5).

Figure 6.17. Binding interaction between full-length factor H and thrombomodulin EGF456 (PDB ID 1DX5).

Figure 6.18. Model of the interaction between factor H SCR19-20 (PDB ID 2G7I) and thrombin-thrombomodulin complex (PDB ID 1DX5).

Figure 7. Factor H affects clotting and regulation of coagulation through strong binding affinities with thrombin, thrombomodulin and fibrinogen.

List of tables

Table 1.1. Factor H interactions with coagulation factors and the impact on complement or coagulation systems.

Table 2.1. Proteins, their stock concentration and storage conditions, as well as their source are listed in their respective rows.

Table 2.2. Table title. Antibodies used in this study are listed, with source information, and their stock concentration.

Table 2.3. Chemicals, reagents, materials, and equipment used for all experiments.

Table 2.4. Protein, volumes, and concentrations for each protein used in the pure protein fibrin turbidity assay.

Table 2.5. Composition of fibrinogen preparations used for the pure protein turbidity assays.

Table 2.6. Volumes and concentrations of components for the plasma-based turbidity assays triggering either the coagulation extrinsic pathway (PPP reagent) or intrinsic pathway (aPTT) reagent.

Table 2.7. Proteins used to perform APC assay and their corresponding volume and final concentrations used.

Table 2.8. Primary antibodies and their concentrations used to detect their respective proteins.

Table 2.9. List of capture antibodies or absorbed proteins used in the enzyme-linked immunosorbent assay against thrombomodulin, factor H and thrombin

Table 2.10. Thrombin structure.

Table 2.11. Factor H structure.

Table 3.1. Fibrinogen level in normal and depleted human plasmas

Table 4.1. Impact of factor H on lag time, velocity, and maximum turbidity in presence of 2.5nM thrombin and 12 μ M fibrinogen.

Table 4.2. Impact of von Willebrand factor in the fibrinogen sample on lag time, velocity and maximum turbidity in presence of increasing factor H concentrations

Table 5.1. Michaelis Menten constant for protein C activation in presence and absence of 100nM factor H, with and without 10nM thrombomodulin, with 3nM thrombin and 200nM protein C.

Table 5.2. The dissociation constant (kd) of factor H for protein C activation in presence and absence of 10nM thrombomodulin, with 2.5nM thrombin and 200nM protein C.

Table 6.1. Binding affinities K_D) of factor H domains SCR1-5, 6-8, 18-20, to C3b, and reported binding affinity from the literature.

Table 6.2. Binding affinities (K_D) of factor H domains SCR6-8 and 18-20, to thrombomodulin captured via antibodies lectin like domain, EGF1-2 and EGF6.

Table 6.3. Binding affinities of factor H domains SCR1-4, 6-8 and 18-20, to thrombin captured to the surface. Kinetics were repeated one time only for each construct.

Table 6.4. List of homologous proteins to SCR14 ranked according to the max score.

Table 6.5. List of homologous proteins to SCR17 ranked according to the max score.

Table 6.6. Residues involved in the interaction between thrombin (PDB ID 1YPG) and factor H SCR19-20 (PDB ID 2G7I).

Table 6.7. Residues involved in the interaction between thrombin (PDB ID 1YPG) and factor H full length.

Table 6.8. Residues involved in the interaction between thrombomodulin (PDB ID 1DX5) and factor H SCR19-20 (PDB ID 2G7I).

Table 6.9. Residues involved in the interaction between thrombomodulin (PDB ID 1DX5) and factor H full length.

Table 6.10. Residues involved in the interaction between thrombin (PDB ID 1DX5) and thrombomodulin (PDB ID 1DX5) in the thrombin-thrombomodulin-factor H interaction.

Table 6.11. Residues involved in the interaction between thrombin (PDB ID 1DX5) and factor H SCR19-20 (PDB ID 2G7I) in the thrombin-thrombomodulin-factor H interaction.

Table 6.12. Residues involved in the interaction between thrombomodulin (PDB ID 1DX5) and factor H SCR19-20 (PDB ID 2G7I) in the thrombin-thrombomodulin-factor H interaction.

Chapter 1: Introduction

Complement and coagulation are two blood-based defence systems composed of proteins that are proteolytically activated, which enable generation of effector molecules essential to immunity and clotting. Complement is involved in the humoral arm of innate immunity, protecting against pathogen invasion and infections of the host (1), and coagulation is involved in haemostasis, preventing fluid loss after vessel injury (2). Both systems evolved from a joint defence system as seen in the horseshoe crab (3), and subsequently components of complement and coagulation share high structural similarity (4). The horseshoe crab's circulating blood, known as hemolymph, carries oxygen and protects against bacterial infection, and uses (it's equivalent) complement and coagulation to clot locally and prevent the spread of bacterial invader (3). Over the past years, mounting evidence has demonstrated the importance of interactions between proteins from each system (3, 5, 6), also known as the crosstalk between complement and coagulation. Although the physiological relevance of some crosstalk has not yet been characterised, many interactions between proteins have significant impact on regulation or activation of one or the other system (7, 8). Diseases where both complement and coagulation are dysregulated include rare renal pathologies such as atypical haemolytic uremic syndrome (aHUS) (9, 10), but also involved in antiphospholipid syndrome (11), or sepsis (12). Often these diseases manifest in overactivation of complement and coagulation commonly leading to host endothelial damage (13). However, the pathophysiological impact of the crosstalk between the two systems in this setting remains poorly understood. Therefore, characterising the crosstalk between complement and coagulation will aid in the understanding of the pathophysiology of diseases where both systems are activated, and ultimately enable the development of targeted therapeutics. A key regulator in the (alternative) complement pathway is factor H (FH). Deficiency or dysregulation of FH due to mutations or polymorphisms is associated with diseases such as aHUS (14), dense deposit disease (DDD) (15), contribute to age-related macular degeneration (AMD) (16), or antiphospholipid syndrome (APS) (17). Dysfunction of FH leads to lack of regulation of the complement alternative pathway and complement overactivation, with increased C3 cleavage, opsonisation, anaphylatoxin generation and membrane attack complex formation on the surfaces of cells, causing damage to the endothelium (18). FH however has also been reported as a ligand for numerous coagulation factors, including factor XII (FXII) (19, 20), factor XIII (FXIII) (21-23), fibrinogen

(FI) (24), platelets (25, 26), von Willebrand factor (vWF) (27, 28) and thrombomodulin (TM) (29), and diseases characterised by dysregulation of factor H have shown coagulopathies also (30, 31). Therefore, it is essential to determine whether excessive complement activation contributes to coagulation dysfunction, and whether FH regulates or impacts coagulation components.

1.1. The complement system

1.1.1. Complement activation

The complement system is an essential component of innate immunity and is the first line of defence against pathogen invasion and altered host cells (1, 32). Complement is constituted of over 30 activator and regulatory proteins, both cell bound and in circulation, and is activated via three different pathways, the classical (CP), lectin (LP) and alternative pathway (AP) (33). The classical pathway is activated via antibody/antigen complexes (34), the lectin pathway by sugar moieties on the surfaces of bacteria (35), and the alternative pathway is constitutively activated by a “tick-over” system and surveys foreign surfaces (34) (Figure 1.1). All pathways converge on the generation of the C3 convertase, C4b,C2a,C3b for classical and lectin pathways, and C3b,Bb for alternative pathway (34, 36, 37), which cleaves C3 (38) (Figure 1.1). The C3 cleavage products by C3 convertase are opsonin C3b (34) that tags the pathogen surface for elimination, and the anaphylatoxin C3a, a soluble mediator recruiting inflammatory chemotactic factors (39), that causes local inflammatory responses and recruitment of immune cells via specific receptor binding to C3a receptors, C3aR (39, 40).

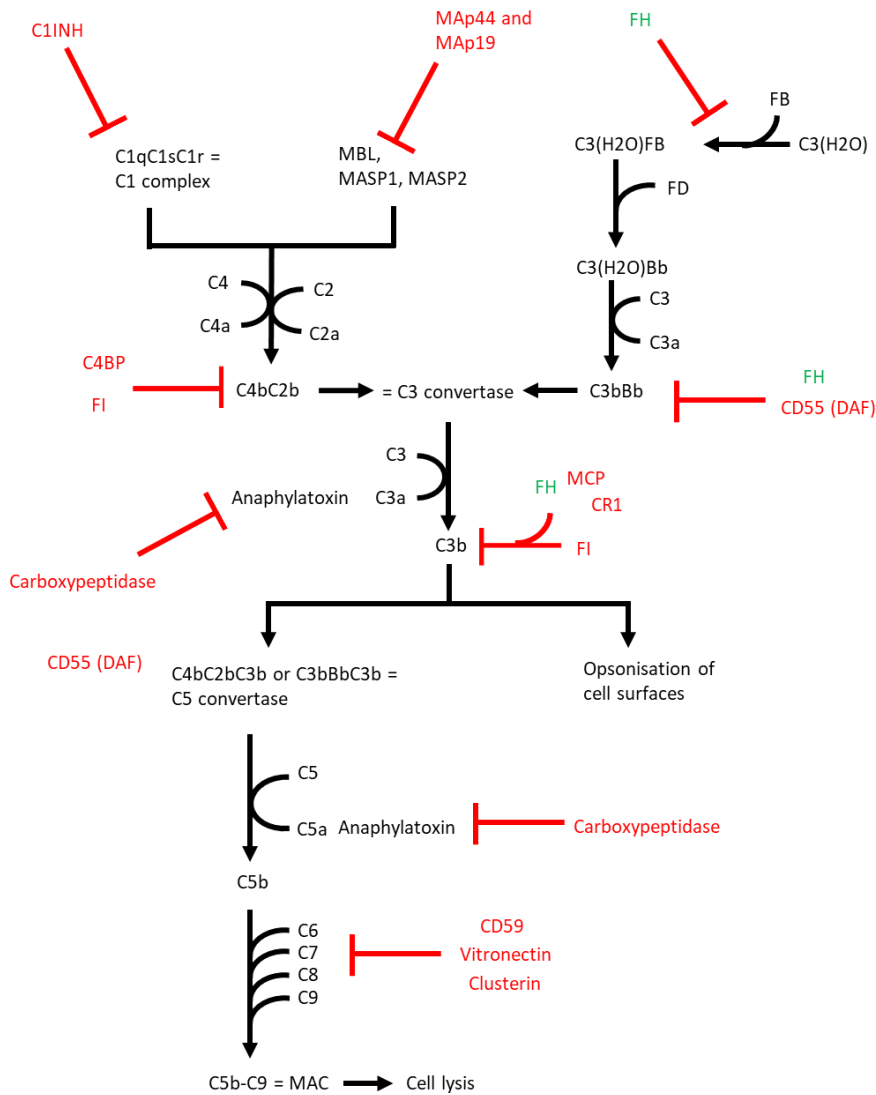


Figure 1.1. The complement cascade. The classical, lectin and alternative pathways antibody/antigen complexes, sugar moieties and spontaneous C3 hydrolysis, respectively, and converge on the formation of the C3 convertase, and cleavage of C3. C3 cleavage product C3b can opsonise cells and is a component to form the C5 convertase, leading to the terminal pathway and MAC formation. Complement is tightly regulated by fluid phase and membrane bound regulators (indicated in red). Complement factor H is a key regulator of the alternative pathway highlighted in green. The “C” for each protein corresponds to “complement component”, eg C5 is complement component 5. C1INH is C1 inhibitor, MBL is mannose binding lectin, MASP1 and 2 are mannose-associated serine protease 1 and 2, MAb44 is mannose-binding lectin-associated protein of 44 kDa, MAb19 is Mannose-binding lectin-associated protein of 19kDa, FH is factor H, FB is factor B, FD is factor D, CD55 or DAF is decay accelerating factor, CD46, or MCP is membrane cofactor protein, CD35, or CR1 is complement receptor 1, FI is factor I, MAC is membrane attack complex, CD59 is MAC inhibitory protein.

1.1.2. The alternative pathway and terminal pathway

This study focusses on components of the alternative pathway -as factor H regulates it- which is activated following spontaneous hydrolysis of C3 (41), happening at a low level (a “tick-over”) (Figure 1.1). C3 is abundant in the plasma, and spontaneous hydrolysis happens at its thioester bond, forming C3(H₂O), enabling binding of factor B (FB) (42). Protease Factor D (FD) then cleaves factor B to give Bb which stays bound to C3(H₂O) (43). The final product is C3(H₂O)Bb a fluid phase C3 convertase, that cleaves C3 molecules (34, 44). The cleavage product C3b is usually inactivated when in the fluid phase but in the presence of pathogen can covalently bind to its surfaces (45, 46), and binds factor B and factor D (47, 48) to generate the C3 convertase of the alternative pathway, C3bBb (44, 46, 49). The alternative pathway also act as an amplification loop of the other pathways, whereby each C3 convertase can cleave more C3 molecules to generate C3b to generate more C3bBb and opsonise the surface of the pathogen (50).

C3b dimerises and binds the C3 convertase (C4bC2bC3b for the classical and MBL pathways, and C3bBbC3b for the alternative pathway) and forms the C5 convertase which cleaves C5 molecules into C5b and C5a (34, 47). C5a anaphylatoxin is a chemotactic factor for recruiting immune cells to the site of complement activation and binds C5a receptor (39, 40) on the surface of immune cells. C5b remains attached to the C5 convertase, binds C6, enabling binding to C7 which renders the complex lipophilic (34, 51). C8 association to the complex is the first membrane insertion event (52), and the C5b8 complex acts as a receptor for C9 and enables its polymerisation (33, 36, 51, 53). Several C9 molecules polymerise and come together to form a pore of about 100Å in diameter, termed the membrane attack complex (MAC), causing osmotic imbalance (51), and breach of the membrane (54).

1.1.3. Complement regulators

Regulatory complement proteins prevent complement activation on host cells, differentiating self from non-self. Complement regulators are present in the fluid phase and expressed on cell surfaces (33, 36, 55, 56). They act either via decay accelerating activity, competitive binding, or cofactor activity.

The thioester bonds of C3b indiscriminately bind to the surface of cells, therefore mechanisms are present to prevent C3 convertases or opsonisation from happening on host or self cells (57). Factor I (CFI), a serine protease circulating in active form, inactivates C3b, preventing further

convertase formation (58, 59) on self surfaces. Factor I cofactors are complement receptor 1 (CR1), membrane cofactor protein (MCP), complement 4 binding protein (C4BP) and complement factor H (FH) (60, 61).

1.1.4. Complement regulator factor H

This work focusses on complement regulator factor H, a 155kDa glycoprotein expressed in the liver, made up of 20 domains named Short Consensus Repeats (SCRs) of approximately 60 amino acids each, and carries 8 glycosylation sites on the C-terminal domain possibly involved in stability and solubility (58, 62-66). It is the most abundant complement regulator (67), and acts in the fluid phase as well as on cell surfaces (49).

Factor H regulates complement via three mechanisms. Its binding will either decay the C3 and C5 convertase (decay-accelerating activity) by accelerating the dissociation of the Bb subunit (50, 68, 69); act as a cofactor to factor I for proteolytic inactivation of C3b (cofactor activity) (66, 68, 69); or will compete with factor B for binding to C3b (competitive binding) (57, 68-73) (Figure 1.2).

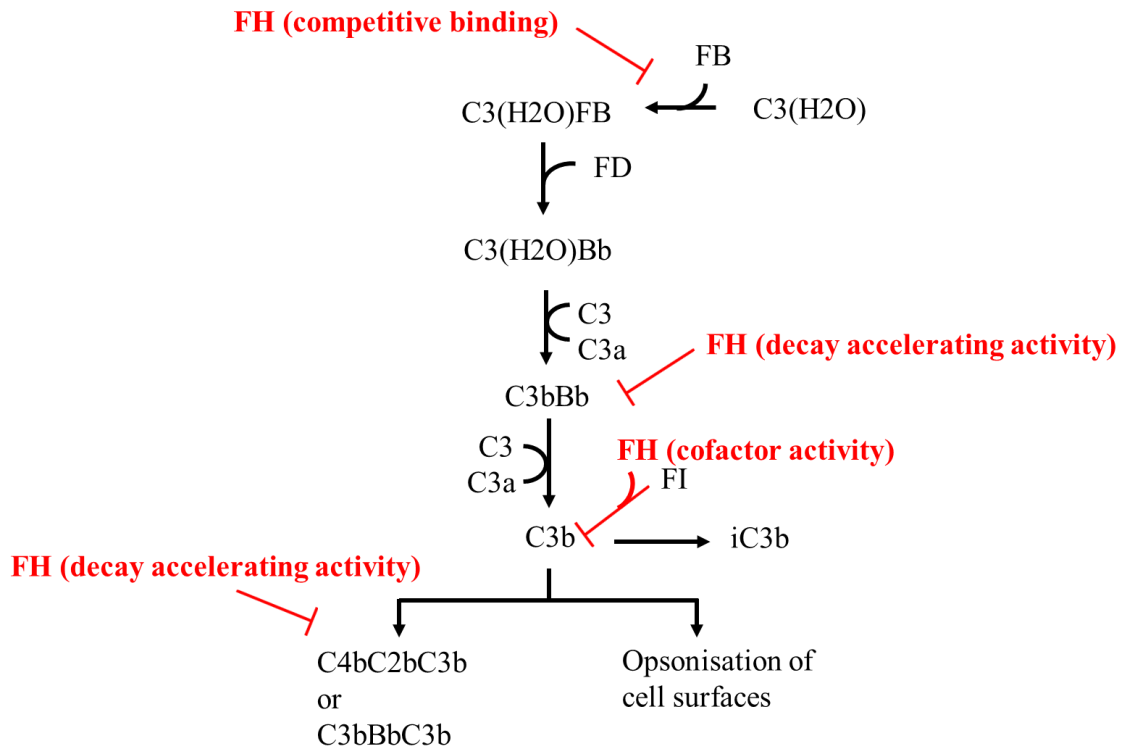


Figure 1.2. Factor H regulates complement through different mechanisms in the alternative pathway. Factor H regulates complement by acting as a cofactor for factor I in C3b inactivation into inactive C3b (iC3b), accelerating the dissociation of the Bb subunit in the convertase, and competing with factor B for binding to C3b. All factor H regulatory activities are indicated in red.

The regulatory domains in factor H are SCRs 1-4, 6-8 and 19-20 (74-77). SCR1-4 promotes the decay accelerating activity, and the cofactor activity for factor I (45, 74, 78). The SCRs 6-8, and 19-20 are involved in the binding to glycosaminoglycans on cell surfaces (79, 80), and all these sites interact with C3b (45, 57, 78, 80, 81) (Figure 1.3).

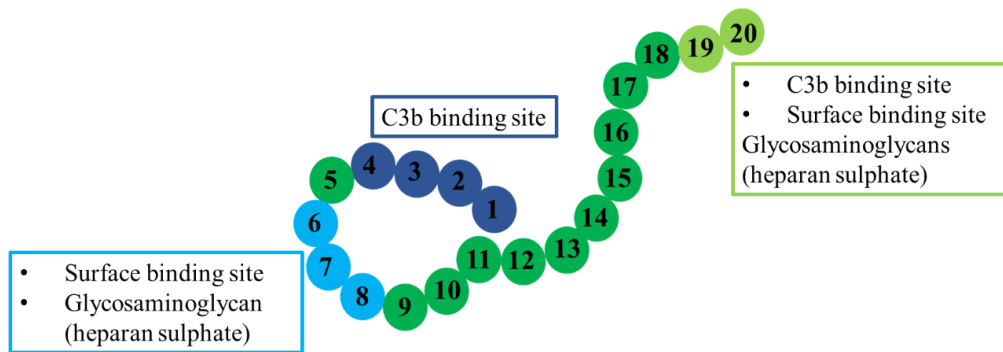


Figure 1.3. Factor H regulates complement through 3 key regions. Factor H is comprised of 20 short consensus domains (SCRs). Factor H binds C3b via its SCR regions 1-4 (dark blue), and SCR 19-20 (light green), and binds cell surfaces via SCR regions 6-8 (light blue) and 19-20 (light green).

In the fluid phase factor H binds to C3b or C3(H₂O), and presence of glycosaminoglycans (GAGs) on cell surfaces enhances factor H binding to C3b, such as by heparan sulphates or sialic acid moieties (42, 78, 82, 83) This aids recognition of self vs non-self surfaces, since pathogens rarely carry these polyanions on their surfaces, thus preventing complement activation on the surface of host cells and targeting complement to the pathogen surface (36, 42).

1.1.5. Factor H deficiency and dysregulation in disease

Mutations and polymorphisms in the factor H gene are causes or are linked to the following diseases: aHUS, dense deposit disease (DDD, or membranoproliferative glomerulonephritis 2), Age-Related Macular Degeneration (AMD), and antiphospholipid syndrome (APS).

1.1.5.1. Factor H dysregulation in disease

AHUS is a rare renal disease characterised by thrombocytopenia, microangiopathic hemolytic anemia and acute renal failure (9, 84). Factor H mutations represent 25% aHUS predisposition (9). The functional factor H V62I polymorphism (I62 being protective) is considered protective in aHUS, with increased binding to C3b, enhanced competition for factor B and binding with factor I (85). Polymorphisms have been identified in factor H SCR11 and SCR16, and increase the risk of aHUS several fold (86), whereas others have been associated with aHUS but have

no apparent functional impact (87). Most of the factor H mutations on the other hand, are heterozygous and present in SCR20, the host recognition domain in factor H (14, 88-90). These mutations lead to a failure to regulate complement on cell surfaces and in particular at the glomerular endothelium (14, 89, 91). Endothelial damage due to lack of complement regulation by factor H causes uncontrolled generation of anaphylatoxins and soluble MAC (92). Some mutations can cause also premature STOP codons in the *cfh* gene and therefore defective synthesis (88). Other mutations in complement proteins of the alternative pathway have been identified also aHUS, notably factor I, C3, factor B, as well as autoantibodies against factor H (9, 92).

The disease AMD (71, 93, 94) is the leading cause of blindness in the western world, due to accumulation of drusen between the pigment epithelium and the Bruch's membrane (71, 93, 95, 96). Factor H has been identified in this drusen (71). The polymorphism, V62I is considered a protective polymorphism against age-related macular degeneration, with I62 showing increased C3b binding, and competition for factor B (16, 85, 97). On the other hand, the Y402H polymorphism in SCR7 is major genetic risk factor for the disease. The risk is increased 2.5-fold when heterozygous and 6-fold when homozygous (97). It has been linked to disease progression, early onset of the disease and drusen composition and size (16). Reports have shown that 402H and 402Y bind differentially to glycosaminoglycans (71), C reactive protein (CRP) and cannot regulate oxidative stressors (16). There is no evidence of the Y402H variant affecting factor H's cofactor activity or decay accelerating activity in SCR 1-4, however affects its binding to glycosaminoglycans on surfaces (97).

1.1.5.2. Factor H deficiency in disease

Factor H deficiency, leading to a lack of regulation of the complement alternative pathway, is due to mutations or polymorphisms, causing defects in key regulatory domains that prevent it from binding surfaces and C3b, or else a premature STOP codon, decreasing the overall protein expression. This leads to diseases such as aHUS and membranoproliferative glomerulonephritis. Membranoproliferative glomerulonephritis (MPGN) is a rare kidney disease, divided into different groups: MPGN caused by immune complexes, and MPGN driven by overactivation of the alternative pathway of complement (98). The latter, also known as C3 glomerulopathy (C3G) is separated into three subgroups, which are dense deposit disease (DDD or MPGN II), C3 glomerulonephritis (C3GN), and CFHR5 glomerulopathy (CFHR5

GP) (49, 99). DDD is characterised by intramembranous glomerular deposits of dense osmophilic material, C3GN by less dense C3 deposits in the mesangial subendothelial and subepithelial area of the glomeruli (49, 100). Dysregulation of factor H due to genetic deficiency or autoantibodies are causative of C3GP, leading to increased alternative pathway activation, therefore low C3 levels in circulation. C3GN and DDD overlap, however they can be differentiated by the levels of properdin (lower in C3GN) and of MAC (higher in C3GN) (49). The C3 depositions are caused by homozygous deficiencies or compound heterozygous mutations in factor H that affect its secretion, and which lead to near undetectable levels in certain cases (98), depending on the mutation which can cause a premature STOP codon. This causes overactivation of complement, and specifically a secondary deficiency in alternative pathway components including C3 and terminal pathway components (98). Polymorphisms have also been shown to be associated with DDD, for instance the V62I, which has shown to be protective and enhance factor H's regulatory activity.

1.1.5.3. Factor H deficiency in CFH^{-/-} mice

Complement factor H knock out mice (*CFH^{-/-}*) are used to study the disease progression of DDD in humans (101, 102). These mice are characterised by uncontrolled C3 activation and spontaneous development of MPGN2, secondary C3 plasma deficiency and renal abnormalities with C3 deposits along the glomerular membrane (103). However, they are not representative of aHUS (102, 104, 105), as this disease is characterised by decreased factor H regulation on cell surfaces, not in circulation. Partial factor H knockout (106), or mice expressing truncated factor H without the C-terminal GAG binding domain of factor H (102) are used to determine effects of aHUS, as there is a decreased regulation of complement on cell surfaces. aHUS disease can be characterised by normal and low factor H levels, depending on the mutations or polymorphisms in the protein. In some cases, normal factor H levels are detected however that only regulate complement in the fluid phase but not on cell surfaces due to mutations in the C-terminal domain. Factor H knockout mice also have decreased visual acuity, increased retinal deposits (107), a thickening of the Bruch's membrane and decreased photoreceptors (108), as well as hallmarks of early AMD and increased amyloid beta deposition (109). There is also disrupted and delayed retinal development and defects in the retina (109, 110).

Reports have also shown increased mortality after infection with bacterial meningitis (111) and higher levels of nucleosomes and necrotic cells (112).

1.2. The coagulation system

1.2.1. The extrinsic and intrinsic pathway

Coagulation is initiated with release of tissue factor expressed within the vessel wall that comes into contact with circulating plasma (113), often in the event of vascular injury. Once released, tissue factor binds to activated factor VII, the latter activated by circulating activated factors IXa, Xa, XIa, XIIa, thrombin (factor IIa), plasmin and the tissue factor/factor VIIa complex itself (114-117). Once the complex formed, it activates factors IX and X. Factors IXa and Xa either stay bound to the complex, or else are diffused into the fluid phase and bind platelets (116). Activated factor IX binds to activated factor VIII -activated by thrombin- forming the tenase complex (118-120). The tenase complex activates factor X, which then binds to factor Va -also activated by thrombin- which form the prothrombinase complex, that converts prothrombin, or factor II, into the serine protease thrombin, or activated factor II (115, 119) (Figure 1.4). Factor V is activated by the first thrombin in circulation however it can also be activated by factor Xa on the surface of platelets (113, 121).

The intrinsic pathway on the other hand, or contact pathway, is initiated by interaction with artificial substrates (113), but is not thought to have an important role in maintenance of haemostasis however, could be important in thrombotic diseases (122, 123). Artificial surfaces enable activation of factor XII, which then activates factor XI. Factor XI activates factor IX, and the intrinsic pathway converges with the extrinsic pathway (Figure 1.4).

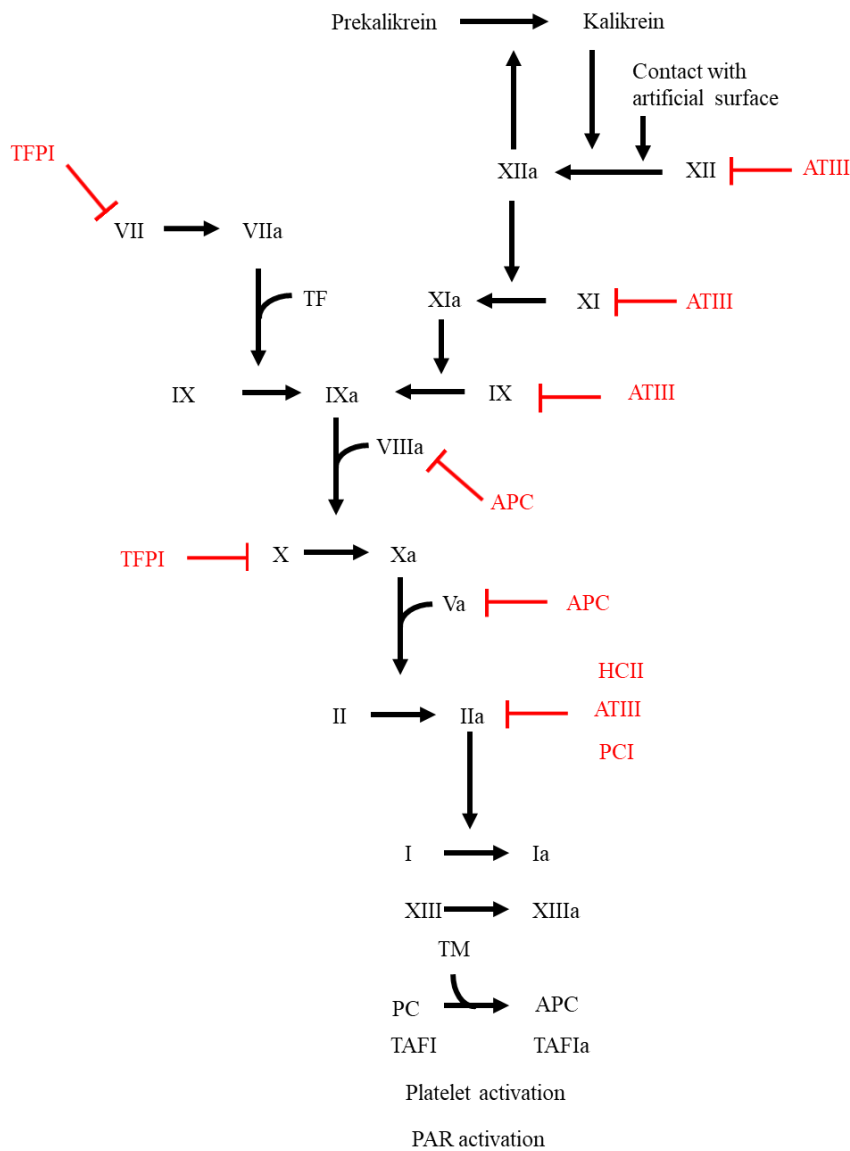


Figure 1.4. The coagulation cascade. The extrinsic pathway, initiated with release of tissue factor into circulation, and the intrinsic pathway, activated by contact activation and activation of factor XII. Both pathways converge on activation of factor IX into IXa, leading to formation of the tenase complex, and then the prothrombinase complex which activates thrombin. Thrombin cleaves and activates factor I, fibrinogen into factor Ia, or fibrin, as well as factor XIII. Regulators are marked in red. Each inactive coagulation factor is represented by its respective roman numeral (for instance X is factor X), and its activated form by the roman numeral followed by a (for instance Xa is activated factor X). TF is tissue factor, II is prothrombin, IIa is thrombin, I is fibrinogen, Ia is fibrin. ATIII is antithrombin III, PC is protein C, APC is activated protein C, TM is thrombomodulin, TAFI is thrombin activating fibrinolysis inhibitor, TAFIa is the activated form, TFPI is tissue factor pathway inhibitor, HClI is heparin cofactor II, PCI is protein C inhibitor, thrombin activates platelets and protease activated receptors, PARs.

Once thrombin is generated, its concentration rapidly increases (123) and cleaves fibrinogen into fibrin, activates platelets, as well as protease activated receptors (PARs) on the surface of platelets (114, 119, 124-133). Thrombin activates factors V, XI and VIII, in a feedback loop and amplifies the pathway (120, 134). Thrombin activates transglutaminase factor XIII that crosslinks fibrin fibres, stabilising the clot (135, 136). Finally, thrombin also activates thrombin-activating fibrinolysis inhibitor (TAFI), which removes lysine residues from the C-terminal of fibrin, therefore preventing fibrinolysis factors from binding and disintegrating the clot (137-139).

1.2.2. The central role of thrombin

1.2.2.1. Structure and function of thrombin

Thrombin is a 37kDa, Na⁺ activated, serine protease from the chymotrypsin family (140) which is characterised by the serine residue in the centre of the active site for nucleophilic attack and targeting the peptide bond (141, 142). Structurally, thrombin contains a serine protease region made up of a catalytic triad His57, Asp189 and Ser195, surface loops and two anion binding exosites (distal from each other) (143). Its specificity for substrates is determined through exosites 1 and 2, the gamma loop, the 60 loop and the sodium binding site.

The 60s loop (or β -insertion, composed of Leu60, Tyr60a, Pro60b, Pro60c, Trp60d, Asp60e, Lys60f, Asn60g, Phe60h, and Thr60i) acts like a “lid” to the active site (144), and plays a role in the entrance of substrates into the active site (145), interacting predominantly with hydrophobic residues on substrates, via the N-terminal of the scissile bond (146). The 60 loop is structurally rigid because of the two consecutive prolines Pro60b and Pro60c (128, 146).

The autolysis (or γ -loop, composed of Thr147, Trp147a, Thr147b, Ala147c, Asn147d, and Val147f) is responsible for substrate specificity filtering substrates (144, 145), and is considered more mobile and hydrophilic (128, 146), interacting with the C-terminal and the body of substrates (Figure 1.5).

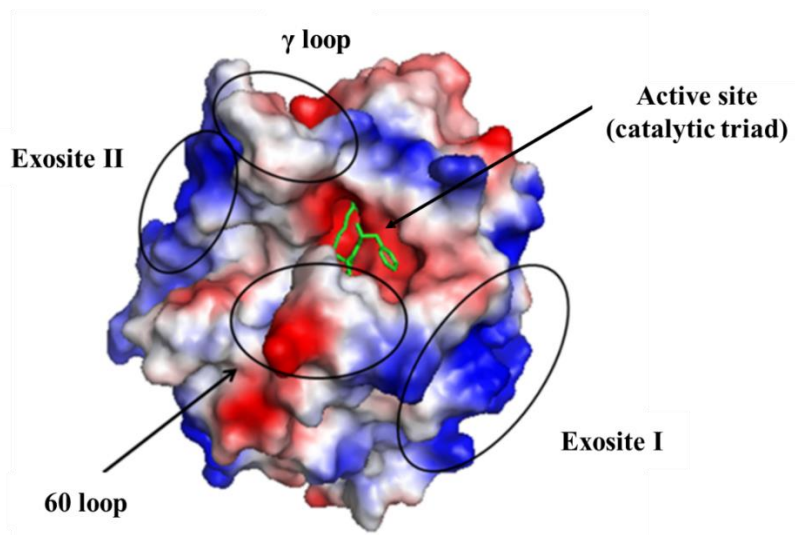


Figure 1.5. Thrombin is a serine protease with several domains enabling its diversity and specificity. Thrombin carries two exosites, exosite I and exosite II, as well as the 60 loops and Gamma loop that define thrombin's specificity for the large cohort of substrates, cofactors, and ligands. Figure adapted from Proteopedia (<https://proteopedia.org/wiki/index.php/Thrombin>).

The anion binding exosites, exosite I (K36, H71, R73, R75, Y76, R77A, K109/110) and exosite II (R93, K236, K240, R101, R233) are charged patches with basic residues, located on opposite regions on the surface of thrombin (147), and interact with the negatively charged residues of substrates (128). They are always involved in thrombin function, and have been shown to play a role in macromolecular substrate binding, inhibitor binding and effector binding (147) attracting and directing substrates to the active site, but also in attracting other regulatory proteins (144). An allosteric linkage between the exosites exists and modulates thrombin activity (145). There are conflicting reports as to whether simultaneous binding of substrates to both exosites or at one or the other affects the binding capacity and specificity opposing exosite (144, 145, 148). Lane and Huntington (149) defined a trend demonstrating which exosite thrombin peptides bound to, based on the ratio of negative charges to hydrophobic residues. When the ratio is below 2, peptides bind exosite I, creating hydrophobic contacts and electrostatic interactions involved in orienting the complementary hydrophobic surfaces. When the ratio is above 2, peptides bind to exosite II and create ionic contacts. In this case hydrophobic contacts are very minimal contributors, and interactions are very reliant on salt concentrations (149). Exosite I is termed the “apolar” binding exosite, and exosite II the “anion” binding exosite (146).

Exosite I binds thrombomodulin, fibrinogen, PARs, hirudin, factor XIII, factor XI, factor V, factor VIII, glycoprotein Iba, and exosite II binds heparin, glycoprotein Iba, factor VIII, factor V, fibrinogen γ' , glycosaminoglycans.

The interaction with sodium causes allosteric changes to the enzyme and determines the “fast” (sodium bound) or “slow” (sodium free) form of thrombin, playing a key role in its recognition of substrates and therefore as a pro or anticoagulant (125, 133). Sodium acts allosterically on thrombin, therefore binds without meeting the substrate and induces conformational transitions to thrombin which enhances catalytic activity (125, 133, 150). Thrombin bound to sodium increases access to smaller substrates and procoagulant substrates. Around 60% thrombin is in the procoagulant form (124, 128) under physiological conditions.

1.2.2.2. Thrombin substrates and ligands

Thrombin has numerous inhibitors, ligands, cofactors and substrates as illustrated in Figure 1.6. The cleavage and activation of substrates are described in the order of the pathway.

Thrombin cleaves and activates the coagulation factors V, XI and VIII which further amplifies the clotting pathway. The activation of these factors is done by early formed thrombin that does a feedback loop (120, 128).

As a procoagulant, thrombin cleaves fibrinogen into fibrin, which forms an insoluble gel, allowing further adhesion of platelets to the site of injury. The interaction is in the micromolar (μM) range and involves the basic exosite I and the active site, binding acidic fibrinogen (120, 146). Thrombin activates transglutaminase factor XIII, and fibrin enhances the cleavage 80-fold by bringing thrombin and factor XIII into proximity (128, 146, 149). Factor XIIIa crosslinks the fibrin fibres together, reinforcing the clot and rendering it resistant to fibrinolysis (136, 151, 152).

Thrombin generation depends on prothrombin availability (153), and procoagulant factors which require a negatively charged surface to activate, indicating that clot formation occurs near cell surfaces (154). Shear blood flow influences the availability of procoagulant factors as it delivers new factors and rids the old ones (155). Thrombin regulates haemostasis, by acting on cell surfaces also, and interacting with protease activated receptors (PARs) present on platelets (Figure 1.6).

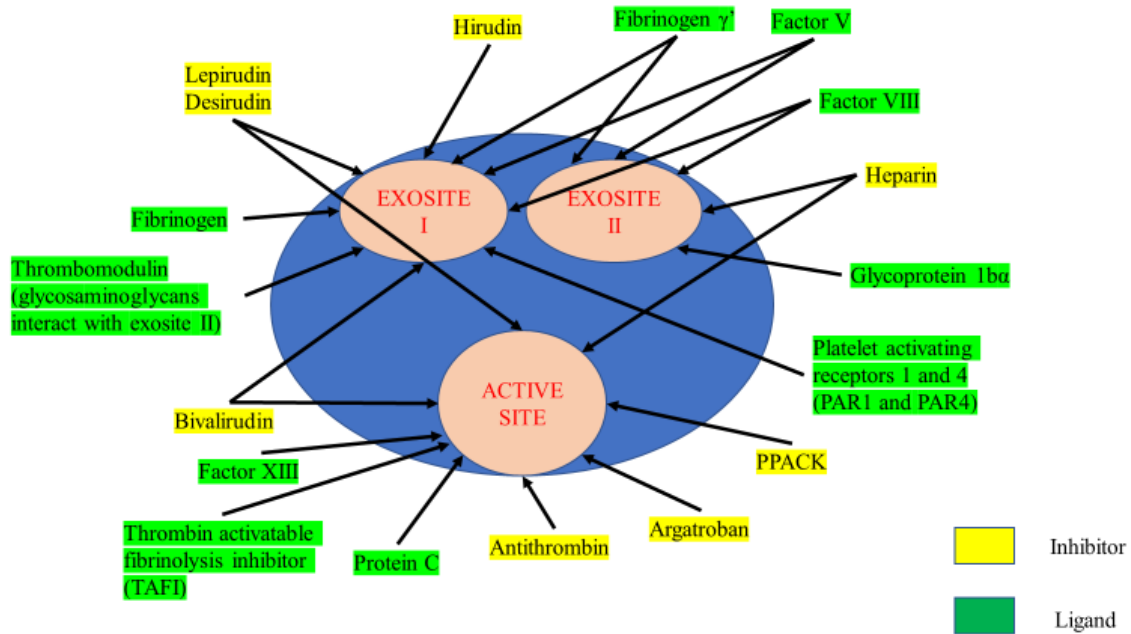


Figure 1.6. Representation of thrombin and its inhibitors and ligands. Many inhibitors of thrombin have been designed artificially based on the natural ones in circulation. Thrombin is multivalent with many ligands in physiological conditions. Thrombin (in blue) interacts with its inhibitors (yellow) and ligands (green) via exosites 1 and 2 and the active site (pink). Some ligands or inhibitors interact with both an exosite and the active site.

Thrombin is carefully regulated also, by being rapidly inhibited by antithrombin (AT), with the cofactor heparin (156). Antithrombin's affinity for thrombin is increased 1000-fold by heparin (146), which acts as a bridge between thrombin and antithrombin (142, 157, 158), bringing them into proximity for antithrombin to block thrombin's active site (149). Li et al (159) described the mechanism as thrombin translating along heparin, bound to antithrombin with high affinity, until thrombin reaches antithrombin.

Thrombin's regulation in the anticoagulant pathway includes its essential anticoagulant activity in the protein C pathway, described further on. Thrombin binds its cofactor thrombomodulin, switching its specificity to protein C. Thrombin cleaves and activates protein C which, with its cofactor protein S, downregulates the coagulation pathway.

Within the fibrinolysis pathway, thrombin, upon binding thrombomodulin activates thrombin-activated fibrinolysis inhibitor, or TAFI, a metallo-carboxypeptidase which prevents lysis and hence increases stability of the clot by cleaving off lysine residues from the N-terminal of fibrin (146).

My supervisor Dr Meike Heurich demonstrated before my arrival in Cardiff, an interaction between thrombin and factor H. No cleavage of factor H by thrombin was observed, nor any impact on the complement system regulation.

1.2.3. Fibrin formation and structure

Fibrinogen is a key thrombin substrate. It is an acute phase, soluble 340-kDa glycoprotein, present in plasma at a concentration of 1.5–4 g/L, expressed in the liver (160) and central to haemostasis, wound healing and inflammation (160).

Thrombin converts fibrinogen into an insoluble fibrin clot (161), which maintains haemostasis, enables wound process repairing, and prevent blood loss (160, 162). Fibrinogen consists of pairs of three disulphide-linked polypeptide chains: A α , B β , and γ (163, 164). The fibrin clot formation depends on pH, calcium, fibrinogen as well as thrombin concentration (135, 165-167), which is important for clot density and thickness of fibrin strands (132).

Thrombin cleaves fibrinogen to fibrinopeptide A (FpA) from the α chain, and fibrinopeptide B (FpB) from the β chain (164), enabling polymerisation. Cleavage of the fibrinogen alpha chain and release of fibrinopeptide A occurs at a faster rate due to the orientation of fibrinogen on surfaces and is essential for protofibril formation (160, 161, 168) and generates thicker fibres (169). Release of fibrinopeptide B is a slower and later stage in fibrin formation and enhances lateral aggregation (160, 169-171) (Figure 1.7).

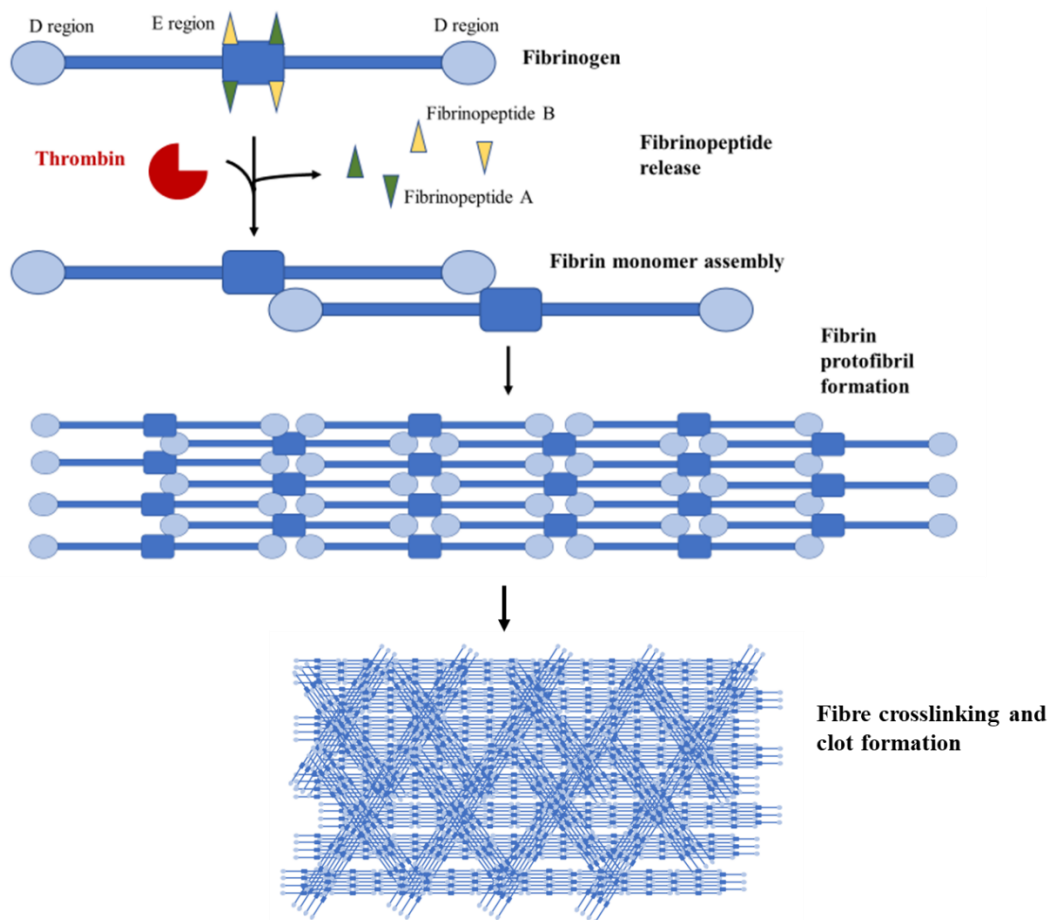


Figure 1.7. Fibrinogen is cleaved by thrombin to yield an insoluble fibrin clot. Fibrinopeptides A (dark green) and B (yellow) are released from fibrinogen upon cleavage by thrombin (red), forming fibrin monomers that assemble into oligomers (2nd image down) and then protofibrils (3rd image down). Fibrin monomers assemble to form the protofibrils through binding of the D region (light blue circles on the fibrin monomer) to the E region (dark square on the fibrin monomer). Protofibrils prolong and with lateral aggregation yield fibres of varying thickness which crosslink and form the clot (4th image down).

Fibrin polymerisation advances with monomers of fibrin assembling and extending longitudinally to begin lateral extension and aggregation (163, 166, 172-174) which is reinforced by factor XIIIa.

Higher concentrations of thrombin generate thinner fibres and a denser and more branched network with smaller and fewer pores, resistant to fibrinolysis (175-179), and decrease the number of protofibrils per fibre, making thinner fibres with increased stiffness (175, 180). On the other hand, lower concentrations of thrombin create a network with thicker fibres and less branching points and larger pores, more susceptible to lysis (132, 160, 175). Protofibrils laterally aggregate and increase the density of the fibrin fibres (155, 181). Fibrin branches out

either by forming a bilateral junction, or a trimolecular junction (155, 160). Gelation of clots corresponds to when around 20% of fibrinogen is converted to fibrin (177).

Other components that have been reported to influence fibrin clot structure include red blood cells (RBCs) (160), neutrophil extracellular traps (NETs) (160), circulating free DNA (CFDNA) (182, 183), von Willebrand factor and protease activated receptors (PARs) (140, 184).

After a clot has fulfilled its haemostatic function, it is dissolved by the fibrinolytic system (114).

1.2.4. The anticoagulant protein C pathway

To assure localised thrombi formation, the endothelium supports regulation of coagulation to maintain the blood in a fluid state (117). The endothelium requires constant surveillance hence platelets and coagulation factors are consumed fast in healthy conditions (123).

Thrombomodulin is an endothelial membrane bound cofactor for thrombin, which enables binding of protein C, a vitamin K-dependent zymogen circulating at 70nM in plasma (185), which is activated into an anticoagulant protease (activated protein C, APC) (186), and enhanced by presence of endothelial protein C receptor (EPCR) (187). Activated protein C, in complex with its cofactor protein S (184, 187), downregulate coagulation by cleaving and degrading the procoagulant factors Va and VIIIa (186, 188), cofactors to factors Xa and XIa, thereby decreasing thrombin generation (189) (Figure 1.8A).

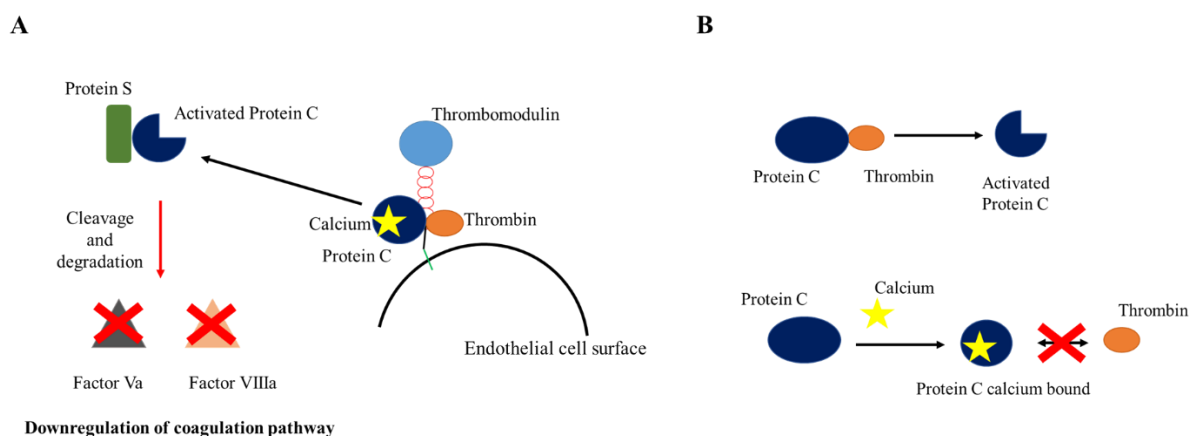


Figure 1.8. Thrombin binding and cleavage of protein C in presence and absence of thrombomodulin. (A) Membrane-bound thrombomodulin (light blue, red figure) acts as a cofactor to thrombin (orange) enabling it to interact with calcium-bound (yellow star) protein C (dark blue circle) to activate it into activated protein C (cleaved dark blue circle). Activated protein C binds protein S (dark green rectangle) enabling inactivation of factors Va (grey triangle) and VIIIa (beige triangle). (B) In absence of thrombomodulin and calcium, thrombin (orange circle) can bind and cleave protein C (dark blue circle, top image) into its active form (cleaved dark blue circle, top image). However physiological concentrations of calcium (yellow star, lower image) inhibit the cleavage of protein C by thrombin (lower image).

Activated protein C also binds protease activated receptor 1 (PAR1), a thrombin receptor, hence competing with thrombin binding and allowing maintenance of endothelial barrier integrity (184, 190).

Thrombin can cleave protein C alone, however the presence of thrombomodulin increases the cleavage 1000-fold (191), upon binding thrombin's exosite I and changing the active site allosterically from a procoagulant to an anticoagulant (192) (Figure 1.8B).

Calcium binding to protein C causes a conformational change and alters the activation peptide (192, 193). Thrombomodulin binds and alters the 37 loop of thrombin and overcomes the inhibitory effect of residue Arginine 35, the latter preventing binding and cleavage of calcium-bound protein C (185, 194-198). Calcium binding also allows formation of an anion binding exosite in protein C, which can bind EGF4 domain of thrombomodulin (185, 197). Overall, calcium binding protein C and thrombomodulin binding thrombin disables the repulsive interaction between Arginine67 in protein C, and Arginine35 in thrombin (194, 199).

Activated protein C further influences down-regulation of proinflammatory and proapoptotic pathways and up-regulation of anti-inflammatory and antiapoptotic pathways (184, 190) and diminishes inflammatory mediator and cytokine release (190).

1.2.5. Thrombomodulin

1.2.5.1. Structure and function of thrombomodulin

Thrombomodulin is a type I glycosylated transmembrane protein located on the endothelium at a density of 50 000 to 100 000 molecules per cell (200). It is expressed mostly on the luminal side of the endothelium but also on neutrophils and monocytes among others (201). Soluble

thrombomodulin is present in plasma (3-50ng/ml) and urine, is generated via proteolytic cleavage by leukocyte-derived proteases such as elastases, and metalloproteases (202-209).

Thrombomodulin binding switches thrombin from a procoagulant protease to an anticoagulant, by binding at exosite 1, preventing thrombin's binding to its substrates, fibrinogen, PARs, FVa, and FXIIIa (134, 191, 210-212). Calcium is crucial for thrombomodulin-thrombin interaction, binding EGF6 (194, 213), and domains EGF456 of thrombomodulin are required for protein C binding and cleavage, allowing optimal alignment for insertion into the active site of thrombin (186, 194, 214, 215). Thrombomodulin increases the catalytic activity of thrombin for protein C 1000-fold, without causing allosteric changes on thrombin's active site (216, 217), allowing generation of activated protein C (Figure 1.9).

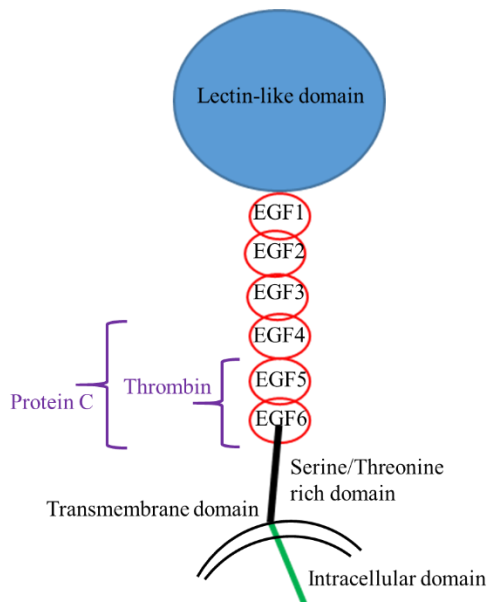


Figure 1.9. Thrombomodulin contains 5 domains. Thrombomodulin contains the N-terminal lectin like domain (LLD, dark blue circle) that plays roles in inflammation and has two N-glycosylation sites. The 6 endothelial-growth factor (EGF)-like domains (red empty circles) are key in regulating coagulation by interacting with thrombin (EGF5) and protein C (EGF4) and calcium (EGF6) which enhances thrombin binding. The serine/threonine rich domain (black stalk) is involved in enhancing thrombin binding with the chondroitin sulphate moiety, the transmembrane domain, and the intracellular domain (green stalk) that are not known to have any relevant regulatory function.

Thrombomodulin is 557 amino acids and made up of five domains (201, 218). The most N-terminal site is the lectin-like domain (LLD) and resembles C-type lectins, and is thought to have a role in endocytosis, inflammation, and tumour growth (219-228). The LLD contains a

hydrophobic domain, two N-glycosylation sites, calcium binding site and carbohydrate recognition sites for homotypic interactions (222).

Attached to this region are the 6 epidermal growth factor-like domains 1 to 6 (EGF1-6) which contain 2 N-glycosylation sites, and two sites prone to oxidisation (229). EGF4, 5 and 6 are involved in calcium binding and the interaction with thrombin and protein C (186, 213, 218). Thrombin binds to thrombomodulin on EGF5 domain and this interaction is enhanced with EGF6 and its calcium binding domain (230). Protein C binds thrombomodulin in EGF-4 (185, 186), and TAFI in EGF3 and 4.

The final soluble part of the transmembrane protein is the Serine/Threonine rich domain (S/T) which can carry a chondroitin sulphate moiety (CS) and enhances thrombin binding (229). The final region is the transmembrane and intracellular region, both about 30 amino acids each (231).

1.2.5.2. Thrombomodulin in other systems

Through binding partners, thrombomodulin adopts roles other than in coagulation, including binding with high mobility group box 1 (HMGB1) (201, 219), decreasing inflammation (201, 225), and with Lewis Y antigen (223, 227, 232), involved in leukocyte function.

Recombinant EGF-like and S/T rich domains compete with membrane bound thrombomodulin for binding to CD14, which decreases release of tumour necrotic factor (TNF) and interleukin 6 (IL6) (229).

Thrombomodulin binds complement regulator factor H and increases its cofactor activity in the inactivation of iC3b (233) and hence complement regulation (29), indicating a molecular crosstalk between anticoagulation and complement systems.

1.3. Coagulation and complement crosstalk

1.3.1 Complement and coagulation crosstalk

Complement and coagulation evolved from the same common ancestor as shown by the horseshoe crab, a “living fossil” which used a fusion of the two systems to prevent infections and blood loss (4). Structural similarities are evident (234) as well as interaction between the cascades at different levels. They act together in inflammation and require a balance to avoid pathological states (7, 235).

Complement activation has been shown to affect the clot structure, rendering the fibres thinner and less permeable (236-238). Complement factors can be found in thrombi and are capable of sustaining inflammation (160, 237-244). The membrane attack complex (MAC), upon disruption of endothelial cells or platelets causes exposure of phosphatidylserine and therefore a surface for prothrombinase formation (3, 18, 235) and ultimately thrombosis (5). Anaphylatoxins C3a and C5a, have been associated with increased tissue factor expression (3, 245). Thrombin activated fibrinolysis inhibitor (TAFI) has also been reported to interact and inactivate anaphylatoxins (246), leading to a decrease in the immune response (Figure 1.10).

C3, C6, and C5 complement components affecting haemostasis is partly illustrated by the knockout mice that have increased bleeding (240, 247-250). Complement C3 binds fibrinogen (240) and factor XIII (22, 240) and increases lysis time (251-253). However, C3 has been shown to be important for tissue factor activation (254), platelet activation and fibrin formation (237, 238). To support this C3 knockout mice have increased bleeding and less platelet aggregation (250) as well as abnormal thrombus formation (238). Complement C5 knockout mice have lower thrombosis, thrombocytopenia, and consumptive coagulopathy (248, 255), have decreased thrombus size and weight (238) and low tissue factor levels (254). Authors determined that C5 played a role in fibrin formation and tissue factor activation (238). Finally in the context of diabetes presence of C3 and C5 rendered fibres thinner and the overall clot denser (237). One report has also demonstrated increased bleeding time and lower platelet aggregation in C6 knockout mice and rats (247, 256), overall indicating a role of the terminal pathway in clot formation.

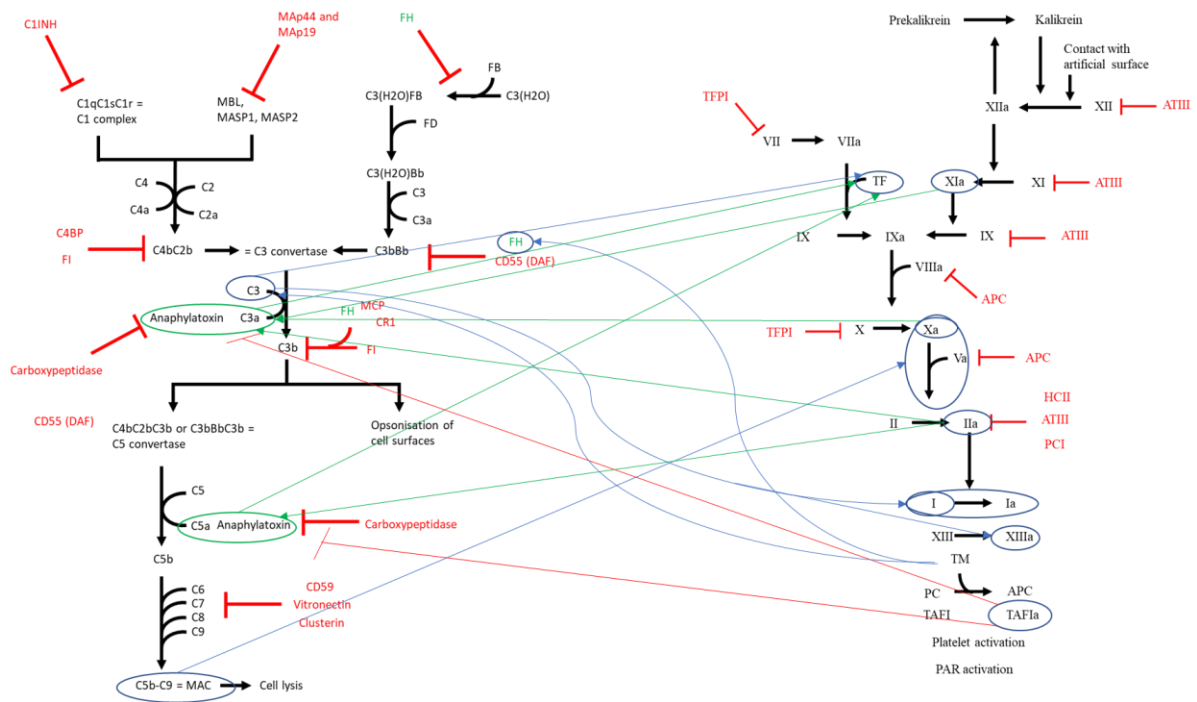


Figure 1.10. Selected crosstalk between complement and coagulation. Illustration of key interactions between complement and coagulation factors that activate or inhibit one or the other system. Red lines indicate inhibition. Colours blue or green are to differentiate the interactions. The crosstalk relevant to my thesis are illustrated only.

Coagulation factors also impact complement regulation and activation (Figure 1.10). Plasminogen and plasmin have been shown to regulate complement by increasing C3b inactivation (257) or act as a convertase in the cleavage of C3 and C5 (6, 258), as well as thrombin, although the physiological relevance of the latter has been debated (259). Thrombin has also been shown to cleave and generate C3a (6). Factors Xa and XIa were also shown to generate biologically active C3a and C5a (6). Kallikrein also cleaves C3 and enables complement activation (260). Previous results have shown the thrombomodulin interacting with factor H (29), and mildly enhancing complement regulation and inactivation of C3b by factor I and factor H (29, 233). Mutations in the lectin like domain and in the serine/threonine rich domain have shown increased binding to both C3b and factor H (233). Furthermore, research has demonstrated an interaction between the lectin like domain of thrombomodulin and C3 and C3b (214, 261-263), and mice lacking the lectin like domain have increased glomerular complement deposition (264) (in the context of diabetic nephropathy), and increased complement activation (in the context of rheumatoid arthritis) (265).

Von Willebrand Factor (vWF) is an adhesive multimeric glycoprotein synthesised by endothelial cells and megakaryocytes (266, 267). It can be stored in Weibel Palade bodies within the endothelial cell, or in platelet alpha granules where it is released into plasma. Von Willebrand factor stabilises factor VIIIa (267) and mediates platelet adhesion to the sub-endothelium and platelet aggregation (123, 268). The dimeric forms of vWF are thought to act in regulating complement by acting as a cofactor for factor I in binding and inactivation of C3b (269-271). However ultra large von Willebrand factor or multimeric forms have a prothrombotic effect and increase complement activation by recruiting complement components (269-271).

1.3.2 Factor H interactions with several coagulation factors

Factor H has been identified as a ligand for numerous coagulation proteins. It has been reported to interact with other components of the fibrin clot (242), including fibrin(ogen) (24, 272), factor XII (19, 20) and factor XIII (23, 240), von Willebrand factor (27, 28) and platelets (25, 26, 273) (Figure 1.11).

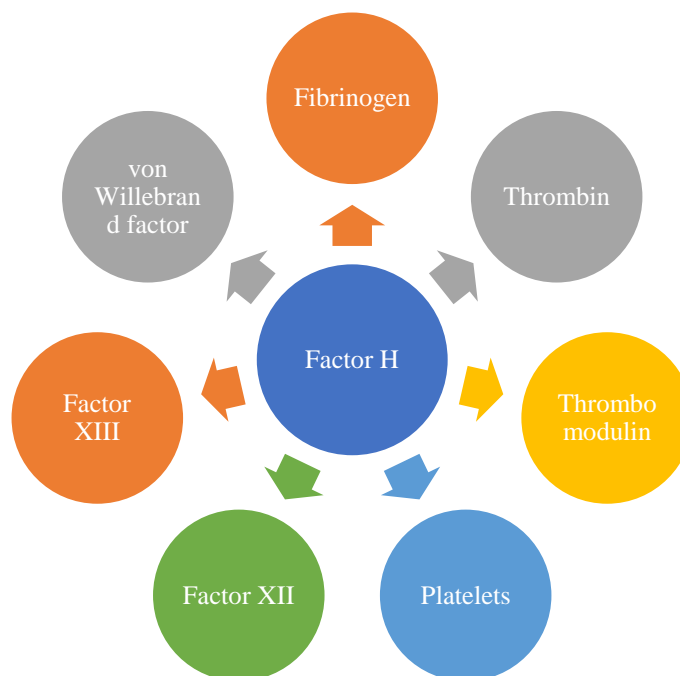


Figure 1.11. Involvement of factor H with clotting and coagulation factors and the effect of the interaction.

Factor H has been reported to interact with factor XII, factor XIII, thrombin, platelets, von Willebrand factor, fibrinogen and thrombomodulin.

The crosstalk of factor H with coagulation ligands and their functional effect on complement or coagulation activity is summarised in table 1.1.

Table 1.1. Factor H interactions with coagulation factors and the impact on complement or coagulation systems. Factor H has been reported to interaction with factor XII, platelets, thrombin, fibrinogen, von Willebrand factor, factor XIII, and thrombomodulin. Different impacts have been reported or not on complement or coagulation.

Complement protein	Coagulation protein/components	Effect on complement system	Effect on coagulation system	Reference
Factor H	Factor XII	No known effect	Inhibits its activation of kallikrein amidolytic activity and complexes detected in plasma	(19, 20)
	Platelets (secrete factor H and uptake of factor H by platelets)	binds platelets in a dose dependent manner via its C-terminal region as it was observed that aHUS mutations in that region bind less	regulates platelet activation and aggregation caused by properdin-mediated complement activation	(25, 26, 273-275)
	Thrombin	No obvious effect	unknown	Previous data from the laboratory
	Fibrinogen	No known effect		

	Von Willebrand factor	Enhances inactivation of C3b by factor H	Decreases cleavage of vWF by ADAMTS13 Increases cleavage of vWF by ADAMTS13	(27, 28, 268-270)
	FXIII	No reported effect	No reported effect	(23)
	Thrombomodulin	Enhances inactivation of C3b by factor H	No known effect	(29, 233)

1.4. Homology modelling of proteins

Nuclear magnetic resonance (NMR) and X-ray diffraction are the spectroscopic techniques that produce high-resolution 3D coordinates of macromolecules (276). Homology modelling is used to determine protein structures when the crystal structure is unavailable and involves calculating a protein's quaternary structure for which only the sequence is known by aligning it with a homologous protein for which the structure is known, using it as a template (277).

Similarity search programs, such as Basic Local Alignment Search Tool BLAST or FASTA, determine homology for newly determined sequences, by comparing and aligning them to sequence databases. Protein-protein sequences are more reliable to compare and determine homology, however, the function of the protein is not as predictable as it is harder to quantify (278). Homology between proteins corresponds to when two sequences have more similarity than chance could predict (278).

BLAST is a program from National Centre for Biotechnological Information (NCBI) that detects similarity between sequences, nucleotides or proteins, by comparing the sequences to those from databases and deducing how significantly different the matches are (279, 280). To construct a homology model, the protein sequence of our region of interest is compared to the databases, specifically in the protein database, PDB. A PSI-BLAST search was done, which is

a Position Specific Iterative search. This setting is used to find distantly related proteins or new members of a protein family (280). A motif or profile is created for a certain family of proteins (based on the search) and this motif is used for subsequent and repeated alignments. At the end of the alignments, a max score, an E-value and percentage identity are generated for each match:

- The max score is the sum of substitutions and gaps, and from this a bit-score is given which considers the statistical properties of the system used.
- The expected value, or E-value is the number of alignments that have a score over or equal to the score which occur in the database by chance (279, 281). It is an estimation of the number of false positives if all scores obtained for the alignment were equal or better than the alignment score from which the E-value comes from. The lower the E-value, the more significant the score and alignment are, The E-value is more accurate for inferring homology and depends on the size of the database that the comparison is done in.
- The percentage identity corresponds to the extent to which the amino acid sequences have the same residues at the same position in the alignment (282). A percentage identity of 98-100% often means that it is the same species. Generally, two sequences are considered homolog when there is over 30% identity over the entire length of the sequence. For homology modelling, a percentage identity of 40% is a good threshold.

To determine a homology model, proteins are superimposed or aligned (positioning a group of structures in a 3D space) into the modelling software Molecular Operating Environment (MOE). The root mean square deviation, RMSD, is determined which is a quantitative measure of the similarity between superimposed atomic coordinates. The lower the RMSD, the better the superimposition (283, 284). It is important to note that measuring the global similarity between two structures can misrepresent the local similarity. For instance, flexible fragments like loops, or relative domain movement are difficult to model and can lead to bad global similarity causing low superimposition (284).

Forcefields in computational modelling measure the force in between atoms within a molecule and between molecules. The one used very often in homology modelling is the assisted model building and energy refinement, or AMBER (specifically AMBER12:EHT). This forcefield is

often used for proteins and DNA, and along with the forcefields CHARMM and GROMOS, is for molecular dynamics of molecules and minimising energy (278, 283).

A total of 10 models are generated, with the final 11th one being the homology model. Once the model was determined, the geometry of the structure is analysed based on the Ramachandran plot, which determines the secondary structures of the peptides within the homology model. The Ramachandran plots the torsional (or dihedral) angles of each residue, or Phi and Psi angles, which ultimately determines the most stable secondary structures for each residue. Each atom is treated as a sphere, corresponding to the Van Der Waals radii. For a give Phi-Psi angle, if two spheres overlap, this is a sterically disallowed conformation of the polypeptide backbone. The most stable conformations are alpha helices or beta strands (Proteopedia).

Full length homology models of factor H have been built, although this was done in 2001 (62) and 2009 (285). Up to date, most SCRs in factor H have been resolved, however no structure (obtained by NMR or X-ray diffraction) exists currently for SCR14 and SCR17 of factor H. The first homology models of full length factor H were not as reliable as they were built without some crystal structures that today are available. Factor H is difficult to study structurally due to its large size and flexible structure. However, the studies performed have demonstrated that factor H is a folded back structure in solution (62, 285).

1.5. Research question and Hypothesis

1.5.1. Functional analysis of thrombin binding to factor H shows no significant effect on complement activity.

Previous research and findings in the lab showed that thrombin bound factor H with nanomolar affinity and does not proteolytically cleave factor H. Studies were done to determine whether thrombin affected factor H's regulatory activity and showed that there was no interference with factor H binding to C3b, nor its regulation of the C3 convertase. Thrombin had a moderate effect on factor H's cofactor activity, in the inactivation of C3b although at supraphysiological concentrations (500nM) and finally did not show any impact on complement activity in haemolytic assays.

1.5.2. Research question

Factor H is a ligand for coagulation protease thrombin, with no significant effect on the complement system but also interacts with other coagulation factors relevant to clot formation, such as factor XII, factor XIII, fibrin(ogen), von Willebrand factor and platelets, as well as anticoagulation, such as thrombomodulin (20, 23-25, 28, 29). This indicates that factor H could play a part in coagulation, fibrin clot formation and the anticoagulant pathway. Therefore, the research questions for this study were:

1. Does the thrombin factor H interaction affect thrombin's role in the coagulation pathway and specifically its role in fibrin clot formation?
2. Does the thrombin factor H interaction affect thrombin's role in the anticoagulation pathway?
3. What are the molecular binding sites and are these relevant to complement or coagulation we observe in disease?

1.5.3. Hypothesis

The underlying hypothesis for this work is that factor H acts as a cofactor for thrombin as a procoagulant in fibrin clot formation and as an anticoagulant in protein C activation.

1.5.4. Aims and objectives

The aim of the project was to understand how factor H binds and affects thrombin's activity as a procoagulant and anticoagulant and what downstream effects were. From this the aim would be determining how mutations in factor H in diseases such as aHUS, could affect the interaction with thrombin and haemostasis. Overall this would allow further understanding of how factor H could regulate coagulation as well as complement, but also deepen the research on the crosstalk between complement and coagulation.

In order to test the hypothesis, the following objectives were set:

- 1) Determine the impact of the absence of factor H on the coagulation profile in factor H knockout (*CFH*^{-/-}) mice by measuring tail bleeding time (experiment performed before my arrival in Cardiff), and levels of soluble thrombomodulin, thrombin-antithrombin complex, and protein C in murine plasma.
- 2) Analyse the impact of the absence of factor H in human factor H-affinity plasma on clotting times. For this, activated partial thromboplastin time (aPTT) and prothrombin times (PT) are measured in human plasma depleted of factor H alone, or factor H and factor B (to prevent alternative pathway activation).
- 3) Determine the role of factor H in thrombin-mediated fibrin clot formation. Turbidity assays are used to monitor how factor H affected thrombin's cleavage of fibrinogen into fibrin in a pure protein system.
- 4) Determine how factor H impacts thrombin's role in anticoagulation. Protein C activation by the thrombin-thrombomodulin complex and by thrombin alone is monitored in presence or absence of factor H, in a pure protein system.
- 5) Determine the binding sites involved in the interaction between factor H and thrombin, and thrombomodulin. Binding assays and surface plasmon resonance is performed to analyse the interaction between thrombin and factor H, and compared to thrombomodulin and factor H, and fibrinogen and factor H. Recombinant short domain constructs of thrombomodulin and factor H will be used to dissect domains involved in binding or function. Molecular modelling is performed with identified thrombomodulin and factor H domains and thrombin, to further analyse the residues involved in the interaction.

Chapter 2: Materials and methods

2.1. Materials

All materials used in this study are listed below. Table 2.1 describes the proteins used, with source information, and their stock concentration. Table 2.2 describes the antibodies used, with source information and their stock concentration and storage condition. Table 2.3 lists the chemicals, reagents and material used for all experiments.

Table 2.1. Proteins, their stock concentration and storage conditions, as well as their source are listed in their respective rows.

Protein name	Stock concentration and storage condition	Source
Factor H	Concentration variable depending on batch. Prepared in 10mM HEPES/150mM NaCl buffer pH7.4 Stored at -80°C	In house (purified from serum or plasma, see purification process in methods)
Factor H constructs SCR1-4, 1-5, 1-6, 6-8, 8-15, 15-18 and 18-20	See appendix A2.1 with information about constructs. Stored at -80°C	Kind gift from Christoph Schmidt, University Ulm, Germany

(expressed in <i>Pichia Pastoris</i>)		
Fibrinogen 1: plasminogen depleted	Concentration variable depending on batch. Prepared in 10mM HEPES/150mM NaCl buffer pH7.4 Stored at -80°C	Enzyme Research Laboratories (Swansea, UK)
Fibrinogen 2: plasminogen depleted, and von Willebrand factor depleted	Concentration variable depending on batch. Prepared in 10mM HEPES/150mM NaCl buffer pH7.4 Stored at -80°C	Enzyme Research Laboratories (Swansea, UK)
Fibrinogen Alexa fluor 488	1mg/ml. Prepared in 10mM HEPES/150mM NaCl buffer pH7.4 Stored at -80°C	Invitrogen
Active Thrombin	93µM, sub-stock 5µM. Prepared in 10mM HEPES/150mM NaCl buffer pH7.4 Stored at -80°C	Enzyme Research Laboratories (Swansea, UK)

PPACK-inhibited thrombin	6.67mg/ml. Prepared in 10mM HEPES/150mM NaCl buffer pH7.4 Stored at -80°C	Enzyme Research Laboratories (Swansea, UK)
Soluble Thrombomodulin (with HIS tag)	9.7µM. Stored at -80°C	R&D Systems
Recombinant EGF456 thrombomodulin construct	8.3mg/ml. Prepared in 10mM HEPES/150mM NaCl buffer pH7.4 Stored at -80°C	Kind gift from Prof. Jim Huntington, Cambridge University, UK
Protein C	67µM. Prepared in 10mM HEPES/150mM NaCl buffer pH7.4 Stored at 4°C	Cambridge Biosciences
Activated protein C	1.72mg/ml. Prepared in 10mM HEPES/150mM NaCl buffer pH7.4 Stored at -80°C	Enzyme Research Laboratories (Swansea, UK)
Hirudin* *recombinant leech	0.1U/ml. Prepared in PBS. Stored at -80°C	Sigma

Table 2.2. Table title. Antibodies used in this study are listed, with source information, and their stock concentration.

Immunogen	Antibody	Type	Stock concentration	Source
Complement				
Factor H	Anti-factor H 35H9 (SCR1-3)	IgM, mouse, monoclonal	2.8mg/ml	In house (Kind gift from Prof. Paul Morgan, Cardiff University, UK)
Factor H	Anti-factor H Ox24 (SCR5)	IgG, mouse, monoclonal	1.4mg/ml	In house (Kind gift from Prof. Paul Morgan, Cardiff University, UK)
Factor H	Anti-factor H SCR10-15	IgG, Monoclonal	2.1mg/ml	In house (Kind gift from Prof. Paul Morgan, Cardiff University, UK)
Factor H	Anti-factor H C18/3 (SCR20)	IgG, mouse, Monoclonal	1mg/ml	Enzo
Factor H	Antibody anti- factor H	IgG, Polyclonal	8mg/ml	In house (Kind gift from Prof. Paul Morgan,

				Cardiff University, UK
Coagulation				
Thrombomodulin	Anti-thrombomodulin-lectin-like domain	IgG, mouse Monoclonal	0.1mg/ml	Santa Cruz Biotechnology
Thrombomodulin	Anti-thrombomodulin against EGF1-2	IgG, mouse monoclonal	0.2mg/ml	Sekisui Diagnostics
Thrombomodulin	Anti-thrombomodulin against EGF 5 PBS-01	IgG, mouse Monoclonal	1mg/ml	Abcam
Thrombomodulin	Anti-thrombomodulin against EGF 6	IgG, rat Monoclonal	0.1mg/ml	Acris
Thrombomodulin	Anti-thrombomodulin	IgG, sheep Polyclonal	0.2mg/ml	R&D Systems biotechne
Thrombin	Anti-thrombin	IgG, sheep Polyclonal	12.2mg/ml	Abcam
Factor B	Anti-factor B JC1	IgG, mouse Monoclonal	1.47mg/ml	In house (Kind gift from Prof. Paul Morgan, Cardiff)

				University, UK
2nd antibodies				
Sheep Ig	HRP-labelled secondary antibody anti- sheep	IgG	0.8mg/ml	Jackson Biolabs
Rat Ig	HRP-labelled secondary antibody anti-rat	IgG	0.8mg/ml	Jackson Biolabs
Mouse Ig	HRP-labelled secondary antibody anti- mouse	IgG	0.8mg/ml	Jackson Biolabs
Rabbit Ig	HRP-labelled secondary antibody anti- rabbit	IgG	0.8mg/ml	Jackson Biolabs
Amboceptor				Siemens

Table 2.3 represents the different chemicals, reagents, materials and equipment used for the different experiments.

Table 2.3. Chemicals, reagents, materials, and equipment used for all experiments. Name of items are indicated in the left row and source indicated in the right row.

Chemicals and reagents (general)	Source
---	---------------

APC substrate CS Biophen 21-66	Quadrachtech
Calcium chloride	Fisherbrand
HEPES	Fisherbrand
NaCl	Sigma
Glycine	Fisherbrand
Trizma Base	Sigma
Coomassie stain	Biorad
PBS	Oxoid
Tween	FisherBrand
Milk powder	Tesco's
Sheep erythrocytes	TCS Biosciences
Normal human serum (NHS)	Pooled, Healthy volunteers, n=3
Normal human plasma (NP)	Pooled, Healthy volunteers, n=3
CFD buffer	Oxoid
Plasmid preparation material	Source
Ampicillin	Sigma
LB Broth	Sigma

LB Broth with Agar	Sigma
Endofree Plasmid Maxi Prep kit	Qiagen
Petri dishes	Corning
Cell culture material	Source
Sterile PBS	Thermo Scientific
RPMI media	Gibco
DMEM media	Sigma Merck
Reduced serum media Opti-MEM	Gibco
Fetal Bovine Serum (FBS)	Gibco
Penicillin-Streptomycin	Sigma Merck
L-glucose	Sigma Merck
Freezing media	Gibco
Flasks (T25, T75, T175)	Fisher Scientific
His-Pur Ni-NTA Spin column	Thermo Scientific
Stripettes	Fisher Scientific
Surface plasmon resonance (Biacore) material	Source
Series S Sensor Chip CM5	GE Healthcare
Amine coupling kit	GE Healthcare

Surfactant p20	GE Healthcare
Coagulometer MCS10 material	Source
SynthAsil (aPTT)	HemosIL
Recomboplastin RTF 2G (PT)	HemosIL
Calcium 0.02M	HemosIL
Fluorescent microscopy	Source
Immunopen	Merk Millipore
Slides	Dixon
Coverslips	Dixon
Western blot	Source
Coomassie stain	Biorad
Milk	Tesco's
4-12% Tris Glycine gradient gels	Life Technologies
PVDF membranes	GE Healthcare
Nitrocellulose membranes	GE Healthcare
Running buffer (MES or MOPS)	Thermo Fisher Scientific
Transfer buffer	Invitrogen

LDS loading sample buffer	Thermo Scientific	Fisher
Reducing agent buffer	Thermo Scientific	Fisher
Protein ladder	New England Biolabs	
ECL	Thermo Fisher	
Gel tank mini gel	Thermo Scientific	Fisher
Transfer tank	Hoeffer system	
Other material	Source	
96 well plates flat bottomed	Fisher Scientific	
96 well plates U-bottomed	Fisher Scientific	
Polystyrene MaxiSorp	Fisher Scientific	
Equipment	Source	
MC10		
Biacore T200	GE Healthcare	
Gbox	Syngene	
Tecan T50 plate reader	Tecan Ltd	
Nanodrop	Thermo Scientific	

AKTA FPLC	GE Healthcare
Centrifuge 5810R	Eppendorf
Centrifuge 5424R	Eppendorf
Clauss Fibrinogen	

2.2. Methods

2.2.1. Complement haemolysis assay to measure complement activation and regulation in serum

Haemolysis assays assess the activity of complement in normal human serum (NHS), and are based on protocols initially described by Mayer (286).

Sheep erythrocytes (2mL) were washed in 20ml of CFD by centrifugation (2000rpm (860xg), 5min) 3 times, by resuspending the pellet in 20ml CFD each time. During the washes, 10ml of CFD, and 10ml of CFD with 5µl of Amboceptor (1/2000 dilution) were preheated to 37 degrees. The sheep erythrocyte pellet was resuspended in 10ml of preheated CFD before addition to the 10ml of CFD + Amboceptor (resulting in 20ml of 2% cell suspension, 1/4000 Amboceptor). The cell suspension is incubated for 30min, at 37°C (water bath) on a shaker. The wash steps were repeated (to remove excess antibody), until the buffer is clear. The pellet was resuspended in 20ml of CFD.

Normal human serum (NHS) was used as a source of complement proteins. NHS was titrated down 50µl/well (0.03%-10%), in a U-bottom plate with CFD, before addition of 50µl of CFD and 50µl of activated and sensitised sheep erythrocytes. The total volume per well was 150µl. The positive control (100% lysis) was 100µl of water/Tween 0.1%, with 50µl sheep erythrocytes. The negative control was 100µl CFD, with 50µl sheep erythrocytes. The plate was then sealed and incubated for 30min-1h to allow haemolysis to take place (check that the first three rows with high NHS concentration are like the positive control). The reaction was

stopped by spinning the plate down at 4 degrees, at 1500rpm (484xg) for 5min. 100µl of supernatant of each row was transferred to a flat-bottom plate (only the supernatant without disrupting the pellet). The plate was read at 405nm in the plate reader, by measuring haemoglobin release, proportional to haemolysis.

The % of haemolysis was calculated with the following formula:

$$\% \text{ haemolysis} = (A(405\text{nm}) \text{ sample} - A(405\text{nm}) \text{ negative CT}) / (A(405\text{nm}) \text{ positive CT} - A(405\text{nm}) \text{ negative CT}) \times 100$$

CT corresponds to control.

Factor H serial dilution in 10mM HEPES/150mM NaCl buffer, pH7.4 is performed in absence or presence of a fixed concentration of catalytically inactive PPACK-thrombin (to assess thrombin-factor H binding only) or active thrombin (to assess impact of thrombin mediated cleavage of complement C3 and C5 in conjunction with factor H binding) at the predetermined NHS dilution. Factor H (0.001-1µM) was diluted in CFD buffer (thrombin was added to the factor H titration or to the serum) before addition of NHS (set at concentration corresponding to 40% lysis of cells according to the NHS titrated) and 2% Amboceptor-activated sheep erythrocytes in CFD buffer.

2.2.2. Mouse plasma preparation

Mouse plasma isolation was performed prior to this work as follows: all animals were housed in conventional cages at the SPF facility, Cardiff University, Cardiff, United Kingdom. Where needed animals were anaesthetized using Isoflurane. All animal studies were carried out under the authority of project license (PPL) 30/3365 granted by the UK Home Office. Both male and female animals were used in our studies, data presented here are male only. Wild-type (WT) mice (C57/Black6 J from Jackson Laboratories) were purchased from Envigo, factor H-deficient mice (*CFH*^{-/-}) on a C57/Black6 background have been described previously and were a kind gift of Prof. Matthew Pickering; bred and maintained in our facility. Factor H knockout mice and wild type mice C57/Black 6 were killed by exsanguination via cardiac puncture under surgical plane anesthesia, Death was confirmed by cervical dislocation. Whole blood was drawn into 3.8% citrate solution (1/8 v/v) or EDTA and underwent centrifuging at 4500 rpm (4355xg) for 5 minutes at room temperature. Murine plasma was removed and stored at -80°C until further analysis.

2.2.3. Human plasma and serum isolation

For the plasma preparation, 50ml of whole blood was taken from 3 consenting healthy volunteers, collected in plastic falcon tubes in 3.8% citrate buffer (1/8 v/v), before spinning down at 4000rpm (3440xg) for 15min. The supernatant (plasma) was collected and spun down a second time at 4000rpm (3440xg) for 15min. The supernatant was collected again and filtered through 0.22µm filter, before aliquoting and freezing down at -80°C until further use.

For the serum preparation, 50ml of whole blood was taken from 3 consenting healthy volunteers and left to clot at room temperature in glass vials for 30 minutes, then put on ice for another 30 minutes to contract the clot before spinning down at 3000rpm (1935xg) for 20min. The serum supernatant was collected and filtered (0.2µm filter) and stored at -80°C until further use.

2.2.4. Affinity depletion of complement factors from citrated human plasma

Human citrated normal plasma was depleted of either:

- factor H and factor B (termed ΔFB/ΔFH plasma)
- factor H only (termed ΔFH plasma)
- factor B only (termed ΔFB plasma)

by using affinity chromatography with factor-specific antibodies. Antibody clone 35H9, against SCR 1-3 of factor H, and anti-factor B antibody, clone JC1, against the Bb fragment of factor B, were coupled each to one Sepharose column via amine coupling.

Monoclonal anti-factor H antibody (clone 35H9, anti SCR1-3) was coupled to a 5ml Hi-Trap NHS-activated column using amine coupling according to manufacturer protocol (GE Healthcare, reference 71-7006-00 AX).

The concentration of the antibody was deduced: $A_{280} \times \epsilon(\text{IgM}) = 5,8 \times 1,8 = 3,2\text{mg/ml}$.

Optimal concentration for 5ml Hi-Trap NHS-activated columns, is 7-10mg/ml. Since the column is 5ml, the total amount of antibody needed is $10\text{mg/ml} \times 5\text{ml} = 50\text{mg/ml}$.

In brief, the antibody was concentrated down to 50mg/ml and dialysed into coupling buffer (0.2M NaHCO₃, 0.5M NaCl, pH8.3) and passed over the activated (1mM HCl) column, which was then washed (0.1M sodium acetate, 0.5M NaCl, pH4) and residual active sites blocked (0.05M Na₂HPO₄, 0.1% NaN₃, pH 7). The coupling efficiency was determined at 97%. The column was then washed and stored in PBS until further use at 4°C.

A volume of human citrated plasma was flown over in the presence of 10mM HEPES/150mM NaCl buffer, pH7.4. For single factor depletion, plasma was flown over each column individually (for the factor H only or factor B only depleted plasmas), or for dual depletion (for the factor H and factor B depleted plasma) plasma was flown over the columns connected sequentially (1st anti-factor B, 2nd anti-factor H) at a flow rate of 1ml/min as shown below (Figure 2.1).

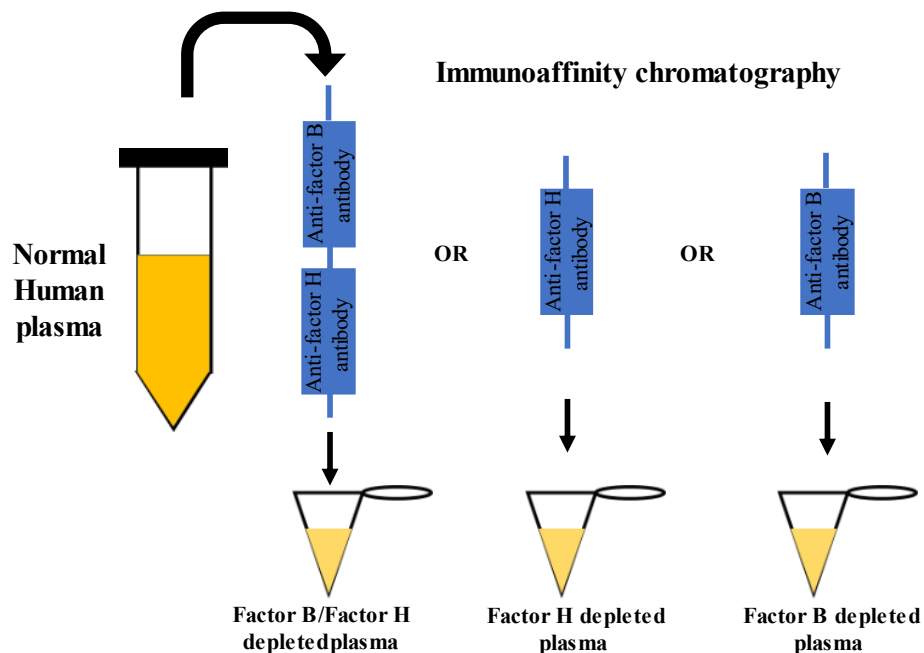


Figure 2.1. Set up and preparation of complement factor B and factor H-depleted normal human plasma using affinity chromatography. Normal human plasma was collected from healthy donors in citrate buffer and was run over Sepharose column(s) coupled with antibodies JC1 (anti-factor B antibody) and/or 35H9 (anti-factor H antibody) to remove factor B first and/or factor H, in the presence of 10mM HEPES/150mM NaCl buffer, pH7.4. Factor B was removed first in the factor B/factor H depleted plasma to prevent activation of complement alternative pathway. Plasma was run over the columns at a 1ml/min flow rate.

Depending on the batch, the plasma was run over the columns once or twice to deplete factor B and factor H fully, respectively. The depleted plasma was collected in fractions after passing

over the column(s), and fractions with the highest absorbance value at 280nm (peak fractions) were collected and pooled before freezing down to -80°C until further use.

Factor B was depleted prior to factor H, to prevent overactivation of the alternative pathway (287). Depletion of only factor H in the presence of Mg^{2+} can cause a lack of regulation of the alternative pathway, and a secondary consumption of complement C3. Therefore, removing factor B simultaneously prevents the alternative pathway C3 convertase from forming, and therefore consumption of C3. Additionally, chelating of Mg^{2+} through the addition of sodium citrate to the plasma and the affinity chromatography running buffer further prevents alternative pathway activation and consumption (287) which I confirmed in the factor H-only depleted plasma using western blotting.

Factor H depleted plasma will be henceforth described as ΔFH -plasma, factor B depleted plasma as ΔFB plasma, factor B and factor H-double depleted plasma is described as $\Delta\text{FB}/\Delta\text{FH}$ -plasma.

2.2.5. Complement factor H purification from human citrate plasma or serum

The purification of factor H was done by preparative affinity chromatography using the same method used for plasma depletion as described above. For factor H purification, the column was attached to an AKTA Pure FPLC system (GE Healthcare), washed with 5 column volumes of equilibration buffer (10mM HEPES, 150mM NaCl, 1/8 citrate 3.8%, pH 7.4) before passing serum or plasma over the column at a flow rate of 1ml/min and peak elution monitored at A280nm. The column was washed with equilibration buffer again with 5 column volumes. Factor H was eluted off the column with elution buffer (100mM Glycine, pH2.5) at a flowrate of 0.3ml/min with 3 column volumes. Factor H peak fractions were collected, dialysed into HEPES buffer (10mM HEPES, 150mM NaCl, pH 7.4) before concentration using a spin concentrator (GE Healthcare) with a molecular weight cut-off of 100kDa to remove any low molecular weight contaminants. Factor H was then aliquoted and frozen at -80°C for further use.

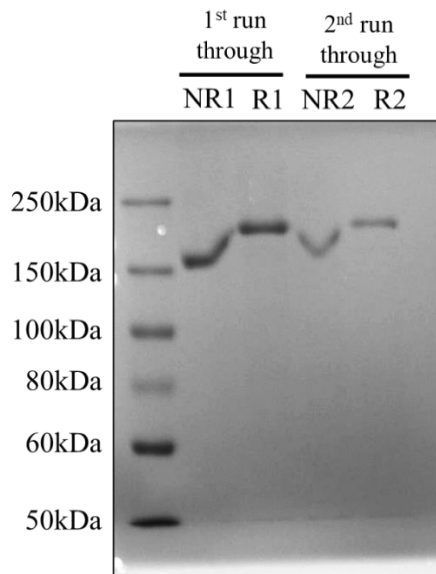


Figure 2.2. Detection of contaminants in factor H purification from human plasma. Plasma was run over a Sepharose column coupled with 35H9 antibody on the FPLC system two times, at a flow rate of 1ml/min. Factor H was eluted off with 100mM glycine, pH 2.5, before dialysing into 10mM HEPES, 150mM NaCl, pH7.5 and concentrated down with a 100kDa molecular weight cut off concentrator. Factor H from each purification run were put on a 4-12% acrylamide gel in non-reduced and reduced conditions, and stained with Coomassie blue to detect bands present in the preparations.

After analysing the Coomassie stained gel (Figure 2.2), it was confirmed that no molecular weight contaminants were present in the purified factor H preparations.

2.2.6. Activated partial thromboplastin time (aPTT) and prothrombin time (PT) in human normal plasma and complement depleted plasma

Assays that measure clotting time in patients include prothrombin time (PT) and activated partial thromboplastin time (aPTT) (288). They are primarily used for the diagnosis of haemophilia A and B, von Willebrand disease (VWD), as coagulation defects impact clotting time, as well as effects of anticoagulant treatments such as warfarin (289, 290). Plasma is preferentially prepared beforehand in citrate, as it puts coagulation in a state of stasis before re-addition of calcium (291). However, there are limitations to both assays, as they only inform on the initial stages of coagulation, and do not give spatio-temporal indications nor effects of natural anticoagulants such as protein C (291, 292). It is also not possible to determine the stability of the clot after it has finished forming (292).

Prothrombin time measures the extrinsic and common pathway of coagulation, notably thrombin, factor V, factor VII, factor X and low levels of fibrinogen (292). Prothrombin time is often used to monitor vitamin K antagonists, heparin, and antiphospholipid antibodies (288, 291).

Activated partial thromboplastin time measures the intrinsic and common pathway, notably thrombin, factor V, factor VIII, factor IX, factor X, factor XI, factor XII and fibrinogen (288, 291, 292). The aPTT assay is often employed to measure inherited and acquired factor deficiencies, and unfractionated heparin treatment (291).

The clotting time of blood is measured, after addition of certain reagents: RecombiPlastin 2G (RTF 2G, or PT reagent), Calcium Chloride 0.020M (CaCl₂) and SnythASil (APTT reagent), purchased from HemosIL. Tissue factor thromboplastin reagent, a mix of tissue factor and phospholipids is added to recalcified plasma (291). The thromboplastin reagent can be from different sources (organ and species), however it is normalised with the international sensitivity index ISI (291):

- Activated partial thromboplastin time (aPTT): reagent added to the plasma which causes activation of intrinsic pathway. The aPTT reagent contains phospholipids and negatively charged surfaces, and partial thromboplastin, a contact activator and a platelet phospholipid substitute enabling factor XII activation.
- Partial thromboplastin time (PT): reagent added to plasma causing activation of extrinsic pathway. The PT reagent contains phospholipids and tissue factor at a high concentration.

An overview of activated partial thromboplastin time assay (aPTT) assay is shown in Figure 2.3.

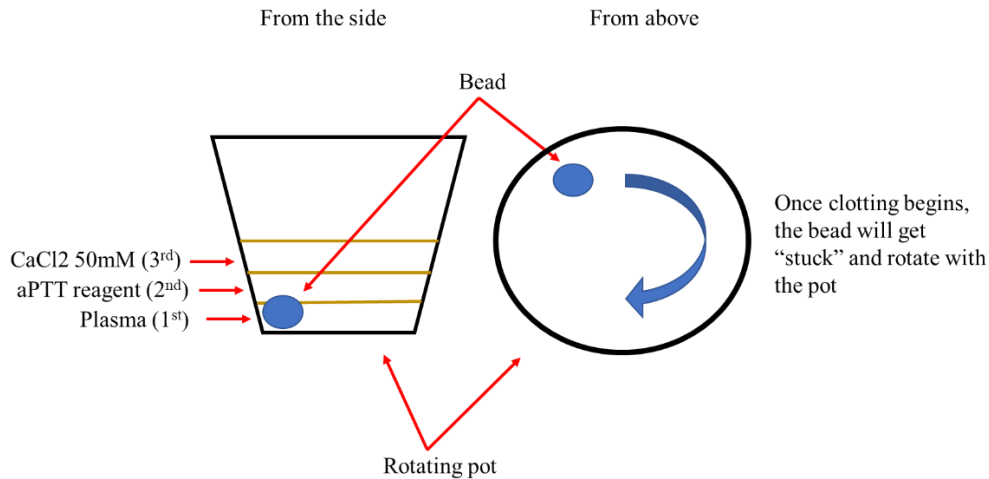


Figure 2.3. Visual representation of activated partial thromboplastin time assay (aPTT). A bead is added to a rotating pot, where it is immobile. Plasma is added for 60sec, before addition of the aPTT reagent for 120sec and finally CaCl₂ is added and time to clot measured. As clotting occurs, the bead gets stuck in the clot and starts rotating with the pot. The prothrombin assay (PT) was the same setup, except for the reagents added, which were 50µl plasma added to the pot for 60sec before addition of 100µl PT reagent and clotting time measured.

APTT and PT tests were performed on the MCS10 coagulometer (Haemostasis lab Heath), according to manufacturer's instructions, testing normal human plasma (NP), factor B depleted plasma, factor H-depleted plasma, factor H/factor B depleted plasma, and depleted plasmas with or without restored factor H.

Depleted plasma with restored factor H was performed as follows: 10µl of Factor H (1µM final in plasma) was added to 50µl of depleted plasma was added back to and left to incubate at room temperature for 30min (1/6 ratio).

Testing blocking antibodies against factor H regions was performed as follows: 10µl of antibody (Anti-SCR1-3, Anti-SCR5, Anti-SCR10-15 and Anti-SCR19, 1µM) was added to 50µl of normal human pooled plasma (NP) and incubated with plasma for 30min at room temperature (1/6 ratio).

For the aPTT measurements, 50µl of plasma are placed in the pot, left for 60 seconds before addition of 50µl of aPTT reagent. The mix is left for 2 minutes, when 50µl of 0.02M CaCl₂ is added, and the time to clot is measured from this point.

For the PT measurements, 50µl of plasma mix are placed in the pot, left for 60 seconds, before addition of 100µl of PT reagent and the time to clot is measured from this point.

2.2.7. Turbidity assays monitoring fibrin clot formation in pure protein system in the presence or absence of factor H

Turbidity based on the literature (177, 293-295), can be detected at 350nm, 405nm and 620nm. Here clot formation was measured at 405nm. Clots are formed upon cleavage of fibrinogen into fibrin by thrombin in the presence of calcium. Turbidity assays were performed in 96 well plates, and the volumes and final concentrations of the proteins are listed in table 2.4. Concentrations were kept as close to physiological as possible. All proteins were prepared in 10mM HEPES, 150mM NaCl, 5mM CaCl₂, pH7.4 buffer.

Table 2.4. Protein, volumes, and concentrations for each protein used in the pure protein fibrin turbidity assay. Factor H and thrombin are preincubated at their respective concentrations, before addition to fibrinogen, in the presence of calcium in the buffer. The clot is then left to form and monitored over 2h at 405nm.

Reagents	VOLUME	CONCENTRATION (final)
Fibrinogen	100µl	12µM
Thrombin	5µl	2.5nM
Calcium	Buffer	5mM
Factor H (or buffer control)	5µl	100nM

The final volume of the mix was 110µl per well. Each condition was tested in triplicate. When factor H was absent, 5µl of buffer was added instead.

Thrombin and factor H were prepared, vortexed and centrifuged together, and preincubated for 20min at 37°C in test tubes before addition to fibrinogen in 10mM HEPES/150mM NaCl/5mM CaCl₂ buffer, pH7.4 in a 96-well plate. The plate was swiftly placed in the plate reader, shaken for 10sec at medium speed to mix the reagents, and turbidity measured by reading absorbance at 405nm, for at least 1h at data points collected at each 60 second interval.

Results were analysed as follows: each turbidity curve represents one condition and gives information about distinct stages of fibrin clot formation.

- **Lag time:** time before increase in absorbance, corresponding to the time thrombin takes to cleave fibrinogen into fibrin, and the oligomerisation of fibrin monomers and formation of protofibrils.

- **Velocity:** slope of the increase in absorbance over time, corresponding to the rate of the reaction and the formation of fibrin fibres from protofibrils.
- **Maximal turbidity:** absorbance at endpoint of the run, corresponding to the final clot formation,

as summarised in Figure 2.4.

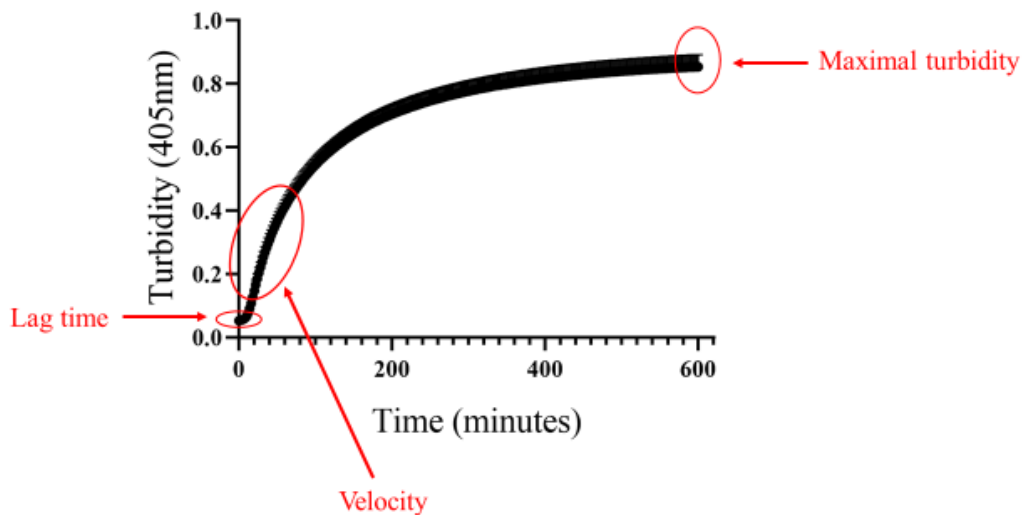


Figure 2.4. Typical representation of a turbidity assay graph. Absorbance at 405nm is measured over time, and from this the lag time, velocity and maximal turbidity are calculated. This is applicable for pure protein systems but also in plasma. The lag time corresponds to the time thrombin takes to cleave fibrinogen into fibrin, and formation of fibrin oligomers and protofibrils. The velocity is the rate of the reaction and the formation of fibres from protofibrils. The maximal turbidity is the end point of the reaction and an indicator of the fibrin clot structure.

From each of these stages, it is possible to determine the impact of factor H on the different stages of fibrin clot formation catalysed by thrombin. The half effective concentration EC50 for velocity and maximal turbidity, and the half inhibitory concentration IC50 for the lag time, were calculated for factor H using GraphPad version 8.0. When a plateau was not reached (where indicated), a top value was defined to attempt to calculate an approximate IC50 or EC50.

The purified fibrinogen preparation used was depleted of plasminogen and contained von Willebrand factor. A fibrinogen preparation depleted of von Willebrand factor was also tested in the turbidity assays. The composition of the fibrinogen preparations are shown in table 2.5.

Table 2.5. Composition of fibrinogen preparations used for the pure protein turbidity assays. Levels of factor XIII, fibrinogen and plasminogen were measured in fibrinogen 1 (plasminogen depleted) and fibrinogen 2 (plasminogen and von Willebrand factor depleted).

Protein	Fibrinogen 1 (plasminogen depleted)	Fibrinogen 2 (plasminogen and von Willebrand factor depleted)
Factor XIII	0.08 IU/ml	0.12 IU/ml
Clauss Fibrinogen	2.9g/l	2.2g/l
Plasminogen	Undetectable	Undetectable

Clauss Fibrinogen is a clinical test to measure levels of fibrinogen in plasma. Plasma is diluted to remove any effects of substances such as fibrin degradation products or heparin. High concentrations of thrombin are then added to the plasma and the ability of fibrinogen to be converted to fibrin is measured. The clotting time (fibrin formation) is interpolated from a standard curve.

2.2.8. Turbidity assays in normal plasma and factor H depleted plasma

Turbidity assays were also performed using plasma (normal or depleted). Different concentrations of calcium, and ratios of calcium buffer to plasma were tested. The aPTT and PT buffers were both tested. All reagents were prepared in 10mM HEPES, 150mM NaCl, pH7.4.

The depleted plasma was prepared beforehand, by adding 10µl of 1µM factor H to 50µl of plasma. After preincubation at 37 °C for 20min in the test tubes, 50µl of the mix was added to the respective reagent and calcium buffer, depending on the pathway analysed (Table 2.6). The plate is rapidly placed in the plate reader, shaken for 10sec at medium speed, and turbidity measured by reading absorbance at 405nm over time (varied according to the experiment and conditions).

Table 2.6. Volumes and concentrations of components for the plasma-based turbidity assays triggering either the coagulation extrinsic pathway (PPP reagent) or intrinsic pathway (aPTT) reagent. Components

for the extrinsic pathway activation were PPP reagent diluted 1/8, calcium 25mM and plasma, and components for the intrinsic pathway activation were aPTT reagent 1/8, calcium 25mM and plasma.

EXTRINSIC pathway assay	INTRINSIC pathway assay
50µl PPP reagent 1/8	50µl aPTT reagent 1/8
50µl CaCl ₂ 25mM	50µl CaCl ₂ 25mM
50µl plasma (NP, ΔFB/ΔFH, ΔFH)	50µl plasma (NP, ΔFB/ΔFH, ΔFH)

The results were analysed in the same manner as the pure protein turbidity assays indicated above.

2.2.9. Fluorescent microscopy of a fibrin clot in the presence or absence of factor H

The fluorescence experiment was performed using the same conditions as the pure protein turbidity assays, to maintain comparable conditions. For one condition tested, 2.5µl of thrombin (2.5nM final) was incubated with 2.5µl of factor H (100nM final) for 20min at 37 °C, before addition to 10µl of fluorescent fibrinogen A488 in a 1/10 ratio to unlabelled fibrinogen 12µM final. The proteins were mixed by pipetting in the Eppendorf tube, and 14µl deposited onto the glass slide in the centre of the area delineated by the Immuno-Pen. The coverslip was rapidly placed on top of the solution. The coverslip was fixed using nail varnish to prevent the coverslip from coming off and the clot from drying out (Figure 2.5).

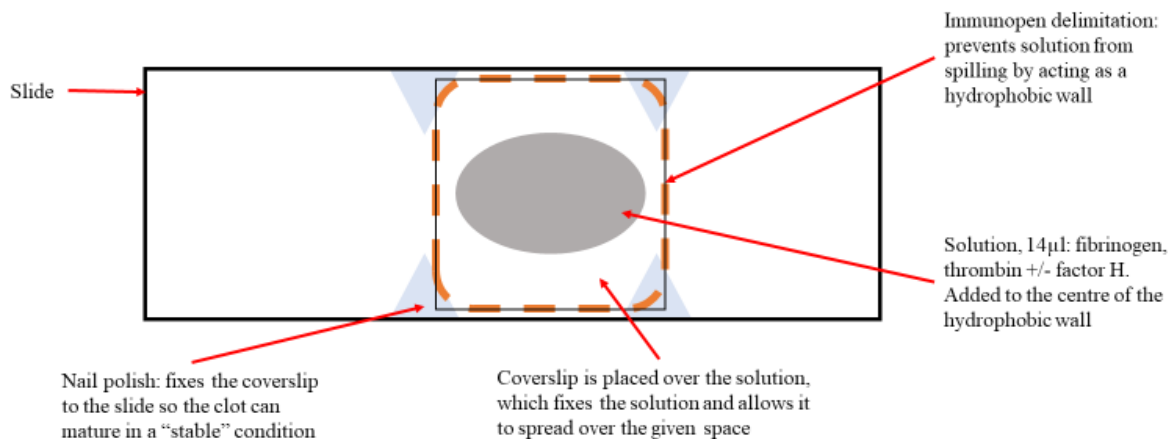


Figure 2.5. Representation of the set up for fluorescent microscopy. The area for the clot to form in is first delineated prior using an immunopen (dashed orange line). Next, the clot (grey circle) is deposited and formed between the slide (large black rectangle) and coverslip (small square in centre of slide), which is sealed with nail varnish (small grey triangles at corners of coverslip). Each element of the experiment is marked by a red arrow. The clot is left to mature for 2h at 37 °C in the dark before imaging.

The mounted slide was then placed in the dark for 2h at 37 °C to let the clot mature.

Images were then taken on the EVOS M7000 fluorescence microscope. Fibrinogen-AF488 was detected by the Green Fluorescent Protein (GFP) channel (excited at 488nm). Factor H was detected with Red Fluorescent Protein (RFP) or Texas Red (excited at 594nm). A total of 10-15 images were taken at 10X, 20X and 40X magnification covering the entire slide and fibrin clot area for each slide and n=3 slides were analysed for each condition.

For quantification analysis, 10-15 images were taken at 20X magnification, and analysed using Image J. To determine pixel intensity, which corresponds to fibre density across a fibrin clot area for each condition, each image 25 lines of 100µm length were drawn via a grid option and results averaged, therefore the average pixel density for each image. Pixel quantification was done using ImageJ, which measured the mean, minimum and maximum pixel density of a given line. In ImageJ, the scale (Analyse > Set scale) is set according to the scale on the image (150µm or 75µm for 20X and 40X respectively), a grid is then drawn across the image to trace 100µm lines accurately (Plugins > Analyse > Grid). The mean, minimum and maximum pixel densities were plotted. The minimum pixel density of each line defines the darker areas in the image that may correspond to pores or less dense fibres in the fibrin clot. The more pores present and the larger they are, the lower the minimum pixel density values.

2.2.10. Activated protein C generation assay

The activated protein C generation assay is a standard method to determine the regulation of coagulation via the protein C pathway. By combining thrombomodulin with thrombin and protein C in the presence of CaCl₂, protein C is proteolytically cleaved by thrombin (in complex with thrombomodulin) to activated protein C. The protein mix is left to incubate for 2h at 37 °C, before adding 1U/ml hirudin to inhibit thrombin enzymatic activity. Activated protein C concentration is determined by its enzymatic activity on a fixed concentration of synthetic substrate CS-Biophen 21-66 and monitored at 405nm. The synthetic substrate is a short peptide sequence imitating the cleavage site of the natural substrate of activated protein C; the chemical group pNA is cleaved off from the peptide p-Glu-Pro-Arg-pNa (CS-Biophen 21-66, Diapharma) resulting in proportional increase of absorbance at 405nm.

After optimisation of the assay by titration of each protein present in the activated protein C assay, the final set up is detailed in Table 2.7.

Table 2.7. Proteins used to perform APC assay and their corresponding volume and final concentrations used. Thrombomodulin is added to protein C, before adding and incubating with thrombin with or without factor H. The protein mix is incubated for 2h at 37°C before addition of hirudin to stop thrombin activity, and APC substrate added to read the absorbance at 405nm.

PROTEIN	VOLUME	CONCENTRATION (final)
Protein C	50µl	200nM
Thrombomodulin (or buffer control)	5µl	10nM
Thrombin	5µl	1.75nM
Factor H (or buffer control)	5µl	100nM
Calcium	Buffer	3mM
Hirudin (thrombin inhibitor)	5µl	12nM
APC substrate (CS-Biophen 21-66)	50µl	1.25mg/ml

The effect of factor H on protein C activation by thrombin-thrombomodulin or thrombin alone was monitored by combining varying concentrations of factor H (0.5-125nM) with thrombin (1.75nM), and then protein C (200nM) in the absence or presence of soluble (human) thrombomodulin (10nM) in 10mM HEPES/150mM NaCl/3mM CaCl₂ buffer, pH7.4.

In another assay, the thrombin substrate protein C (0-400nM) was titrated and incubated with thrombin (1.75nM) in the presence or absence of factor H (100nM) or soluble thrombomodulin (10nM), in 10mM HEPES/150mM NaCl/3mM CaCl₂ buffer, pH7.4.

The proteins were incubated for 2 hours at 37°C, followed by 1U/well (5µl) hirudin for 10 minutes to inhibit thrombin activity. Activated protein C was quantified by subsequent addition of activated protein C synthetic substrate (CS21(66), 1.25mg/ml) and absorbance read at 405nm for 1 hour at 60second intervals.

An activated protein C standard curve was generated to deduce the concentration of activated protein C. From there the Michaelis-Menten KM constant was calculated in the protein C titration in presence and absence of factor H with the GraphPad version8.0.

The dissociation constant k_d was calculated for the factor H titration by taking the concentration of factor H that reached half maximum velocity in the presence and absence of thrombomodulin.

2.2.11. Thrombomodulin EGF456-ST domain plasmid vector design

The mutations in aHUS present on thrombomodulin that affected factor H binding and activity were situated in the serine/threonine rich domain and lectin like domain. Therefore, it was interesting to determine the binding affinity of these regions to factor H, and whether the binding of factor H to the serine-threonine rich domain affected thrombomodulin regulatory function. Therefore, the EGF456-serine/threonine rich domain was designed and expressed to study this.

The plasmid used as a vector to carry the thrombomodulin variants was the pcDNA3.1+C-6HIS plasmid, 5.4kb from Thermo Fisher. The vector carries a 6HIS tag allowing the protein to be purified and detect them in other assays. The plasmid is specifically designed for transfections into mammalian cells and contains an Ampicillin Resistant (AmpR) and Neomycin Resistant (NeoR) genes allowing selection of the stable cell lines (when growing the plasmids in bacteria). The pUC origin of replication (pUC Ori and f1 ori) was used to achieve expression of as many copies as possible. The CMV promoter was present as it allows strong mammalian gene expression. Plasmids contained the native signal peptide of thrombomodulin. The MCS, or multiple cloning site, was where the gene sequences were inserted, which is followed by the 6HIS tag and a stop codon. The Kozak sequence was added to enhance translation of the mRNA for each protein. The thrombomodulin signal peptide allowed the recombinant proteins to be excreted out of the cells and into the media, as the transmembrane domain was not included in the sequence.

Plasmid pcDNA3.1+6HIS is shown in Figure 2.6.

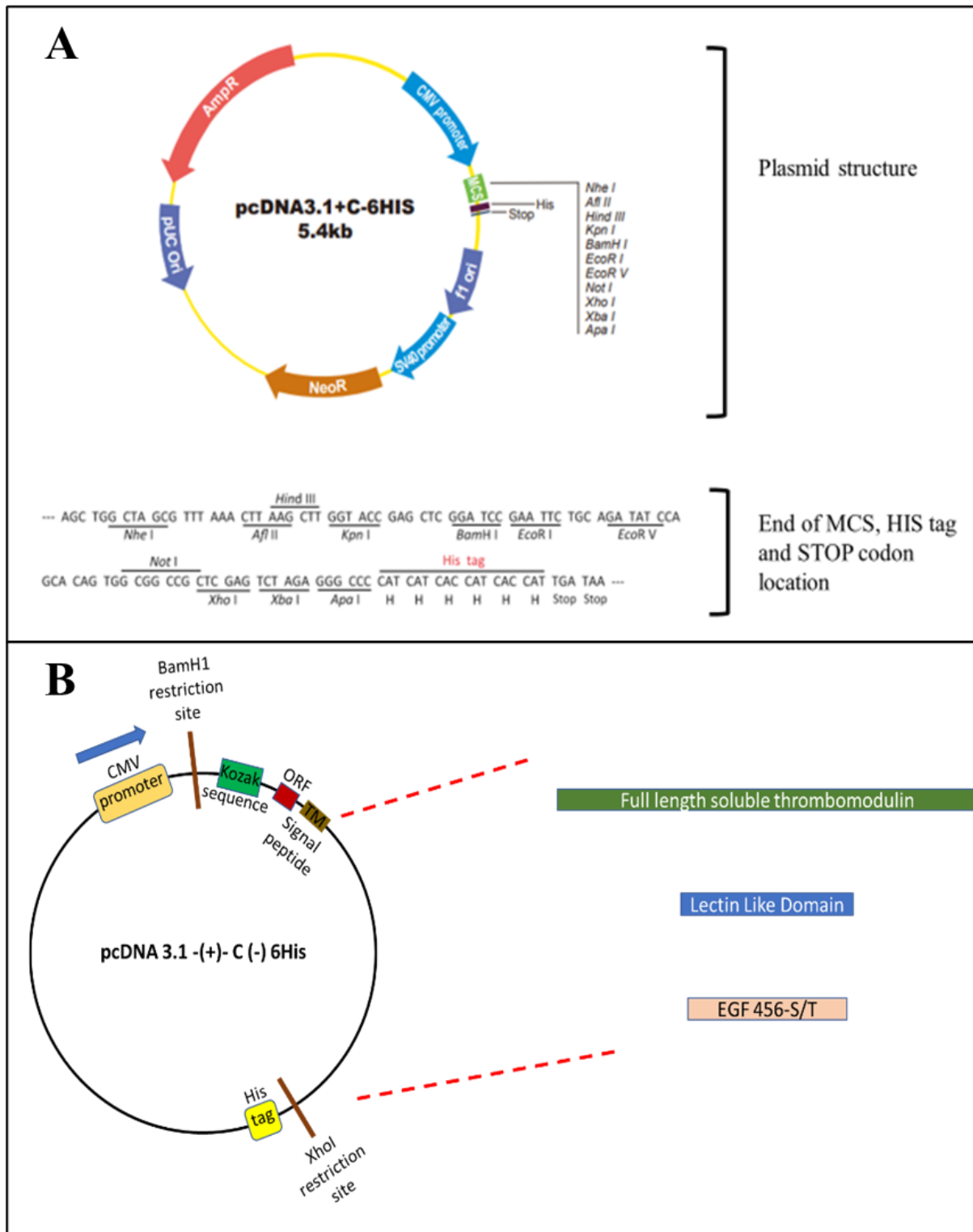


Figure 2.6. Plasmid pcDNA3.1+6HIS design used as a vector for transport and transfection of the thrombomodulin constructs. (A) Plasmid illustration with all the key regions for optimal protein expression. (B) Genes for the constructs full length soluble thrombomodulin, soluble lectin like domain, and soluble EGF-like456 + S/T rich domain, were inserted into the multiple cloning site between BamH1 and Xho1. The plasmid contained a CMV promoter, Ampicillin resistant gene and a 6HIS tag for the protein of interest to be expressed. An additional

Kozak sequence was added to further enhance expression. The ORF was present followed by the endogenous signal peptide of thrombomodulin and finally the sequence of interest.

The full-length soluble form of thrombomodulin (sTM) was from amino acid Pro20 to Ser515, the lectin-like domain (sLLD) was from amino acid Pro20 to Phe169, and the EGF456-Serine/Threonine rich domain (sEGF456-S/T) was from Val365 to Ser515 (Appendix Figure A2.2). The sequence for the full-length form was stopped at the end of the Serine/Threonine rich domain, Ser515, and the transmembrane and intracellular domains were not included to render the protein soluble and excreted out of the cell.

The expression vectors were commercially obtained from Genscript Ltd. The bacterial stab was provided in the *E.coli* strain TOPO10 (upon receipt), and amplified in the same *E.coli* strain in-house. The plasmid was purified using maxi-prep from Qiagen and then transiently transfected into HEK293 cells (https://www.lgcstandards-atcc.org/products/all/crl-1573.aspx?geo_country=gb#) using Turbofect system from Thermo Scientific.

2.2.11.1. Plasmid transformation and expansion in E.coli

Transformed TOP10 *E.coli* bacteria (bacterial stab) were spread on Agar plates (15g/l agar, 10g/l tryptone, 5g/l yeast extract, 5g/l NaCl) supplemented with 1/500 Ampicillin overnight at 37 °C. One colony of each was picked and incubated in a LB Broth (10g/l Tryptone, 5g/l yeast extract, 5g/l NaCl, 0.6g/l inert binder) supplemented with 1/500 Ampicillin, for 8h at 37 °C on a shaker (total volume was), of which 500µl were then added to 250ml of LB Broth supplemented with 1/500 Ampicillin, overnight at 37 °C on a shaker. The bacterial cultures were spun down at 6000xg for 15min at 4 °C. Plasmid purification was done according to manufacturer's protocol (Qiagen, reference 12362). After air-drying the plasmid pellet and adding TE Buffer (10mM Tris, 1mM EDTA, pH8), the absorbance was measured at 260nm to determine DNA concentration and levels of contamination.

2.2.11.2. Cell culture -maintenance of HEK293 cells

Human embryonic kidney cells (HEK293) were cultured and grown in T75 flasks in minimum essential medium eagle (MEME) supplemented with 10% foetal bovine serum (FBS), 2mM L-glutamine and 1U/ml of penicillin/streptomycin. Media was changed every 3 days and cells

passed once a week (a 1 in 10 dilution of cells was done for passaging). The maximum passage number was set at 30.

2.2.11.3. Transient transfection

The cells were seeded fresh before the transfection in T175 flasks and left to reach 70% confluency (48hours). Cells were washed once in sterile PBS and resuspended in reduced serum medium (Opti-MEM is a chemically defined, low protein Minimum Essential Medium allowing a reduction of Fetal Bovine Serum supplementation by 50% without affecting growth or morphology). A master-mix of 18 μ g of soluble thrombomodulin plasmid with 60 μ l of TurboFect reagent was prepared according to manufacturer's protocol (Thermo Scientific, reference R0533), in 3ml of reduced serum medium, and added to the cells.

2.2.11.4. Protein purification from cell culture media

After 48 hours, the media of the transfected cells was collected and spun down at 1500g for 5min. The supernatant was collected, transferred into concentrator columns 10,000Da molecular weight cut-off, and spun down to 200 μ l (75 times concentrated). The concentrated media was flowed over a HisPur™ Ni-NTA Spin column. Protein purification was done following manufacturer's protocol in non-denaturing conditions (Thermo Scientific, reference 88226). The column was equilibrated to room temperature and with equilibration buffer (PBS, imidazole 25mM, pH 7.4) before incubation of the samples in the same equilibration buffer, which were left to adhere to the column for 30min at 4°C. The column was then washed with wash buffer (PBS, imidazole 25mM, pH 7.4) three times by centrifuging at 700xg, for 2min. Proteins were eluted with elution buffer (PBS, imidazole 250mM, pH 7.4) three times by centrifuging at 700g for 2min.

Each flow through for each step was preserved to run on a Coomassie stain to determine purity. The column resin was regenerated using MES buffer (20mM 2-(N-morpholine)-ethane sulfonic acid, 0.1M sodium chloride, pH 5), and stored in ethanol 20%.

2.2.12. Coomassie staining

Protein concentrate was loaded onto 4-12% gradient gels (ThermoScientific, reference NW04125BOX), in reducing (sample reducing agent 5X and LDS Sample Buffer 2X) or non-reducing buffers (LDS Sample Buffer 2X). The gel was left to run for 2h at 120V (time and voltage were optimised), before being placed in Coomassie stain overnight at room temperature. De-staining of the gel was done the following day at room temperature, with distilled water changed every 1h for 3h. The gel was imaged using Syngene G:BOX XT4 (Syngene).

2.2.13. Western blotting of recombinant thrombomodulin constructs

For the dot blot, 2-3 μ l of concentrated media were dotted onto a nitrocellulose membrane and blocked in milk 5% PBS, 0.01% Tween overnight at room temperature. The membrane was incubated with a polyclonal sheep anti-thrombomodulin in PBS, 0.01% Tween (1 μ g/ml) for 1hour at room temperature and then a secondary anti-sheep HRP-conjugated antibody in PBS, 0.01% Tween (0.02 μ g/ml) for 1hour at room temperature. Three washes of 5min in 5ml PBS, 0.01% Tween were performed after incubation of primary, and then secondary antibodies. To develop the dot blot, the chemiluminescent HRP substrate Pierce ECL was added to the membrane for 2-3min before exposure using a Syngene G:BOX XT4 (Syngene).

For the western blot, 1-10 μ g of protein (protocol was optimised) with 20 μ l of loading (non-reducing) buffer were loaded onto a 4-12% Tris Glycine gel and ran for 1h30 at 150V using 1X MES running buffer (50mM MES, 50mM Tris Base, 0.1% SDS, 1mM EDTA, pH7.3) in a mini-gel tank. The proteins were then transferred onto nitrocellulose or Polyvinylidene difluoride (PVDF) membranes for 1 hour at 90V in 1X transfer buffer (25mM Tris-HCl pH7.6, 192mM glycine, 20% methanol, 0.03% sodium dodecyl sulphate (SDS)). The membrane was blocked in 5% milk in PBS, 0.01% Tween for 2h, and incubated overnight at 4 $^{\circ}$ C with monoclonal antibody in PBST 0.05% (5ml total volume). Each antibody at their respective concentration is shown in table 2.8.

Table 2.8. Primary antibodies and their concentrations used to detect their respective proteins. Antibodies names and specificity are indicated on the left hand side, and the working concentrations are indicated on the right.

Antibody	Concentration
35H9 (mouse)	1µg/ml
Polyclonal anti-factor H (rabbit)	1µg/ml
Polyclonal anti-thrombomodulin (sheep)	1µg/ml
Anti-lectin like domain thrombomodulin (mouse)	1µg/ml
Anti-EGF5 thrombomodulin (mouse)	1µg/ml

The next day the membrane was washed 3 times 10min with 5ml of PBS, 0.01% Tween and incubated with the horseradish peroxidase (HRP)-conjugated secondary antibody 1/5000 (anti-sheep, anti-mouse or anti-rat, all 0.16µg/ml final, 10ml total volume) in milk 2.5% PBS, 0.01% Tween for 1 hour at room temperature on a roller. The membrane was washed 3 times for 10min in 5ml PBS, 0.01% Tween before addition of enhanced chemiluminescence (ECL) substrate for 3 minutes and the membrane was read using using a Syngene G:BOX XT4 (Syngene).

2.2.14. Enzyme-linked immunosorbent assay for thrombomodulin-factor H complex detection

Either proteins or capture antibodies were coated onto polystyrene wells in 50µl of carbonate buffer, pH 9.6, for two hours at 37°C, then blocked overnight at 4°C, with 200µl of 2.5% milk in phosphate buffered saline containing 0.01% Tween (PBS, 0.01% Tween). In the case of capture antibodies (anti-thrombomodulin antibodies anti-lectin like domain, anti-EGF12, anti-EGF5, anti-EGF6, or anti-factor H antibodies anti-SCR1-2, anti-SCR5, anti-SCR10-15 and anti-SCR20), proteins (thrombomodulin or factor H) were captured at 2.5µg/ml or 5µg/ml in PBS, 0.01% Tween and incubated for 1h at 37°C. The binding ligand was then added at 5µg/ml for 1h at 37°C and then were detected using polyclonal antibodies at 5µg/ml in PBS, 0.01% Tween for 1h at 37°C, before addition of 50µl secondary HRP-conjugated antibody for detection, diluted 1/5000 (0.16µg/ml) or 1/10000 (0.08µg/ml) in milk 2.5% PBS, 0.01% Tween. HRP substrate OPD was added and the reaction was stopped using 10% H₂SO₄, before reading the absorbance at 492nm. A list of antibodies used in the enzyme-linked immunosorbent assay for thrombomodulin, factor H and thrombin is shown in Table 2.9.

Table 2.9. List of capture antibodies or absorbed proteins used in the enzyme-linked immunosorbent assay against thrombomodulin, factor H and thrombin. Coating proteins and antibodies with their specificities are listed on the left hand side (thrombomodulin and anti-thrombomodulin antibody coat, factor H and anti-factor H antibody coat, or thrombin coat) and working concentrations for each is listed on the right.

Capture antibody or ligand protein or analyte	Concentration
Soluble thrombomodulin	2.5µg/ml
Anti-thrombomodulin monoclonal antibody against lectin like domain (mouse)	10µg/ml
Anti-thrombomodulin monoclonal antibody against EGF-like 1-2 (mouse)	10µg/ml
Anti-thrombomodulin monoclonal antibody against EGF-like 5 (mouse)	10µg/ml
Anti-thrombomodulin monoclonal antibody against EGF-like 6 (rat)	10µg/ml
Anti-thrombomodulin polyclonal antibody (sheep)	10µg/ml
Complement factor H	10µg/ml (ligand) or 2.5µg/ml (captured protein)
Anti-factor H monoclonal antibody against SCR 1-3 (35H9, mouse)	5µg/ml
Anti-factor H monoclonal antibody against SCR 5 (ox24, mouse)	5µg/ml
Anti-factor H monoclonal antibody against SCR 10-15	5µg/ml
Anti-factor H polyclonal antibody (rabbit)	5µg/ml
Thrombin inactive (PPACK inactivated)	5µg/ml
Anti-thrombin polyclonal antibody (sheep)	5µg/ml

2.2.15. Surface Plasmon Resonance (SPR) binding interaction and affinity analysis

All experiments were performed on a Biacore T200 equipment using Series S Sensor Chip CM5. The surface of the chip has a carboxymethylated dextran matrix, and all proteins were attached to the dextran matrix surface using amine coupling (NHS/EDC) according to manufacturer protocol. The running buffer used was 10mM HEPES, 150mM NaCl, 0.05% P20 surfactant, pH 7.4 0.22µm sterile filtered. Regeneration of the surface was done using 10mM Acetate/1M NaCl buffer, pH4.5, after each dissociation.

Factor H/thrombomodulin interaction analysis: Domain specific thrombomodulin antibodies were immobilised to a level of 4000 resonance units (4000RU) to each flow cell (reference cell was flow cell 1) and soluble recombinant thrombomodulin (1µM) was captured to each antibody indirectly via the respective lectin like domain, EGF1-2 or EGF6. Thrombomodulin capture was performed at a flow rate of 20µl/min for 120 seconds and repeated twice or until binding curve saturated and stable binding was observed. As a control surface C3b was immobilised using amine coupling to a level of 1500RU on an adjacent flow. Full length factor H and short recombinant factor H constructs comprising SCR1-5, SCR6-8, SCR8-15, SCR15-18, SCR18-20 were tested for binding to domain-specific captured thrombomodulin. The flow over each flow cells is shown below (Figure 2.7).

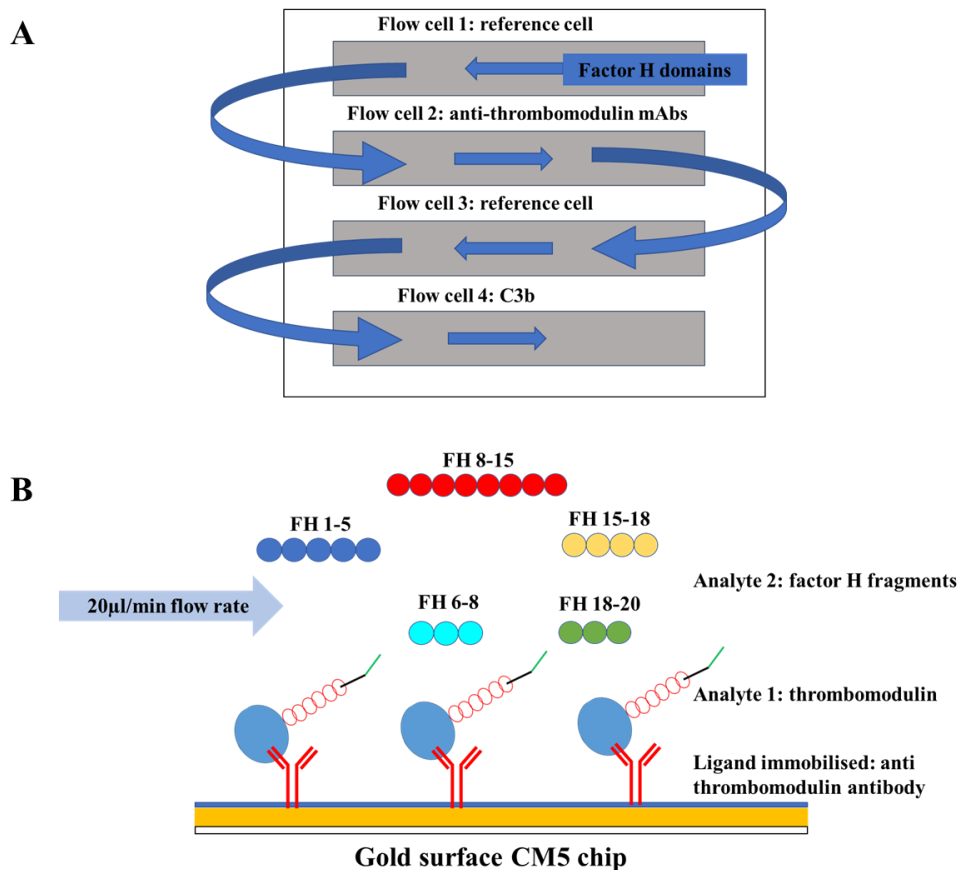


Figure 2.7. Factor H fragments flowed over thrombomodulin captured via monoclonal domain-specific antibodies. A) Anti-thrombomodulin antibodies (anti-lectin like domain, anti-EGF12, and anti-EGF6) were attached to the surface of flow cell with a reference flow cell as control and binding with factor H compared to its binding to C3b immobilised on an adjacent flow cell flow cell 4. B) Thrombomodulin was captured with the antibodies before flowing over factor H constructs to determine binding. Flow cell 1 was used as reference flow cell. Flow rate was 20µl/min.

Single injections of each 2µM factor H constructs were flowed at 10µl/min for 120sec association followed by 120sec dissociation to assess binding. Kinetics and affinity was determined by flowing a concentration series of factor H constructs (0.0094-10µM, 8 concentrations) at a flow rate of 20µl/min, with an association time of 120sec and a dissociation time of 180sec.

Factor H/thrombin and factor H/fibrinogen interaction analysis: PPACK-thrombin was immobilised to a level of 1000RU on flow cell 2 (reference cell was flow cell 1). Fibrinogen was immobilised to a level of 10000RU on adjacent flow cell 4 (reference cell was flow cell 3). Full length factor H (100nM) and short recombinant factor H constructs SCR1-5, SCR6-8,

SCR8-15, SCR15-18, SCR18-20 (100nM) were flowed and tested for binding to thrombin or fibrinogen (Figure 2.8).

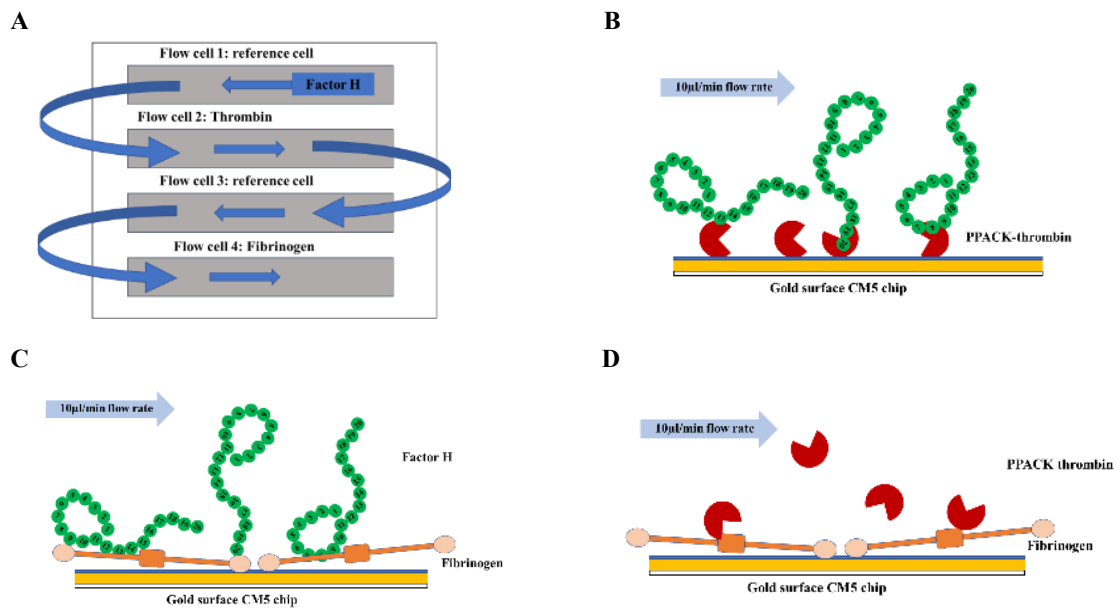


Figure 2.8. Factor H or thrombin flowed over thrombin and fibrinogen to determine binding affinity. A) Thrombin was captured on flow cell 2 and fibrinogen was captured on flow cell 4. B) Set up on flow cell 2 to determine the binding interaction between thrombin and factor H, C) set up on flow cell 4 to determine the binding interaction between fibrinogen and factor H and D) set up on flow cell 4 to determine the binding interaction between fibrinogen and thrombin (control). Flow cell 1 was used as reference flow cell. Flow rate was 20µl/min.

Single injections of 100nM factor H were flowed at 20µl/min for 120 seconds association followed by 120sec dissociation. Kinetics and affinity were determined by preparing and flowing a concentration series of factor H (3.125-100nM, 8 concentrations) at a flow rate of 30µl/min, with an association time of 120sec and a dissociation time of 180sec.

2.2.16. Molecular modelling

To look at the binding interaction between thrombin, thrombomodulin and factor H, it was important to have a full-length model of each protein.

Thrombin has a light and heavy chain and exerts its enzymatic activity and regulatory function through the heavy chain. Thrombin is allosterically altered by its binding partner

thrombomodulin, therefore thrombin's binding partners were also noted (Table 2.10), to analyse the binding of factor H on thrombin depending on the presence of other proteins such as thrombomodulin (which also binds factor H) or PPACK which inhibits thrombin's active site.

Table 2.10. Thrombin structure. List of thrombin full length structure pdb files, with their corresponding pdb ID, amino acid sequence, method of crystallisation (solution NMR, X-ray diffraction or solution scattering), with resolution and their respective binding partners.

Name	aa sequence	Technique	Resolution	Binding partner(s)
aSHH	1-14 and 16-245	Xray diffraction	1.55A	slow form, PPACK
1SG8	1-14 and 16-245	Xray diffraction	2.30A	fast form, Na ⁺ , C8H15NO6
1SGI	1-15 and 16-246	Xray diffraction	2.30A	slow form, C8H15NO6
1E0F	1-15 and 16-247	Xray diffraction	3.10A	haemadin (exosite II inhibitor)
1TB6	1-14 and 16-247	Xray diffraction	1.50A	Antithrombin II, GAGs (15 ligands)
1XMN	1-14 and 16-246	Xray diffraction	1.85A	heparin ; 9 ligands
1YPG	1-14 and 16-245	Xray diffraction	1.80A	hirudin
1DX5	1-15 and 16-247	Xray diffraction	2.30A	thrombomodulin; 5 ligands
1HLT	1-14 and 16-244	Xray diffraction	3.0A	EGF5 of TM; 1 ligand
1FPH	1-15 and 16-247	Xray diffraction	2.5A	FpA; hirudin; ligands
2A45	1-15 and 16-246	Xray diffraction	3.65A	E region fibrin, alpha beta and gamma chain
4DT7	1-15 and 16-247	Xray diffraction	1.9A	active site of protein C
1VR1	1-14 and 16-243	Xray diffraction	1.90A	hirudin
1EGT				
3GIS	1-15 and 16-247	Xray diffraction	2.40A	TM

Only some SCR domains of factor H have been crystallised individually, as the protein is too large and extremely flexible to crystallise the full length (62, 285). Solution scattering has been done on the whole protein (28), however the resolution of solution scattering is very high, and the models not very reliable. Therefore, in this study, homology modelling was performed on the regions of factor H without NMR or X-ray diffraction to obtain a model of the full-length protein.

Each PDB file for factor H obtained with solution NMR or X-ray diffraction were listed (Table 2.11), and the missing regions determined.

Table 2.11. Factor H structure. List of factor H region structure pdb files, with their corresponding domain (SCR), pdb name, amino acid sequence for each structure and method of crystallisation (solution NMR, X-ray diffraction or solution scattering), with resolution and their respective binding partners.

Domain	Name	aa sequence	Technique	Resolution	Binding partner(s)
SCR 1-2	2RLP	20-142	solution NMR		none
SCR2-3	2RLQ	84-206	solution NMR		none
SCR1-4	5O35		Xray diffraction	4.20A	C3; C8H15NO6
	5O32		Xray diffraction	4.21A	C3 ; Factor I; small molecules
	2WII	3-247	Xray diffraction	2.70A	C3b beta and alpha chain; small molecules
SCR1-5	2QFG	17-328	solution scattering		none
SCR4-5	4MUC	205-329	Xray diffraction	2.90A	SO4
SCR6-7	4AYD	321-443	Xray diffraction	2.40A	Factor H binding protein; C2H6O2
	4AYE	321-443	Xray diffraction	2.80A	Factor H binding protein; C2H6O2
	4AYI	325-443	Xray diffraction	2.31A	lipoprotein GNA 1870; C2H6O2
	4AYM	325-443	Xray diffraction	3.0A	factor H binding protein
	2W80	321-443	Xray diffraction	2.35A	factor H binding protein
	2W81	322-443	Xray diffraction	2.35A	factor H binding protein
SCR6-8	2IC4 (mutation)	320-506	solution scattering		none
	2UWN	320-506	Xray diffraction	2.35A	L-peptide linking modif residue; SO4; C3H8O3; Cl;C12H22O35S8
	2V8E	320-506	Xray diffraction	2.50A	L-peptide linking modif residue; SO4; C3H8O3; Cl;C12H22O35S8
SCR7	2JGX (mutation)	386-444	solution NMR		none
	2JGW	386-444	solution NMR		none
SCR9	4K12	508-567	Xray diffraction	1.08A	choline binding chain A

SCR10-11	4B2R	566-687	solution NMR		none
SCR11-12	4B2S	627-747	solution NMR		none
SCR12-13	2KMS	690-804	solution NMR		none
SCR 15	1HFI	866-927	solution NMR		none
SCR16	1HCC	927-985	solution NMR		none
SCR 15-16	1HFH	866-985	solution NMR		none
SCR16-20	2QFH	922 - 1254	solution scattering		none
SCR18-20	3SWO	1046-1231	Xray diffraction	1.80A	PO4 ; C3H8O3
SCR19-20	2G7I	1109-1230	Xray diffraction	1.75A	none
	2BZM	1107-1231	solution NMR		none
	3R62 (mutation)	1107-1231	Xray diffraction	1.52A	C3H8O3
	3KZJ (mutation)	1109-1230	Xray diffraction	1.65A	SO4
	3KXV (mutation)	1109-1230	Xray diffraction	2.00A	SO4
	2XQW (mutation)	1109-1230	Xray diffraction	2.31A	C3
	4ZH1	1104-1228	Xray diffraction	2.24A	C3 ; small molecules
	4ONT	1106-1231	Xray diffraction	2.15A	C3d fragment; small molecules
	4J38	1106-1228	Xray diffraction	2.83A	outer surface protein E; SO4
	5NBQ	1104-1230	Xray diffraction	3.18A	C3; outer surface protein E
	3OXU		Xray diffraction	2.10A	C3; glycerol
SCR20	5WTB	1206-1222	Xray diffraction	3.30A	ser-asp repeat cont. protein E
SCR1-20	3GAU	1-1213	solution scattering		none
	3GAV	1-1213	solution scattering		none
	3GAW	1-1213	solution scattering		none

Homology modelling

First a Basic Local Alignment Search Tool, or BLAST search was performed to determine which protein sequence available in PDB is the most similar, or homolog to the protein in question. In the program Molecular Operating Environment (MOE), the fasta sequences of the protein of interest and the template PDB file was uploaded from BLAST, before construction of the homology model.

While structures for most SCRs in factor H have been resolved, no structure (obtained by NMR or X-ray diffraction) existed currently for SCR14 and SCR17 of factor H. Therefore, homology modelling was required on these regions to obtain a full-length structure. Although there was a structure based on solution scattering for SCR16-20, the resolution was too low.

A PSI-BLAST in PDB was performed on the sequence for SCR14 and SCR17 from factor H. Only NMR or X-ray diffraction structures are considered, and the parameters to take into account are the lowest E-value and the highest percentage identity.

The fasta sequence of the region to model, and the PDB file for the most homolog protein was uploaded into MOE. To determine a homology model, proteins were superimposed or aligned (positioning a group of structures in a 3D space). The root mean square deviation, RMSD, was determined. The forcefield used was the assisted model building and energy refinement, or AMBER (specifically AMBER12:EHT).

A total of 10 models were generated, with the final 11th one being the homology model. Once the model was determined, the fasta sequence for the protein of interest was uploaded again, along with the template protein. From there, the model, the fasta sequence of the protein of interest, and the template protein sequence were aligned. The residues that were aligned with the template were constrained and a new homology model was built. Again 10 models were generated, and the 11th was the final homology model, however this time the final model was refined and set as “fine”, and the RMS gradient at 0.1.

Once the model was determined, the geometry of the structure is analysed based on the Ramachandran plot, which determines the secondary structures of the peptides within the homology model.

Protein-protein docking analysis

All molecular modelling studies were performed on a Viglen GenieIntel@CoreTMi7-3770 vPro CPU@ 3.40 GHz × 8 running Ubuntu 14.04. Molecular Operating Environment 2014 was used for the homology model building, and Molecular Operating Environment (MOE) 2019.10 for the “protein-protein docking” program. The Protein Data Bank (PDB, www.rcsb.org) was accessed to upload available PDB files of crystal structures.

The following PDB files were uploaded for protein-protein docking analysis:

- PDB 1DX5: Thrombomodulin EGF456/thrombin complex
- PDB 1YPG: thrombin complexed to hirudin
- PDB 2G7I: factor H SCR 19-20
- full length factor H model resulting from homology model

The proteins of interest were selected for binding interaction analysis as follows:

- Thrombin AND factor H SCR19-20
- Thrombin AND full-length factor H
- Thrombomodulin EGF456 AND factor SCR19-20
- Thrombomodulin EGF456 AND full-length factor H
- Thrombomodulin EGF456/thrombin complex AND factor H SCR19-20
- Thrombomodulin EGF456/thrombin complex AND full-length factor H

MOE generates a conformational search and lists all the possible interactions, from the highest to the lowest energy score (the lowest binding energy, kcal/mol). The best scores were analysed, and the binding sites were analysed by plotting which amino acids were involved in the interaction. The top best scores, therefore the interactions requiring the lowest energy, were analysed and the interaction corresponding most to the experimental data was selected as a potential model.

2.2.17. Statistical methods

All statistical analyses were performed in GraphPad Prims version 8. Normality and Lognormality tests were performed when appropriate to determine whether the data followed a Gaussian normal distribution. Depending on this, a Mann Whitney U test was performed (not normal distribution) or a Welch's t-test (normal distribution). For the reagent titrations and to determine concentration dependent effects, nonparametric Spearman correlation was computed. All data is presented as mean \pm SD (standard deviation) or median with interquartile range. All data points were collected in triplicate (n=3) or more and each experiment repeated at least three times.

Chapter 3: Factor H effect on fibrin clot generation in plasma-based turbidity assays

I first confirmed the effect of thrombin on factor H's regulation of haemolysis (Figure 3.1) and showed no impact on factor H activity. I tested the presence of physiological concentrations of active thrombin (10nM), supraphysiological concentration inactive (PPACK) and active thrombin (500nM).

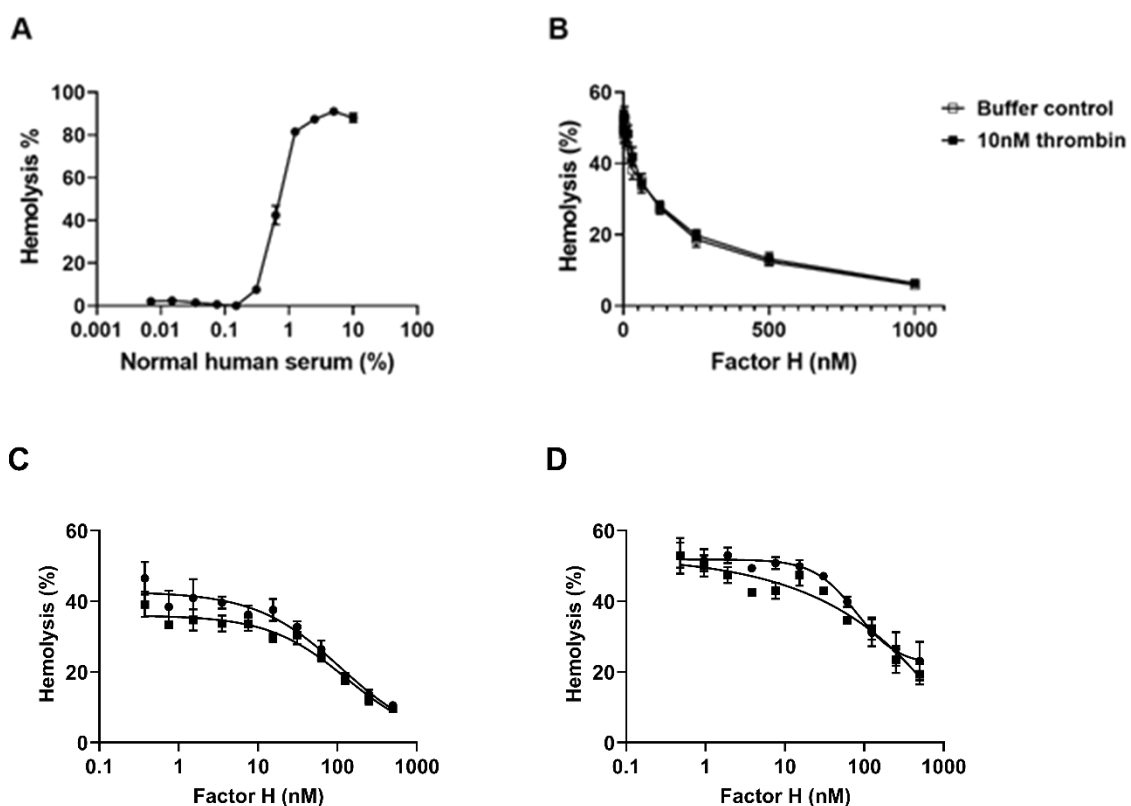


Figure 3.1. Thrombin does not impact complement haemolysis regulation by factor H in serum. (A) Normal human serum was titrated (0.007-10%) and concentration corresponding to 50% haemolysis of antibody-coated sheep erythrocytes was selected (1.25%). (B) Factor H was titrated (3.25-1000nM) into normal human serum in presence or absence of (B) 10nM active thrombin, (C) 500nM of PPACK inactive thrombin and (D) 500nM of active thrombin. There was no difference in the IC₅₀ in absence and presence of 10nM thrombin. Presence of 500nM PPACK inactive thrombin and active thrombin do not significantly affect the IC₅₀. Results show mean +/-SD (n=3). Welch's t-test was performed on the physiological concentration of thrombin, Mann-Whitney U test on the supraphysiological thrombin concentrations (PPACK inactive and active). Experiment representative of three independent experiments.

Previous data generated by my supervisor Dr Meike Heurich before the start of the PhD demonstrated that there was no obvious effect of thrombin on factor H and I was able to conclude that thrombin, at physiological concentrations ($IC_{50}=206.1\pm 58.58\text{nM}$ in the absence and $IC_{50}=191.0\pm 91.92\text{nM}$ in the presence of thrombin, p-value 0.82), did not interfere with factor H's regulation of haemolysis. Supraphysiological concentrations of PPACK inactive ($IC_{50}=85.75\pm 24.64\text{nM}$ in absence and $IC_{50}=120.7\pm 37.4\text{nM}$ in presence, p-value 0.4, Figure 3.1C) and active ($IC_{50}=78.73\pm 20.97\text{nM}$ in absence and $IC_{50}=115.2\pm 25.73\text{nM}$ in presence, p-value 0.8, Figure 3.1D) thrombin were tested also, and a small but non-significant difference was seen in presence of thrombin. However, the concentration of thrombin tested, 500nM, would never occur in physiological settings.

From this I concluded that thrombin did not affect factor H or its regulatory activity in the complement system. Therefore, I wanted to investigate the functional effect of factor H interaction with thrombin, first on clot formation.

Further previous research by Dr Heurich demonstrated that factor H knockout mice ($CFH^{-/-}$) had increased tail bleeding time compared wild type mice. The impact of the absence of factor H in murine plasma was further analysed by quantifying coagulation parameters relevant to coagulation and thrombin generation (thrombin-antithrombin complex, TAT) as well as anticoagulation (soluble thrombomodulin, sTM; protein C, PC).

3.1. Absence of factor H and complement C3 increase levels of soluble thrombomodulin in mice

Tail bleeding assays performed in the laboratory previously demonstrated an increase in bleeding time in both $CFH^{-/-}$ and $C3^{-/-}$ mice compared to their wild type counterparts (Appendix A3.1). The colony was discontinued therefore I was not able to obtain data of my own, furthermore the number of repeats or mice was sufficient to perform statistical analysis. Coagulation biomarkers in murine plasma were quantified to determine the coagulation profile of these mice using ELISA kits for thrombin-antithrombin complexes (TAT, coagulation components), soluble thrombomodulin, and activated protein C (sTM and APC, anticoagulation components) (Figure 3.2).

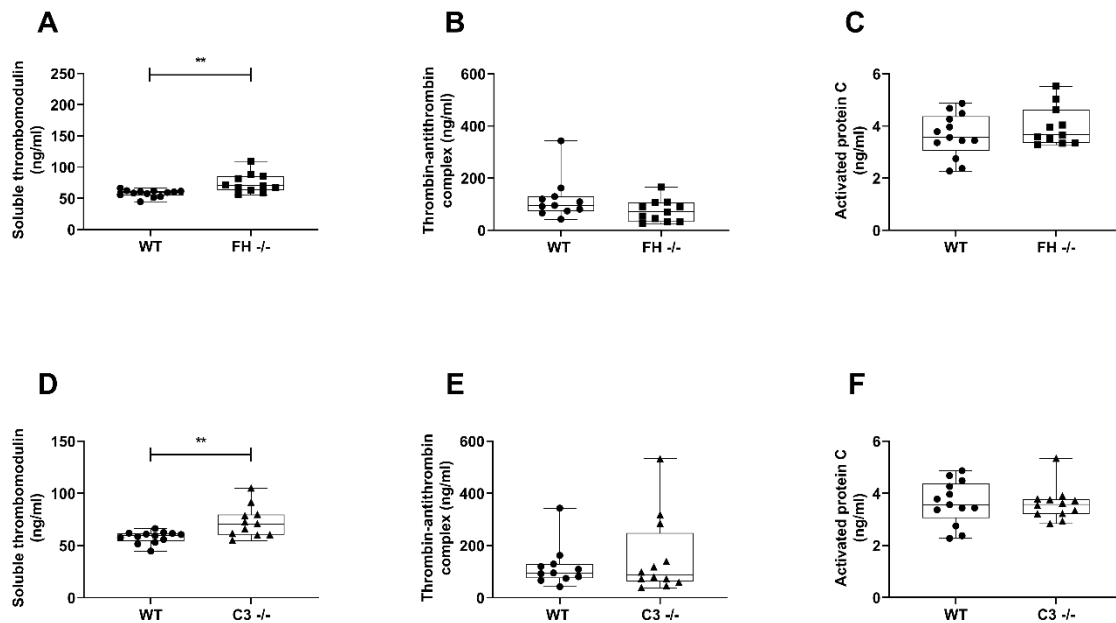


Figure 3.2. Quantification of murine plasma soluble thrombomodulin, thrombin-antithrombin complex and activated protein C in *CFH*^{-/-} and *C3*^{-/-} mice. Whole blood was obtained by cardiac puncture. (A, D) Soluble thrombomodulin, (B, E), thrombin-antithrombin complex and (C, F) protein C was quantified in murine plasma of *CFH*^{-/-} (■) and *C3*^{-/-} (▲) compared to wild-type (WT) (●). (A) Soluble thrombomodulin was increased in *CFH*^{-/-} and (D) *C3*^{-/-} compared to wild type. Thrombin-antithrombin complex was not statistically significant different for (B) *CFH*^{-/-} and (E) *C3*^{-/-} compared to WT. Activated protein C did not differ significantly for (C) *CFH*^{-/-} nor (F) *C3*^{-/-}, compared to WT. Data are expressed as mean±SD, n=13 for WT, n=11 for *CFH*^{-/-} and n=12 for *C3*^{-/-} and analysed using nonparametric Mann–Whitney test.

Thrombin-antithrombin complexes are indicative of the concentration of thrombin and coagulopathy in plasma (296). Results showed that levels of thrombin-antithrombin complex were not significantly altered in the *CFH*^{-/-} mice (75±43ng/ml for *CFH*^{-/-}, 120±81ng/ml for WT, p-value 0.0879, Figure 3.2B). Soluble thrombomodulin is considered a marker for endothelial damage (200, 297). *CFH*^{-/-} mice had increased levels of soluble thrombomodulin compared to the wild type mice (74±16ng/ml for *CFH*^{-/-}, 58±6ng/ml for WT, p-value 0.0012, Figure 3.2A). Levels of activated protein C help determine the anticoagulant state of plasma (195). No differences were seen in the levels of activated protein C in the *CFH*^{-/-} mice (3.99±0.8ng/ml for *CFH*^{-/-}, 3.6±0.8ng/ml for WT, p-value 0.494, Figure 3.2C). Overall, results indicate that the *CFH*^{-/-} mice have increased levels of soluble thrombomodulin, indicative of increased haemolysis and endothelial damage. Previous data from the lab indicated increased

haemolysis in the *CFH*^{-/-} mice, but not the *C3*^{-/-} or wildtype mice, which opposes with previous findings for the latter (298), whereby authors demonstrated increased haemolysis via the classical pathway in C3 knockout mice.

The *C3*^{-/-} mice had increased soluble thrombomodulin levels (72.8±15ng/ml for *C3*^{-/-}, 58±6ng/ml for WT, p-value 0.0097, Figure 3.2D), but no significant differences were seen in the levels of thrombin-antithrombin complexes (154±149ng/ml for *CFH*^{-/-}, 120±81ng/ml for WT, p-value 0.6389, Figure 3.2E), nor of activated protein C (3.6±0.7ng/ml for *C3*^{-/-}, 3.6±0.8ng/ml for WT, p-value 0.7283, Figure 3.2F). The difference between *CFH*^{-/-} mice and *C3*^{-/-} mice models is that the *CFH*^{-/-} mice have C3b deposits, contrary to *C3*^{-/-} mice that have none. The C3b deposits are likely responsible for the increased endothelial damage illustrated by increased haemolysis and soluble thrombomodulin.

Previous data from the lab generated by Dr Heurich demonstrated that *CFH*^{-/-} mice had increased tail bleeding time as well as increased haemolysis. Haemolysis in plasma was quantified by release of haemoglobin, by measuring absorbance at 405nm. The results here showed an increase in soluble thrombomodulin levels, an indicator of endothelial damage which could explain the increased haemolysis in the knockout mouse models. However, they do not explain the increased tail bleeding time. Therefore, I wanted to understand whether the absence of factor H in human plasma affected clotting time.

3.2. Restoration of factor H decreases activated partial thromboplastin time in human factor H-depleted plasma

To determine the impact of factor H or factor B on clotting, human plasma was depleted of factor H and/or factor B, and depletion of the plasmas was done via western blotting analysis. Depletion of factor B and/or factor H was verified by western blot using the JC1 antibody against the Bb fragment of factor B, and the 35H9 monoclonal antibody against SCR1-3 of factor H (Figure 3.3). Each membrane probed had a control condition with only the secondary antibody.

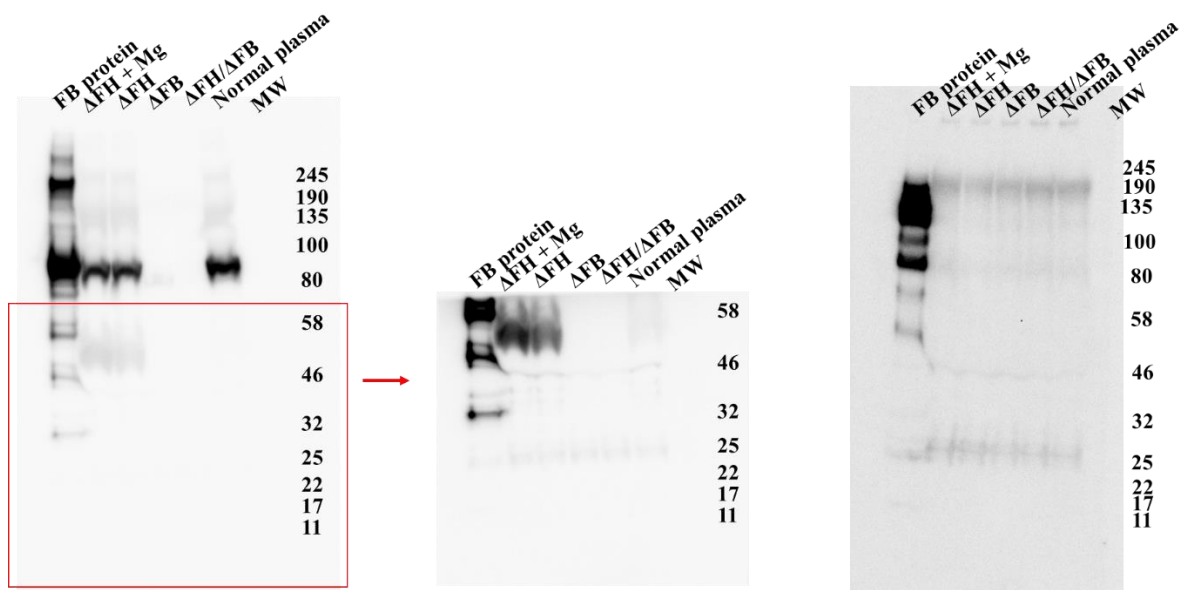


Figure 3.3. Detection of factor B in normal, FH depleted, FB depleted and FH/FB depleted plasmas. Normal plasma, FH depleted, FH depleted with magnesium (Mg), FB depleted and FH/FB depleted plasmas were loaded onto 10% acrylamide gels, left to migrate for 1h45 at 120V, before transfer onto a PVDF membrane at 100V for 55min, and blocked in PBST milk 5% for 3h at room temperature. Membranes were probed with JCI monoclonal antibody at 0.1 μ g/ml overnight at 4 $^{\circ}$ C. Secondary mouse HRP-conjugated antibody was added at 1/5000. The membrane was cut at 70kDa and re-exposed to determine presence of Bb fragment, therefore complement activation. The secondary only control was the same set-up without addition of JCI monoclonal antibody. Illustration representative of three independent experiments.

A band was detected in the normal plasma pre-depletion and in FH depleted plasma with and without magnesium, around 80-100kDa marker. Factor B before cleavage by factor D weighs 90kDa, corresponding to the correct band. No bands at this molecular weight were detected in the FH/FB depleted and the FB depleted plasmas, demonstrating that factor B had been removed (Figure 3.3 left). The secondary only control condition showed some non-specific binding at around 190kDa (Figure 3.3 right). Hence, factor B had been correctly removed from the FH/FB depleted, and the FB depleted plasmas.

To determine whether there was complement activation, the bottom half of the membrane was re-exposed, to see the breakdown fragment Bb (Figure 3.3 middle). When exposing the lower half of the membrane, bands were present in FH depleted with and without magnesium around 46-50kDa (Figure 3.3 middle). The Bb fragment is 60kDa as seen in the control condition with only factor B protein, however a band was detected around 50kDa in the FH depleted plasma with and without magnesium.

Depletion of factor H was verified using the 35H9 antibody (Figure 3.4), and not the rabbit polyclonal antibody, as there was too much background and non-specific binding generated.

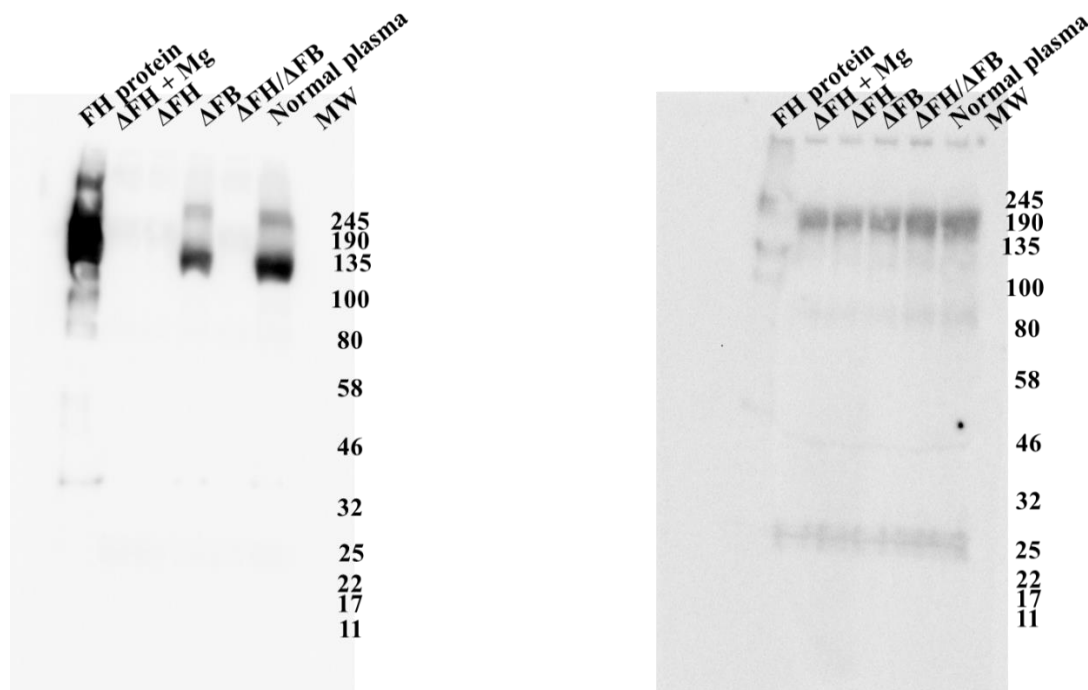


Figure 3.4. Verification of factor H depletion in normal pre-depletion, FH depleted, FB depleted and FH/FB depleted plasmas. Normal plasma, FH depleted, FH depleted with magnesium (Mg), FB depleted and FH/FB depleted plasmas were loaded onto 10% acrylamide gels, left to migrate for 1h45 at 120V, before transfer onto a PVDF membrane at 100V for 55min, and blocked in PBST milk 5% for 3h at room temperature. Membranes were probed with mouse 35H9 antibody at 0.1µg/ml overnight at 4 °C. Secondary mouse HRP-conjugated antibody was added at 1/5000. The secondary only control was the same set-up without addition of 35H9 monoclonal antibody. Illustration representative of three independent experiment.

Using the 35H9 antibody, bands were visible in the normal plasma condition, and the FB depleted plasma, at around 100-135kDa marker bands (Figure 3.4 left). Control condition with only the factor H protein showed a smear at 135-190kDa. Some non-specific binding was present at 190kDa (Figure 3.4 right). Factor H was successfully removed from the FH depleted and FH/FB depleted plasma.

Activated partial thromboplastin time (aPTT) and prothrombin times (PT) were measured in depleted plasmas, to determine the time to clot in plasma in absence of factor H and/or factor B (Figure 3.5).

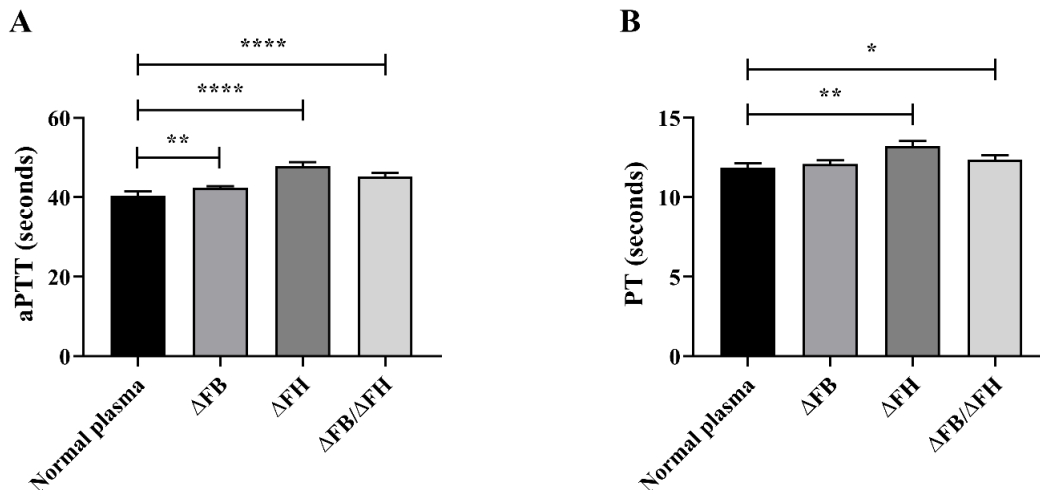


Figure 3.5. ΔFB/ΔFH, and ΔFH plasmas have significantly increased activated partial thromboplastin time and prothrombin time compared to normal plasma. (A) Activated partial thromboplastin times, aPTT and (B) prothrombin time were measured in normal, ΔFB/ΔFH, ΔFB and ΔFH plasmas. (A) ΔFB plasma, ΔFH plasma and ΔFB/ΔFH plasma had significantly increased aPTT compared to normal plasma. (B) Prothrombin times were increased in ΔFH plasma and ΔFB/ΔFH plasma compared to normal plasma and ΔFB plasma. Results show mean \pm SD (n=3). APTT data was normally distribution, whereas the PT did not, therefore a Welch's t-test were performed on aPTT results and a Mann-Whitney U test on the PT results. Illustration representative of 2 independent experiments. Only two experiments were performed due to limitation on the plasma volume available to deplete of each factor.

Results showed that all depleted plasmas had a significantly increased aPTT (Figure 3.5A) compared to the same plasma pre-depletion. ΔFB plasma clotted in 42.42 ± 0.4 seconds (p-value 0.0082), ΔFH plasma in 47.95 ± 0.9 seconds (p-value <0.0001), and ΔFB/ΔFH plasma in 45.22 ± 0.9 seconds (p-value <0.0001) compared to normal plasma that clotted in 40.37 ± 1.2 seconds (Figure 3.5A). Therefore, absence of factor B and/or factor H affect the activated partial thromboplastin time of normal plasma, indicating a role for the complement proteins in the coagulation system.

Prothrombin time (Figure 3.5B) was significantly increased in ΔFH (13.22 ± 0.3 seconds, p-value 0.0022), and ΔFB/ΔFH (12.37 ± 0.3 seconds, p-value 0.03) plasmas, compared to normal (11.88 ± 0.3 seconds) and ΔFB (12.1 ± 0.2 seconds) plasmas (Figure 3.5B). These results demonstrated that time to clot via the extrinsic pathway is increased in absence of factor H, indicating a role of factor H in coagulation.

To confirm whether the difference in aPTT and PT was due to the absence of factor H and/or factor B, or whether it was due to a dilution effect after the affinity depletion of the plasma, Clauss fibrinogen was performed to measure levels of fibrinogen in the depleted plasmas.

Fibrinogen levels were measured using Clauss fibrinogen (see Materials and Methods) in the depleted plasmas, presented in Table 3.1, and compared to normal plasma pre-depletion, to determine whether the depletion procedure had caused dilution of the plasma and therefore increased time to clot.

Table 3.1. Fibrinogen level in normal and depleted human plasmas. Levels of fibrinogen (g/l) presented as mean +/-SD measured with Clauss Fibrinogen, in depleted plasmas (FB depleted, FH depleted, and FB/FH depleted) compared to normal plasma. The data points were not normally distributed (n=2) and a Mann-Whitney U test was performed to determine the difference between the levels of fibrinogen in the plasmas. ns is non-significant.

Plasma	Fibrinogen (g/l) (mean +/- SD)	P-value
Normal plasma (NP)	2.035 +/- 0.064	
Factor B depleted (Δ FB)	2.08 +/- 0.029	0.67 (ns)
Factor H depleted (Δ FH)	1.795 +/-0.007	0.33 (ns)
FB/FH depleted (Δ FB/ Δ FH)	2.225 +/- 0.11	0.33 (ns)

Only two repeats were performed for the Clauss fibrinogen test, therefore it is not possible to conclude certainly (impossible to perform statistical tests due to low repeats) that there is no significant difference between the plasma preparations. The results show that the factor H depleted plasma has a lower concentration of fibrinogen, which could explain in part why the clotting time is increased. The Clauss Fibrinogen assay required a significant volume to perform the test (700 μ l for a duplicate), and I was informed that the Clauss Fibrinogen is highly accurate and that I would not need to repeat the measurement multiple times to get a reliable result.

After measuring aPTT and PT in depleted plasma, the measurements were done on the depleted plasma with restored physiological concentrations of factor H (Figure 3.6).

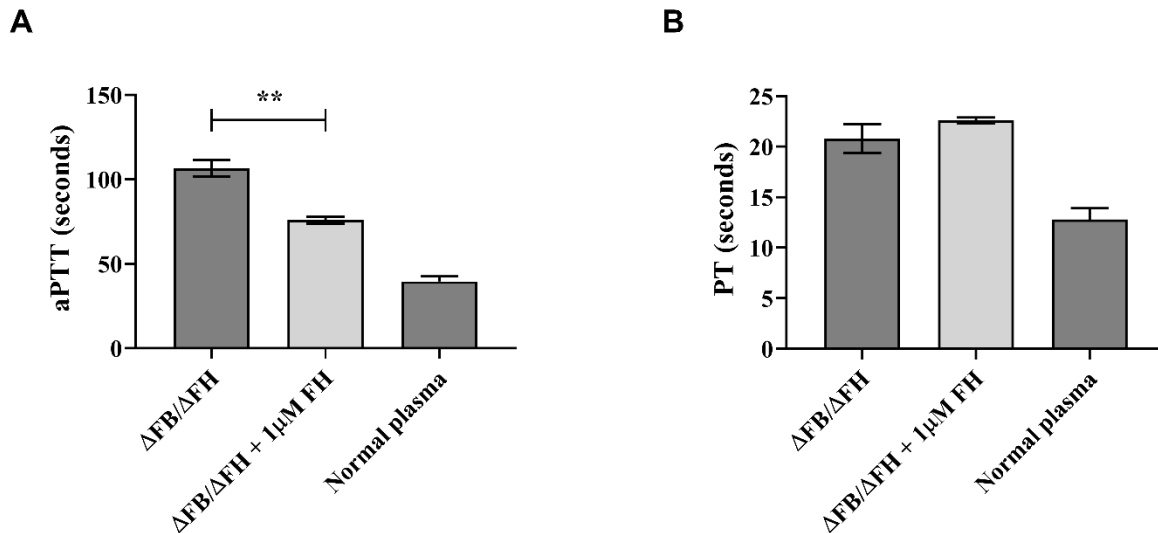


Figure 3.6. Restoration of physiological concentration of factor H decreases aPTT in ΔFB/ΔFH plasma. (A) Activated partial thromboplastin times, aPTT and (B) prothrombin time (PT) were measured in normal, ΔFB/ΔFH plasmas. (A) aPTT was decreased with 1μM factor H (39.61±/−2.93 seconds in normal plasma). PT was not significantly altered upon restoration of factor H (12.79±/−1.12 seconds in normal plasma). APTT data was normally distribution, whereas the PT did not, therefore a Welch’s t-test were performed on aPTT results and a Mann-Whitney U test on the PT results. Results show mean ±/−SD (n=3). Illustration representative of 2 independent experiments.

Results showed that upon restoration of physiological concentration of factor H (1μM), there was a significant decrease in aPTT in ΔFB/ΔFH plasma (106.5±/−4.9 seconds in ΔFB/ΔFH plasma, 75.97±/−2.07 seconds with 1μM factor H, p-value 0.022, Figure 3.6A), although normal plasma clotting time was not reached, likely due to the dilution effect of the affinity depletion. No effect was seen in prothrombin time PT (20.8±/−1.4 seconds in ΔFB/ΔFH plasma, 22.6±/−0.28 seconds with 1μM factor H, Figure 3.6B) after restoration of factor H. It was hypothesised that this was due to high levels of tissue factor present in the PT reagent, which mask the effect of factor H on time to clot.

After demonstrating that the most significant difference in aPTT and PT was with the factor H only depleted plasma, and that in absence of factor H alone, there was no significant overactivation of complement in the plasma, physiological concentrations of factor H were added back to factor H only depleted plasma (Figure 3.7).

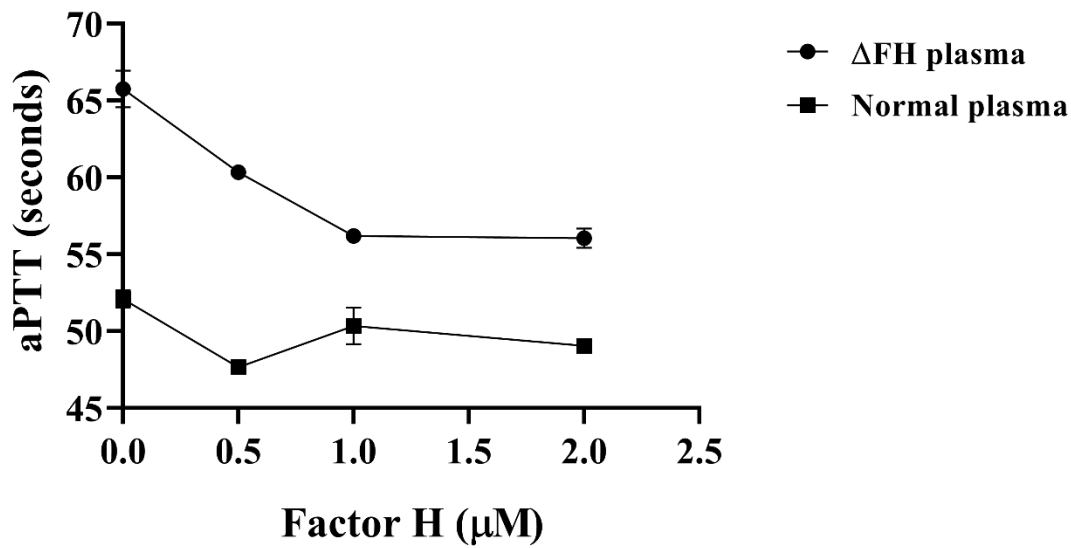


Figure 3.7. Factor H decreases activated partial thromboplastin time in factor H depleted plasma in a dose dependent manner. Activated partial thromboplastin times, aPTT was measured in normal plasma or Δ FH plasma in the presence of varying concentrations of factor H (0.5 μ M-2 μ M). Number of repeats were too low to measure statistics. Results show mean +/-SD (n=2). Illustration representative of one independent experiments.

The results showed that activated partial thromboplastin time decreased with increasing concentrations of factor H added back in the Δ FH plasma, non-significantly however as the internal repeats were too low (Figure 3.7). No effect of factor H was seen in the normal plasma. Therefore, absence of factor H caused an increase in time to clot in the aPTT assay, and restoration of physiological concentrations of factor H decreased it.

3.3. Anti-factor H antibodies against SCR1-3 and SCR19-20 decreased activated partial thromboplastin time in human plasma

Next, I wanted to determine whether specific regions of factor H relevant to its regulatory function, were involved in the effect on clot formation in plasma. For this, domain specific anti-factor H antibodies were added to normal human plasma (NP). Different antibodies binding specific factor H SCRs are summarised in Figure 3.8.

FACTOR H monoclonal antibodies and their binding sites:

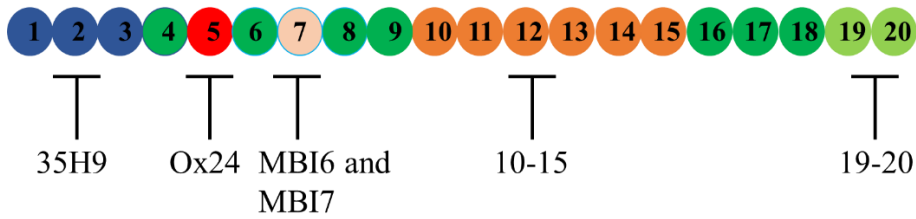


Figure 3.8. Diagram representing the binding sites of the anti-factor H monoclonal antibodies. Clone 35H9 binds SCR 1-4, clone ox24 binds SCR5, clone 10-15 binds SCR 10-15, all made in house. Commercial antibody C18 was bought against SCR20.

The antibodies target different SCRs in factor H. All antibodies were Immunoglobulin G (IgG), except monoclonal 35H9 antibody against SCR 1-3, which was immunoglobulin M (IgM). Ox24 is raised against factor H SCR5, clone 10-15 is against SCR10-15, MBI6 and 7 are against a polymorphism in SCR7 (MBI6 against Y402 and MBI7 against H402) and clone C18 is against SCR20. Activated partial thromboplastin time was measured in plasma in presence of each anti-factor H antibody or buffer control (Figure 3.9).

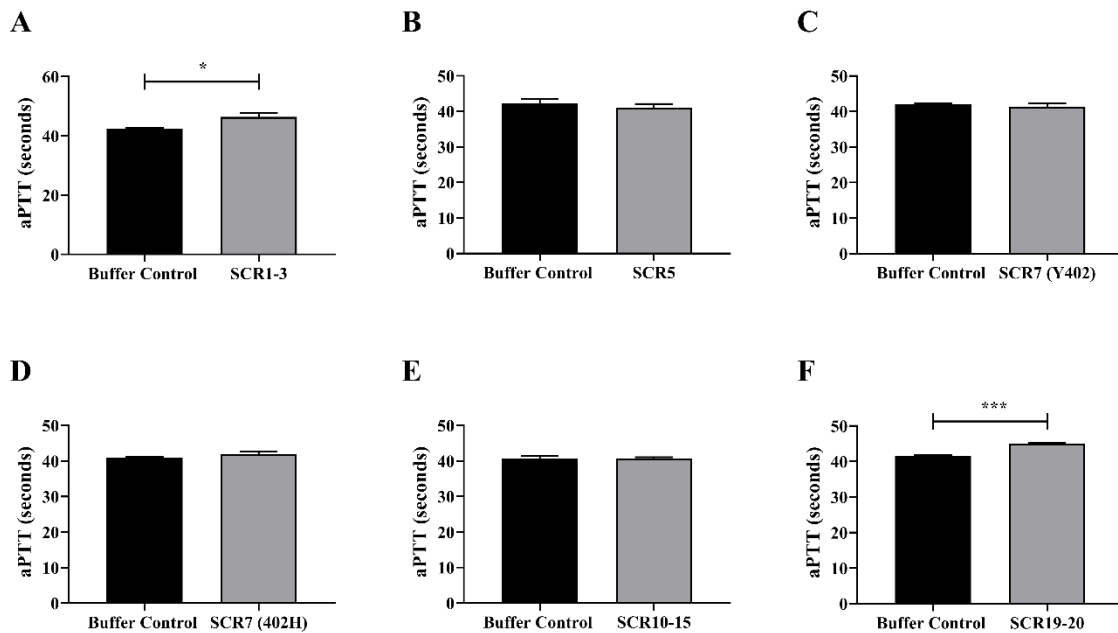


Figure 3.9. Factor H antibodies against SCR1-3 and SCR20 decrease activated partial thromboplastin time. Antibodies against different regions of factor H to normal human plasma, at 1µM, for 30min at room temperature, each alongside a buffer control incubated for the same time, before measuring activation partial thromboplastin time. Antibodies against SCR20 and SCR1-3 increased the aPTT significantly. Antibodies against SCR5, SCR7

(MBI6 and MBI7), and SCR10-15, showed no significant effect on time to clot. Results show mean +/-SD (n=3). Illustration representative of three independent experiments.

IgMs are about 900kDa, whereas IgGs are about 150kDa. This characteristic was important to consider as it was not possible to add 1 μ M of 35H9 to plasma (10 μ l of antibody into 50 μ l of plasma). Activated partial thromboplastin time was increased in presence of the 35H9 antibody (IgM, buffer control 42.35 \pm 0.35 seconds, with antibody 46.37 \pm 1.39 seconds, p-value 0.029), targeting SCR1-3 (Figure 3.9A), and C18 antibody (IgG, buffer control 41.57 \pm 0.31 seconds, with antibody 44.97 \pm 0.31 seconds, p-value 0.0002), targeting SCR20 (Figure 3.9F). No effect was seen when plasma was in presence of Ox24 (IgG, buffer control 42.3 \pm 1.13 seconds, with antibody 41.1 \pm 1.015 seconds, p-value 0.347), targeting SCR5 (Figure 3.9B), MBI6 and 7 (MBI6 and MBI7, MBI6 buffer control 42 \pm 0.36 seconds, with MBI6 antibody 41.4 \pm 0.964 seconds, p-value 0.399; MBI7 buffer control 40.93 \pm 0.25 seconds, with MBI7 antibody 41.87 \pm 0.81 seconds, p-value 0.178), targeting SCR7 (Figure 3.9C and D), and 10-15 (IgG, buffer control 40.7 \pm 0.7 seconds, with antibody 40.67 \pm 0.42 seconds, p-value 0.96), targeting SCR10-15 (Figure 3.9E). The 35H9 antibody is an IgM, with increased molecular weight therefore the volume added to obtain 1 μ M in plasma was higher, diluting the plasma, explaining the increased time to clot time also observed in the buffer control (Figure 3.9A).

To further analyse how factor H could affect time to clot in plasma, turbidity assays were done in normal plasma and depleted plasma to determine the lag time, velocity and maximal turbidity.

3.3.1. Factor H depleted plasma has increased time to clot compared to factor H and factor B depleted plasma

Plasma was depleted of factor H and factor B (FH/FB depleted), factor H alone (FH depleted) and factor B alone (FB depleted), and the depletion verified by western blot with the 35H9 and JC1 antibodies (Figure 3.10).

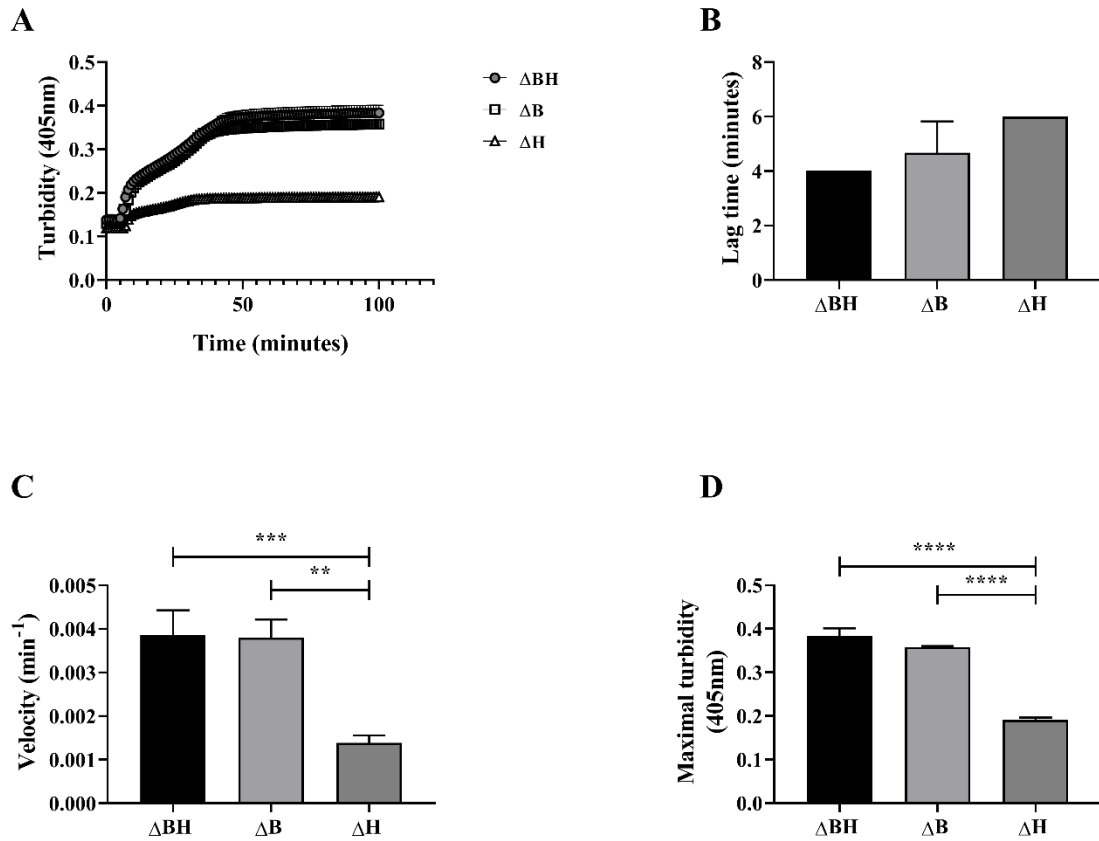


Figure 3.10. FH depleted plasma has a lower velocity and maximal turbidity compared to FH/FB depleted and FB depleted plasmas. Δ BH, Δ B, and Δ H plasmas were tested in a turbidity assay. Fibrin clot formation was triggered using aPTT reagent containing factor XII activator and phospholipids, to trigger the intrinsic pathway of coagulation. The reagent was diluted 1/16, and calcium 10mM. (A) Turbidity (A405nm) was monitored over time. (B) Impact of factor H and B depletion on lag time showed no significant difference. (C) FH depleted plasma had a significantly decreased velocity compared the FH/FB depleted and FB depleted plasma. (D) FH depleted plasma also had decreased maximal turbidity compared to FH/FB depleted and FB depleted plasmas. Results show mean +/-SD (n=3). Illustration depicts one independent experiment.

The turbidity assays showed that all depleted plasmas showed robust fibrin clot generation monitored as turbidity over time (Figure 3.10A). The lag times did not significantly differ (Figure 3.10B) however the velocity (Figure 3.10C) was lower for the Δ FH plasma, which was 0.0014min^{-1} compared to 0.00385min^{-1} and 0.0038min^{-1} for Δ FB/ Δ FH and Δ FB plasmas respectively (p-value 0.0009 and 0.001 respectively). The maximal turbidity (Figure 3.10D) was 0.19 for Δ FH plasma, was also significantly decreased compared to Δ FB/ Δ FH and Δ FB plasmas (0.38 and 0.36 respectively, p-value <0.0001 for both). Therefore, absence of factor H and factor B, and factor B only does not significantly affect fibrin clot generation. However,

absence of factor H increases lag time of fibrin clot formation and decreases velocity and maximal turbidity. Overall, these results indicate that absence of factor H affects thrombin's cleavage of fibrinogen into fibrin (lag time), the rate at which the clot is formed and the formation of fibres (velocity), as well as the final structure of the fibrin clot (maximal turbidity).

3.3.2. Restoration of factor H to factor H/factor B depleted plasma moderately affects fibrin clot formation in plasma

I next wanted to determine, whether restoration of factor H into Δ FH plasma affects fibrin clot formation. This was monitored in turbidity assay to assess lag time, velocity, and maximum turbidity (Figure 3.11).

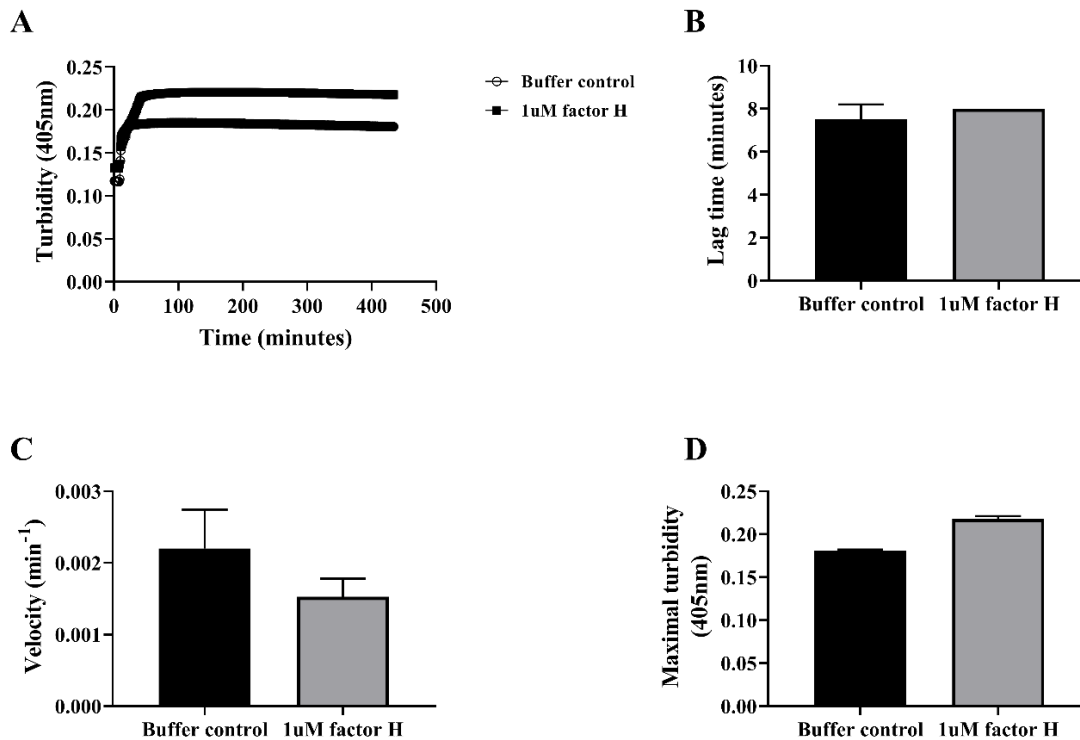


Figure 3.11. Factor H moderately affects the lag time and velocity in Δ FH plasma. Factor H was added back at 1 μ M to factor H only depleted plasma and compared to a buffer control. (A) Fibrin clot generation was triggered using aPTT reagent diluted 1/16, and calcium 10mM, and turbidity (A405nm) was monitored over time. (B) Upon factor H restoration, there was a trend showing that factor H increased lag time of the depleted plasma, as well as (C) velocity. (D) There was no effect on the maximal turbidity. Results show mean \pm SD (n=3). Illustration representative of one independent experiment.

Fibrin clot generation was initiated in Δ FH plasma by adding factor H 1 μ M (Figure 3.11A). A non-significant increase in lag time (7.5 \pm 0.7 to 8 minutes, p-value >0.99, Figure 3.11B) was observed, as well as decreased velocity (from 0.0022 \pm 0.0005 min⁻¹ to 0.0015 \pm 0.0003 min⁻¹, p-value 0.33, Figure 3.11C) and increased maximal turbidity (0.18 to 0.22, p-value 0.33, Figure 3.11D) in presence of factor H. These results indicate that restoration of factor H to Δ FH plasma has no significant impact on the lag time, velocity nor maximal turbidity in turbidity assays. However, this experiment was not repeated enough to pull solid conclusions.

Next, I tested the effect of factor H restoration to Δ FB/ Δ FH depleted plasma with 1 μ M factor H (Figure 3.12).

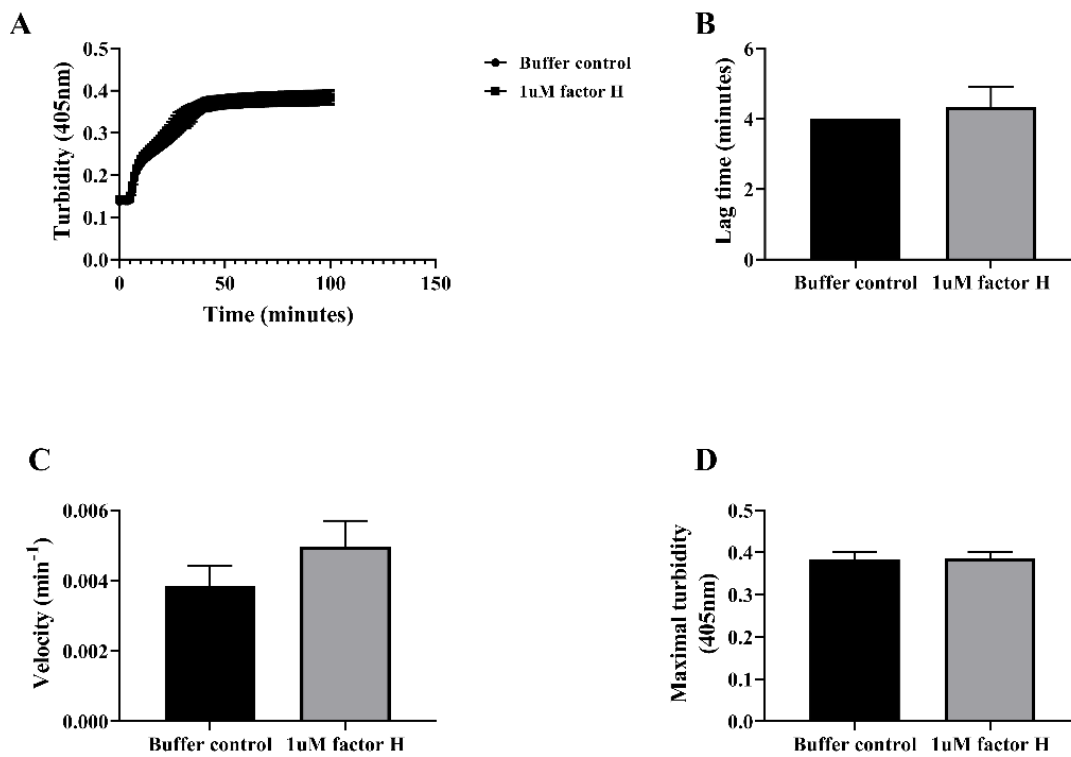


Figure 3.12. Factor H moderately affects the velocity in Δ FB/ Δ FH depleted plasma. Factor H was added back at 1 μ M to Δ FB/ Δ FH depleted plasma (A). Clotting was triggered using aPTT reagent diluted 1/16, and calcium 10mM. Re-addition of factor H non-significantly increased (C) velocity. There was no evident effect (B) on the lag time, nor (D) maximal turbidity in FH/FB depleted plasma. Results show mean \pm SD (n=3). Illustration representative of one independent experiments.

Upon addition of factor H at 1 μ M, there was no significant difference in the lag time (4 minutes to 4.3 \pm 0.6 minutes, Figure 3.12B), velocity (from 0.004 \pm 0.0006 min⁻¹ to 0.005 \pm 0.0007

min⁻¹, Figure 3.12C) nor maximal turbidity (Figure 3.12D). However, there was a trend with increased lag time and increased velocity, which would need to be verified by increasing sample number. The increase in velocity concurs with the increased time to clot in the aPTT assays. Overall, absence of factor H and factor B does not significantly affect fibrin clot formation in plasma, although a trend is observed showing an increase in lag time and velocity after restoration of factor H. It was observed that turbidity assays in plasma were prone to variability and high error bars, therefore pure protein turbidity assays were designed to dissect the effect of factor H on fibrin clot generation.

Chapter 4: Factor H effect on fibrin clot generation in pure protein turbidity assays

After analysing the impact of factor H in plasma, the effect of factor H on thrombin's mediated fibrin clot formation were investigated in a pure protein assay.

4.1 Fibrin generation depends on thrombin concentration, and is enhanced by factor H

Turbidity assays were used to analyse factor H's impact on thrombin's procoagulant role in the conversion of fibrinogen into fibrin by monitoring fibrin clot formation over time in a pure protein assay.

Two fibrinogen preparations were used in the turbidity assays:

- Fibrinogen 1 preparation was plasminogen-depleted and contained von Willebrand factor and FXIII that contribute to clot formation and fibre crosslinking (for concentration of each fibrinogen preparation see Materials and Methods).
- Fibrinogen 2 preparation was also tested where indicated, which was plasminogen and von Willebrand factor depleted (termed vWF-depleted plasma).

First, thrombin concentration was titrated to determine a concentration-dependent effect in the presence and absence of factor H. Fibrin clot formation was followed by measuring turbidity at 405nm over time to assess lag time, reaction rate (velocity) and the maximal turbidity (Figure 4.1).

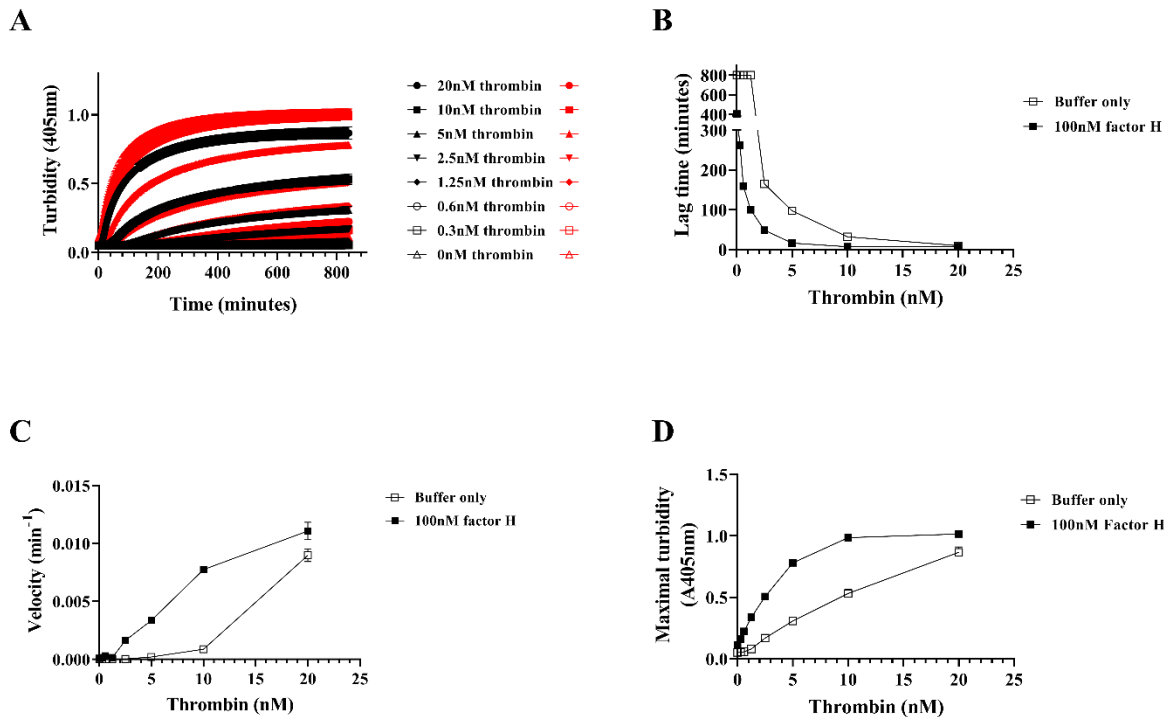


Figure 4.1. Fibrin clot formation depends on thrombin concentration and is enhanced in the presence of factor H by decreasing lag time and increasing velocity and maximal turbidity. Thrombin was titrated (0.3-20nM) in the presence (red) or absence (black) of 100nM factor H before addition to 12 μ M fibrinogen (plasminogen depleted) in the presence of 5mM calcium. (A) Thrombin increased fibrin clot formation in a concentration dependent manner and is enhanced in presence of factor H. (B) Lag time decreased in the presence of factor H and the (C) velocity was increased in the presence of factor H as well as (D) maximum turbidity. IC₅₀ was calculated for lag time and the EC₅₀ for the velocity and maximal turbidity using nonlinear regression fit. Results show mean \pm SD (n=3). A non-parametric Spearman correlation was performed for each curve and p-values were calculated with Welch's t-test as data followed Gaussian distribution. Illustration representative of seven independent experiments.

Turbidity increased over time (Figure 4.1A), and increasing thrombin decreased the lag time and increased velocity and maximal turbidity in a dose dependent manner. The lag time (Figure 4.1B) was inversely correlated to thrombin concentration (r value -0.9386, p-value 0.0012). Velocity (Figure 4.1C) was positively correlated to thrombin concentration (r value 0.9762, p-value 0.0004), as was maximum turbidity (Figure 4.1D) also (r value 1, p-value <0.0001). Therefore, cleavage of fibrinogen into fibrin and protofibril assembly, as well as fibre formation and the structure of the fibrin clot are dependent on thrombin concentration.

In presence of factor H, there was a significant increase in lag time (Figure 4.1B), which was inversely correlated to thrombin concentration in the presence of factor H (r value -0.994, p-value <0.0001). The velocity significantly increased in the presence of factor H (Figure 4.1C) and was correlated to thrombin concentration (r value 0.9762, p-value 0.0004). The maximum turbidity (Figure 4.1D) was significantly correlated to thrombin concentration in the presence of factor H (r value 1, p-value <0.0001).

The IC50 for the lag time, and EC50 for the velocity and maximal turbidity were calculated and compared in presence and absence of factor H (Table 4.1).

Table 4.1. Impact of factor H on lag time, velocity, and maximum turbidity in presence of 2.5nM thrombin and 12µM fibrinogen. Comparison of half inhibitory and effective concentrations (IC50 and EC50 respectively) for buffer control or with added factor H for lag time, velocity and maximum turbidity. Fold change describes the fold differences between IC50/EC50 values for each condition, in presence and absence of 100nM factor H, and the p-value associated.

	Buffer control	100nM factor H	Fold change	P value
Lag time IC50 (nM)	2.13 +/- 0.0058	0.38 +/-0.0058	5.6	<0.0001 ****
Velocity EC50 (nM)	142.4 +/- 0.4163	8.733 +/-1.332	16.3	<0.0001 ****
Maximum turbidity EC50 (nM)	18.97 +/- 2.239	3.103 +/- 0.1332	6.1	0.0064 **

The presence of factor H affected lag time by decreasing the IC50 5.6-fold, the velocity by increasing the EC50 16.3-fold and the maximum turbidity 6.1-fold, showing factor H significantly enhances all steps of fibrin clot generation in a thrombin concentration dependent manner.

4.2. Factor H affects fibrin clot formation in a dose dependent manner

Next, I wanted to determine whether factor H affects fibrin clot formation in a concentration dependent manner. Factor H was titrated while maintaining fibrinogen and thrombin at a fixed concentration (Figure 4.2). The fibrinogen preparation used was fibrinogen 1, in the presence of von Willebrand factor.

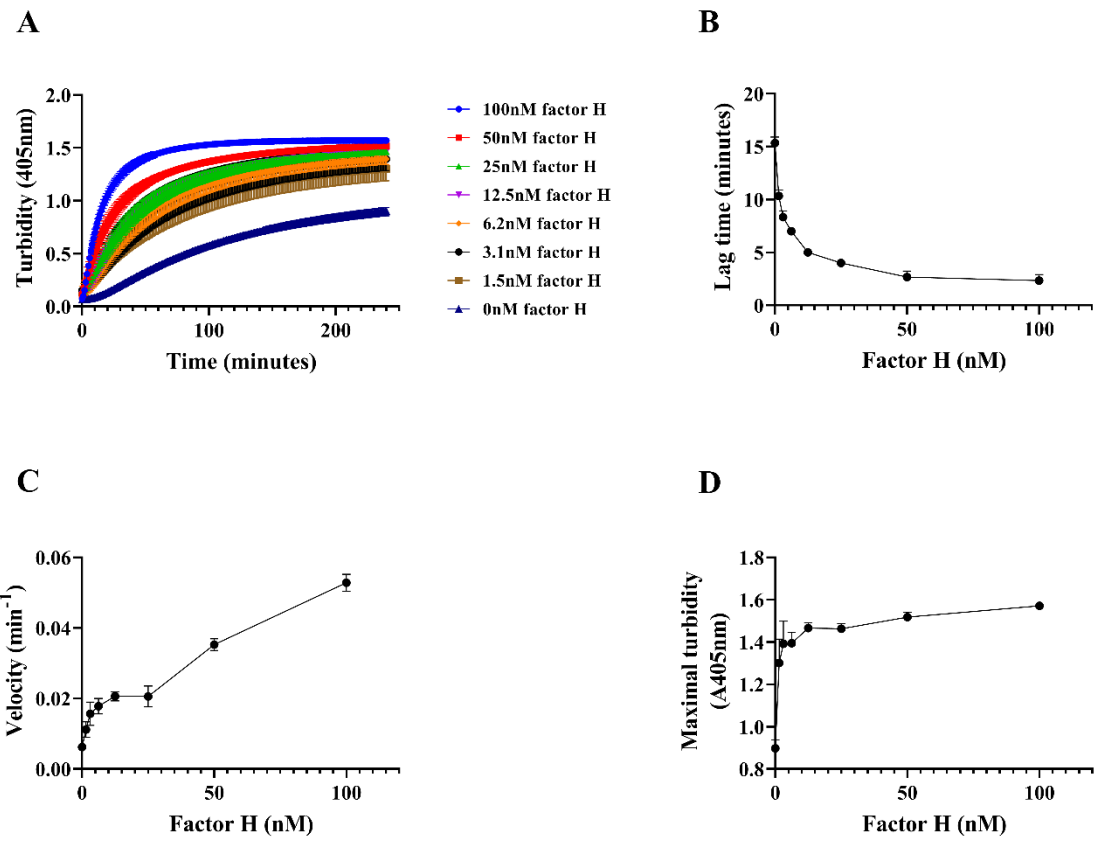


Figure 4.2. Factor H enhances fibrin clot formation in a dose dependent manner by decreasing lag time and increasing velocity and maximal turbidity. Factor H was titrated (1.5nM-100nM) in the presence of 2.5nM thrombin, before addition to 12 μ M fibrinogen, with 5mM calcium. Factor H enhanced fibrin formation in a concentration dependent manner by reducing lag time (A) and increasing velocity (B) and maximum turbidity (C). Results show mean +/-SD (n=3). A non-parametric Spearman correlation was performed for each criterion. Illustration representative of six independent experiments. This experiment was performed together with MPharm project student James Taylor.

Results demonstrated that lag time (Figure 4.2B) was inversely correlated to the concentration of factor H (r value -0.994, p-value <0.0001). The velocity significantly correlated to the factor H concentration (Figure 4.2C) (r value 0.9762, p-value 0.0004); maximal turbidity (Figure 4.2D) increased with factor H concentration (r value 0.9762, p-value 0.0004). Therefore, the results indicated that factor H affected the formation of protofibrils (decreased lag time),

promoted their assembly into fibres (increased velocity), and accelerated the formation of a final clot (increased maximal turbidity) in a concentration dependent manner.

4.3. Factor H affects fibrin clot formation in a dose dependent manner also in the absence of von Willebrand factor

Next, I wanted to test whether the same effect with vWF-depleted fibrinogen was observed (Figure 4.3). In addition, von Willebrand factor has been shown to bind factor H (28, 269, 299).

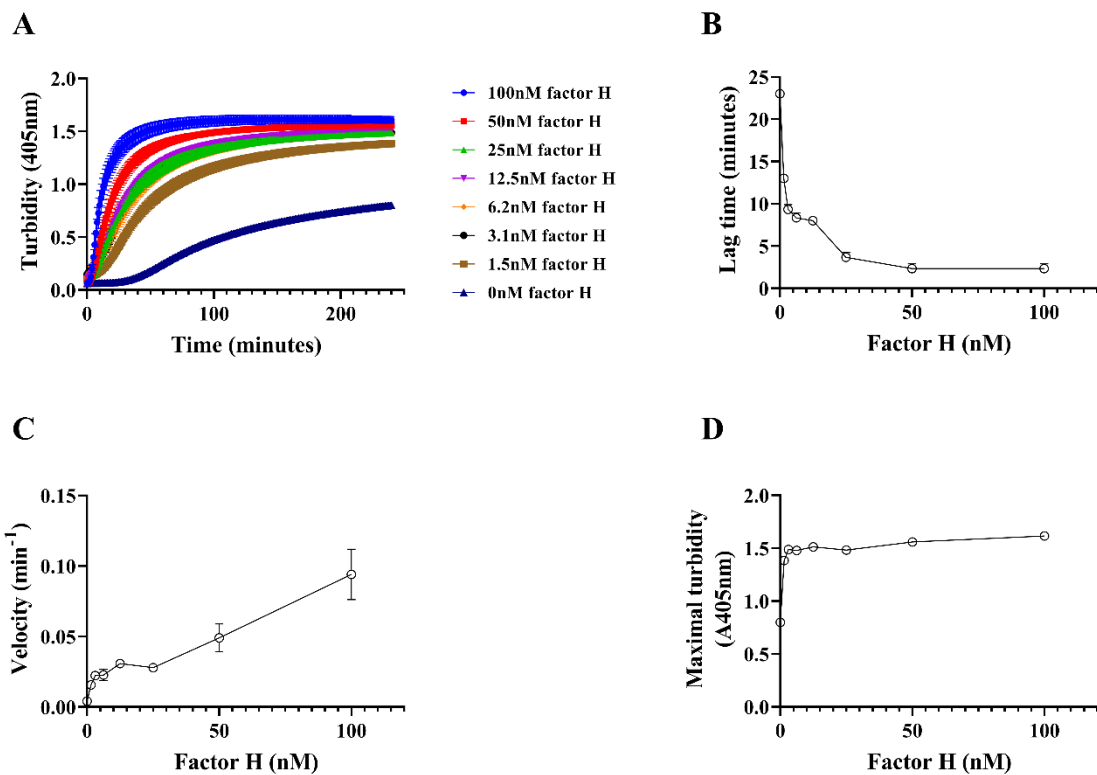


Figure 4.3. Factor H enhances fibrin clot formation in a dose dependent manner by decreasing lag time and increasing velocity and maximal turbidity with vWF-depleted plasma. Factor H was titrated (1.5nM-100nM) in the presence of 2.5nM thrombin, before addition to 12 μ M vWF-depleted fibrinogen, with 5mM calcium. Factor H enhanced fibrin formation in a concentration dependent manner by reducing lag time (A) and increasing velocity (B) and maximum turbidity (C). Results show mean \pm SD (n=3). A non-parametric Spearman correlation was performed for each criterion. Illustration representative of six independent experiments. This experiment was performed together with MPharm project student James Taylor.

Results demonstrated that turbidity increased over time dependent on factor H concentration in and absence of von Willebrand factor (Figure 4.3A).

The lag time (Figure 4.3B) was inversely correlated to the concentration of factor H, in absence (r value -1.0, p-value <0.0001) of von Willebrand factor. The velocity significantly correlated to the factor H concentration (Figure 4.3C) in absence (r value 0.9762, p-value 0.0004) of von Willebrand factor; maximal turbidity (Figure 4.3D) increased with factor H concentration in absence (r value 0.881, p-value 0.0072) of von Willebrand factor. Therefore, the results indicated that factor H affected the formation of protofibrils (decreased lag time), promoted their assembly into fibres (increased velocity), and accelerated the formation of a final clot (increased maximal turbidity) in a concentration dependent manner, in presence and absence of von Willebrand factor.

The IC50 and EC50 for lag time, velocity and maximal turbidity were calculated in presence and absence of von Willebrand factors and compared (Table 4.2).

Table 4.2. Impact of von Willebrand factor in the fibrinogen sample on lag time, velocity and maximum turbidity in presence of increasing factor H concentrations. Comparison of effective concentration needed for vWF-depleted fibrinogen or standard fibrinogen for lag time, velocity and maximum turbidity. Fold change describes the fold differences between IC50 or EC50 values for each condition.

	Fibrinogen	vWF-depleted fibrinogen	Fold change	P value
Lag time IC50 (nM)	3.0 +/-0.697	1.86 +/-0.064	1.6	0.7 (ns)
Velocity EC50 (nM)	No plateau reached	No plateau reached	-	-
Maximum turbidity EC50 (nM)	0.257 +/-0.89	0.432 +/-0.043	1.7	0.0857 (ns)

No significant difference was observed for lag time IC50 (p-value 0.7), or maximum turbidity (p-value 0.0857) when comparing vWF-depleted fibrinogen with standard fibrinogen in a factor H dose-dependent manner. When plotting the velocity, no plateau was reached, therefore it was not possible to calculate the EC50 accurately.

4.4. Factor H affects fibrin clot formation in a dose dependent manner by specific domains

To determine which regions were involved in affecting fibrin clot formation by factor H, recombinant factor H fragments representing SCR1-4, SCR1-6, SCR6-8, SCR8-15, SCR15-18 and SCR18-20 were titrated and preincubated with thrombin before addition to fibrinogen (Figure 4.4).

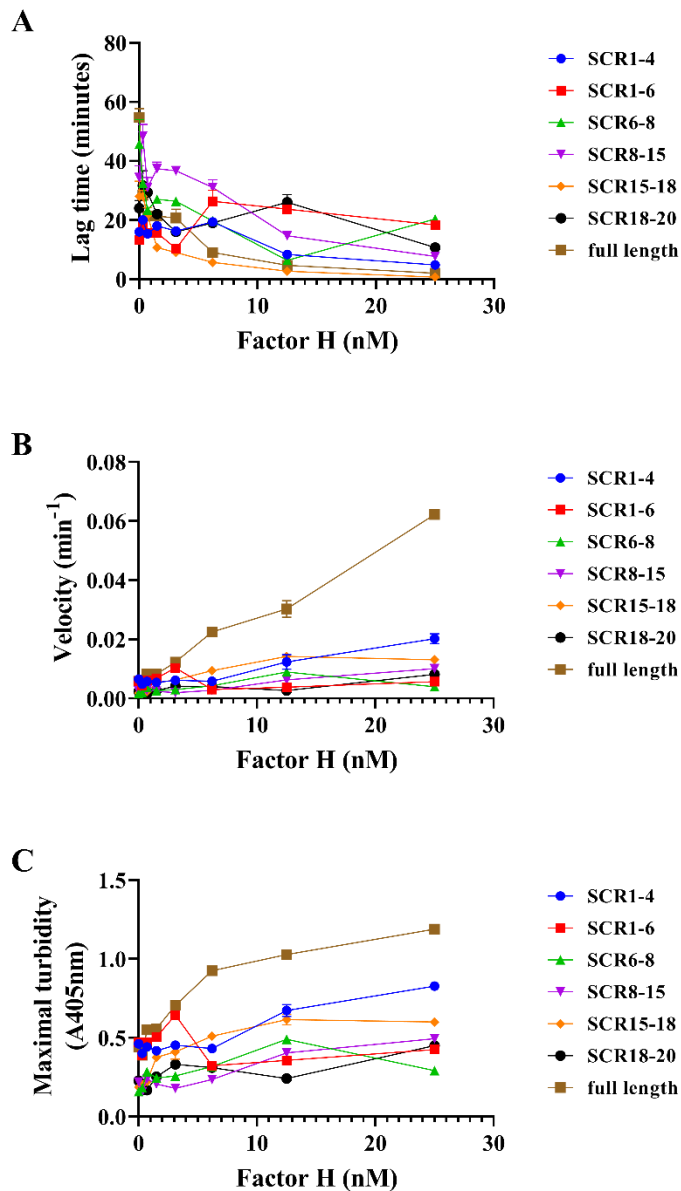


Figure 4.4. Impact of factor H fragments on lag time, velocity and maximal turbidity in fibrin clot formation. Factor H full length and recombinant fragments were titrated (0.035-25nM) in the presence of 2.5nM thrombin, before addition to 12 μ M fibrinogen with von Willebrand Factors, and 5mM calcium. Factor H full length (■) enhanced fibrin formation in a concentration dependent manner by reducing lag time (A) and increasing velocity (B) and maximum turbidity (C). Factor H SCR6-8 (▲) and SCR15-18 (◆) decreased lag time, SCR1-4 (●), SCR1-6 (■), SCR8-15 (▼) and 18-20 (●) did not affect lag time. Fragments 6-8, 15-18 and 18-20 increased velocity, fragments 1-4, 1-6 and 8-15 did not. Fragments 6-8, 15-18 and 18-20 increased maximal turbidity, fragments 1-4, 1-6 and 8-15 did not. Data presented as mean \pm SD, n=3. A non-parametric Spearman correlation was performed for each criterion. Representative of 2 experimental repeats.

Results showed that factor H full length control decreased the lag time (Figure 4.4A), and increased velocity (Figure 4.4B) and maximal turbidity (Figure 4.4C) as previously demonstrated. Of the factor H domain constructs, SCR6-8 (lag time p-value 0.0107, velocity p-value 0.0107, maximal turbidity p-value 0.0107) and SCR15-18 (lag time p-value <0.0001, velocity p-value 0.0004, maximal turbidity p-value 0.0004) also decreased lag time, increased velocity and maximal turbidity, and SCR18-20 (velocity p-value 0.0154, maximal turbidity p-value 0.0458) increased velocity and maximal turbidity significantly. Fragments 1-4, 1-6 and 8-15 did not affect clot formation. Therefore, the regions SCR6-8, 15-18 and 18-20, some key in factor H surface binding and C3b binding, could be involved in the impact on clot formation. However this assay would require further repeats before concluding surely; the dialysis and concentration could have had an effect on the fragments.

4.5. Factor H influences the fibrin clot structure by affecting fibre thickness, increasing pore size and number, and decreasing fibre density

4.5.1. Factor H impacts fibrin clot structure

Factor H enhanced maximum turbidity of fibrin clot generation, which is an indicator of the structure of the clot; with a more turbid clot indicating increased fibre thickness (132). Therefore, after determining the impact of factor H on the rate of fibrin clot generation, its effect on clot structure was analysed. For this, fibrin clots were formed in pure protein assays as was done for the turbidity assays, imaged under the fluorescent microscope and fibre density analysed in the presence or absence of factor H (Figure 4.5).

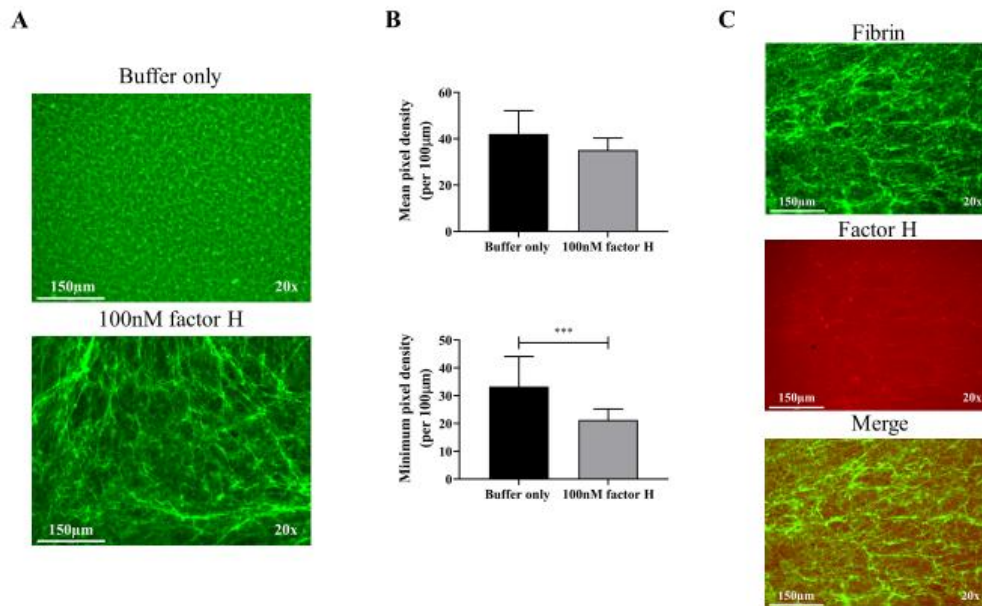


Figure 4.5. Factor H binds with the fibrin network, decreases fibre density and affects structure. 2.5nM thrombin, in presence or absence of 100nM factor, was added to fibrinogen 12µM, in presence of 5mM calcium. The clot was formed and matured on a glass slide for 2h in the dark at 37 degrees. (A) Top panel represents the buffer control mature clot, and the bottom panel is a mature clot in presence of factor H. Fluorescent microscopy at 20x magnification showed factor H altered the clot structure, by making the fibrin clot (green) more porous and less dense and increasing fibre thickness. (B) Mean (top graph) and minimum (bottom graph) pixel densities, which correspond to the fibre density and the presence of pores, respectively, were calculated in presence and absence of factor H (mean p-value 0.00524, min p-value 0.0002). This was done by taking 10 images in different areas of the clot and measuring the pixels along a 100µm line (drawn in 25 spots on each image). (C) Factor H was also tagged and visualised, and was present within the clot around thicker fibres. Images representative of 9 experimental repeats. Scale bars represent 150µm. Fibre density represented as pixel intensity with calculated mean \pm SD and p values calculated using Mann Whitney.

In the absence of factor H (buffer control), it was observed that the fibrin clot showed thinner fibres with few and smaller pores (Figure 4.5A), as well as more branching points and an overall denser clot. In the presence of factor H, larger fibres (Figure 4.5B) with less branching points, with more and larger pores were observed.

The density of the clot was determined by measuring the pixel density through 100µm lines on each image. Factor H decreased the mean pixel density (p-value 0.00524), which corresponds to the fibre density of the clot (Figure 4.5B upper graph). The minimum pixel density is the lowest pixel intensity value per line, therefore the “darkest” areas of the images, theoretically

corresponding to the pores of the clot. The minimum pixel density in presence of factor H was decreased (Figure 4.5B, lower graph) compared to the buffer control (p-value 0.0002). Therefore, the measurement of the mean and minimum pixel density confirmed that factor H decreases the fibre density of the clot and seemed to increase pore size and number, however further analysis is required to affirm this (quantification of the pores within the clot using ImageJ).

Co-localisation experiments observing factor H in the fibrin clot showed that fluorescently labelled factor H was present throughout the clot, and specifically at a higher intensity along the fibrin fibres indicating that factor H may bind here (Figure 4.5C).

Overall, the presence of factor H alters clot structure and reduces fibre density.

4.5.2. Factor H impacts fibrin clot structure when formed with vWF-depleted fibrinogen

As studies have shown that factor H binds with von Willebrand factor (28, 269, 299), the effect of factor H on fibrin clot structure was also analysed in presence of fibrinogen preparation 2, depleted of von Willebrand factor (vWF-depleted fibrinogen) (Figure 4.6).

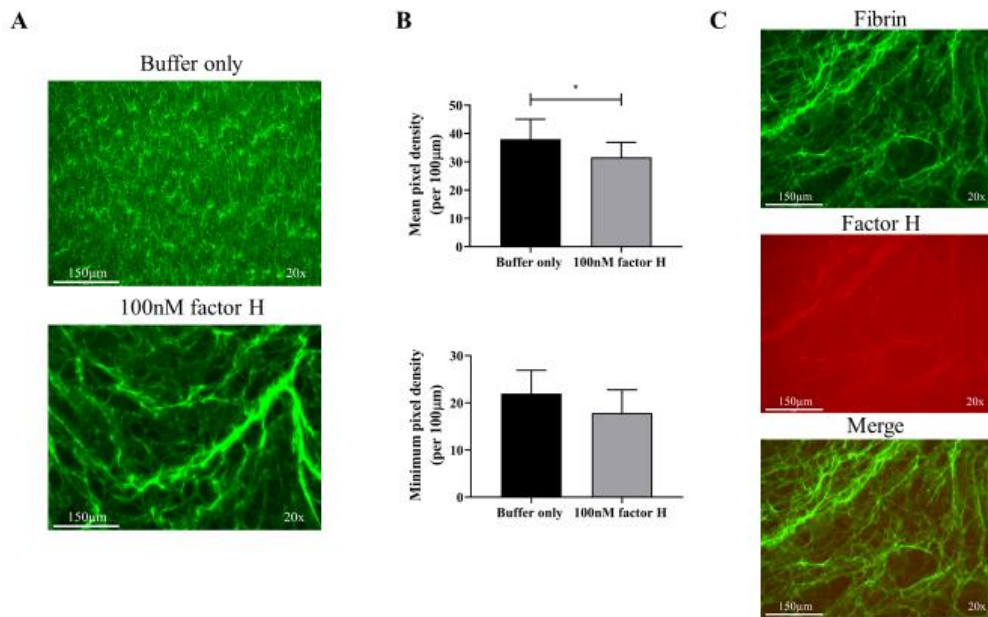


Figure 4.6. Factor H binds with the fibrin network, decreases fibre density and affects structure with vWF-depleted fibrinogen. 2.5nM thrombin, in presence or absence of 100nM factor, was added to vWF-depleted fibrinogen 12µM, in presence of 5mM calcium. The clot was formed and matured on a glass slide for 2h in the dark at 37 degrees. (A) Top panel represents the buffer control mature clot, and the bottom panel is a mature clot in presence of factor H. Fluorescent microscopy at 20x magnification showed factor H altered the clot structure, by making the fibrin clot (green) more porous and less dense and increasing fibre thickness. (B) Mean (top graph) and minimum (bottom graph) pixel densities, which correspond to the fibre density and the presence of pores, respectively, were calculated in presence and absence of factor H (mean p-value 0.00524, min p-value 0.0002). This was done by taking 10 images in different areas of the clot and measuring the pixels along a 100µm line (drawn in 25 spots on each image). (C) Factor H was also tagged and visualised, and was present within the clot around thicker fibres. Images representative of 9 experimental repeats. Scale bars represent 150µm. Fibre density represented as pixel intensity with calculated mean \pm SD and p values calculated using Mann Whitney.

When clots were formed with vWF-depleted fibrinogen, the control condition showed a similar profile to fibrinogen containing von Willebrand factor, whereby the fibres were thinner and denser, with fewer and smaller pores (Figure 4.6A). In the presence of factor H, as in the presence of von Willebrand factor, fibres were thicker with less branching points, with numerous larger pores (Figure 4.6A).

The mean and minimum pixel density values were plotted and showed a similar trend to the assay in presence of von Willebrand factor (Figure 4.6B). There was a decrease in fibre density (Figure 4.6B, upper graph), and a lower minimum pixel density (Figure 4.6B, lower graph).

Factor H seemed to bind along the fibres, as was the case in the presence of von Willebrand factor (Figure 4.6C). Therefore, factor H affects the fibrin clot structure in presence and absence of von Willebrand factor.

Chapter 5: Factor H impact on thrombin's anticoagulant role

After determining the impact of factor H on fibrin clot formation and more specifically on thrombin's procoagulant role, I wanted to also understand whether factor H affected thrombin's role in the anticoagulant system, therefore in protein C activation.

5.1. Impact of factor H on protein C activation

Previous work has shown that factor H interacts with both thrombin and thrombomodulin (29, 233). After demonstrating the impact of factor H on thrombin's procoagulant role in fibrin clot formation, I wanted to determine whether factor H binding to thrombin also affects the thrombin-mediated anticoagulant protein C pathway and the activation of protein C.

5.1.1. Factor H enhances protein C activation in a protein C concentration dependent manner by the thrombin-thrombomodulin complex and thrombin alone

To determine whether factor H affected thrombin's anticoagulant role, the substrate protein C was titrated in presence of the thrombin-thrombomodulin complex or thrombin alone, and the effect of factor H analysed (Figure 5.1).

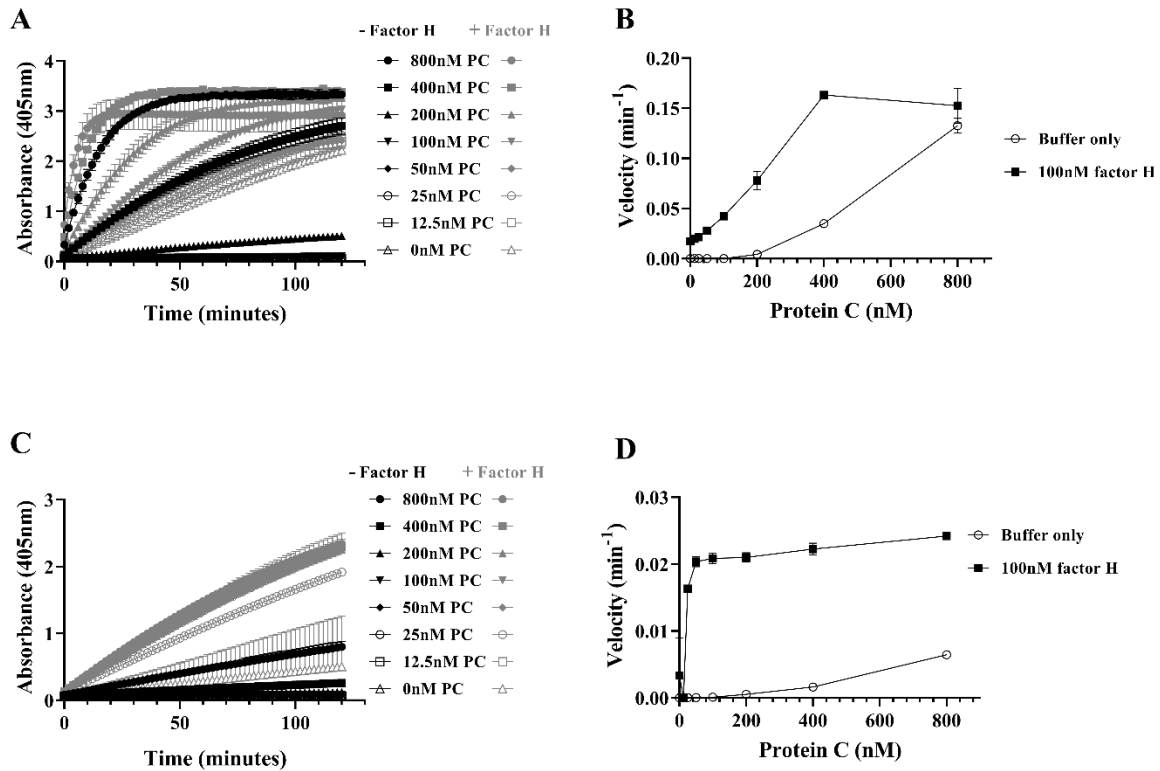


Figure 5.1. Factor H enhances thrombin-mediated protein C activation in presence and absence of thrombomodulin. Protein C (PC) was titrated (12.5-800nM) and added to thrombomodulin-thrombin (A and B) or thrombin-only (C and D). Velocity of protein C activation was calculated in the presence (grey graphs, and ■ velocity) or absence (black graphs, ○ velocity) of 100nM factor H. Activation of protein C was monitored at 405nm over time in (A and B) presence and (C and D) absence of thrombomodulin (A) and the velocities were calculated. Protein C activation (APC generation) increased proportionally to protein C concentration and was significantly higher in presence of factor H. Results show mean +/-SD (n=3). (C) Thrombomodulin-thrombin mediated protein C activation in the presence (■, KM 80+/-28nM) or absence (○KM 187+/-105nM) of factor H (p-value 0.004). (D) Thrombin mediated protein C activation in the presence (■, KM 199+/-38nM) or absence (○ KM 752+/-99nM) of factor H (p-value 0.004). KM were compared using Mann-Whitney test. Data presented as (mean +/-SD, n=3). P value calculated by Mann-Whitney. Illustration representative of six independent experiments.

Factor H significantly enhances protein C activation (p-value 0.0363) by the thrombin/thrombomodulin complex (Figure 5.1A with increasing concentrations of protein C). No plateau was reached when analysing the effect of factor H on protein C activation by thrombin alone (Figure 5.1C), however it seemed to enhance its activation. (Figure 5.1B and D). Using an activated protein C standard curve, the Michaelis Menten constant (KM) was calculated in presence and absence of factor H for each condition (Table 5.1).

Table 5.1. Michaelis Menten constant for protein C activation in presence and absence of 100nM factor H, with and without 10nM thrombomodulin, with 3nM thrombin and 200nM protein C. The KM of activation of protein C was calculated using GraphPad version 8.0, in presence and absence of factor H. There was a significant increase in the KM in presence of factor H by the thrombin-thrombomodulin complex (p-value 0.004, fold change 2.3) and also by thrombin alone (p-value 0.004, fold change 3.8).

	10nM thrombomodulin, 1.75nM thrombin, 200nM protein C	No thrombomodulin, 1.75nM thrombin, 200nM protein C	Fold change	p-value
Buffer control	187+/-105nM	752+/-99nM	With thrombomodulin: 2.3-fold	0.004
100nM factor H	80+/-28nM	199+/-38nM	Without thrombomodulin: 3.8-fold	0.004

The KM values calculated showed that factor H significantly increased the rate of activation of protein C, by the thrombin-thrombomodulin complex and by thrombin alone. There was a 2.3 fold increase in KM by the thrombin-thrombomodulin complex (p-value 0.004), and a 3.8-fold increase in activation by thrombin alone (p-value 0.004).

Factor H from different plasma purifications, as well as commercial factor H (Complement Technology, catalogue number A137) were tested and the same results were observed (Figure 5.2).

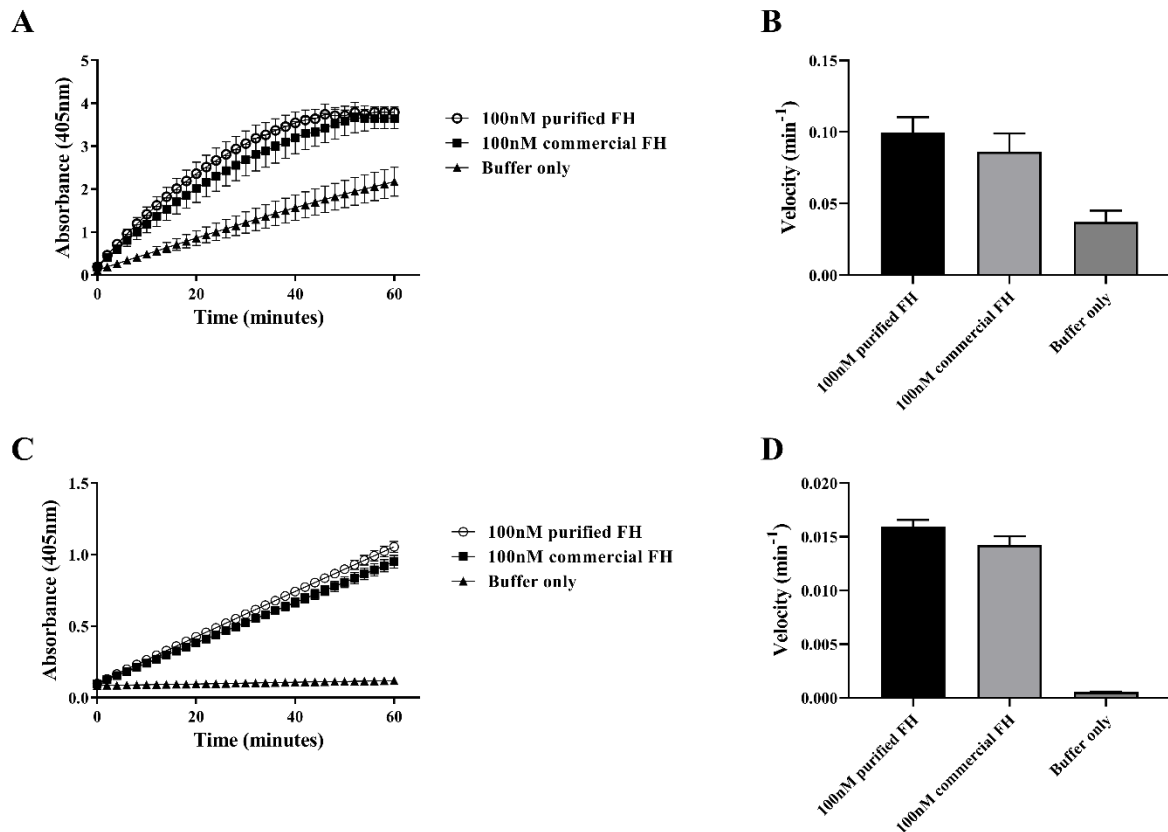


Figure 5.2. Commercial factor H enhances protein C activation in presence and absence of thrombomodulin. 100nM factor H purified from plasma (in-house) or commercial (Comptech) was incubated with 1.75nM thrombin before addition to (A and B) 10nM thrombomodulin or (C and D) buffer and added to 200nM protein C. (A and C) Activation of protein C was monitored at 405nm over time and (B and D) velocity was calculated. Commercial and purified factor H enhance protein C activation significantly in presence and absence of thrombomodulin. Results show mean \pm SD (n=3). Welch's t-test was performed, comparing absence and presence of factor H.

For the commercial factor H test, only with and without factor H, was tested on a fixed concentration of protein C, thrombomodulin and thrombin. commercial factor H significantly increased protein C activation in presence ($0.086 \pm 0.01 \text{ min}^{-1}$ with factor H, $0.037 \pm 0.008 \text{ min}^{-1}$ with buffer, p-value 0.0085) and absence ($0.014 \pm 0.0008 \text{ min}^{-1}$ with factor H, $0.0005 \pm 0.00004 \text{ min}^{-1}$ with buffer, p-value 0.0011) of thrombomodulin as did purified factor H in presence ($0.01 \pm 0.01 \text{ min}^{-1}$ with factor H, $0.037 \pm 0.008 \text{ min}^{-1}$ with buffer, p-value 0.0018) and in absence ($0.016 \pm 0.0006 \text{ min}^{-1}$ with factor H, $0.0005 \pm 0.00004 \text{ min}^{-1}$ with buffer) of thrombomodulin. Purified factor H, in absence of thrombomodulin, enhanced protein

C activation more significantly than commercial factor H, possibly due to the purification processes of each preparation.

5.1.2. Factor H enhances protein C activation in a concentration dependent manner

Next, I wanted to determine whether factor H affects protein C generation in dose dependent manner (Figure 5.3). Therefore, factor H was titrated, and protein C activation monitored in presence of thrombin-thrombomodulin complex and of thrombin alone.

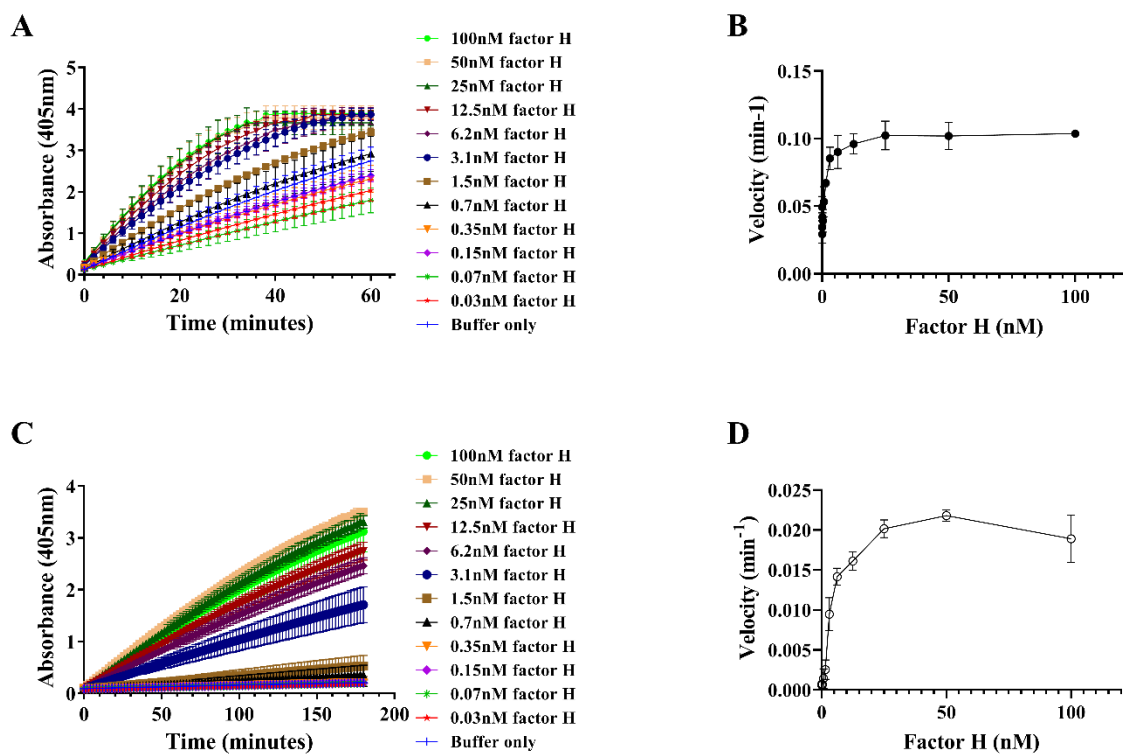


Figure 5.3. Factor H increases thrombin-thrombomodulin and thrombin-only mediated protein C activation in a dose dependent manner. Factor H was titrated (0.035-100nM) and preincubated with 1.75nM thrombin and added to 100nM protein C in the presence (●) or absence (○) of 10nM thrombomodulin. Activation of protein C was monitored at 405nm over time in (A and B) presence and (C and D) absence of thrombomodulin (A) and the velocities were calculated. Protein C activation rate increased with factor H concentration. In presence and absence of thrombomodulin the concentration of factor H was significantly correlated to the generation of activated protein C generation. Results show mean +/-SD (n=3). Dissociation constant was calculated by nonlinear regression. Illustration representative of four independent experiments.

The results demonstrated that factor H increased protein C activation in a dose dependent manner in the presence (Figure 5.3A) and absence (Figure 5.3C) of thrombomodulin. The rate of activation was significantly correlated to factor H concentration in presence (r value 0.9286, p-value <0.0001, Figure 5.3B) and absence (r value 0.9231, p-value <0.0001, Figure 5.3D) of thrombomodulin. Thrombomodulin (Figure 5.3A and B) increases the overall dose response by factor H compared to its absence (Figure 5.3C and D).

The dissociation constant for factor H in presence and absence of thrombomodulin was calculated (Table 5.2).

Table 5.2. The dissociation constant (kd) of factor H for protein C activation in presence and absence of 10nM thrombomodulin, with 2.5nM thrombin and 200nM protein C.

	No thrombomodulin, 1.75nM thrombin, 200nM protein C	10nM thrombomodulin, 1.75nM thrombin, 200nM protein C	Fold change	p-value
Dissociation constant kd	34.3 +/-04.8nM	3.5 +/-0.6nM	9.8-fold	0.0003

The dissociation constant kd, is an indicator of the affinity between a protein and a ligand, in this case the affinity between factor H and the thrombin-thrombomodulin complex, and thrombin alone. The presence of thrombomodulin significantly increased the affinity of factor H for thrombin kd 9.8-fold (p-value 0.0003).

Factor H was also tested with activated protein C to determine whether it affected activated protein C enzymatic activity in the cleavage of its synthetic substrate. Results proved that factor H did not affected activity of activated protein C, indicating that it only impacts thrombin's enzymatic activity (Appendix Figure A5.1).

5.1.3. Factor H enhances the thrombomodulin-thrombin-mediated protein C activation with purified rabbit thrombomodulin

The key regulatory domain of thrombomodulin in the anticoagulant pathway is EGF-like 456 (215, 217, 218), whereby thrombin binds EGF5 (218), calcium binds EGF6 to enhance thrombin binding, and protein C interacts with thrombin and EGF456 (185). Binding sites of factor H on thrombomodulin are still unknown, as well as the binding sites on thrombin. Therefore, it was interesting to determine whether factor H could enhance protein C activation with only the regulatory domain of thrombomodulin, EGF456. Rabbit thrombomodulin (purified from lung tissue) shows little difference in structure based on cDNA analysis compared to human form, however the post-translational modifications may cause different phenotype expression (300-302). The effect of factor H was tested in presence of rabbit thrombomodulin to determine if the effect seen was validated with a different source of thrombomodulin (Figure 5.4), and of recombinant thrombomodulin EGF456 to determine whether factor H enhanced protein C activation with only the regulatory domain (Figure 5.4).

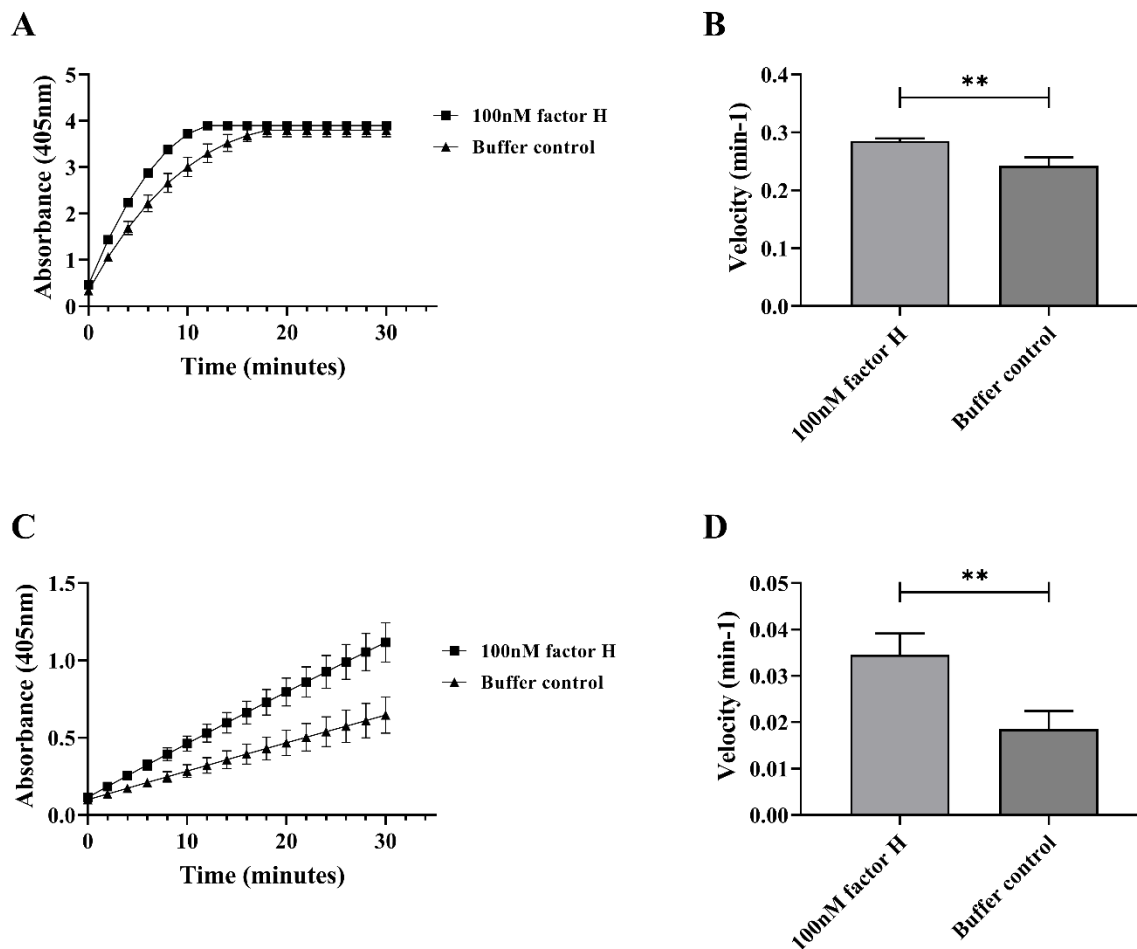


Figure 5.4. Factor H enhances protein C activation in the presence of the soluble rabbit form of thrombomodulin and EGF456. 100nM factor H was incubated with 1.75nM thrombin before addition to (A and B) 10nM rabbit thrombomodulin or (C and D) 500nM EGF456 and added to 200nM protein C. (A and C) Activation of protein C was monitored at 405nm over time and (B and D) velocity was calculated. Factor H enhanced protein C activation significantly in presence of rabbit thrombomodulin (p-value 0.0027) and EGF456 (p-value 0.0038). Results show mean +/-SD (n=3). Welch's t-test was performed, comparing absence and presence of factor H. Illustration representative of two independent experiments.

Rabbit soluble thrombomodulin showed an increase in absorbance at 405nm over time (Figure 5.4A and C), confirming that it could activate human protein C with human thrombin. The highest velocity was observed in presence of rabbit thrombomodulin, at 0.243min^{-1} (Figure 5.4B), then the human form with 0.0812min^{-1} .

These differences could be explained by the glycosylation profiles of each, but also the molecular weight (300, 301). It has been suggested that rabbit thrombomodulin has a higher affinity and a chondroitin sulphate moiety, not always present in the human recombinant form (dependent on expression system), which increases its binding affinity to human thrombin (301, 302). This could explain why there is a higher protein C activation with the rabbit rather than human form of thrombomodulin. The glycosylation profile could also enhance binding of factor H to thrombomodulin and therefore further enhancing protein C activation.

Factor H also enhances protein C activation in the presence of recombinant EGF456. The recombinant EGF456 domains of thrombomodulin is missing the serine-threonine rich domain, which acts as a second binding site for thrombin and enhances the interaction (299, 300). Therefore, a higher concentration of recombinant thrombomodulin EGF456 was required, although there was still lower protein C activation. These results could also indicate that factor H needs other binding sites or interactions on thrombomodulin to exert its full enhancing potential.

Overall, the results demonstrated that factor H enhances protein C activation by the thrombin-thrombomodulin complex regardless of thrombomodulin source, in part through the regulatory domain EGF456.

5.2. In house soluble recombinant full length thrombomodulin and EGF456-ST domains enhance protein C activation

I expressed recombinant constructs of thrombomodulin, including full length (sTM), the lectin-like domain (LLD) and EGF-like 456-Ser/Thr domain (EGF456S/T), and confirmed expression on dot blot and western blot (Appendix A5.2).

The activity of full length soluble thrombomodulin was compared to the R&D construct, and the thrombomodulin EGF456-S/T was compared to TM456 in the activation of protein C activation to determine whether the proteins were expressed and functional (Figure 5.5). Neat volume of the thrombomodulin in house preparations were added to the assay, as the concentration calculation required a specific ELISA kit which was not available during the time of the PhD.

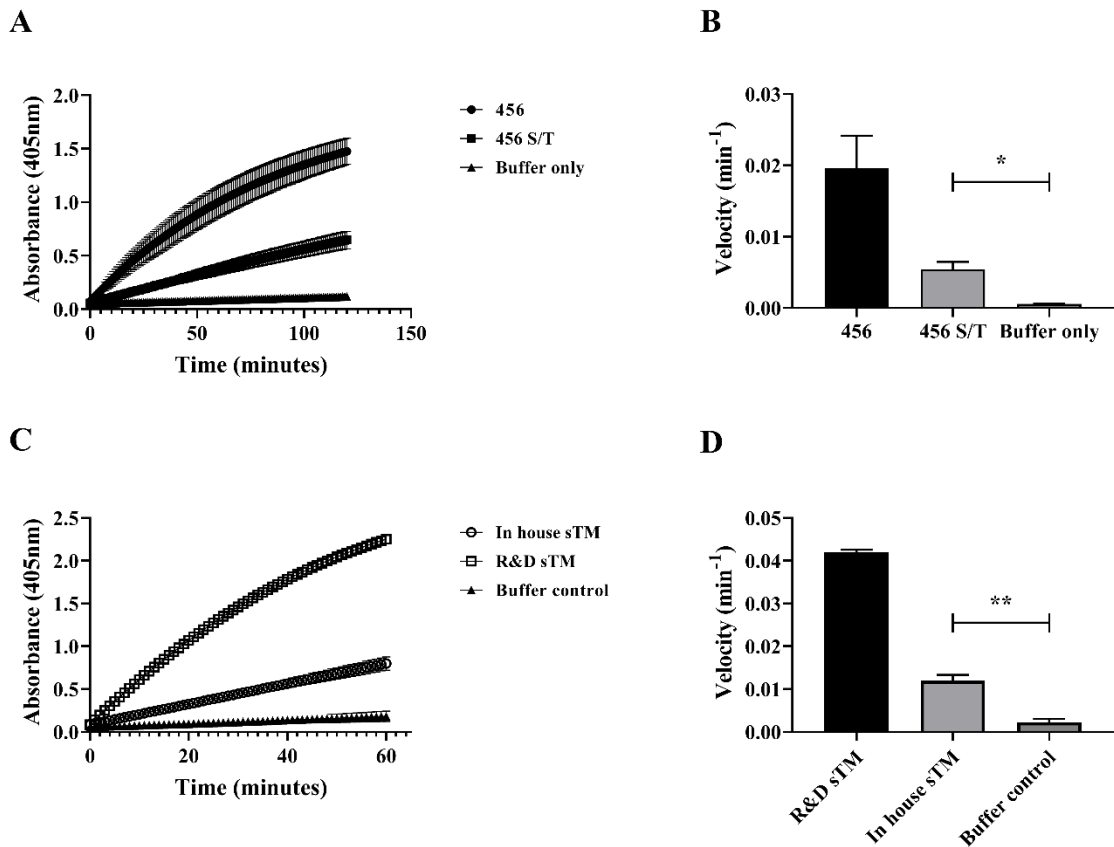


Figure 5.5. Recombinant thrombomodulin constructs soluble full length and 456-S/T generate activated protein C at a low level. (A and B) Recombinant EGF456-S/T (in house) was compared to the recombinant TM456 at 500nM (p-value 0.0142), in presence of 3nM thrombin and 200nM protein C and (C and D) in house soluble recombinant thrombomodulin was compared to R&D recombinant thrombomodulin in the same conditions (p-value 0.0021). (A and C) Activation of protein C was monitored at 405nm over time and (B and D) velocity was calculated. Both constructs showed increased protein C activation compared to the buffer control condition (no thrombomodulin). Results show mean \pm SD (n=3). Welch's t-test was performed comparing thrombomodulin constructs to buffer control condition. Illustration representative of two independent experiments.

Results showed that the recombinant EGF456-S/T enabled protein C activation (p-value 0.0142, Figure 5.5A), compared to the TM456 construct provided by Jim Huntington (Figure 5.5B). Recombinant soluble full length thrombomodulin also showed some activity compared to the buffer only condition (Figure 5.5C), illustrated in the significant increase in rate of activation (p-value 0.0021, Figure 5.5D). The activity is still lower compared to the control thrombomodulin, due to the much lower concentration in the preparation. The next step is to

test the presence of factor H with the thrombomodulin constructs to determine whether factor H can still increase protein C activation.

Chapter 6: Binding of factor H with thrombomodulin, thrombin and fibrinogen

Factor H has been reported to bind with thrombomodulin (1,2), and previous findings from the lab (unpublished) demonstrated that factor H could also bind thrombin with nanomolar affinity. This study confirmed that factor H binding thrombin affected protein C activation by the thrombin/thrombomodulin complex and by thrombin alone. It was also confirmed that factor H enhanced thrombin-mediated fibrinogen cleavage and fibrin clot formation. Next, I wanted to investigate which regions of factor H were involved with specific regions on thrombomodulin and compare binding affinity with thrombin and fibrinogen.

6.1. Analysis of binding between factor H and thrombomodulin

6.1.1. Domain specific anti-thrombomodulin capture antibodies influence thrombomodulin-factor H binding in solid phase binding assays

To determine the binding sites involved in the interaction between thrombomodulin and factor H, domain-specific anti-thrombomodulin antibodies were used as capture antibodies for soluble recombinant thrombomodulin. The specificity of the anti-thrombomodulin antibodies to thrombomodulin was tested first in binding assays (Appendix A6.1), before monitoring the binding of factor H or thrombin to antibody-captured thrombomodulin.

A ligand binding assay on a microtitre plate was designed to analyse the binding of factor H and thrombin and thrombomodulin, in presence or absence of competing anti-thrombomodulin antibodies against EGF5 and EGF6 (Figure 6.1A and C).

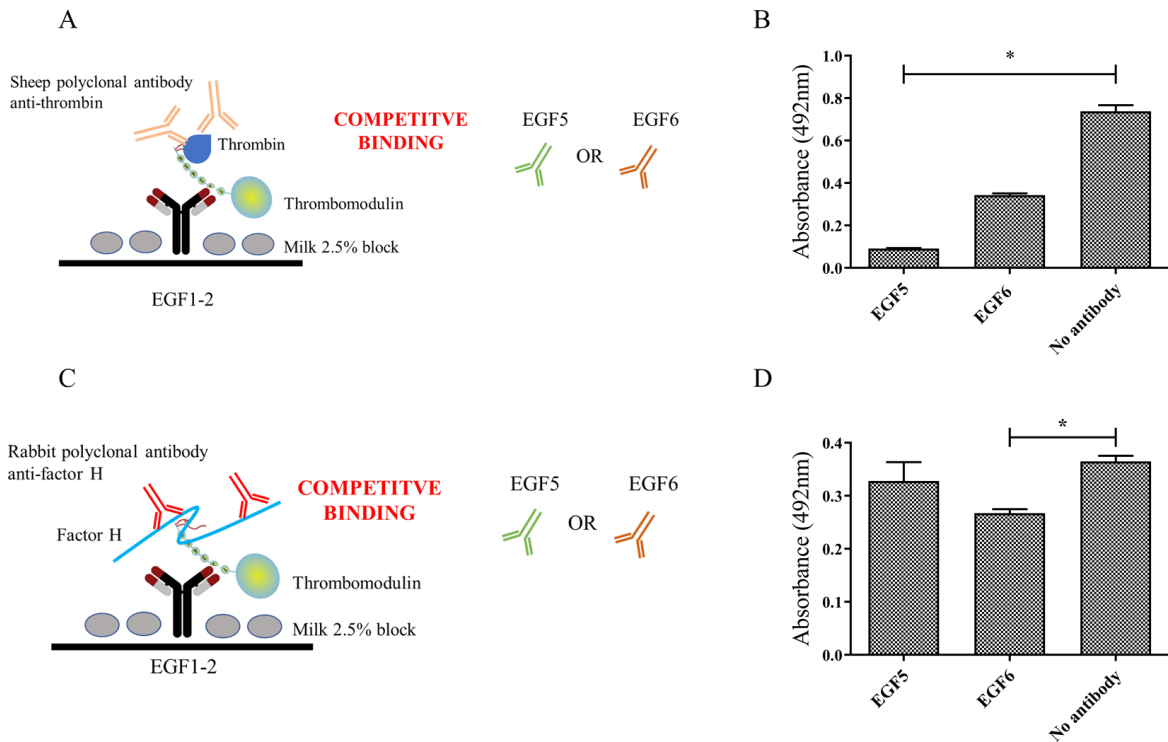


Figure 6.1. Thrombin binds EGF5 and EGF6 of thrombomodulin, and factor H binds EGF6 of thrombomodulin. Thrombomodulin was antibody-captured via anti-EGF1-2 antibody (EGF1-2 is not involved in thrombomodulin binding to thrombin) before addition of (A) factor H or (C) thrombin before addition of anti-thrombomodulin antibodies against EGF5 or EGF6. Thrombin or factor H were detected using specific polyclonal antibodies. Absorbance at 492nm was measured with HRP-conjugated secondary anti-sheep (B) Anti-thrombomodulin EGF5 antibody and EGF6 decreased binding of thrombin to thrombomodulin compared to buffer control. (D) EGF6 antibody decreased binding of factor H to thrombomodulin compared to buffer control. Absorbance at 492nm was measured with HRP-conjugated secondary anti-sheep. Data did not follow Gaussian distribution therefore Kruskal Wallis analysis was performed, results represented by mean +/- SD (n=3), representative of two independent experiment.

Binding of thrombin to thrombomodulin was significantly decreased in presence of anti-EGF5 antibody (0.091 ± 0.002 , p-value 0.0146) and EGF6 antibody (0.343 ± 0.009 , non-significant) antibodies compared to the buffer control (0.738 ± 0.029) (Figure 6.1B). This confirms the literature, stating thrombin binds via exosite I to EGF5 of thrombomodulin and binds in part to EGF6 via exosite II (7). Therefore, the decrease in binding of thrombin in presence of the antibodies confirms its binding sites on thrombomodulin.

This was compared to factor H binding, which was significantly decreased in the presence of the EGF6 antibody (0.267 ± 0.008 , p-value 0.0225) compared to buffer control ($0.365 \pm$

0.011), however not when competing with the EGF5 antibody (0.328±0.036) (figure 6.1D). These results indicated that factor H could potentially bind on EGF6 of thrombomodulin. It is important to consider influences such as steric hindrance of the antibody and factor H's structure in solution, which could interfere with the binding of factor H with thrombomodulin.

6.1.2. Binding interaction analysis of factor H domains interaction with domain specific antibody-captured thrombomodulin using surface plasmon resonance

The binding interaction between factor H and thrombomodulin has been reported previously, and the solid phase binding assay indicated that factor H may bind via EGF6. Therefore, thrombomodulin was captured onto a sensor chip surface via domain-specific antibodies against its LLD, EGF1-2 or EGF6 domains and binding with full length factor H and factor H domain constructs (SCR1-5, 6-8, 8-15, 15-18, 18-20) monitored in real-time. It is important to note that these fragments were expressed in *Pichia pastoris*, therefore did not have the same glycosylation profile as human factor H.

First, we confirmed (this experiment was performed by Dr Heurich) factor H constructs binding to its ligand C3b (Figure 6.2). For all experiments analysing the binding of factor H to C3b or thrombomodulin, factor H full length was not tested due to reagent limitation and as previous reports had already demonstrated the binding (29, 81).

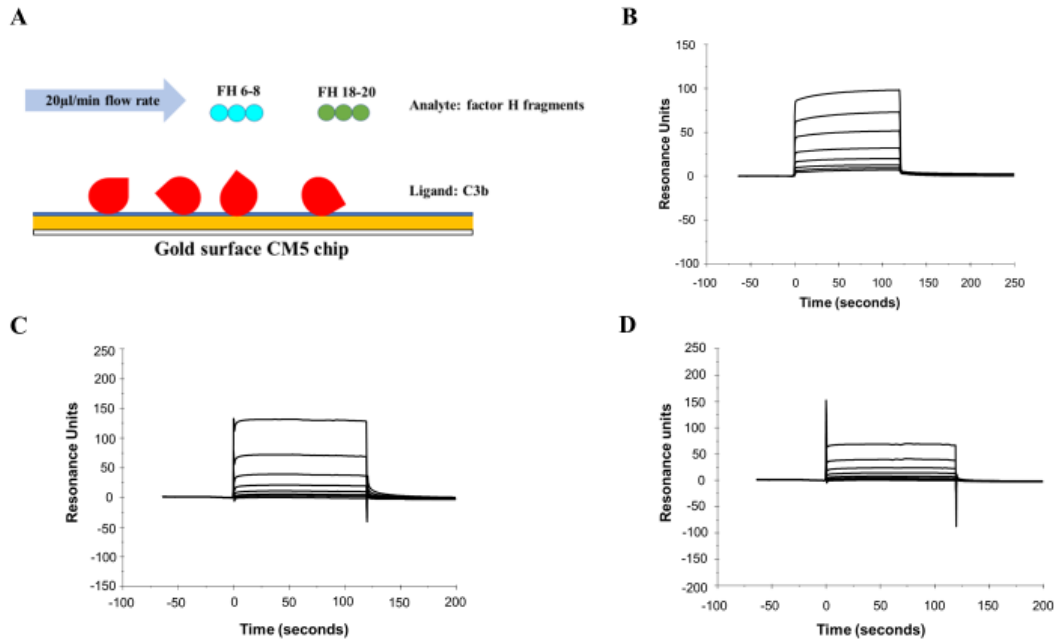


Figure 6.2. Factor H constructs SCR1-5, SCR6-8 and SCR18-20 bind C3b. (A) C3b was immobilised onto a CM5 sensor by amine coupling and factor H or factor H construct binding was monitored at 20 μ l/min. Single injection of factor H constructs SCR1-5, 6-8, 8-15, 15-18, 18-20 (2 μ M) over 120 seconds association (triplicate, repeated once) showed binding of SCR1-5, SCR6-8 and SCR18-20. (B) Affinity (K_D) analysis of binding factor H constructs SCR 1-5 (0.07-5 μ M, K_D 12 μ M, n=1), (C) SCR 6-8 (0.07-5 μ M, K_D =21 μ M, n=1) and (D) SCR 18-20 (0.07-5 μ M, K_D =16 μ M, n=1).

Factor H is known to have three distinct binding sites for C3b (12). Domains SCR1-5 (Figure 6.2B), SCR6-8 (Figure 6.2C), and SCR18-20 (Figure 6.2D) bound to C3b confirming factor H functionality. Binding affinity values for each were:

Table 6.1. Binding affinities K_D of factor H domains SCR1-5, 6-8, 18-20, to C3b, and reported binding affinity from the literature.

Factor H domain	Binding affinity K_D	Reported K_D (70, 80, 303)
SCR1-5	12 μ M (n=1)	SCR1-6: 0.08 μ M
SCR6-8	21 μ M (n=1)	
SCR18-20	16 μ M (n=1)	SCR19-20: 1-2 μ M

The fragments showed binding to C3b, however affinity (K_D) values were lower compared to the literature (13), possibly due to the setup of the experiments and the low number of repeats.

Using the factor H constructs, the interaction between thrombomodulin and factor H was analysed. Thrombomodulin was captured on the surface of a CM5 chip using monoclonal antibodies binding specific thrombomodulin domains. The factor H short recombinant domains were then flowed over to determine binding to thrombomodulin. (Figure 6.3).

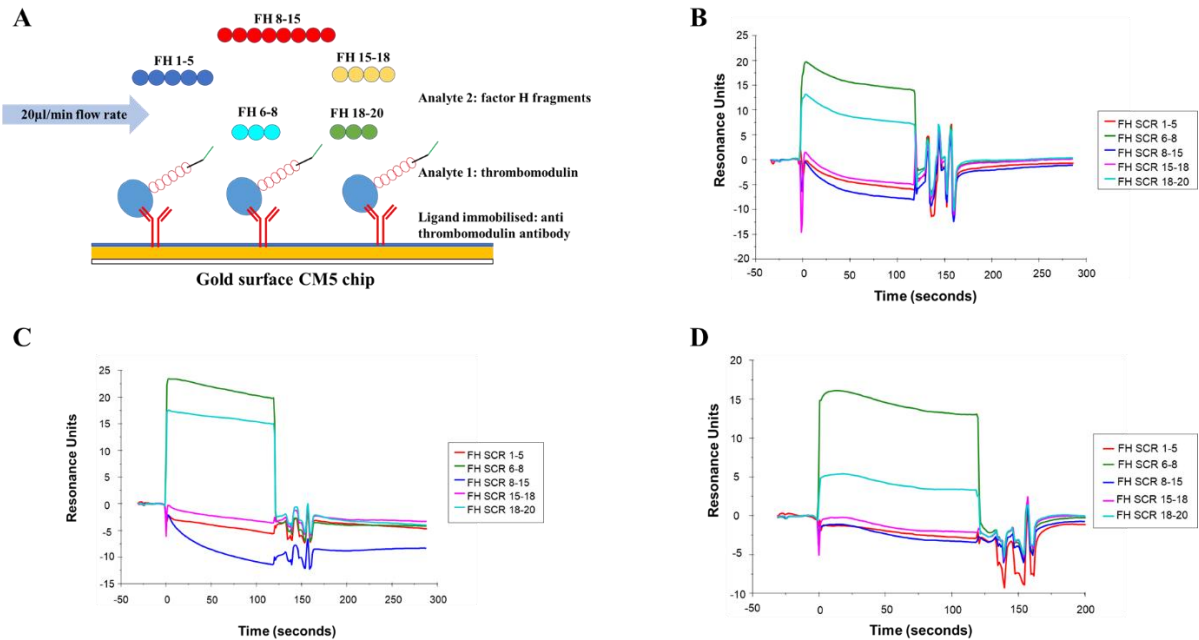


Figure 6.3. Factor H domains SCR6-8 and SCR18-20 bind thrombomodulin independent of capture antibody. (A) Thrombomodulin was captured by domain specific antibodies that were immobilised onto a CM5 sensor by amine coupling and factor H construct binding was monitored at 20µl/min. Single injection of factor H constructs SCR1-5, 6-8, 8-15, 15-18, 18-20 (2µM) over 120 seconds association (triplicate, repeated once) showed binding of SCR6-8 and SCR18-20 when flowed over thrombomodulin captured by domain specific antibodies against (B) lectin like domain, (C) EGF1-2, and (D) EGF6.

Thrombomodulin was captured via the lectin like domain, EGF1-2 and EGF6 and results showed that factor H domains SCR6-8 and SCR18-20 bound to thrombomodulin independent of capture antibody (Figure 6.3B, C, D). The domains corresponding to SCR1-5, SCR8-15 and SCR15-18 did not bind thrombomodulin, regardless of the capture antibody.

Following these results, binding kinetics were performed with SCR6-8 (Figure 6.4) and SCR18-20 (Figure 6.5) to determine binding affinity.

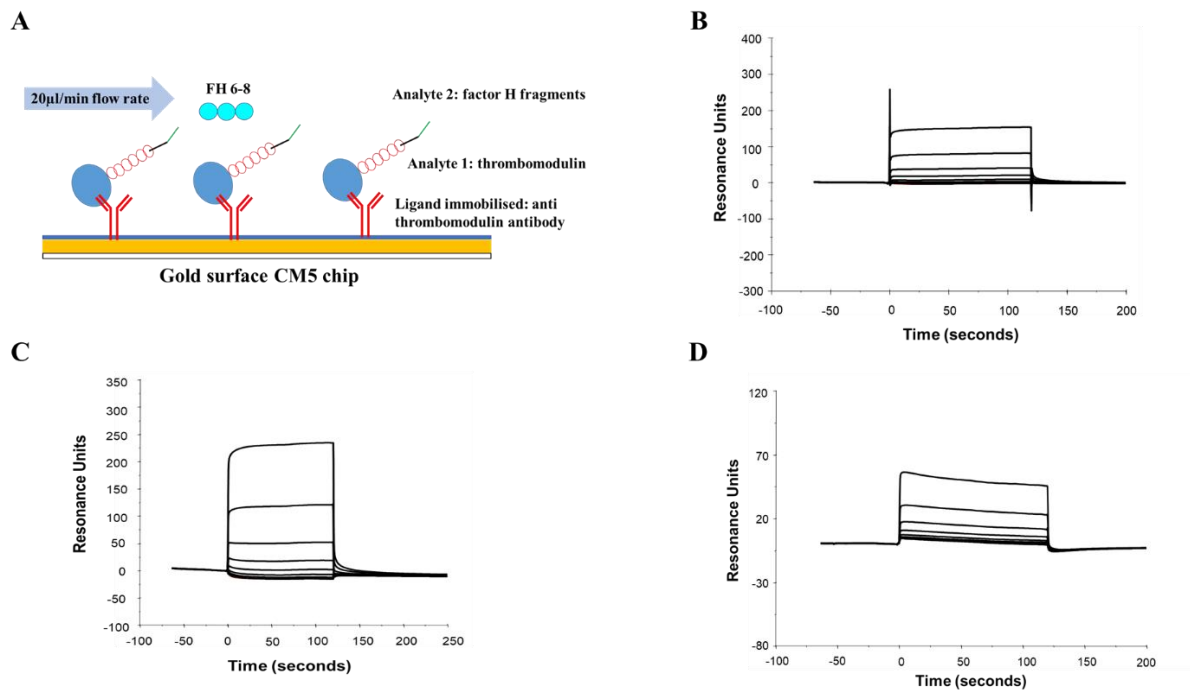


Figure 6.4. Factor H SCR6-8 binds thrombomodulin A) Illustration of binding interaction of $2\mu\text{M}$ factor H domain SCR6-8 titrated ($0.0325\text{-}2\mu\text{M}$) and flowed over at $20\mu\text{l}/\text{min}$, to antibody-captured thrombomodulin. Kinetics were performed and affinity calculated for SCR6-8 binding thrombomodulin captured (B) via the lectin like domain with a K_D of $58.16\mu\text{M}$, (C) via EGF1-2 with a K_D of $169\mu\text{M}$, and (D) via EGF6 with a K_D of $57\mu\text{M}$ ($n=1$ for each antibody setup).

Kinetics results demonstrated that domain SCR6-8 bound with rapid on/off rate to thrombomodulin when captured via the lectin like domain specific antibody (Figure 6.4B) with a K_D of $58.16\mu\text{M}$, EGF1-2 (Figure 6.4B) with a K_D of $169\mu\text{M}$ (Figure 6.4C), and EGF6 (Figure 6.4D) with a K_D of $57\mu\text{M}$. These results show that factor H SCR6-8 binds less to thrombomodulin when the latter is captured via EGF1-2, indicating that factor H may bind EGF1-2 of thrombomodulin, via SCR6-8.

Kinetics were also performed with the factor H SCR18-20 (Figure 6.5).

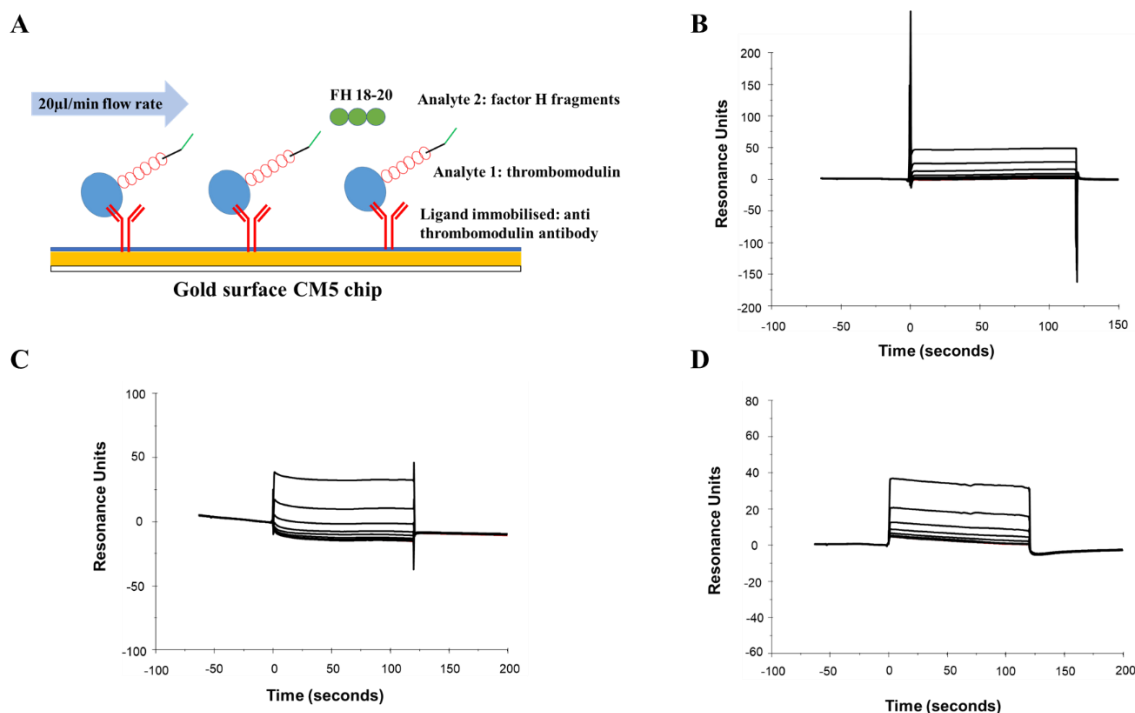


Figure 6.5. Factor H constructs 18-20 bind thrombomodulin. A) Illustration of binding interaction of $2\mu\text{M}$ factor H domain SCR18-20 titrated ($0.0325\text{-}2\mu\text{M}$) and flowed over at $20\mu\text{l}/\text{min}$, to antibody-captured thrombomodulin. Kinetics were performed using steady state affinity and affinity calculated for SCR18-20 binding thrombomodulin captured (B) via the lectin like domain with a K_D of $35.87\mu\text{M}$, (C) via EGF1-2 with a K_D of $66.36\mu\text{M}$, and (D) via EGF6 with a K_D of $237\mu\text{M}$ ($n=1$ for each antibody setup).

Factor H SCR18-20 bound with rapid on/off rate to thrombomodulin when captured via the lectin like domain (Figure 6.5B) with a K_D of $35.87\mu\text{M}$, EGF1-2 (Figure 6.5B) with a K_D of $66.36\mu\text{M}$ (Figure 6.5C), and EGF6 (Figure 6.5D) with a K_D of $237\mu\text{M}$. These results show that factor H SCR18-20 binds less to thrombomodulin when the latter is captured via EGF6, indicating that factor H could bind EGF6 of thrombomodulin via SCR18-20. This supports the solid phase binding assays (Figure 6.1), whereby factor H competed with anti-EGF6 antibody for binding to thrombomodulin.

The affinity values corresponding to binding interaction between factor H domains SCR6-8 and SCR18-20 are summarised in Table 6.2.

Table 6.2. Binding affinities (K_D) of factor H domains SCR6-8 and 18-20, to thrombomodulin captured via antibodies lectin like domain, EGF1-2 and EGF6.

Thrombomodulin capture antibody	Factor H SCR6-8 (K_D)	Factor H SCR18-20 (K_D)
Lectin like domain	58.16μM (n=1)	35.87μM (n=1)
EGF1-2	169μM (n=1)	66.36μM (n=1)
EGF6	57μM (n=1)	237μM (n=1).

Overall, the results indicate that the binding of factor H SCR 6-8 and SCR 18-20 to thrombomodulin is not blocked by capturing thrombomodulin via its lectin-like domain, EGF1-2 nor EGF6, as binding was detectable when using these antibodies. However, binding affinity was reduced for SCR6-8 binding to thrombomodulin when captured via anti-EGF1-2 antibody and was also reduced for SCR18-20 when captured via anti-EGF6 antibody, the latter also confirming the solid phase binding assay. Factor H domains SCR 1-5 containing its regulatory ability (9), did not bind thrombomodulin with any capture method.

6.2. Binding analysis of factor H with thrombin

6.2.1. Binding affinity of factor H with thrombin

After determining that factor H had an impact on thrombin's pro and anticoagulant roles, their binding interaction was analysed using surface plasmon resonance (Figure 6.6).

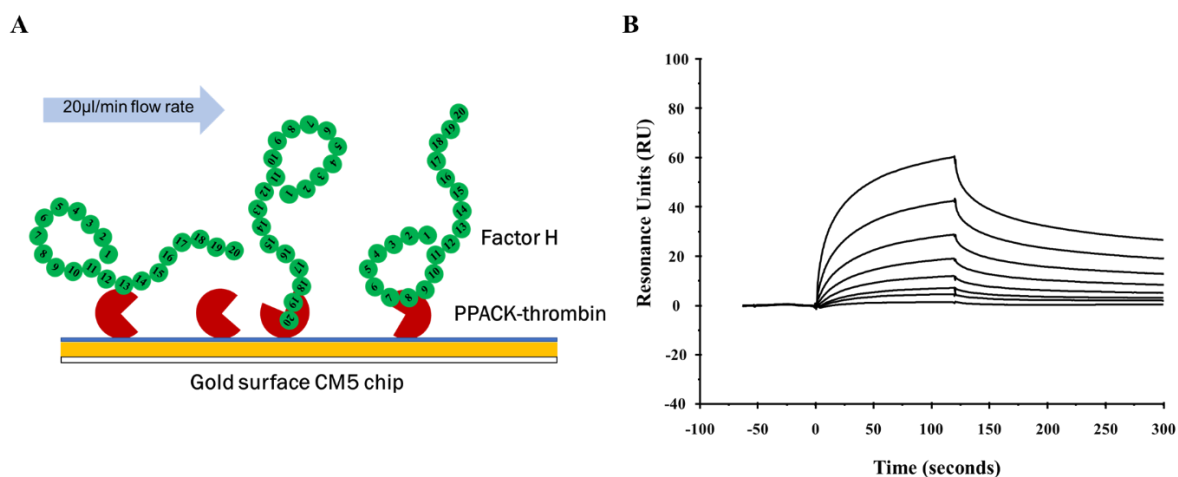


Figure 6.6. Factor H binds with nanomolar affinity to immobilised PPACK-thrombin. (A) Thrombin was immobilised onto a CM5 sensor by amine coupling and factor H binding was monitored at 20 µl/min. (B) Kinetics were measured by flowing factor H (3.125-200nM) and affinity calculated using 1:1 binding with binding affinity K_D of 29.7 +/- 1.08nM. (n=3).

After testing binding with single injects, kinetics were performed and binding affinity of factor H with catalytically inactive PPACK-thrombin (Figure 6.6A) was estimated at 29.7 +/- 1.08nM (Figure 6.6B). This indicated a strong interaction between both proteins. It is important to note that the binding interaction between factor H and thrombin is extremely avid, as no plateau is reached therefore steady state binding is not reached, indicating potentially multiple binding sites involved. Therefore the analysis chosen may not be as accurate as it assumes one to one binding, with only one binding site on each protein.

6.2.2. Binding of factor H SCR domains with thrombin

Next, factor H SCR constructs were flowed over immobilised thrombin to determine which sites in factor H were involved in the binding interaction (Figure 6.7). These results were generated by my supervisor Dr Meike Heurich when I was learning the technique.

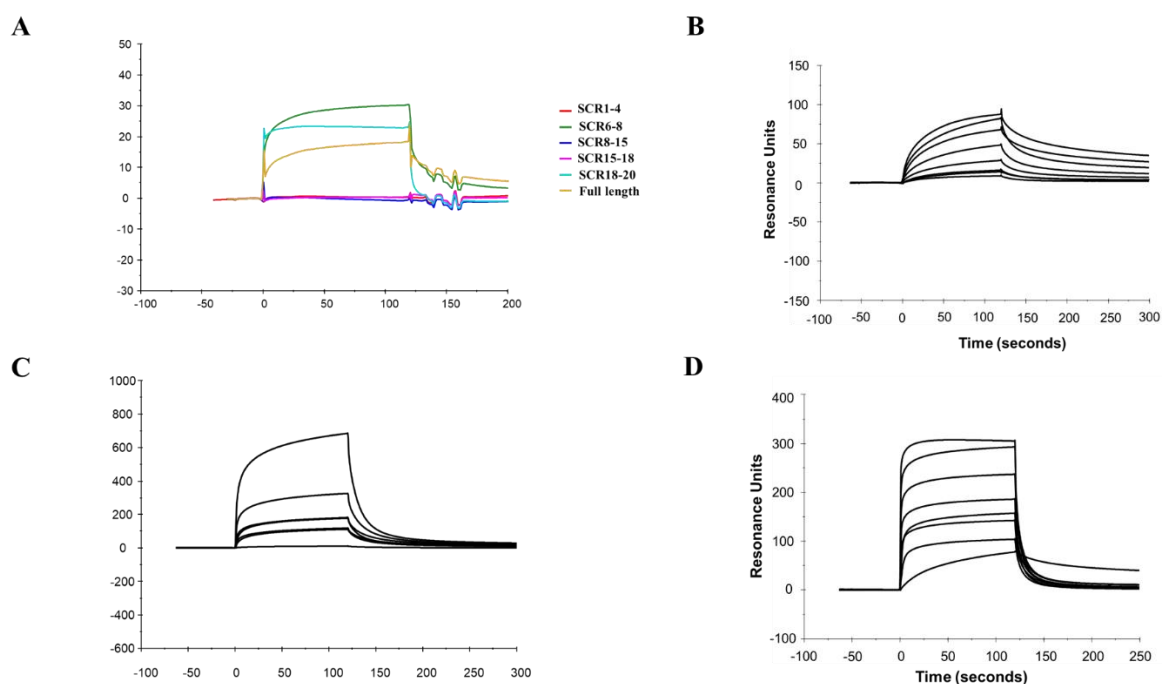


Figure 6.7. Factor H SCR1-4, SCR6-8 and SCR18-20 bind thrombin. Binding interaction of factor H SCR constructs flowed over at 20 μ l/min, to thrombin immobilised to the chip surface. (A) Single injection of factor H constructs SCR1-4, 6-8, 8-15, 15-18, 18-20 (2 μ M) over 120 seconds association (triplicate n=1). Affinity K_D analysis of binding factor H constructs (B) SCR1-4 was calculated with 1:1 binding analysis ($K_D=2.96\mu$ M, n=1), (C) SCR6-8 was calculated with 1:1 binding ($K_D=2.9\mu$ M, n=1) and (D) SCR18-20 was calculated with steady-state binding analysis ($K_D=1.14\mu$ M, n=1).

Factor H SCR 1-4 (Figure 6.7B), 6-8 (Figure 6.7C) and 18-20 (Figure 6.7D) constructs all bound thrombin with micromolar affinity, although there were differences in kinetics. Binding affinities were calculated and are summarised in Table 6.3.

Table 6.3. Binding affinities of factor H domains SCR1-4, 6-8 and 18-20, to thrombin captured to the surface. Kinetics were repeated one time only for each construct.

Factor H domain	SCR1-4	SCR6-8	SCR18-20
Binding affinity (K_D) for thrombin (n=1)	2.96 μ M	2.9 μ M	1.14 μ M

Results demonstrated factor H binds thrombin at SCR1-4, albeit with relatively weak affinity, indicating that a potential effect of thrombin on factor H regulatory activity is minor, as Dr.

Heurich had observed previously in complement regulatory assays (results were generated before my arrival in Cardiff). This also confirms the observation of the potential binding site of thrombin with factor H SCR2-3 due to structural homology with factor I (59).

The binding affinity of factor H SCR6-8 and SCR18-20 with thrombin indicates that these regions are likely important for the interaction between factor H and thrombin, and both contribute to the overall binding affinity of factor H with thrombin.

6.3. Binding of factor H with fibrinogen

6.3.1. Binding of factor H with fibrinogen using a solid phase binding assay

Factor H has been reported to bind both fibrinogen and fibrin (14,15) and has been found within the clot (239, 240, 242-244). To validate this, fibrinogen was attached to the well surface via passive adhesion, and factor H was titrated and detected using a polyclonal anti-factor H antibody (Figure 6.8).

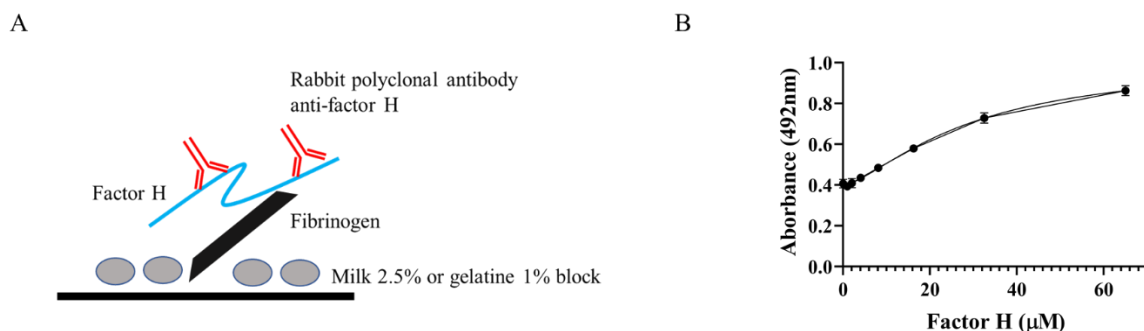


Figure 6.8. Factor H binds fibrinogen in a concentration dependent manner. (A) ELISA set up for fibrinogen (15µM) captured on the surface by passive adhesion and blocked using milk 2.5% with binding to factor H (1.01-65µM), and absorbance measured at 492nm. Factor H binds fibrinogen in a dose dependent manner (r value 0.9762, p-value 0.0004). EC50 was calculated and estimated at 47.05±11.05µM. EC50 was calculated using non-linear regression fit. Correlation was calculated using nonparametric Spearman correlation. Results represented as mean ± SD (triplicate), figure representative of 3 independent experiments.

Factor H binding to fibrinogen was detected using a polyclonal anti-factor H antibody (Figure 6.8A). Factor H bound to fibrinogen increasingly in a factor H concentration dependent manner (Figure 6.8B) and factor H concentration was significantly correlated to absorbance (r value 0.9762, p-value 0.0004 for both blocking agents). The half effective concentration EC50 was estimated at $47.05 \pm 11.05 \mu\text{M}$. It was important to note that there was These results indicated that factor H bound significantly to fibrinogen.

6.3.2. Binding of factor H with fibrinogen

To further analyse the interaction between factor H and fibrinogen, surface plasmon resonance was performed with fibrinogen immobilised to the chip surface and factor H flowed over (Figure 6.10) and compared to thrombin (Figure 6.9), also immobilised to the surface.

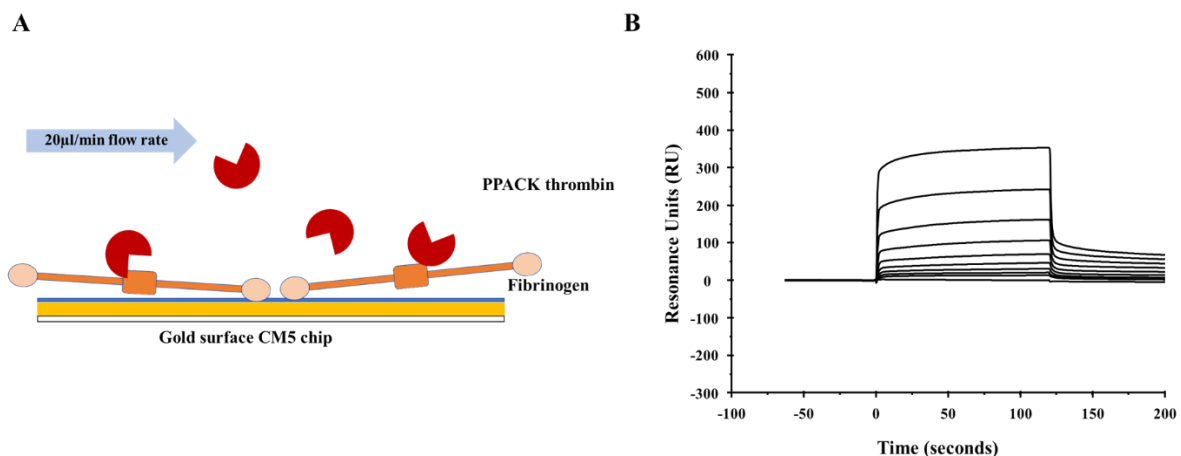


Figure 6.9. Thrombin binds with micromolar affinity to immobilised fibrinogen. A) Illustration of binding interaction of thrombin ($0.0075\text{--}2 \mu\text{M}$) at $20 \mu\text{l}/\text{min}$, to immobilised fibrinogen (10000 resonance units captured on the surface). (B) Kinetics were performed, and affinity calculated using steady state affinity for thrombin binding to fibrinogen, $K_D = 1.37 \pm 0.23 \mu\text{M}$. ($n=3$).

The binding affinity between thrombin and fibrinogen, based on the results was $1.37 \pm 0.23 \mu\text{M}$ (Figure 6.9B) was comparable to the literature ($2\text{--}5 \mu\text{M}$, (149)), confirming fibrinogen's functionality.

Next, factor H binding to fibrinogen was further explored using surface plasmon resonance and the binding affinity determined (Figure 6.10).

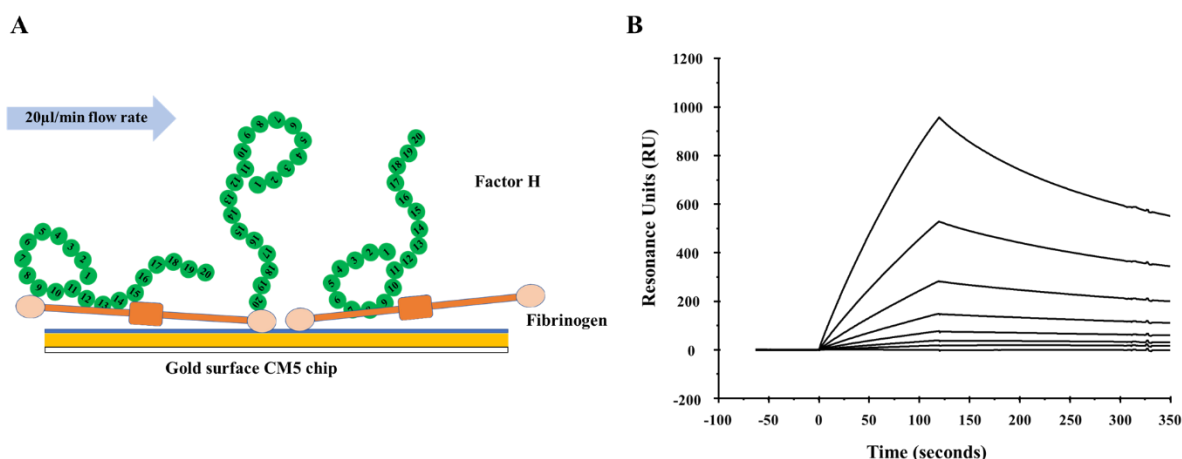


Figure 6.10. Factor H binds with nanomolar affinity to immobilised fibrinogen. A) Illustration of binding interaction of factor H (3.125-200nM) at 20 μ l/min, to immobilised fibrinogen (10000 resonance units captured on the surface). (B) Kinetics were performed, and affinity calculated using 1:1 binding for factor H binding to fibrinogen, $K_D=38.21\pm 0.93$ nM. (n=6).

Results showed that factor H bound strongly with fibrinogen, with a binding affinity of $K_D\sim 38.21\pm 0.93$ nM (Figure 6.10B), indicating significant interaction. This is approximately 25-fold higher than thrombin binding fibrinogen. A very dense surface of fibrinogen was generated, due to a mistype when setting up the chip. The interaction between factor H and fibrinogen is extremely avid once again, indicating that a 1:1 binding may not be accurate. It would be interesting to repeat the experiment with a less dense surface of fibrinogen. However, despite this result, I can confirm the strong binding occurring between factor H and fibrinogen, as the control interaction between thrombin and fibrinogen is comparable to the literature as mentioned above.

6.4. *In silico* analysis of binding interactions of thrombin and factor H

To further understand the interactions between factor H and thrombin, molecular modelling was used to analyse the residues involved in the binding interaction, and to support the experimental data. For this, the software Molecular Operating Environment (MOE) was used to first build a full-length factor H model using homology modelling, and then to analyse the residues involved in the interaction between factor H and thrombin. It is important to note that

these are not fixed data, rather a model that supports the experimental data. Further studies are required to determine the exact residues involved in the interaction.

6.4.1. Building the full-length factor H homology model

No crystal structure is available for full-length factor H, as the protein is too long and flexible in solution (277). Individual sections of the protein have been crystallised using nuclear magnetic resonance (NMR) or X-ray diffraction (276, 277). A structure of the full-length protein has been done using solution scattering (62, 285), however this method has very low resolution, making the model unreliable.

I determined that no structure exists for SCR 14 and 17 of factor H (Materials and Methods, Table 2.11), therefore homology modelling was performed to obtain the missing pieces for building the full-length structure. Although there was a structure based on solution scattering for SCR 16-20, the resolution was too high.

A PSI-BLAST search was performed to determine which protein available in PDB was the most similar, or homolog to SCR14 and SCR17. In MOE, the FASTA sequences of the protein of interest and the template PDB file are uploaded from BLAST, before construction of the homology model. The structure built is verified with the Ramachandran plot. Table 6.4 represents the hits with the highest scores, the structures with the E-value (the expected value, therefore the number of alignments that have a score above or equal to the score which occurred in the database by chance) higher than the threshold for the PDB files homologous to SCR14 and the percentage identity (which corresponds to the extent to which the amino acid sequences have the same residues at the same position in the alignment).

Table 6.4. List of homologous proteins to SCR14 ranked according to the max score. The sequence corresponding to SCR14 was entered into protein-protein BLAST, and a PSI-BLAST search in Protein Database Bank (PDB) was performed. The E-value is the number of alignments that have a score above or equal to the score which occurred in the database by chance), and the percentage identity corresponds to how many base pairs are the same between the two sequences compared). 1HF1A was obtained by solution NMR and had the highest percentage identity, therefore was selected as the template for SCR14 homology modelling.

	Description	Max score	Total score	Query cover	E value	Per. Ident	Accession	Select for PSI blast	Used to build PSSM	Newly added
<input checked="" type="checkbox"/>	Chain A_Four Models Of Human Factor H Determined By Solution Scattering Curve-Fitting	122	477	100%	5e-35	100.00%	1HAQ_A	<input checked="" type="checkbox"/>		
<input checked="" type="checkbox"/>	Chain A_Complement factor H [Homo sapiens]	122	479	100%	5e-35	100.00%	3GAU_A	<input checked="" type="checkbox"/>		
<input checked="" type="checkbox"/>	Chain A_FACTOR H_15TH C-MODULE PAIR [Homo sapiens]	38.5	38.5	93%	5e-06	35.09%	1HFL_A	<input checked="" type="checkbox"/>		
<input checked="" type="checkbox"/>	Chain A_COMPLEMENT FACTOR H [Homo sapiens]	39.7	39.7	98%	5e-06	32.76%	4B2R_A	<input checked="" type="checkbox"/>		
<input checked="" type="checkbox"/>	Chain A_COMPLEMENT FACTOR H [Homo sapiens]	39.7	70.5	98%	5e-06	32.76%	4B2S_A	<input checked="" type="checkbox"/>		
<input checked="" type="checkbox"/>	Chain A_Complement Factor H-related Protein 2 [Homo sapiens]	39.7	39.7	96%	5e-06	35.09%	3ZD1_A	<input checked="" type="checkbox"/>		
<input checked="" type="checkbox"/>	Chain A_FACTOR H_15TH AND 16TH C-MODULE PAIR [Homo sapiens]	38.1	67.8	94%	2e-05	35.09%	1HFH_A	<input checked="" type="checkbox"/>		
<input checked="" type="checkbox"/>	Chain A_Complement Factor H-related Protein 1 [Homo sapiens]	36.6	36.6	96%	7e-05	33.33%	4MUC_A	<input checked="" type="checkbox"/>		
<input checked="" type="checkbox"/>	Chain A_COMPLEMENT FACTOR H [Homo sapiens]	36.6	36.6	96%	7e-05	33.33%	2BZM_A	<input checked="" type="checkbox"/>		
<input checked="" type="checkbox"/>	Chain D_Complement Factor H-related Protein 1 [Homo sapiens]	36.6	59.3	96%	7e-05	33.33%	3RJ3_D	<input checked="" type="checkbox"/>		
<input checked="" type="checkbox"/>	Chain D_Complement factor H [Homo sapiens]	36.6	36.6	96%	7e-05	33.33%	5NBQ_D	<input checked="" type="checkbox"/>		

Structures obtained by solution scattering were excluded from the search as the resolution obtained with this technique is too high. 1HAQ.A and 3GAU.A were not considered. 1HFI.A, 4B2R.A, 4B2S.A, 3ZD1.A had the same lowest E-value (the homologs generated least due to chance), however 1HFI.A (structure obtained from NMR) had the highest percentage identity out of all of them, therefore the highest identity between the sequence of interest and the homolog sequence). Therefore, this PDB file was selected to obtain the homology model of SCR14 of factor H.

The homology search was also performed in MOE, to compare with the PSI-BLAST search. MOE determined that the closest sequence was 1HFH.A, which according to BLAST, had a lower E-value compared to 1HFI.A, but a higher query cover. As the E-value gives more reliable homologs, 1HFI.A was selected as the homolog sequence to determine the model of SCR14 (Figure 6.11).

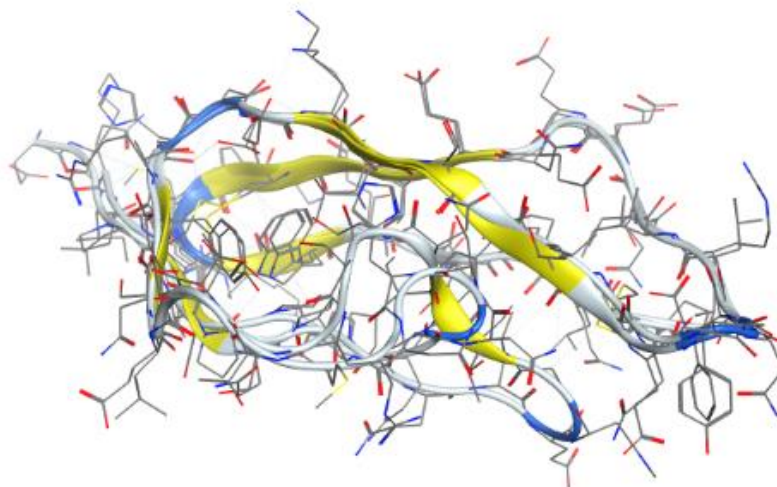


Figure 6.11. Homology model of SCR14 of factor H. SCR14 model was obtained using the pdb 1HFI.A as a template, and running a AMBER12:EHT forcefield. Atoms are represented as ball and stick, and protein backbone as yellow ribbon. The model was verified using a Ramachandran plot

After determining the model for SCR14 (Figure 6.11), a Ramachandran plot is done to verify and analyse accuracy of the model, by looking at the secondary structure of the peptides within the homology model (Appendix Figure A6.2). Based on the Ramachandran plot, the predominant secondary structures of SCR14 are beta strands, as the Phi-Psi coordinates for most residues are located in the upper left region of the plot. Two outliers were noted, proline 5 and proline 10 of the homology model.

Next, the homology model was created for SCR17 of factor H also following the same procedure as for the construction of the SCR14 homology model. The best fitted model was selected using PSI-BLAST (Table 6.5).

Table 6.5. List of homologous proteins to SCR17 ranked according to the max score. The sequence corresponding to SCR17 was entered into protein-protein BLAST, and a PSI-BLAST search in Protein Database Bank (pdb) was performed. The E-value is the number of alignments that have a score above or equal to the score which occurred in the database by chance), and the percentage identity corresponds to how many base pairs are the same between the two sequences compared). 3SWO.X was obtained by solution NMR and had the highest percentage identity, therefore was selected as the template for SCR17 homology modelling.

	Description	Max score	Total score	Query cover	E value	Per. Ident	Accession	Select for PSI blast	Used to build PSSM	Newly added
<input checked="" type="checkbox"/>	Chain A_Solution Structure Of The C-Terminal Scr-1620 FRAGMENT OF Complement Factor H [Homo sapiens]	127	255	100%	6e-38	100.00%	2QFH_A	<input checked="" type="checkbox"/>		
<input checked="" type="checkbox"/>	Chain A_Complement factor H [Homo sapiens]	125	442	100%	5e-36	100.00%	3GAU_A	<input checked="" type="checkbox"/>		
<input checked="" type="checkbox"/>	Chain A_Four Models Of Human Factor H Determined By Solution Scattering Curve-Fitting And Homology Modelling [Homo sapiens]	125	442	100%	5e-36	100.00%	1HAQ_A	<input checked="" type="checkbox"/>		
<input checked="" type="checkbox"/>	Chain X_Complement Factor H [Homo sapiens]	51.2	87.4	100%	4e-10	37.29%	3SW0_X	<input checked="" type="checkbox"/>		
<input checked="" type="checkbox"/>	Chain A_16TH COMPLEMENT CONTROL PROTEIN [Homo sapiens]	41.6	41.6	93%	3e-07	30.91%	1HCC_A	<input checked="" type="checkbox"/>		
<input checked="" type="checkbox"/>	Chain A_FACTOR H_15TH AND 16TH C-MODULE PAIR [Homo sapiens]	41.2	71.6	94%	1e-06	30.91%	1HFH_A	<input checked="" type="checkbox"/>		
<input checked="" type="checkbox"/>	Chain A_Complement Factor H-related Protein 2 [Homo sapiens]	40.8	40.8	66%	2e-06	38.46%	3ZD1_A	<input checked="" type="checkbox"/>		
<input checked="" type="checkbox"/>	Chain A_Structure Of Complement Factor H Variant Q1139a [Homo sapiens]	38.1	38.1	93%	3e-05	30.91%	3KXV_A	<input checked="" type="checkbox"/>		
<input checked="" type="checkbox"/>	Chain C_COMPLEMENT FACTOR H [Homo sapiens]	37.7	37.7	93%	3e-05	30.91%	2XQW_C	<input checked="" type="checkbox"/>		
<input checked="" type="checkbox"/>	Chain B_Complement Factor H [Homo sapiens]	37.7	37.7	93%	3e-05	30.91%	4J38_B	<input checked="" type="checkbox"/>		
<input checked="" type="checkbox"/>	Chain D_Complement factor H [Homo sapiens]	36.2	36.2	93%	1e-04	29.09%	5NBQ_D	<input checked="" type="checkbox"/>		
<input checked="" type="checkbox"/>	Chain A_Complement Factor H [Homo sapiens]	36.2	36.2	93%	1e-04	29.09%	2G7I_A	<input checked="" type="checkbox"/>		
<input checked="" type="checkbox"/>	Chain A_Complement Factor H-related Protein 1 [Homo sapiens]	36.2	36.2	93%	1e-04	29.09%	4MUC_A	<input checked="" type="checkbox"/>		
<input checked="" type="checkbox"/>	Chain D_Complement Factor H-related Protein 1 [Homo sapiens]	36.2	36.2	93%	1e-04	29.09%	3RJ3_D	<input checked="" type="checkbox"/>		
<input checked="" type="checkbox"/>	Chain A_COMPLEMENT FACTOR H [Homo sapiens]	36.2	36.2	93%	1e-04	29.09%	2BZM_A	<input checked="" type="checkbox"/>		
<input checked="" type="checkbox"/>	Chain A_Complement factor H [Homo sapiens]	36.2	36.2	93%	1e-04	29.09%	3R62_A	<input checked="" type="checkbox"/>		
<input checked="" type="checkbox"/>	Chain A_Structure Of Complement Factor H Variant R1203a [Homo sapiens]	36.2	36.2	93%	1e-04	29.09%	3KZJ_A	<input checked="" type="checkbox"/>		
<input checked="" type="checkbox"/>	Chain C_Complement factor H, Complement factor H [Homo sapiens]	36.2	67.0	96%	2e-04	29.09%	5Q35_C	<input checked="" type="checkbox"/>		

The pdb file 3SWO.X was selected as a template for the homology model of SCR17 of factor H. 2QFH.A, 3GAU.A, and 1HAQ.A had the highest percentage identities however the structures were obtained by solution scattering therefore were not selected due to high resolution. 3SWO.X had the highest percentage identity, and the lowest E-score (Table 6.5).

With 3SWO.X as a template, the homology model of SCR17 was built (Figure 6.12).

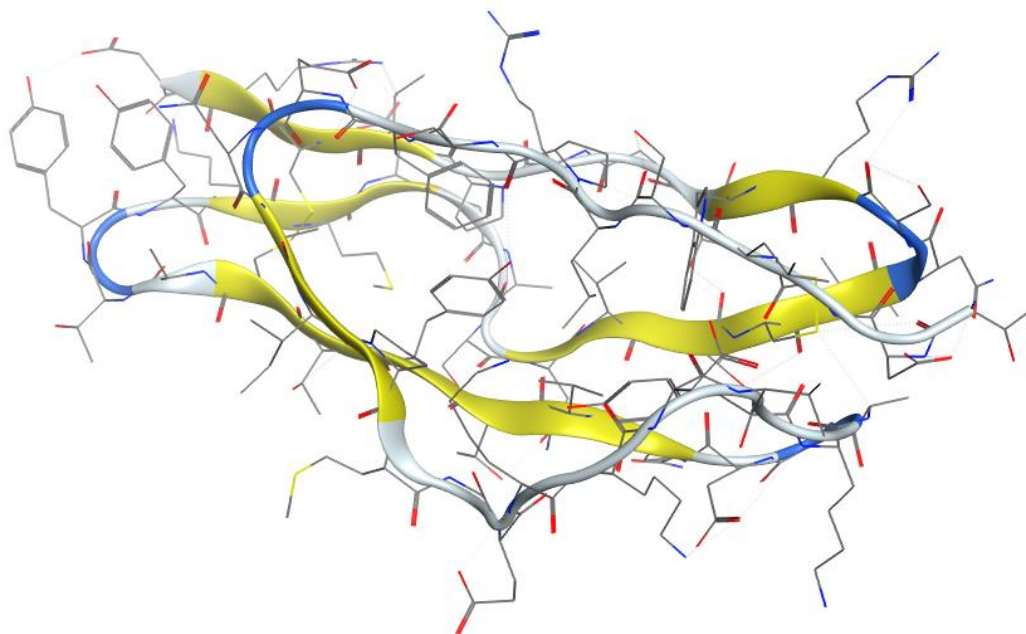


Figure 6.12. Homology model of SCR17 of factor H. SCR14 model was obtained using the pdb 3SWO.X as a template, and running a AMBER12:EHT forcefield. Atoms are represented as ball and stick, and protein backbone as ribbon.

The homology model of SCR17 (Figure 6.12) was verified using a Ramachandran plot (Appendix Figure A6.3). Based on the Ramachandran plot, the predominant secondary structures of SCR17 are beta strands, as the Phi-Psi coordinates for most residues are located in the upper left region of the plot. One outlier was noted, aspartate 2, of the homology model.

After building homology models for the two regions that did not have corresponding structures, the factor H molecule was built. The individual structures were manually assembled using overlapping residues with help from Professor Andrea Brancale (Pharmacy, Cardiff University) (Figure 6.13).

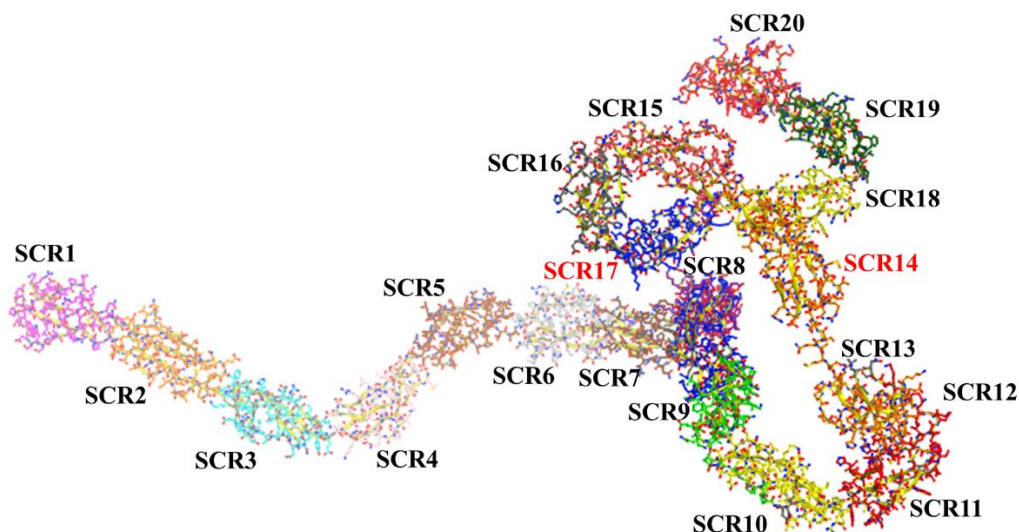


Figure 6.13. Model of full-length factor H. Homology models were performed for domains SCR14 (residues in orange, red marking) and SCR17 (residues in blue, red marking), for which no pdd file was available. Each structure for each region was manually assembled using overlapping residues. This work was performed by Andrea Brancale. Atoms are represented as ball and stick, and protein backbone as ribbon.

After assembling and building the full-length factor H structure, protein-protein docking was performed between factor H and thrombin, factor H and thrombomodulin and factor H and the thrombin-thrombomodulin complex, therefore I modelled the interaction using individual domain constructs, based on the data obtained with the ELISA work and SPR analysis. First, the binding of SCR19-20 was analysed with each protein individually (thrombin or thrombomodulin EGF456) or complexed together (thrombin-EGF456), before performing the same binding interaction with full length factor H. SCR19-20 was chosen, as it is a key regulatory domain of factor H and was involved in the binding to thrombin and thrombomodulin based on the experimental data.

6.4.2. Modelling the binding interaction between factor H SCR19-20 and full-length, and thrombin

Based on the experimental surface plasmon resonance data, factor H SCR18-20 bound with thrombin, and evidence showed that thrombin competed with factor H for binding to heparin

(Appendix Figure A6.4), which is in part mediated through overlapping SCR19-20. Mutations linked to aHUS on factor H are situated in SCR19-20, therefore to narrow down one of the regions involved in the interaction, SCR19-20 was selected to test the binding to thrombin (Figure 6.14).

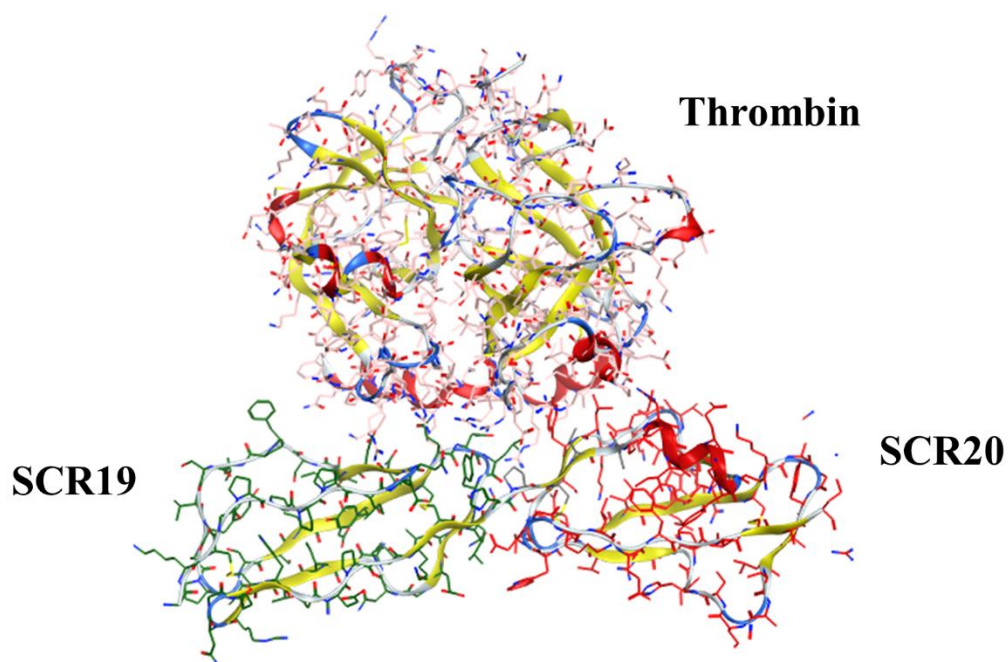


Figure 6.14. Binding interaction between SCR19-20 (PDB ID 2G7I) of factor H and thrombin (PDB ID 1YPG). The binding interaction model between SCR19 (in green) and SCR20 (in red) of factor H SCR19-20 (PDB ID 2G7I), and thrombin (PDB ID 1YPG), was performed using protein-protein docking in MOE, and the interaction with the 1st lowest score, that is equivalent to the least energy required for the interaction, was chosen. Thrombin exosite II is engaged in the interaction. Atoms are represented as ball and stick, and protein backbone as ribbon.

Figure 6.14 represents the interaction between SCR19-20 of factor H and thrombin with the lowest score, therefore the least energy required for the interaction to occur (score -64.07, E_refine -64.0706). The residues involved in the interaction were reported for each protein:

Table 6.6. Residues involved in the interaction between thrombin (PDB ID 1YPG) and factor H SCR19-20 (PDB ID 2G7I). Residues from thrombin exosite I are noted in bold, exosite II are underlined and the 60 loop in turquoise. Factor H SCR19 is noted in green, SCR20 in red.

Thrombin	Factor H SCR19-20
----------	-------------------

Exosite I: in bold Exosite II: underlined 60 loop: turquoise	SCR19 (aa1107-1165): green SCR20 (aa1170-1230): red
H91, P92, R93 , <u>R101</u> , R126, A129a, S129b, L130, Q131, A132, E164, R165, P166, D178, N179, M180, H230, F232, <u>R233</u> , L234, K235, <u>K236</u> , W237, I238, <u>K240</u> , Q244, F245.	P1114, I1115, D1116, N1117, G1118, D1119, I1120, T1121, S1122, F1123, Q1137, C1138, Q1139, N1140, L1141, Y1142, P1166, V1168, I1169, S1170, R1171, E1172, Q1187, K1188, L1189, Y1190, R1192, E1195

Exosite II of thrombin comprises residues R93, K236, K240, R101 and R233, which are all involved in the interaction with SCR19-20 described above. Exosite I is composed of K36, H71, R73, R75, Y76, R77a, K109/110. Therefore, the model supports the experimental data, whereby thrombin competed with heparin for the binding to factor H (Appendix Figure A6.4) and binds with SCR18-20 with an affinity $K_D=1.14\mu\text{M}$. Therefore, exosite II could be involved in the binding to factor H SCR19-20.

The interaction between thrombin and the full-length factor H protein was then modelled, as presented in figure 6.15.

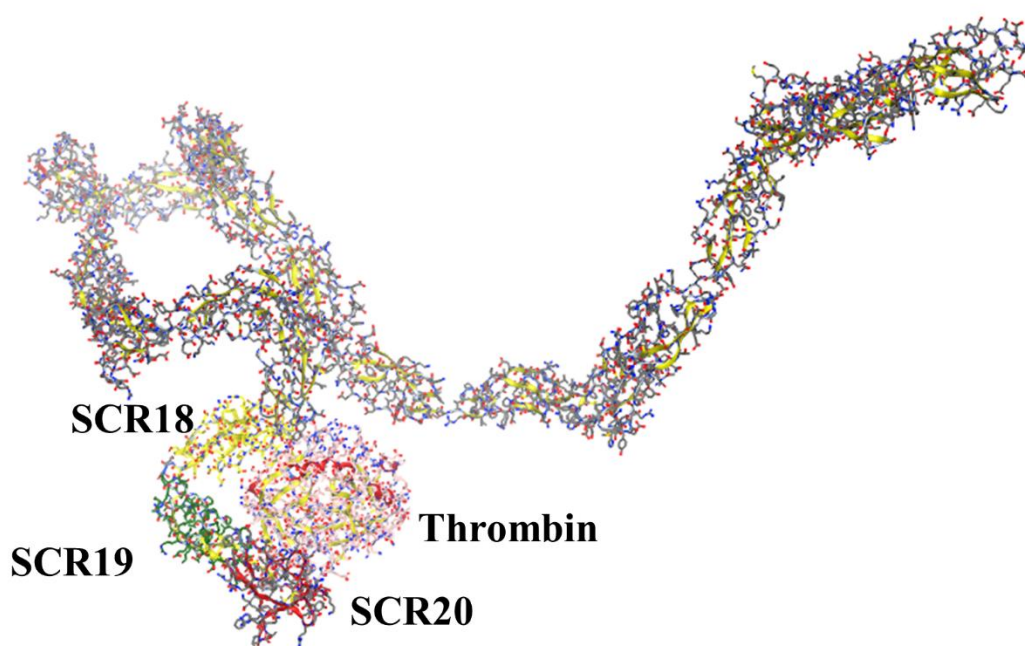


Figure 6.15. Binding interaction between full-length factor H and thrombin. The binding interaction model was performed using protein-protein docking in MOE, and the interaction with the second lowest score, so the least energy required was chosen, as SCR19-20 of factor H (SCR19 in green, SCR20 in red) and Exosite II of thrombin (blue), are engaged in the interaction. Atoms are represented as ball and stick, and protein backbone as ribbon.

The heavy chain of thrombin was modelled with full length factor H. Figure 6.15 corresponds to the interaction with the second lowest score, as it involved SCR19-20 interaction with thrombin. The residues involved in the interaction were the following:

Table 6.7. Residues involved in the interaction between thrombin (PDB ID 1YPG) and factor H full length. Residues from thrombin exosite I are noted in bold, exosite II are underlined and the 60 loop in turquoise. Factor H SCR18 is noted in yellow, SCR19 in green, SCR20 in red.

Thrombin	Factor H full length
Exosite I: in bold	SCR18: (aa1046-1104): yellow
Exosite II: underlined	SCR19 (aa1107-1165): green
60 loop: turquoise	SCR20 (aa1170-1230): red
K36 , S36a, Q38, <u>L60</u> , P60b, P60c, D60e,	D1045 , S1047, C1048, V1049, N1050,
<u>N60g</u> , F60h, T60i, E61, D63, L65, Y76 ,	P1051 , P1052, T1053, R1062, Q1063,

R77a, N78, I79, E80, K81, I82, S83, M84, K87, I88, Y89, I90, H91, P92, Y94, W96, R97, K110 , P111, V112, A113, F114, S115, D116, R175, W237, <u>K240</u> , V241, Q244, F245	M1064, S1065, K1066, Y1067, G1094, P1114, D1116, N1117, Q1139, N1140, L1141, Y1142, H1165, P1166, C1167, V1168, S1170, E1172, I1173, Y1190, D1220, G1221, K1222, L1223
--	--

The results demonstrated also that there could be multiple binding sites involved in the interaction between factor H and thrombin. The thrombin 60loop, a rigid structure that restrict and mediates access to the catalytic site of thrombin to hydrophobic substrates (of note, the second letter for each residue of the 60 loop is not a mutation, it is how the residue is numbered in the loop), interacts with SCR18, whereas parts of exosites I and II seem to be involved in the interaction with SCR19 and 20. After analysis of the other interactions generated from lowest to highest score, thrombin did not often bind with SCR19-20 in the full-length factor H. Thrombin does not interact only via SCR19-20, but also SCR6-8 (based on the experimental data) and the docking simulation is part of future work. Further investigation and experiments are required before concluding on the most accurate model representing the interaction between thrombin and full-length factor H.

6.4.3. Modelling the binding interaction between factor H and thrombomodulin

The binding assay (Figure 6.1) and SPR data (Figure 6.4) demonstrated that there was binding between factor H SCR18-20 and thrombomodulin EGF6. Therefore, the binding interaction between the structures of SCR19-20 and EGF456 of thrombomodulin was modelled to determine which amino acid residues could be involved in the interaction (Figure 6.16).

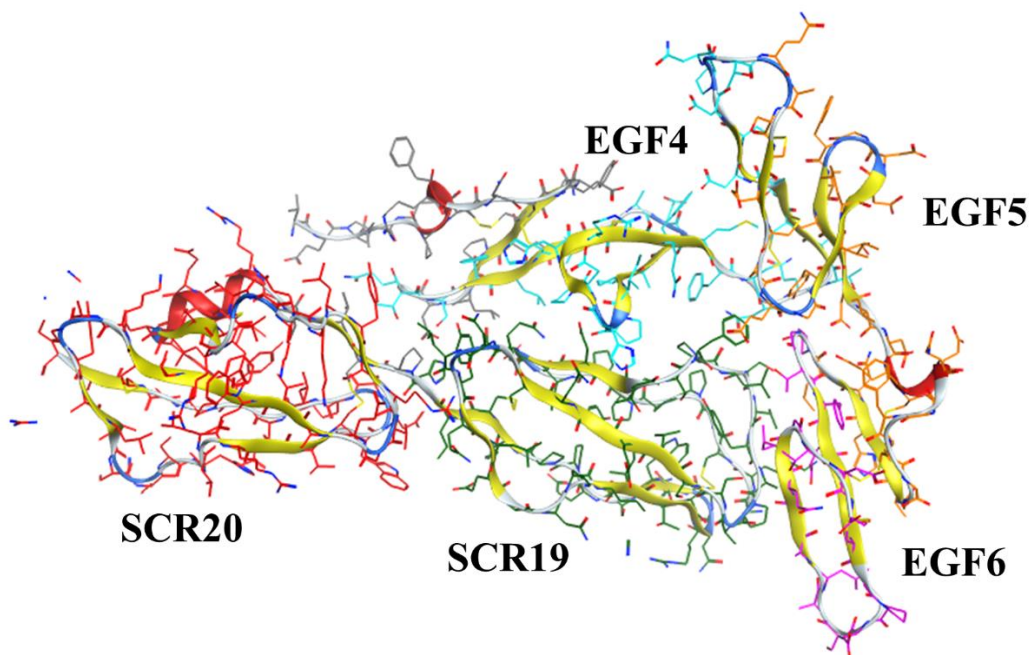


Figure 6.16. Binding interaction between SCR19-20 of factor H (PDB ID 2G7I) and thrombomodulin EGF456 (PDB ID 1DX5). The binding interaction model between SCR19 (in green) and SCR20 (in red) of factor H (PDB ID 2G7I), and thrombomodulin (EGF4 light blue, EGF5 orange, EGF6 purple, PDB ID 1DX5), was performed using protein-protein docking in MOE, and the interaction with the 2nd lowest score (least energy required for the binding to occur) was chosen as EGF6 was engaged in the interaction, supporting the experimental work. Atoms are represented as ball and stick, and protein backbone as ribbon.

The binding interaction model shown above between factor H SCR19-20 and thrombomodulin EGF456 had the second lowest score (corresponding to the interaction requiring the second least energy for the binding to occur), as EGF6 was involved, and supported the experimental data. The residues engaged in the interaction were:

Table 6.8. Residues involved in the interaction between thrombomodulin (PDB ID 1DX5) and factor H SCR19-20 (PDB ID 2G7I). Residues from thrombomodulin EGF4 are noted in light blue, EGF5 in dark green and EGF6 in purple. Factor H SCR19 is noted in green, SCR20 in red.

Thrombomodulin EGF456	Factor H SCR19-20
EGF4 (aa365-405): light blue	SCR19 (aa1107-1165): green
EGF5 (aa404-440): dark green	SCR20 (aa1170-1230): red
EGF6 (aa441-481): purple	

V345, R353, L363, D364, T366, S367, Y368, L369, P378, I379, P380, H381, P383, H384, Q387, M388, F389, C390, N391, P410, E411, Y413, H438, L440, P441, G442, T443, F444, E445, A455, G456, I458	K1108, I1115, D1116, N1117, G1118, D1119, I1120, T1121, S1122, F1123, P1124, L1125, S1126, V1127, Y1128, A1129, P1130, A1131, S1132, Q1137, Q1139, N1140, Y1142, H1165, I1166, V1168, E1172, Y1190
--	---

This model demonstrated that EGF6 binds factor H SCR19-20, primarily through SCR19, and EGF5 is only partly involved in the binding, which supports previous results (Figure 6.1). Furthermore, the SPR data showed the binding affinity of SCR18-20 was decreased when the EGF6 domain was blocked (Table 6.2), indicating that the modelled interaction in Figure 6.16 is representative of the experimental data. However, the model also presents significant binding with EGF4, which was not investigated experimentally (no antibody against this region).

Next the binding interaction between the full-length factor H and thrombomodulin EGF456 was modelled, to determine if there were other binding sites involved other than SCR19-20 (Figure 6.17).

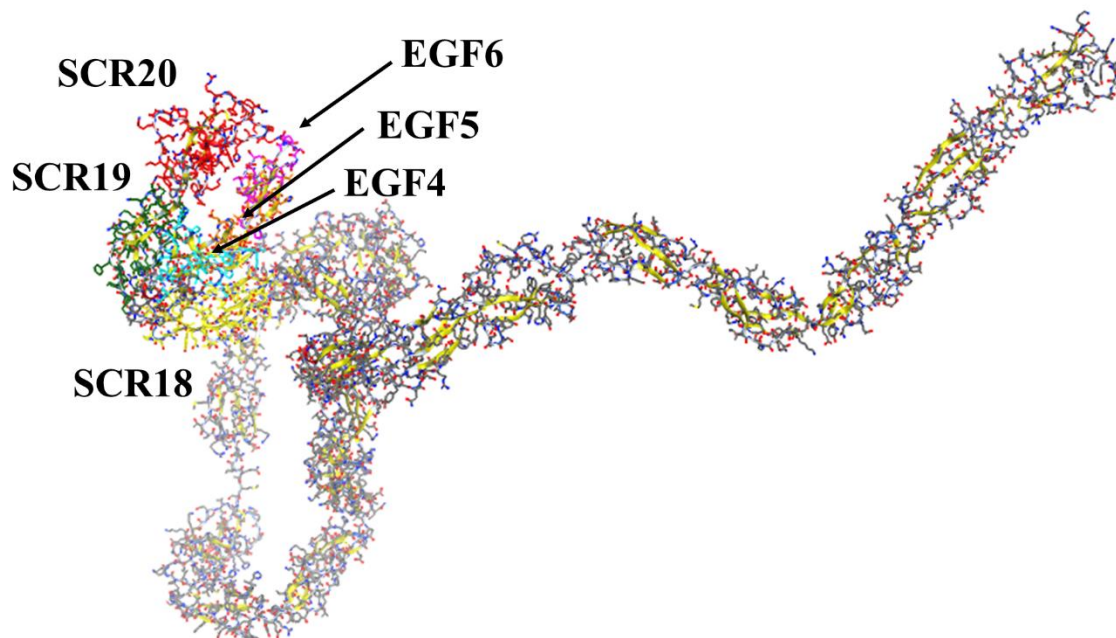


Figure 6.17. Binding interaction between full-length factor H and thrombomodulin EGF456 (PDB ID 1DX5). The binding interaction model was performed using protein-protein docking in MOE, and the interaction with the 4th lowest score (least energy required) was chosen, as SCR19-20 of factor H (SCR19 in green, SCR20 in red) was engaged in the interaction with EGF456 (EGF4 light blue, EGF5 orange, EGF6 purple). Atoms are represented as ball and stick, hydrogens not presented, and protein backbone as ribbon.

The model chosen to represent the interaction between factor H full length and thrombomodulin EGF456 had the 4th lowest score (corresponding to the interaction with the 4th lowest energy required for the binding to occur), as the SCR19-20 domain was involved (Figure 6.17). The residues engaged in the binding were:

Table 6.9. Residues involved in the interaction between thrombomodulin (PDB ID 1DX5) and factor H full length. Residues from thrombomodulin EGF4 are noted in light blue, EGF5 in dark green and EGF6 in purple. Factor H SCR18 is noted in yellow, SCR19 in green, SCR20 in red.

Thrombomodulin EGF456	Factor H full length
EGF4 (aa365-405): light blue	SCR18: (aa1046-1104): yellow
EGF5 (aa404-440): dark green	SCR19 (aa1107-1165): green
EGF6 (aa441-481): purple	SCR20 (aa1170-1230): red
E374, G375, F376, I379, H381, E382, R385, C386, Q387, Q392, T393, A394, P396, C399, D400, P401, N402, T403, Q404, S406, E408, E411, D417, G418, F419, I420, C448, G449, P450, D451, Q457, G459, T460, D461, C462	D1045, S1047, V1049, N1050, P1052, T1053, V1054, Q1055, K1066, F1084, G1094, N1095, W1096, T1097, E1098, P1099, Q1101, K1103, P1111, P1112, P1113, P1114, I1115, D1116, N1117, Q1139, Y1142, Q1156, W1157, S1158, E1159, P1160, H1165, V1168, S1209, R1210, S1211, H1212, D1220, K1222, L1223, E1224

The binding model demonstrated that SCR18, 19 and 20 are involved in the interaction. This model corresponds to the SPR data, as the binding affinity of the SCR18-20 domain was decreased when thrombomodulin was captured via EGF6. In this model, EGF6 of thrombomodulin is engaged in the interaction, however a significant number of residues from

EGF5 are also involved in the interaction, which does not concur with the experimental data. Therefore further experiments are required to conclude whether this model corresponds to the correct interaction.

6.4.4. Modelling the binding interaction between the thrombin-thrombomodulin complex and factor H SCR19-20

After modelling the interaction of factor H SCR19-20 and full length with thrombin and thrombomodulin EGF456 individually, the resolved structure of the thrombin-thrombomodulin complex (PDB ID 1DX5) was modelled with SCR19-20, to determine which residues are involved in the binding and whether factor H bound differently to thrombin or the thrombin-thrombomodulin complex (Figure 6.18).

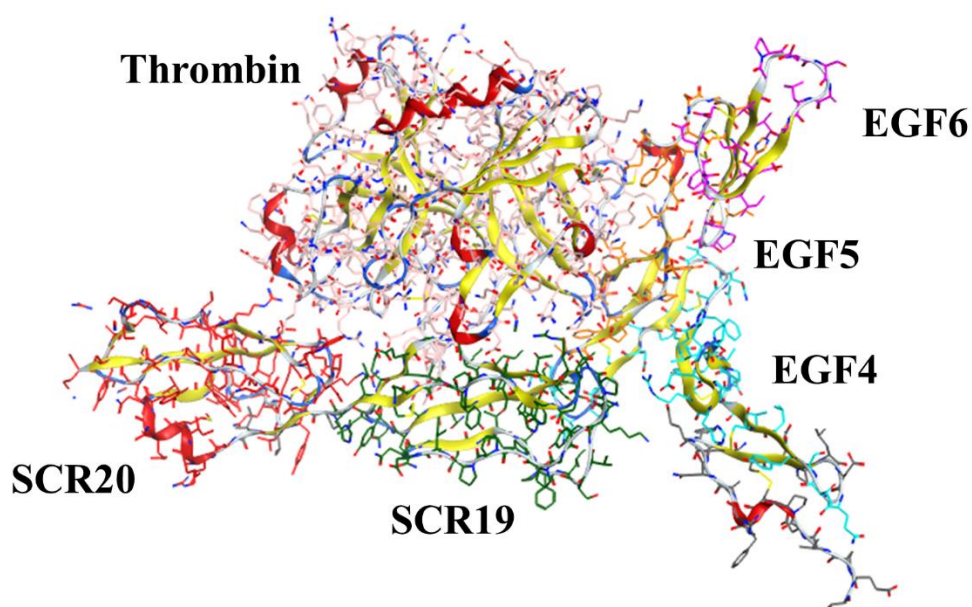


Figure 6.18. Model of the interaction between factor H SCR19-20 (PDB ID 2G7I) and thrombin-thrombomodulin complex (PDB ID 1DX5). The binding interaction model between SCR19 (in green) and SCR20 (in red) of factor H (PDB ID 2G7I), and thrombin-thrombomodulin (PDB ID 1DX5) complex (thrombin in pink, EGF4 in light blue, EGF5 in orange, EGF6 in purple), was performed using protein-protein docking in MOE. The interaction with the 3rd lowest score (least energy required) was chosen, as the 60 loop of thrombin was involved in the interaction with factor H as shown in the full length factor H and thrombin model interaction. Atoms are represented as ball and stick, and protein backbone as ribbon.

The binding interaction represented between factor H SCR19-20 and the thrombin-thrombomodulin complex, corresponded to the model with the 3rd lowest score, as there was the 60 loop of thrombin engaged in the interaction, as was demonstrated in the model between the full length factor H and thrombin in Figure 6.15. The residues engaged in each interaction were:

Table 6.10. Residues involved in the interaction between thrombin (PDB ID 1DX5) and thrombomodulin (PDB ID 1DX5) in the thrombin-thrombomodulin-factor H interaction. Residues from thrombomodulin EGF4 are noted in light blue, EGF5 in dark green and EGF6 in purple. Thrombin exosite I is noted in bold, exosite II underlined and 60 loop in turquoise.

Thrombin Exosite I: in bold Exosite II: underlined 60 loop: turquoise	Thrombomodulin EGF456 EGF4 (aa365-405): light blue EGF5 (aa404-440): dark green EGF6 (aa441-481): purple
F34, K36 , S36a, P37, Q38, E39, L65, R67, T74, R75 , Y76 , R77a , N78, E80, K81, I82, S83, M84, K110	T393 , S406, C407, E408, C409, Y413, I414, L415, D416, D417, T422, D423, I424, D454, E428, N429, G430, G431, F432, S434, N439, D461

Table 6.11. Residues involved in the interaction between thrombin (PDB ID 1DX5) and factor H SCR19-20 (PDB ID 2G7I) in the thrombin-thrombomodulin-factor H interaction. Residues from thrombin exosite I are noted in bold, in exosite II underlined and 60 loop in turquoise. Factor H SCR19 is noted in green, SCR20 in red.

Thrombin Exosite I: in bold Exosite II: underlined 60 loop: turquoise	Factor H full length SCR19 (aa1107-1165): green SCR20 (aa1170-1230): red
R35, S36a, P37, E39, L41, P60c , W60d , D60e , K60f , F60h , N143, E146, T147, W148, T149, D170, S171, T172, R173, I174, P186, E192, E218, G219, R221a, D222, G223, K224, Y225	A1131 , S1133 , Y1136 , Q1137 , C1138 , N1140 , Q1143 , L1144 , E1145 , G1146 , N1147 , K1148 , R1149 , T1151 , R1153 , S1158 , E1159 , P1160 , P1161 , K1162 , R1192 , G1194 , E1195 , S1196 , H1212

	R1215, T1216, T1217, C1218, W1219, K1222, L1223, E1224
--	---

Table 6.12. Residues involved in the interaction between thrombomodulin (PDB ID 1DX5) and factor H SCR19-20 (PDB ID 2G7I) in the thrombin-thrombomodulin-factor H interaction. Residues from thrombomodulin EGF4 are noted in light blue, EGF5 in dark green and EGF6 in purple. Factor H SCR19 is noted in green, SCR20 in red.

Thrombomodulin EGF456 EGF4 (aa365-405): light blue EGF5 (aa404-440): dark green EGF6 (aa441-481): purple	Factor H full length SCR19 (aa1107-1165): green SCR20 (aa1170-1230): red
N355, E357, R385, D400, N402, T403, S406, E408	K1108, S1122, F1123, P1124, L1125, Y1128, A1129, P1130, A1131, S1132, S1133, V1134, E1135

Experimental data demonstrated that EGF6 of thrombomodulin bound with factor H SCR19-20, which concurred with experimental data as well as the models of factor H and thrombomodulin alone. Based on the resolved structure of thrombin and thrombomodulin EGF456 complexed together (PDB ID 1DX5), the interaction between thrombomodulin and thrombin is also maintained, whereby thrombomodulin binds via EGF5 to exosite I of thrombin (residues 36, 71, 73, 75, 76, 77A, 109/110). This would be in accordance with the experimental data, as thrombin -thrombomodulin complex generates activated protein C in presence of factor H. Factor H binds thrombin in part via the 60 loop, which was also observed in the full length factor H-thrombin interaction model, however exosite II is not involved, which was observed in the SCR19-20 interaction with thrombin. SCR19 interacts with thrombomodulin, whereas SCR20 with thrombin. In the model of thrombomodulin EGF456 with factor H SCR19-20 and full length, SCR19 is engaged in the binding to thrombomodulin, supporting the model of the thrombin-thrombomodulin-factor H complex. Factor H SCR19-20 shares the binding with thrombomodulin to thrombin P37, which relieves the inhibition preventing thrombin from activating calcium bound protein C (191, 230).

Modelling of the interactions supports experimental data, and the lowest score binding model does not always correspond to the exact interaction happening. Therefore, further investigation of the interaction is necessary before validating these models.

Chapter 7. Discussion

Results obtained demonstrated that factor H significantly impacted proteins in the coagulation and anticoagulation pathways. Factor H *CFH*^{-/-} mice had increased soluble thrombomodulin levels indicating increased endothelial damage, and human plasma depleted of factor H had increased clotting time, suggesting a key role of factor H in clot formation. Factor H impacted the fibrin clot by enhancing the clot formation and significantly altering the structure of the fibrin clot. This further supports a role of factor H in fibrin clot formation by thrombin and that there it plays a role in clot structure and maintenance. Activated protein C generation was increased in presence of factor H by the thrombin/thrombomodulin complex and by thrombin alone, which demonstrates that factor H also affects thrombin's role in the anticoagulant pathway in presence and absence of thrombomodulin. Factor H binds both thrombin and fibrinogen with nanomolar affinity, illustrating that factor H affects clotting and anticoagulant pathway possibly directly through binding interactions with thrombin, fibrinogen and thrombomodulin. Overall, there was important evidence that factor H acts as a cofactor for thrombin in its pro and anticoagulant roles, and its absence in factor H *CFH*^{-/-} mice or human plasma, seems to primarily affect regulation of coagulation.

7.1. Soluble thrombomodulin is increased in *CFH*^{-/-} mice, with normal thrombin-antithrombin levels

Previous work demonstrated increased bleeding time in *CFH*^{-/-} mice (304). Results demonstrated that *CFH*^{-/-} mice have increased soluble thrombomodulin levels, and normal levels of thrombin-antithrombin complex. Soluble thrombomodulin levels vary between 3-

50ng/ml (202, 229) in circulation in physiological conditions, and upon vascular damage these levels increase (305, 306). The enzymes responsible for cleaving thrombomodulin off the cell surface have not been fully characterised (307) but likely include neutrophil derived enzymes (202, 297, 308), released in response to damaged tissue and infections (309). Soluble thrombomodulin is widely accepted as a marker of endothelial injury (200, 205, 297), although it is still debated (203, 297). For instance, soluble thrombomodulin levels correlate with worsened chronic kidney disease (CKD) and increased inflammatory markers such as creatinine, cystatin C and oxidised low density lipoprotein (oxLDL) (203, 308), and is elevated in diseases such as thrombotic thrombocytopenic purpura (TTP), aHUS, sepsis patients with disseminated intravascular coagulopathy (DIC) and multiple organ dysfunction syndrome (MODS), and preeclampsia (205, 231). *CFH*^{-/-} mice develop C3 glomerulonephritis, as a result of uncontrolled C3 activation due to alternative complement pathway consumption, leading to spontaneous development of MPGN2, secondary C3 plasma deficiency and renal abnormalities with C3 deposits along glomerular membrane (104, 310, 311). The increased C3b deposition on the glomerular membrane increases complement activation (312) which leads to release of anaphylatoxins and MAC, as well as increased leukocyte infiltration, ultimately causing cell injury (313). The leukocytes release proteinases (182), which could explain the increased levels of soluble thrombomodulin in the *CFH*^{-/-} mice (Figure 3.1A).

Additionally, levels of thrombin-antithrombin complex (TAT) were analysed (Figure 3.1B), which are indicators of coagulation activation, and how much thrombin is generated (314). Normal levels confirm that *CFH*^{-/-} mice do not have a coagulopathy, and the absence of factor H does not significantly affect thrombin generation. Therefore, the conclusion was reached that increased bleeding time in *CFH*^{-/-} mice cannot be explained by a dysfunction of thrombin generation. Vascular damage leads to endothelial dysfunction and activation (315), promoting thrombus formation (316). Increased soluble thrombomodulin is a marker of vascular damage, which does not concur with increased bleeding as seen in the *CFH*^{-/-} mice. Nevertheless, bleeding and clotting are observed simultaneously in disseminated intravascular coagulopathy (DIC), although bleeding is due to consumption of coagulation factors with the progression of the disease (317). Reports have shown recurrence of bleeding in mice, which they believe is due to problems with platelets, causing an unstable clot structure and the thrombi to not adhere to the vessel wall correctly (318). Therefore, the absence of factor H in mice could be linked to a lack of stability in the thrombus formation or in platelet activation. In addition reports have shown significant links between factor H and platelet regulation (25, 26, 319) and activation.

Complement knockout mouse models have shown to have coagulation complications. C3 knock out mice have been shown to bleed longer and have decreased platelet aggregation, and are protected from thrombosis (238, 250, 254, 320, 321), as well as lower thrombus weight and size (238). Studies have shown that C3 can activate tissue factor (254) and bind platelets to allow platelet-neutrophil and platelet-monocyte aggregates (322), but also binds fibrinogen and increases fibrinolysis time (251-253) Anaphylatoxin C3a stimulates platelet activation (323) but also causes thrombosis after complement activation by infection (324), overall demonstrating why C3 knockout mice bleed more. C5 knockout mice also have decreased thrombus size and weight, (238), and are protected against lethal thrombosis (248). The authors of the study conclude that C5a drives platelet aggregation, therefore leading to thrombus formation (248) in the mice. One report has shown that C3 and C5 affect the fibrin clot structure by causing smaller fibres and less pores, and consequently a higher lysis time (237), and removing them increases fibre thickness and pores, and decreases lysis time. This is further supported by Shats-Tseytlina finding (236) that complement activation within the clot renders the fibres thinner and the clot less permeable. In addition, C6 deficient mice and rats have increased bleeding time and lower platelet aggregation (247). Although the authors of the study do not speculate, this could indicate the involvement of the terminal pathway of complement in clot formation.

Therefore, the stop/start bleeding observed in the *CFH*^{-/-} mice could be due to unstable clots or platelet activity, but it could also be linked to the increased complement activation and secondary consumption of C3. The consumption of C3 leading to its absence is similar to the C3 knockout mouse, which has increased bleeding time. However factor H knockout and C3 knockout mice differ in complement activation profiles; factor H knockout mice have increased complement activation which promotes thrombosis according to previous findings, although this does not concur with the finding that *CFH*^{-/-} mice have increased bleeding time. One possible explanation for the stop/start bleeding is the overactivation of complement leading to thrombi, before consuming complement factors and hence causing bleeding. It remains difficult to conclude on the role of complement activation thus far based on these results. Another explanation is that factor H is having a direct effect on clotting and clot formation.

7.2. Absence of factor H in human plasma increases clotting time via activated partial thromboplastin time and prothrombin time.

Citrated plasma depleted of only factor H showed some minor complement activation as determined through the appearance of Bb fragment, whereas alternative pathway activation was prevented in factor H and factor B double-depleted plasma (Figure 2.2). Results showed that plasma depleted of factor H alone had significantly increased activated partial thromboplastin time (aPTT) and prothrombin time (PT) (Figure 3.3). Plasma depleted of factor H and factor B also had significantly increased activated thromboplastin time and prothrombin time, although when comparing to normal plasma, the difference was not as significant. Normally, an increase in prothrombin time (PT) indicates dysregulation of the extrinsic and common pathway of coagulation either of thrombin, factor V, factor VII, factor X and fibrinogen (288, 291, 292). Increased activated partial thromboplastin time (aPTT) indicates dysregulation in the intrinsic or common pathway, either of thrombin, factor V, factor VIII, factor IX, factor X, factor XI, factor XII and fibrinogen (288, 291, 292). Activated partial thromboplastin time is a slower clotting time as the intrinsic pathway takes longer to activate compared to prothrombin time (116, 122). Therefore, the results suggest that absence of factor H and factor B may affect, either directly or indirectly: thrombin, factor V, factor VIII, factor IX, factor XI, factor XII or fibrinogen. when both aPTT and PT are prolonged, this is often an indicator of vitamin K deficiency (325) but can also indicate a liver disease (326). Oral anticoagulants can also increase aPTT PT (326). In addition, aPTT and PT are indicative of the state and stability of the fibrin clot (327, 328), demonstrating whether or not there is an increased risk of bleeding or thrombosis (132). Significant binding affinity of factor H to both thrombin and fibrinogen was observed, hence factor H could affect fibrin clot formation through direct interaction with those proteins. Specifically, factor H is thought to inhibit factor XIIa activity (19), by preventing contact or intrinsic pathway activation. This study was done by measuring only the activation of kallikrein, not the downstream activation of thrombin and formation of the clot.

Complement overactivation can lead to enhanced coagulation, as MAC formation, anaphylatoxin generation affect tissue factor expression (3) and promote prothrombotic surfaces, as well as C3 and C5 affecting the density of the fibrin clots (238, 254). However

after analysing complement activation in the Δ FB/ Δ FH versus Δ FH plasmas, there was not complete complement consumption (detection of the Bb fragment, Figure 2.2) likely due to magnesium, required for alternative pathway activation (37), which is mostly chelated by citrate present in the plasma. Therefore, this indicated that overactivation of complement was possibly not the main driver of the increase in time to clot. Increases in aPTT and PT can inform on the formation and structure of the fibrin clot (132, 329). Deficiency in thrombin, von Willebrand factor and fibrinogen levels are detected by aPTT and PT (288, 289, 326), and factor H has been reported to interact with all these components. However, the effect of factor H on von Willebrand factor regulation are conflicting (27, 28), therefore aPTT and PT would not be able to dissect the impact of this interaction. The function or impact of the interaction between fibrin(ogen) and factor H has not been reported (24). Factor XIIa has been reported to impact the clot structure and increases fibrin density (330), and that this role may be more predominant compared to the activation of the intrinsic pathway. As factor H has a strong affinity for factor XIIa (331), one could speculate that factor H is also acting as a cofactor for factor XIIa in the clot formation, which has not been explored yet. The interaction between factor XIII and factor H has been shown to have no functional effect on factor XIII regulatory activity (23). However factor XIII deficiency is not detected with aPTT and PT (332), therefore if this interaction affected clotting it would not be detected with this method. In conclusion, the absence of factor H affecting time to clot could be a direct effect, as there is likely no complement consumption in the plasma, therefore might not be linked to it. Therefore, the next step taken was to determine more specifically the impact of factor H on the fibrin clot formation and structure, and whether its interaction with thrombin, fibrinogen, or von Willebrand factor could be linked to the effect on time to clot.

7.3. Factor H enhances fibrin clot formation by decreasing lag time, and increasing velocity and maximal turbidity, and alters fibrin clot structure

Fibrin clot and thrombus formation are affected by ionic strength, pH, polyphosphate, polysaccharides, peptides, lipids, proteins, nucleic acids, medications, natural and artificial compounds in blood and tissues (160). Factor H has been identified within the fibrin clot structure by numerous reports, and specifically has been shown to interact within and with other components of the clot (242), including factor XII (19, 20), fibrin(ogen) (24, 272), von

Willebrand factor (27, 28), factor XIII (23, 240) and platelets (25, 26, 275). Based on the data showing increased bleeding time in factor H knockout mice, as well as increased clotting time in human plasma depleted of factor H, I wanted to determine whether factor H affects thrombin-mediated fibrinogen cleavage and fibrin clot formation. Results demonstrated that factor H enhanced fibrin clot formation in a dose dependent manner (Figure 4.5), and further showed that the effect of factor H on fibrinogen in the presence of von Willebrand factor was less important (Figure 4.6). This is supported by the previous reports illustrating the interaction between von Willebrand factor and factor H, which could prevent factor H's direct effect on fibrin clot formation (27, 28). I also observed that factor H significantly altered the structure of the fibrin clot.

I demonstrated that factor H enhanced clot formation in a concentration dependent manner (Figure 4.2). Thrombin is an acute phase serine protease and a visible clot in blood appears from 10-30nM of the protease (129), requiring explosive generation to deal with the injury to the vessel immediately (131). Thrombin activity at 1nM is not detectable in *in vitro* assays and correspond to the coagulation pathway initiating (Figure 1.4), and from around 5nM thrombin there is propagation of coagulation activation and the acute response (129, 132). Physiological concentrations of factor H are around 2 μ M (58). Results herein showed that thrombin bound directly to factor H with an affinity of 29.7 \pm 1.08nM (Figure 6.6), demonstrating that around 30nM of factor H is required to maximally occupy thrombin, corresponding to a low proportion of total factor H in circulation. Fibrinogen is present in circulation at a concentration of 2-4 μ M (160). My results showed that the binding affinity between factor H and fibrinogen is 38.2nM (Figure 6.10), indicating that only a small proportion of factor H is necessary to fully occupy fibrinogen binding sites. The lag time corresponds to the speed at which thrombin cleaves fibrinogen into fibrin and subsequent formation of fibrin oligomers and then protofibrils. The velocity is the reaction rate at which protofibrils are assembled into fibres. The maximal turbidity is the point of formation of the mature clot, and an indicator of clot structure, whereby increased turbidity signifies a more porous clot (132). The results showed that factor H decreased the lag time, and increased the velocity and maximal turbidity in a dose dependent manner. Therefore, factor H increased thrombin-mediated cleavage of fibrinogen, oligomerisation and protofibril formation, the assembly into fibres through lateral aggregation, and the final structure of the clot. Howes et al (240) detected the presence of factor H within the clot using one-dimensional gel electrophoresis bands using MALDI/TOF-MS peptide mass fingerprinting, and showed that factor H stays bound to the fibrin clot when they spiked plasma

with increasing concentrations of factor H detected with ELISA. They found no impact of factor H on maximal turbidity in their pure protein assays, which was not in accordance with our results as we demonstrated a dose dependent effect of factor H on maximal turbidity. However, the conditions used by Howes et al were different to my set up, as their concentration of fibrinogen and thrombin were 10-fold lower (they used 0.5mg/ml fibrinogen and 0.025U/ml thrombin, whereas I used 4mg/ml fibrinogen and 0.28U/ml thrombin), and the concentration of factor H were 1000-fold higher (factor H was titrated from 65 μ M and I from 100nM). My results showed that a plateau was reached at quite low concentrations of factor H (Figure 4.2), indicating that the effect happens at lower concentrations, and why Howes et al did not see an effect. Singh et al (23) with size exclusion chromatography, showed the interaction between factor H and the B subunit of factor XIII, however, did not report any effect of factor H on thrombin-mediated activation of factor XIII. The experiment was done by triggering clotting with tissue factor, phospholipids, and factor XIII A subunit, before addition of factor XIII B subunit and factor H, all to plasma depleted of factor XIII. I did not evaluate the impact of factor H on factor XIII activation, however based on the plasma turbidity assays, it proved to be more difficult to pull out effects of factor H (its absence and restoration of physiological concentrations), compared to pure protein assays.

Factor H was shown to significantly alter the structure of the fibrin clot, as well as decrease fibre density (Figure 4.5). Different factors influence the fibrin clot structure and density, including factor XII, that increases the density of the clot (330), and has been reported to significantly interact and bind with factor H, although the impact on regulation of complement and coagulation has not been elucidated yet. Red blood cells render the clot less dense and enable fibrinolysis factors to access the clot (136, 172, 333). Complement C3 on the other hand has been reported to increase fibre density and delay fibrinolysis (240, 252, 334). Platelets and von Willebrand factor are key to generating a denser and more stable clot (28, 113). Therefore, factor H could play a key role within the clot, maintaining a certain structure to enable accessibility of lytic factors to the clot.

Thicker fibres are associated with less dense fibrin networks, larger pores, and higher susceptibility to fibrinolysis (160, 175, 176, 335). Thinner fibres are associated with smaller pores, and a denser network, and are more resistant to lysis (160, 175, 176, 293). Factor H promoted a less dense fibre network by enhancing thrombin enzymatic activity and lateral aggregation, which increases fibre diameter, and consequently decreases the number of branching points (176) and the density of the clot. Overall, this information indicates that in

the presence of factor H, the fibrin clot formed is less dense and therefore more susceptible to fibrinolysis, regulating the clot structure and formation, which decreases the risk of thrombi forming.

Results showed that factor H increased fibrin clot formation in the presence and absence of von Willebrand factor (Figure 4.5 and Figure 4.6). Although the difference was not significant, there was a trend showing that the presence of von Willebrand factor increased lag time (IC₅₀ was 3.0±0.7min with von Willebrand factor, 1.86±0.06min without von Willebrand factor, p-value 0.7) and decreased maximal turbidity (EC₅₀ was 0.26±0.9 with von Willebrand factor, 0.4±0.04 without von Willebrand factor, p-value 0.086). These results indicated that the presence of von Willebrand factor slowed the effect of factor H on clotting. Factor H has been reported to bind von Willebrand factor through factor H SCR6-8 and SCR19-20 according to Rayes et al (28), and Feng et al (27) show that the C-terminal region is key (they only state that SCR1-5 does not bind) (27, 28). However the effects of the interaction reported were conflicting, as Feng et al (27) reported that factor H enhanced von Willebrand factor cleavage by ADAMTS13, whereas Rayes et al (28) saw that presence of factor H decreased it. Both experimental setups were done with pure proteins, however the methods of detection of ADAMTS13 cleavage activity were different, which could explain the discrepancies (Rayes used an ELISA technique, and Feng a fluorometric assay). Von Willebrand factor is thought to act in regulating complement by acting as a cofactor for factor I in binding and inactivation of C3b, in the absence of factor H (269-271). However ultra large von Willebrand factor or multimeric forms have a prothrombotic effect and increase complement activation by recruiting complement components (269-271). As von Willebrand factor may be involved in factor H regulation of complement, it is possible that this interfered with factor H's cofactor activity towards thrombin in enhancing clot formation or compete with thrombin for a factor H binding site. The reports demonstrating the interaction between factor H and von Willebrand reported affinity values of 33nM (27) and 180nM (28), therefore in the same range as factor H affinity for thrombin. In addition, my results showed that SCR6-8 and SCR18-20 of factor H bound directly to thrombin, which are also the binding regions on von Willebrand factor (27, 28). Therefore, thrombin and von Willebrand factor could share a binding site on factor H, explaining the delayed clot formation in presence of von Willebrand factor.

Plasma turbidity assays showed increased lag time after restoration of factor H to factor H-depleted plasma (Figure 3.9), whereas in the pure protein assays factor H caused a decrease. In plasma other factors are present that interact with factor H, for instance. Factor H also interacts

with factor XIIIa of the intrinsic pathway (19, 20) and inhibits it. This could explain why the lag time is enhanced in plasma-based assays when comparing factor H depleted plasma to when it is restored with physiological concentrations of factor H. Factor H further increased the velocity in plasma which is reflected the pure protein assays, indicating a role in the lateral fibrin aggregation, of which the mechanisms and driving forces are still unknown (160). However, clot structure and stability depend on thrombin concentration, as well as calcium, pH and ionic strength (132).

To conclude, factor H significantly impacted thrombin's role in fibrin clot formation, by decreasing the lag time, and increasing the velocity and maximal turbidity, and also affected the fibrin clot structure. Overall, factor H could play a vital role in the regulation and maintenance of the fibrin clot. However, thrombin also participates in the anticoagulant protein C pathway; factor H has been reported to interact with thrombomodulin, therefore the impact of factor H on protein C activation by the thrombin thrombomodulin complex was analysed.

7.4. Factor H enhances thrombin's anticoagulant role by increasing protein C activation by the thrombin-thrombomodulin complex and by thrombin alone

I further investigated the role of factor H on thrombin's anticoagulant role. Results showed that factor H increased protein C activation by the thrombomodulin-thrombin complex (Figure 5.1). Thrombin alone cannot activate protein C and requires its cofactor thrombomodulin to enable cleavage and activation. Other factors that enhance protein C activation by the thrombin-thrombomodulin complex include the endothelial protein C receptor (EPCR), present on the endothelium and lowers the Michaelis Menten KM value for protein C activation (336). Platelet factor 4, an abundant platelet alpha-granule protein, also enhances protein C activation by the thrombin-thrombomodulin complex, in the fluid phase but also on surface of the endothelium (337), by rendering protein C more accessible to the thrombin-thrombomodulin complex. Authors hypothesise that upon platelet activation, PF4 is released onto the endothelium, promoting protein C activation and anticoagulation, thereby keeping the thrombus local (337). My results demonstrated that factor H also significantly enhanced the KM of activation, by the

thrombin-thrombomodulin complex (without factor H K_M 187nM, with factor H 80nM, p-value 0.004) in a concentration dependent manner ($K_D=3.5nM$). Factor H is present in circulation but also binds cell surfaces, therefore could act in a similar way to PF4, enhancing protein C activation around the fibrin clot to prevent thrombosis from spreading.

My results showed that factor H enhanced protein C activation by thrombin alone (without factor H 752nM, with factor H 199nM, p-value 0.004) in a concentration dependent manner ($K_D=34.3nM$, Figure 5.1). Thrombin binds thrombomodulin and cleaves calcium-bound protein C into its activated form (186, 194). Calcium binding to protein C conformationally alters the activation peptide of protein C (192, 193), revealing the anion binding exosite which enables thrombomodulin binding at EGF4 (185, 197). Thrombomodulin binds thrombin and allosterically alters the 37-loop of thrombin, overcoming the inhibitory effect of residue Arginine 35 that prevents thrombin's cleavage of calcium-bound protein C (185, 194-198). Calcium binding protein C, and thrombomodulin binding thrombin allows interaction between protein C and thrombin, and activation of protein C. My results suggest that in absence of thrombomodulin, factor H enhances protein C activation by thrombin 3.7-fold, indicating that factor H could overcome the inhibitory effect of calcium via its strong binding interaction with thrombin -affinity of 28nM- allowing the latter's cleavage of protein C. As a cofactor to factor I, which has a significant homology to thrombin (59), factor H acts as a contact interface between factor I and C3b, bringing them into proximity (57). This stabilises the C3b domains during factor I cleavage (59). In presence of thrombomodulin, factor H could proximate thrombin to thrombomodulin, and thrombomodulin presence could be an additive effect. Thrombomodulin has been described as a scaffold for thrombin and protein C interaction (185, 196, 230); factor H could act in a similar fashion or else further enhance this action.

These interactions were studied in solution using recombinant soluble thrombomodulin, representing events in circulation. Thrombomodulin is primarily surface bound on the endothelium, therefore further understanding of the regulation by factor H of protein C activation would require analysis of the interaction on cell surfaces.

Overall, these results suggest that factor H, through significant binding affinity to thrombin, could enhance protein C activation at the cell surface, where membrane-bound thrombomodulin is present, although this needs further investigation. This would therefore reduce thrombin generation and clot formation in that area and decrease endothelial damage due to thrombosis. The enhanced protein C activation in the absence of thrombomodulin could

occur in circulation away from thrombomodulin, potentially contributing to protein C's roles elsewhere, for instance its anti-inflammatory or anti-apoptotic roles (184, 190).

After determining the impact of factor H on thrombin's regulatory activity in both coagulation and in the anticoagulant pathway, I wanted to understand how the proteins were interacting and which binding sites were involved.

7.5. Factor H interacts with EGF1-2 and EGF6 of thrombomodulin and exosite II of thrombin, via SCR6-8 and SCR18-20

The model of full-length factor H was built using homology modelling and was manually assembled using overlapping residues (Figure 6.13). The full-length structure of factor H has been previously resolved at low resolution using solution scattering (62, 285), and showed a folded back and flexible structure which was presented in the model built in this work. Building the full-length model of factor H was important to be able to analyse the binding interaction between factor H and thrombin, thrombomodulin and the thrombin-thrombomodulin complex.

Results from the SPR analysis demonstrated that factor H binds thrombomodulin, potentially to EGF1-2 and EGF6 via SCR regions 6-8 and 18-20, as there was a lower binding affinity when thrombomodulin was captured via these regions. The molecular modelling illustrated binding between thrombomodulin via these regions also, specifically through SCR19 which would support these results (Figure 6.16). Previous results have shown the interaction and binding affinity between factor H and thrombomodulin (29), as well as the impact on complement regulation and inactivation of C3b by factor I and factor H (29, 233). Mutations in the serine/threonine rich domain, as well as the lectin like domain have shown increased binding to both C3b and factor H (233). The SPR results demonstrated that there was potential binding of factor H fragments SCR6-8 nor SCR18-20 to EGF1-2 and EGF6, respectively. One hypothesis could be that factor H twists around thrombomodulin and binds on the EGF-like domains EGF1-2 and EGF6, via SCR 6-8 and 18-20 respectively, enabling thrombin's binding to thrombomodulin and subsequent anticoagulant activity. The models showed that SCR19 was involved in the binding to thrombomodulin, which concurs with this hypothesis. It also was evident that factor H bound EGF6 of thrombomodulin alone which was in line with the experimental SPR data. Factor H did not bind EGF6 when thrombomodulin was bound to

thrombin however. EGF6 binds calcium to enable increased thrombin binding, which could explain why factor H is not interacting with EGF6 in these conditions. SCR18 could be binding thrombin 60 loop, as demonstrated by the interaction modelled between thrombin and full length factor H (Figure 6.15). Further investigation is required concerning the involvement of SCR6-8 in the interaction however.

Competitive binding between heparin and thrombin, and hirudin and thrombin, indicated that heparin and thrombin (Appendix Figure A6.4) share a binding site to factor H, in exosite II (149, 338-340). No competitive binding was seen between thrombin and hirudin for factor H, in exosite I (134, 149, 339) (Appendix Figure A6.5). The modelling of factor H SCR19-20 binding to thrombin showed that the interaction requiring the least energy was when SCR19-20 bound in part via exosite II. However when analysing the interaction with full length factor H, the 60 loop of thrombin was involved in the binding, a structure in thrombin responsible for mediating hydrophobic substrates binding within the active site. In the model of factor H SCR19-20 and the thrombin-thrombomodulin complex, the 60 loop was involved in the binding also, indicating that this model is the most likely (Figure 6.18). However, further studies into the role of the 60 loop in the interaction with factor H is required. In addition, thrombin and factor H could bind differently compared to when thrombin is complexed to thrombomodulin, explaining the differences in the models.

Factor I and thrombin have shown structural homology, and authors showed that SCR2-3 of factor H binds factor I loop 358-363 and loop 394-408, which correspond to the 37s and 70s loops of thrombin (59), both situated in exosite I. The models generated showed that it was the 60 loop that could be more involved in the binding to factor H, and some of exosite I. I only studied the binding interaction of SCR19-20 to thrombin, however the authors did not report an interaction between SCR19-20 and factor I in their model (59). Binding between SCR1-5 and thrombin was observed in SPR (Figure 6.7), however thrombin had no impact on factor H complement regulation, therefore SCR2-3 could bind thrombin, though this interaction would have no functional effect. Further analysis is required however before concluding, including analysing the interaction of factor H SCR2-3 with thrombin.

Thrombomodulin binds in exosite I of thrombin to relieve the inhibitory effect of Arginine35, and therefore enable its binding and cleavage of protein C. In the model illustrating the thrombin-thrombomodulin complex bound to SCR19-20, thrombomodulin is still bound to exosite I of thrombin, indicating that protein C activation can still occur in presence of factor

H. In the report from Xue et al (59), SCR2-3 could bind exosite I of thrombin, which does not concur with my model. However, it could be that SCR2-3 binds thrombin in exosite I when alone rather than complexed to thrombomodulin. SCR2-3 was not involved in the interaction with thrombin in the model of full length factor H and thrombin. However binding data demonstrated that the affinity of SCR18-20 was higher ($K_D=1.14\mu\text{M}$) than that of SCR1-5 ($K_D=2.96\mu\text{M}$) to thrombin, justifying that this model may be more reliable. However, the model of factor H bound to the thrombin-thrombomodulin complex showed that factor H shared the binding to arginine35, with thrombomodulin. In addition factor H only binds Arginine35 of thrombin when the latter is complexed to thrombomodulin. Thrombomodulin releases the inhibitory effect of arginine35 which prevents thrombin from binding and cleaving protein C (191, 197). Results showed that factor H enhances protein C activation by thrombin-thrombomodulin, and based on the model, factor H could be removing the inhibitory effect of Arginine35 in thrombin to enable its interaction with protein C. The models indicate that factor H likely binds thrombin differently compared to when it is complexed to thrombomodulin.

In conclusion, the binding study showed that factor H SCR18-20 could be one of the sites significantly involved in the interaction with thrombin and thrombomodulin. This region of factor H, specifically SCR19-20, contains mutations responsible for aHUS, a renal disease characterised by decreased regulation of complement and micro-clots. Therefore, understanding the involvement of factor H in this disease leads to a better understanding of how factor H could be involved in regulating coagulation. In addition, the region of thrombomodulin likely involved in the interaction with factor H also contains mutations causing this disease.

7.6. Factor H deficiency and dysregulation in disease states

Factor H dysregulation and deficiency is noted in the following diseases: aHUS (15, 43, 64, 90, 98, 106, 341-345), DDD (10, 49, 100, 106, 346-350) and antiphospholipid syndrome (APS) (11, 17, 19, 351-355). More specifically, aHUS and DDD are characterised by thrombotic microangiopathy (9, 10, 92, 356) and APS by thrombosis (11, 17, 242, 354, 355), and highlight an impact of complement dysregulation on clotting. Thrombotic microangiopathy is an umbrella term for diseases characterised by thrombocytopenia and haemolytic anaemia (10, 31, 357). It corresponds to when the vessel wall thickening is damaged, leading to swelling,

detachment of endothelial cells from the basement membrane, platelet accumulation and thrombosis, and ultimately obstruction of the vessel lumina (358). Genetic defects in diseases aHUS and TTP lead to thrombotic microangiopathies (10, 31). Importantly, thrombotic microangiopathies in aHUS derive from complement dysregulation, mostly as a result of mutations in the C-terminal of factor H located in SCR19-20 primarily (14, 15, 43, 90, 91, 319, 342-345, 359, 360), that impair factor H's complement regulation on cell surfaces.

My results showed that the binding sites on thrombin and thrombomodulin are likely located on SCR18-20, demonstrated by the SPR data and supported to a certain extent by the modelling. Therefore, mutations in this region could affect binding to thrombin, and regulation of clot formation but also of the anticoagulant pathway. Identifying the residues involved in the interaction would shed light on how the mutated forms could affect the binding (increasing or decreasing it), and what downstream effects are on fibrin clot formation (enhancing or decreasing it) or on protein C generation (enhancing or decreasing it). The state of coagulation in aHUS patients can vary, and one could hypothesise that the mutations in factor H could contribute to this in part, through its' interaction with thrombin. SCR18-20 also interacted with thrombomodulin, and mutations causing aHUS could impact this interaction too. Mutations have been identified in aHUS located on thrombomodulin, in EGF5 and EGF6 (231, 233, 361), one region likely involved in the interaction with factor H based on the SPR and ELISA data, and supported in part by the molecular modelling. Therefore, mutations on both factor H and thrombomodulin could significantly alter the binding interaction and downstream regulation of complement but also of coagulation, as the interaction enhances inactivation of C3b and is involved in increasing protein C activation.

Complement dysregulation can favour a procoagulant environment (10, 31), therefore one could hypothesise that a lack of factor H regulation on surfaces indirectly enhances clotting. However my results demonstrated that in presence of antibody against SCR20 of factor H, there was an increase in activated partial thromboplastin time, indicating that a loss of SCR20 affects factor H's role in fibrin clot formation. This assay could reflect to a certain extent, mutations in factor H SCR20 from aHUS that cause a defect in factor H binding surfaces, but is still able to regulate complement in the fluid phase (14, 64, 91). This is supported by the SPR analysis which showed that SCR18-20 is involved in the binding to thrombin. The significant effect of factor H on fibrin clot formation and on the structure of the clot also, also supported the hypothesis that SCR20 is involved in affecting clotting. This indicates that mutations in SCR20 could cause a decrease in fibrin clot generation, or an unstable clot, leading to increased

bleeding. Binding between factor H and fibrinogen was also demonstrated, although the binding sites were not identified. Nevertheless, this interaction could also influence the effects of factor H observed in fibrin clot generation, though further investigation is needed.

The relevance of SCR20 was demonstrated by a report that studied an aHUS mutation, identified in human, in a mouse model (the equivalent was W1206R) (362). The results revealed decreased complement regulation on cell surfaces but normal regulation in circulation, and a more prothrombotic phenotype. This indicated that this amino acid residue could be involved in the regulation of clotting as was demonstrated in my results. This residue could be key in the interaction with thrombin, and the mutation could cause alteration of the regulation of thrombin by factor H in clot formation. When measuring the aPTT of plasma in the presence of anti-factor H antibody against SCR20, there was an increase in the time to clot, which would not agree with the findings that the W1206R mutant factor H mice have a prothrombotic phenotype (362). However, it is not possible to know whether the mutation affected thrombin binding. Therefore, the surface binding region of factor H SCR20 domain is likely important in the regulation of clotting, and in its absence, clotting is delayed. However, mutations in this domain may affect this regulation differently.

There was a significant increase in tail bleeding time in factor H knockout mice, and increased clotting time in human plasma depleted of factor H, measured with aPTT and PT, which indicated that factor H could play a key role in clot formation and regulation, and loss of factor H leads to dysregulation of clotting. There is very little data on the state of clotting in aHUS patients, only one recent study reported increased activated partial thromboplastin time for aHUS patients (363), which concurs with our results.

It is important to note that there is not complete deficiency or loss of factor H function in aHUS, and the main effect reported is on cell surfaces contributing to endothelial damage leading to thrombosis (7). Factor H knockout mice are characterised by overactivation of complement alternative pathway, and secondary consumption of C3 (104). Consequently, there is increased anaphylatoxin and MAC formation, and high complement deposition along the glomerular membrane (310). Human plasma depleted of factor H showed low complement activation, due to the citrate chelating the magnesium and prevent overactivation. In aHUS patients, there is a decreased regulation by factor H on the surfaces of cells, due to mutations in the surface binding region (SCR19-20) that prevent it from regulating complement on self-cells (14). However, there is still regulation in the fluid phase. Vernon et al (106) designed a mouse model with only

partial factor H deficiency (factor H was knocked out in hepatocytes only), which was more representative of aHUS. Another mouse model before this was designed by expressing a truncated form of factor H, missing the SCR16-20 region (102), a model characterised by fluid phase regulation of complement but not on cell surfaces, as seen in aHUS patients. The human plasma depleted of factor H, as well as the factor H knockout mice, are not quite representative of aHUS disease, as there is no regulation by factor H in the fluid phase nor on cell surfaces. Complement component C5 has been reported to be responsible for the thrombotic microangiopathy in the mouse models of aHUS (104, 364), as its cleavage due to overactivation of complement leads to increased anaphylatoxin generation and MAC formation, which promote thrombosis (106, 248). However, the factor H knockout mice had increased bleeding time, which would not concur with the increased thrombosis in the aHUS model, however it is important to note the difference in complement regulation in the models. This indicates that levels of complement activation could play a role in clot formation, dependent on levels of regulation by factor H in the fluid phase and on cell surfaces.

Based on these results, it would be interesting to determine whether aHUS patients with low factor H levels, or else dysregulated factor H function due to mutations, have altered clotting times, therefore measuring aPTT and PT in these patients, and from there analyse where the mutations lie in factor H. One study measured aPTT and PT in aHUS patients, however there was no classification with regards the mutations leading to the disease (363).

AHUS is also characterised by thrombocytopenia, or a low platelet count. Platelets in aHUS can be activated and consumed by complement activation due to poor regulation by factor H (26, 273, 319, 345). Factor H is secreted by platelets (273) and also binds in a dose dependent manner via the C-terminal region (273, 322), as aHUS mutations in the C-terminal bound less (25, 26, 273). Factor H is thought to regulate platelet activation and aggregation due to complement activation by properdin (274, 275). Therefore, the effect of factor H observed could be explained in a physiological setting by the presence of platelets secreting and recruiting factor H to their surfaces to enhance the clot formation and the platelet plug. The pool of factor H expressed by platelets corresponds to only 0.05% of total factor H present in plasma, therefore a hypothesis is that it plays a more specific role (322), possibly in enhancing fibrin formation by thrombin.

The results demonstrated that loss of factor H caused increased bleeding time in mice, and prolonged clotting time in human plasma. Factor H enhanced fibrin clot formation, and altered

the structure, causing thicker fibres and larger pores, and enhances thrombin's anticoagulant role, all through its interaction with thrombin, fibrinogen and thrombomodulin (Figure 6.21).

Overall, in disease where factor H is deficient or dysfunctional, binding interactions and downstream mechanisms will be dysregulated, specifically with coagulation factors such as von Willebrand factor (27, 28), factor XII (20), factor XIII (23), fibrin(ogen) (24), platelets (25, 26) and thrombin (304). Mutations in factor H may affect clot formation, clot structure, localisation of the clot, the anticoagulant pathway, and overall clotting time in patients with factor H deficiency or dysfunction. The below illustration summarises the proposed mechanisms of factor H function in the coagulation and anticoagulation pathways (Figure 7). In presence of factor H, the fibrin clot is less dense and therefore more accessible to fibrinolytic factors. Platelet activation is carefully regulated by factor H as well as von Willebrand factor, the latter also regulating complement activation.

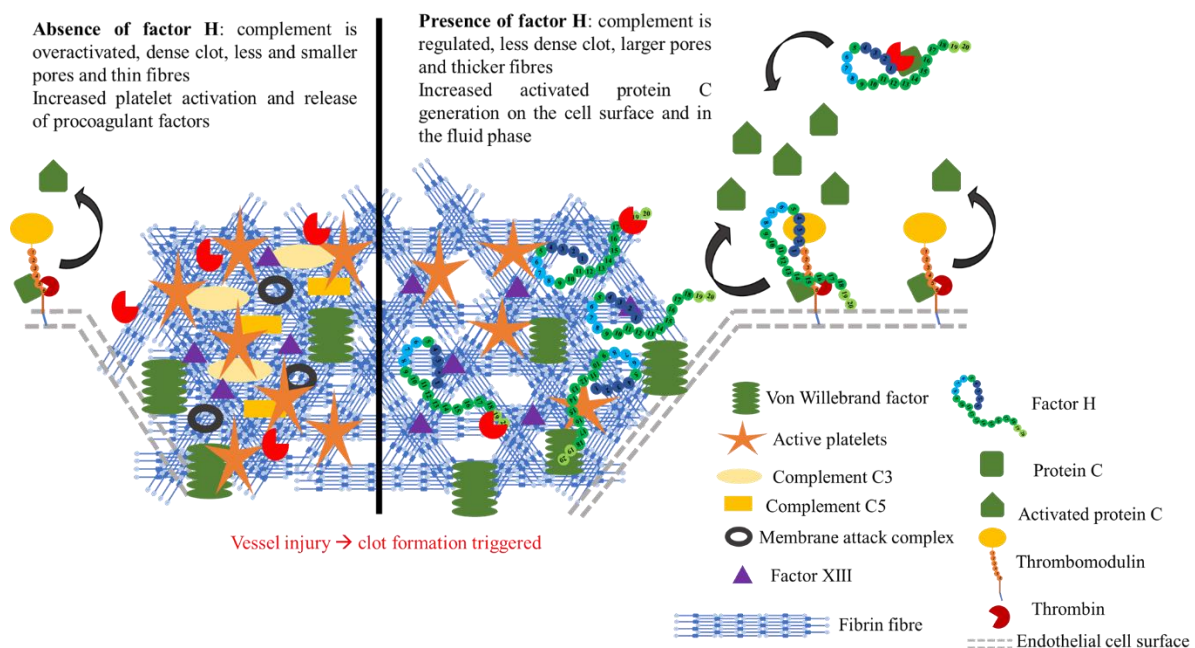


Figure 7. Factor H affects clotting and regulation of coagulation through strong binding affinities with thrombin, thrombomodulin and fibrinogen. The proposed effect is that factor H enhances thrombin-mediated formation of fibrin clots and alters the structure (by decreasing fibre density) and interactions with clot components von Willebrand factor, platelets, factor XIIIa and factor XIIa. Factor H enhances protein C activation on cell surfaces by the thrombin-thrombomodulin complex, and by thrombin alone in circulation.

Mutations in factor H or deficiency would impair its interactions with these coagulation factors. Reports have demonstrated that factor H's interaction with platelets is affected in aHUS (25, 319, 345), leading to increased complement activation on platelet surfaces. The C-terminal of

factor H was key to the interaction with von Willebrand factor (27, 28); reports of the effects of factor H on ADAMTS13-mediated cleavage of von Willebrand factor were contradictory (27, 28), hence effects of mutations in the C-terminal are inconclusive in this regard. Analysing the impact of aHUS mutations on the interaction of factor H with thrombin, fibrinogen and thrombomodulin would be key to understanding how factor H is regulating the anticoagulation and the coagulation pathway, which highlights the importance of the complement and coagulation crosstalk, and the severity of their dysregulation in diseases.

The hypothesis of the project was that factor H acted as a ligand for thrombin and affects both its procoagulant role in fibrin clot formation, and its anticoagulant role, in protein C activation. The following objectives were set, and results shed light and resolved them:

The coagulation profiles of the factor H knockout mice were analysed, and showed increased tail bleeding time as well as increased soluble thrombomodulin, and normal levels of thrombin-antithrombin complexes, indicating that the mice were characterised by increased vascular damage, but no coagulopathy. The stop/start bleeding observed could be due to unstable clotting.

The time to clot (activated partial thromboplastin time and prothrombin time) in plasma depleted of factor H was analysed and demonstrated that clotting time was increased in absence of factor H, and decreased upon restoration of physiological concentrations of factor H. These results indicated that factor H could play a crucial role in clot formation in human plasma. This was observed in plasma where little complement activation was seen, therefore the increased clotting time was likely due to factor H rather than complement activation.

The impact of factor H on thrombin-mediated fibrin clot formation was determined, and factor H significantly increased fibrin clot generation, in a dose dependent manner, as well as altering the structure of the fibrin clot. This indicated that factor H could be an essential component in haemostasis, by regulating fibrin clot formation by thrombin and influences the clot structure.

Factor H effect on thrombin's anticoagulant role was analysed also and showed that there was a significant increase in protein C activation by the thrombin-thrombomodulin complex but also by thrombin alone. This finding meant that factor H could have the potential to regulate protein C activation on cell surfaces in presence of thrombomodulin (although cell surface experiments need to be done), but also in circulation in absence of thrombomodulin.

Finally, the binding interaction analysis between factor H and thrombin and thrombomodulin was done. The results illustrated that SCR6-8 and 18-20 were likely involved in the interaction with thrombin, likely on one of the exosites, and thrombomodulin, likely via the EGF1-2 and EGF6. This meant that the surface binding domains of factor H are involved in the interaction with thrombin and thrombomodulin and influence the regulation of coagulation. This is a key finding to be able to further investigate the impact of mutations on factor H on coagulation.

7.7. Future perspectives:

Based on the results obtained during this project, different follow up experiments could be performed.

Regarding the factor H knock out mice, it could be interesting to measure activated partial thromboplastin time and prothrombin time. This would further support the tail bleeding assays performed and indicate the state of the intrinsic and extrinsic pathways in the absence of factor H in mice. The mice had normal levels of thrombin-antithrombin complexes, indicating that the thrombin generation pathway may not be severely affected, however measuring aPTT and PT would indicate whether clot formation is affected by factor H deficiency, therefore downstream of thrombin generation. The results demonstrated that there was low complement activation in human factor H depleted plasma (due to the citrated buffer), which is not representative of the FH knockout plasma where complement is consumed. Therefore, it would be key to measure aPTT and PT in human factor H depleted plasma with complement overactivation and consumption.

After concluding that factor H impacted fibrin clot formation by thrombin by enhancing the rate of formation, as well as altering its structure, it would be important to confirm the effect of factor H on clot structure and fibre thickness. Using the ROTEM technique, we would further establish what the effects of factor H are on fibre thickness, lateral aggregation, and clot density in pure protein assays. Using scanning electron microscopy (SEM) would allow more in-depth analysis of factor H's impact on clot structure, specifically the fibre formation and size, as well as the pores in the clot. This would confirm the fluorescent imaging performed. Also visualising clot formed in normal plasma as well as factor H depleted plasma would indicate the role of factor H on clot structure in a more physiological setting.

In addition, it would be interesting to determine whether factor H also had an impact on fibrinolysis. Clots with thinner fibres are harder to lyse, whereas thicker fibres are more rapidly lysed. We could hypothesise at this stage that the presence of factor H would enhance fibrinolysis, as it increases fibre thickness and the number and size of pores, as well as decrease fibre density.

A strong link has been demonstrated between factor H and platelets. Therefore, further analysing the effect of factor H on clot formation, aPTT and PT, and the clot structure in the presence of platelets would be a future analysis.

Results showed a significant interaction of factor H with fibrinogen. It would therefore be interesting to investigate further the binding sites involved on factor H and fibrinogen, and also whether factor H binds fibrin also, therefore after cleavage by thrombin.

It was also observed that factor H enhanced protein C activation, by the thrombin-thrombomodulin complex and by thrombin alone. As the interaction between factor H and thrombin, and factor H and thrombomodulin were established, the next analysis is the interaction between factor H and protein C. However, identifying all residues involved in the interaction between thrombin and factor H, thrombomodulin and factor H, and the thrombin-thrombomodulin complex and factor H, is key. In addition, analysing whether factor H enhances protein C activation on the surfaces of cells would enable a more physiological setting. Investigating the role and impact of calcium in the presence of factor H would also be key to understanding thrombin only mediated enhancement of protein C activation.

Thrombin activated fibrinolysis inhibitor (TAFI) is also activated by the thrombin-thrombomodulin complex, therefore it would be interesting to determine if factor H can also enhance activation of TAFI by thrombin, in presence and absence of thrombomodulin.

AHUS is driven by mutations mainly situated in factor H, specifically the C-terminal domain SCR19-20. Therefore, after determining the impact of factor H full length on thrombin's role in fibrin clot formation as well as anticoagulation, it is key to determine the impact of mutant factor H. Results illustrated that the SCR19-20 could be involved in the interaction with thrombin, therefore the mutations in that region could have an impact on the binding with thrombin and the impact on clotting and protein C activation. Determining how the mutations in factor H alter the binding to thrombin, thrombomodulin or fibrinogen, as well as whether they cause differential regulation of clotting or protein C activation would help understand the pathophysiology of the disease. Performing these experiments on the mutant forms of factor H

would also further deepen the knowledge of the role of factor H in the clot microenvironment, where it interacts also with von Willebrand factor, factor XII, factor XIII and platelets. The SCR19-20 region has also been identified as a binding site with these factors.

A significant number of mutations in aHUS have been identified on thrombomodulin. Previous data from the lab demonstrated the effect that thrombomodulin has on factor H regulatory activity, therefore looking at the impact of these mutations on protein C activation is essential, to determine any impact on the regulation of coagulation. Therefore determining whether the thrombomodulin mutations also affect factor H's effect on protein C activation by the thrombin-thrombomodulin complex would help deepen the function of these mutations. It would be essential to analyse the impact of a thrombomodulin and factor H dual mutation.

Further understanding the binding sites by doing an alanine scanning experiment for instance would help identify the exact residues involved in the interaction, and also further validate the molecular models set.

7.8. Limitations of the study

Despite the results obtained throughout the project, there were some limitations which impeded the completion of some results. The factor H knockout mouse colony was discontinued at the end of my first year of thesis, and therefore we were not able to perform more repeats or other experiments on them. More specifically, we wanted to measure aPTT and PT in mouse plasma, which we were not able to do, due to low sample number and the EDTA buffer that the blood was collected in. In the future, I would like to obtain more *CFH*^{-/-} murine citrate plasma to conduct aptt and pt.

A section of the work planned was to generate a recombinant thrombomodulin domain construct, however, development of the protocol and expression conditions as well as difficulties with isolation of the product, caused significant delay. While TM456-ST was produced, protein concentration was only sufficient to compare its functionality but not the impact of factor H. In the future, I would like to generate a higher yield to conduct further experiments with this fragment.

The factor H fragments I had access to were a limited resource and I needed to carefully measure how much could be used. Also, the storage buffer, largely interfered with calcium-

sensitive assays, which caused false positives in experiments which were excluded from the final analysis. In the future, it is key to request more protein or consider generating my own stock of relevant fragments to conduct more in-depth analysis on the factor H binding sites.

The molecular modelling was self-taught, therefore spending more time on training would have been beneficial to complete the modelling section. There was also a limitation on time available to spend working with the software.

Having other anti-thrombomodulin antibodies to be able to further dissect the potential binding sites between factor H and thrombomodulin, would have been useful. For instance, the modelling showed a potential involvement of EGF4 in the interaction with factor H, therefore an antibody against EGF4 would have been interesting.

The covid-19 pandemic caused the labs to be closed for a significant amount of time in the final and most productive year of the PhD. Although it was an opportunity for me to write my thesis, it delayed work (which needed re-optimisation after returning to the lab), and caused me to have to cancel certain experiments. Some of my work was also done in the haemostasis laboratory in Heath hospital; with the lockdown I was not able to access the facilities to do the experiments. The pandemic also occasionally caused delays in orders, as well as constraints with regards to using laboratory facilities, as there was a limit on the number of people in one given space, and equipment had to be booked.

References

1. ALPORT MAJW. Complement First of Two Parts. *New England Journal of Medicine*. 2001;344(14):1058-66.
2. Tomaiuolo M, Brass LF, Stalker TJ. Regulation of Platelet Activation and Coagulation and Its Role in Vascular Injury and Arterial Thrombosis. *Interv Cardiol Clin*. 2017;6(1):1-12.
3. Dzik S. Complement and Coagulation: Cross Talk Through Time. *Transfus Med Rev*. 2019;33(4):199-206.
4. Conway EM. Reincarnation of ancient links between coagulation and complement. *J Thromb Haemost*. 2015;13 Suppl 1:S121-32.
5. Afshar-Kharghan V. Complement and clot. *Blood*. 2017;129(16):2214-5.
6. Amara U, Flierl MA, Rittirsch D, Klos A, Chen H, Acker B, et al. Molecular intercommunication between the complement and coagulation systems. *J Immunol*. 2010;185(9):5628-36.
7. Chapin J, Terry HS, Kleinert D, Laurence J. The role of complement activation in thrombosis and hemolytic anemias. *Transfus Apher Sci*. 2016;54(2):191-8.
8. Foley JH. Examining coagulation-complement crosstalk: complement activation and thrombosis. *Thrombosis Research*. 2016;141:S50-S4.
9. Kavanagh D, Goodship TH, Richards A. Atypical hemolytic uremic syndrome. *Semin Nephrol*. 2013;33(6):508-30.
10. Meri S. Complement activation in diseases presenting with thrombotic microangiopathy. *Eur J Intern Med*. 2013;24(6):496-502.
11. Chaturvedi S, Brodsky RA, McCrae KR. Complement in the Pathophysiology of the Antiphospholipid Syndrome. *Front Immunol*. 2019;10:449.
12. Lupu F, Keshari RS, Lambris JD, Coggeshall KM. Crosstalk between the coagulation and complement systems in sepsis. *Thromb Res*. 2014;133 Suppl 1:S28-31.
13. Foley JH, Conway EM. Cross Talk Pathways Between Coagulation and Inflammation. *Circ Res*. 2016;118(9):1392-408.
14. Jozsi M, Heinen S, Hartmann A, Ostrowicz CW, Halbich S, Richter H, et al. Factor H and atypical hemolytic uremic syndrome: mutations in the C-terminus cause structural changes and defective recognition functions. *J Am Soc Nephrol*. 2006;17(1):170-7.
15. Goodship TH. Factor H genotype-phenotype correlations: lessons from aHUS, MPGN II, and AMD. *Kidney Int*. 2006;70(1):12-3.
16. Toomey CB, Johnson LV, Bowes Rickman C. Complement factor H in AMD: Bridging genetic associations and pathobiology. *Prog Retin Eye Res*. 2018;62:38-57.
17. Foltyn Zadura A, Memon AA, Stojanovich L, Perricone C, Conti F, Valesini G, et al. Factor H Autoantibodies in Patients with Antiphospholipid Syndrome and Thrombosis. *J Rheumatol*. 2015;42(10):1786-93.
18. Wiegner R, Chakraborty S, Huber-Lang M. Complement-coagulation crosstalk on cellular and artificial surfaces. *Immunobiology*. 2016;221(10):1073-9.
19. Ferluga J, Kishore U, Sim RB. A potential anti-coagulant role of complement factor H. *Mol Immunol*. 2014;59(2):188-93.
20. Thangaraj SS, Christiansen SH, Graversen JH, Sidelmann JJ, Hansen SWK, Bygum A, et al. Contact activation-induced complex formation between complement factor H and coagulation factor XIIa. *J Thromb Haemost*. 2020;18(4):876-84.

21. Akhter MS, Singh S, Yadegari H, Ivaskевичius V, Oldenburg J, Biswas A. Exploring the structural similarity yet functional distinction between coagulation factor XIII-B and complement factor H sushi domains. *J Thromb Thrombolysis*. 2019;48(1):95-102.
22. Nikolajsen CL, Dyrland TF, Poulsen ET, Enghild JJ, Scavenius C. Coagulation factor XIIIa substrates in human plasma: identification and incorporation into the clot. *J Biol Chem*. 2014;289(10):6526-34.
23. Singh S, Akhter MS, Dodt J, Volkens P, Reuter A, Reinhart C, et al. Identification of Potential Novel Interacting Partners for Coagulation Factor XIII B (FXIII-B) Subunit, a Protein Associated with a Rare Bleeding Disorder. *Int J Mol Sci*. 2019;20(11).
24. Abbow H. Studies on ligand interactions of human complement factor H: University of Leicester; 2016.
25. Blatt AZ, Saggi G, Cortes C, Herbert AP, Kavanagh D, Ricklin D, et al. Factor H C-Terminal Domains Are Critical for Regulation of Platelet/Granulocyte Aggregate Formation. *Front Immunol*. 2017;8:1586.
26. F. VAZIRI -SANI JH, P . F . ZIPFEL, A. G. SJOHOLM, R. IANCU and D. KARPMAN. Factor H binds to washed human platelets. *Journal of Thrombosis and Haemostasis*. 2005;3.
27. Feng S, Liang X, Cruz MA, Vu H, Zhou Z, Pemmaraju N, et al. The interaction between factor H and Von Willebrand factor. *PLoS One*. 2013;8(8):e73715.
28. Rayes J, Roumenina LT, Dimitrov JD, Repesse Y, Ing M, Christophe O, et al. The interaction between factor H and VWF increases factor H cofactor activity and regulates VWF prothrombotic status. *Blood*. 2014;123(1):121-5.
29. Heurich M, Preston RJ, O'Donnell VB, Morgan BP, Collins PW. Thrombomodulin enhances complement regulation through strong affinity interactions with factor H and C3b-Factor H complex. *Thromb Res*. 2016;145:84-92.
30. Abe T, Sasaki A, Ueda T, Miyakawa Y, Ochiai H. Complement-mediated thrombotic microangiopathy secondary to sepsis-induced disseminated intravascular coagulation successfully treated with eculizumab: A case report. *Medicine (Baltimore)*. 2017;96(6):e6056.
31. Palma LMP, Sridharan M, Sethi S. Complement in Secondary Thrombotic Microangiopathy. *Kidney Int Rep*. 2021;6(1):11-23.
32. Dunkelberger JR, Song WC. Complement and its role in innate and adaptive immune responses. *Cell Res*. 2010;20(1):34-50.
33. Carroll MV, Sim RB. Complement in health and disease. *Adv Drug Deliv Rev*. 2011;63(12):965-75.
34. Merle NS, Church SE, Fremeaux-Bacchi V, Roumenina LT. Complement System Part I - Molecular Mechanisms of Activation and Regulation. *Front Immunol*. 2015;6:262.
35. Kozarcenin H, Lood C, Munthe-Fog L, Sandholm K, Hamad OA, Bengtsson AA, et al. The lectin complement pathway serine proteases (MASPs) represent a possible crossroad between the coagulation and complement systems in thromboinflammation. *J Thromb Haemost*. 2016;14(3):531-45.
36. Bajic G, Degn SE, Thiel S, Andersen GR. Complement activation, regulation, and molecular basis for complement-related diseases. *EMBO J*. 2015;34(22):2735-57.
37. PIKE RSAMC. Interaction of Complex Polysaccharides with the Complement System: Effect of Calcium Depletion on Terminal Component Consumption. *Infection and Immunity*. 1975;11(2):273-9.
38. Fung KW, Wright DW, Gor J, Swann MJ, Perkins SJ. Domain structure of human complement C4b extends with increasing NaCl concentration: implications for its regulatory mechanism. *Biochem J*. 2016;473(23):4473-91.
39. Klos A, Tenner AJ, Johswich KO, Ager RR, Reis ES, Kohl J. The role of the anaphylatoxins in health and disease. *Mol Immunol*. 2009;46(14):2753-66.
40. Sarma JV, Ward PA. The complement system. *Cell Tissue Res*. 2011;343(1):227-35.
41. Kerr H, Richards A. Complement-mediated injury and protection of endothelium: lessons from atypical haemolytic uraemic syndrome. *Immunobiology*. 2012;217(2):195-203.

42. Pangburn SMMK. Regulation of Alternative Pathway complement activation by glycosaminoglycans: specificity spe of polyanion binding site on factor H. *Biochemical and Biophysical Research Communications*. 1994;198:52-9.
43. Maga TK, Nishimura CJ, Weaver AE, Frees KL, Smith RJ. Mutations in alternative pathway complement proteins in American patients with atypical hemolytic uremic syndrome. *Hum Mutat*. 2010;31(6):E1445-60.
44. Williams JA, Stampoulis D, Gunter CE, Greenwood J, Adamson P, Moss SE. Regulation of C3 Activation by the Alternative Complement Pathway in the Mouse Retina. *PLoS One*. 2016;11(8):e0161898.
45. Ferreira VP, Herbert AP, Cortes C, McKee KA, Blaum BS, Esswein ST, et al. The binding of factor H to a complex of physiological polyanions and C3b on cells is impaired in atypical hemolytic uremic syndrome. *J Immunol*. 2009;182(11):7009-18.
46. Ramadass M, Ghebrehiwet B, Smith RJ, Kew RR. Generation of multiple fluid-phase C3b:plasma protein complexes during complement activation: possible implications in C3 glomerulopathies. *J Immunol*. 2014;192(3):1220-30.
47. de Cordoba SR, Tortajada A, Harris CL, Morgan BP. Complement dysregulation and disease: from genes and proteins to diagnostics and drugs. *Immunobiology*. 2012;217(11):1034-46.
48. Morgan BP. *Complement Methods and Protocols* 2000.
49. Smith RJH, Appel GB, Blom AM, Cook HT, D'Agati VD, Fakhouri F, et al. C3 glomerulopathy - understanding a rare complement-driven renal disease. *Nat Rev Nephrol*. 2019;15(3):129-43.
50. Sanchez-Corral P, Pouw RB, Lopez-Trascasa M, Jozsi M. Self-Damage Caused by Dysregulation of the Complement Alternative Pathway: Relevance of the Factor H Protein Family. *Front Immunol*. 2018;9:1607.
51. Serna M, Giles JL, Morgan BP, Bubeck D. Structural basis of complement membrane attack complex formation. *Nat Commun*. 2016;7:10587.
52. Hadders MA, Bubeck D, Roversi P, Hakobyan S, Forneris F, Morgan BP, et al. Assembly and regulation of the membrane attack complex based on structures of C5b6 and sC5b9. *Cell Rep*. 2012;1(3):200-7.
53. Afshar-Kharghan V. The role of the complement system in cancer. *J Clin Invest*. 2017;127(3):780-9.
54. Morgan BP. The membrane attack complex as an inflammatory trigger. *Immunobiology*. 2016;221(6):747-51.
55. Carroll MC. The complement system in regulation of adaptive immunity. *Nat Immunol*. 2004;5(10):981-6.
56. Noris M, Remuzzi G. Overview of complement activation and regulation. *Semin Nephrol*. 2013;33(6):479-92.
57. Wu J, Wu YQ, Ricklin D, Janssen BJ, Lambris JD, Gros P. Structure of complement fragment C3b-factor H and implications for host protection by complement regulators. *Nat Immunol*. 2009;10(7):728-33.
58. Ferreira VP, Pangburn MK, Cortes C. Complement control protein factor H: the good, the bad, and the inadequate. *Mol Immunol*. 2010;47(13):2187-97.
59. Xue X, Wu J, Ricklin D, Forneris F, Di Crescenzo P, Schmidt CQ, et al. Regulator-dependent mechanisms of C3b processing by factor I allow differentiation of immune responses. *Nat Struct Mol Biol*. 2017;24(8):643-51.
60. Ricklin D, Reis ES, Lambris JD. Complement in disease: a defence system turning offensive. *Nat Rev Nephrol*. 2016;12(7):383-401.
61. Rose KL, Paixao-Cavalcante D, Fish J, Manderson AP, Malik TH, Bygrave AE, et al. Factor I is required for the development of membranoproliferative glomerulonephritis in factor H-deficient mice. *J Clin Invest*. 2008;118(2):608-18.

62. Aslam M, Perkins SJ. Folded-back solution structure of monomeric factor H of human complement by synchrotron X-ray and neutron scattering, analytical ultracentrifugation and constrained molecular modelling. *J Mol Biol.* 2001;309(5):1117-38.
63. David. Gordon RMK, Timothy K. Blackmore, Jeffrey Kwong, and Douglas M. Lublin. Identification of Complement Regulatory Domains in Human Factor H. *J Immunol.* 1995;155:348-56.
64. de Cordoba SR, de Jorge EG. Translational mini-review series on complement factor H: genetics and disease associations of human complement factor H. *Clin Exp Immunol.* 2008;151(1):1-13.
65. Jozsi M, Schneider AE, Karpati E, Sandor N. Complement factor H family proteins in their non-canonical role as modulators of cellular functions. *Semin Cell Dev Biol.* 2019;85:122-31.
66. Jozsi M, Zipfel PF. Factor H family proteins and human diseases. *Trends Immunol.* 2008;29(8):380-7.
67. Wu YQ, Qu H, Sfyroera G, Tzekou A, Kay BK, Nilsson B, et al. Protection of nonself surfaces from complement attack by factor H-binding peptides: implications for therapeutic medicine. *J Immunol.* 2011;186(7):4269-77.
68. Perkins SJ, Nan R, Li K, Khan S, Miller A. Complement factor H-ligand interactions: self-association, multivalency and dissociation constants. *Immunobiology.* 2012;217(2):281-97.
69. Pouw RB, Vredevoogd DW, Kuijpers TW, Wouters D. Of mice and men: The factor H protein family and complement regulation. *Mol Immunol.* 2015;67(1):12-20.
70. Blaum BS, Hannan JP, Herbert AP, Kavanagh D, Uhrin D, Stehle T. Structural basis for sialic acid-mediated self-recognition by complement factor H. *Nat Chem Biol.* 2015;11(1):77-82.
71. Clark SJ, Bishop PN, Day AJ. Complement factor H and age-related macular degeneration: the role of glycosaminoglycan recognition in disease pathology. *Biochem Soc Trans.* 2010;38(5):1342-8.
72. Dopler A, Guntau L, Harder MJ, Palmer A, Hochsmann B, Schrezenmeier H, et al. Self versus Nonself Discrimination by the Soluble Complement Regulators Factor H and FHL-1. *J Immunol.* 2019;202(7):2082-94.
73. Parente R, Clark SJ, Inforzato A, Day AJ. Complement factor H in host defense and immune evasion. *Cell Mol Life Sci.* 2017;74(9):1605-24.
74. Bhattacharjee A, Lehtinen MJ, Kajander T, Goldman A, Jokiranta TS. Both domain 19 and domain 20 of factor H are involved in binding to complement C3b and C3d. *Mol Immunol.* 2010;47(9):1686-91.
75. Hocking HG, Herbert AP, Kavanagh D, Soares DC, Ferreira VP, Pangburn MK, et al. Structure of the N-terminal region of complement factor H and conformational implications of disease-linked sequence variations. *J Biol Chem.* 2008;283(14):9475-87.
76. Okemefuna AI, Gilbert HE, Griggs KM, Ormsby RJ, Gordon DL, Perkins SJ. The regulatory SCR-1/5 and cell surface-binding SCR-16/20 fragments of factor H reveal partially folded-back solution structures and different self-associative properties. *J Mol Biol.* 2008;375(1):80-101.
77. Perkins SJ, Fung KW, Khan S. Molecular Interactions between Complement Factor H and Its Heparin and Heparan Sulfate Ligands. *Front Immunol.* 2014;5:126.
78. Morgan HP, Schmidt CQ, Guariento M, Blaum BS, Gillespie D, Herbert AP, et al. Structural basis for engagement by complement factor H of C3b on a self surface. *Nat Struct Mol Biol.* 2011;18(4):463-70.
79. Herbert AP, Deakin JA, Schmidt CQ, Blaum BS, Egan C, Ferreira VP, et al. Structure shows that a glycosaminoglycan and protein recognition site in factor H is perturbed by age-related macular degeneration-linked single nucleotide polymorphism. *J Biol Chem.* 2007;282(26):18960-8.
80. Schmidt CQ, Herbert AP, Kavanagh D, Gandy C, Fenton CJ, Blaum BS, et al. A new map of glycosaminoglycan and C3b binding sites on factor H. *J Immunol.* 2008;181(4):2610-9.
81. Jokiranta TS, Hellwage J, Koistinen V, Zipfel PF, Meri S. Each of the three binding sites on complement factor H interacts with a distinct site on C3b. *J Biol Chem.* 2000;275(36):27657-62.

82. Ormsby RJ, Jokiranta TS, Duthy TG, Griggs KM, Sadlon TA, Giannakis E, et al. Localization of the third heparin-binding site in the human complement regulator factor H1. *Mol Immunol*. 2006;43(10):1624-32.
83. Osborne AJ, Nan R, Miller A, Bhatt JS, Gor J, Perkins SJ. Two distinct conformations of factor H regulate discrete complement-binding functions in the fluid phase and at cell surfaces. *J Biol Chem*. 2018;293(44):17166-87.
84. Janssen van Doorn K, Dirinck E, Verpooten GA, Couttenye MM. Complement factor H mutation associated with membranoproliferative glomerulonephritis with transformation to atypical haemolytic uraemic syndrome. *Clin Kidney J*. 2013;6(2):216-9.
85. Tortajada A, Montes T, Martinez-Barricarte R, Morgan BP, Harris CL, de Cordoba SR. The disease-protective complement factor H allotypic variant Ile62 shows increased binding affinity for C3b and enhanced cofactor activity. *Hum Mol Genet*. 2009;18(18):3452-61.
86. Caprioli J, Castelletti F, Bucchioni S, Bettinaglio P, Bresin E, Pianetti G, et al. Complement factor H mutations and gene polymorphisms in haemolytic uraemic syndrome: the C-257T, the A2089G and the G2881T polymorphisms are strongly associated with the disease. *Hum Mol Genet*. 2003;12(24):3385-95.
87. Tortajada A, Pinto S, Martinez-Ara J, Lopez-Trascasa M, Sanchez-Corral P, de Cordoba SR. Complement factor H variants I890 and L1007 while commonly associated with atypical hemolytic uremic syndrome are polymorphisms with no functional significance. *Kidney Int*. 2012;81(1):56-63.
88. Vaziri-Sani F, Holmberg L, Sjöholm AG, Kristoffersson AC, Manea M, Fremeaux-Bacchi V, et al. Phenotypic expression of factor H mutations in patients with atypical hemolytic uremic syndrome. *Kidney Int*. 2006;69(6):981-8.
89. Perez-Caballero D, Gonzalez-Rubio C, Gallardo ME, Vera M, Lopez-Trascasa M, Rodriguez de Cordoba S, et al. Clustering of missense mutations in the C-terminal region of factor H in atypical hemolytic uremic syndrome. *Am J Hum Genet*. 2001;68(2):478-84.
90. Sanchez-Corral P, Perez-Caballero D, Huarte O, Simckes AM, Goicoechea E, Lopez-Trascasa M, et al. Structural and functional characterization of factor H mutations associated with atypical hemolytic uremic syndrome. *Am J Hum Genet*. 2002;71(6):1285-95.
91. Kerr H, Wong E, Makou E, Yang Y, Marchbank K, Kavanagh D, et al. Disease-linked mutations in factor H reveal pivotal role of cofactor activity in self-surface-selective regulation of complement activation. *J Biol Chem*. 2017;292(32):13345-60.
92. Jokiranta TS. HUS and atypical HUS. *Blood*. 2017;129(21):2847-56.
93. Clark SJ, Bishop PN. Role of Factor H and Related Proteins in Regulating Complement Activation in the Macula, and Relevance to Age-Related Macular Degeneration. *J Clin Med*. 2015;4(1):18-31.
94. Clark SJ, Schmidt CQ, White AM, Hakobyan S, Morgan BP, Bishop PN. Identification of factor H-like protein 1 as the predominant complement regulator in Bruch's membrane: implications for age-related macular degeneration. *J Immunol*. 2014;193(10):4962-70.
95. Cipriani V, Lores-Motta L, He F, Fathalla D, Tilakaratna V, McHarg S, et al. Increased circulating levels of Factor H-Related Protein 4 are strongly associated with age-related macular degeneration. *Nat Commun*. 2020;11(1):778.
96. Prosser BE, Johnson S, Roversi P, Herbert AP, Blaum BS, Tyrrell J, et al. Structural basis for complement factor H linked age-related macular degeneration. *J Exp Med*. 2007;204(10):2277-83.
97. Maugeri A, Barchitta M, Mazzone MG, Giuliano F, Agodi A. Complement System and Age-Related Macular Degeneration: Implications of Gene-Environment Interaction for Preventive and Personalized Medicine. *Biomed Res Int*. 2018;2018:7532507.
98. Pickering MC, Cook HT. Translational mini-review series on complement factor H: renal diseases associated with complement factor H: novel insights from humans and animals. *Clin Exp Immunol*. 2008;151(2):210-30.

99. Ankawi GA, Clark WF. Atypical haemolytic uremic syndrome (aHUS) and membranoproliferative glomerulonephritis (MPGN), different diseases or a spectrum of complement-mediated glomerular diseases? *BMJ Case Rep.* 2017;2017.
100. Smith RJ, Harris CL, Pickering MC. Dense deposit disease. *Mol Immunol.* 2011;48(14):1604-10.
101. Goetz L, Laskowski J, Renner B, Pickering MC, Kulik L, Klawitter J, et al. Complement factor H protects mice from ischemic acute kidney injury but is not critical for controlling complement activation by glomerular IgM. *Eur J Immunol.* 2018;48(5):791-802.
102. Pickering MC, de Jorge EG, Martinez-Barricarte R, Recalde S, Garcia-Layana A, Rose KL, et al. Spontaneous hemolytic uremic syndrome triggered by complement factor H lacking surface recognition domains. *J Exp Med.* 2007;204(6):1249-56.
103. Fakhouri F, de Jorge EG, Brune F, Azam P, Cook HT, Pickering MC. Treatment with human complement factor H rapidly reverses renal complement deposition in factor H-deficient mice. *Kidney Int.* 2010;78(3):279-86.
104. Pickering MC, Warren J, Rose KL, Carlucci F, Wang Y, Walport MJ, et al. Prevention of C5 activation ameliorates spontaneous and experimental glomerulonephritis in factor H-deficient mice. *Proc Natl Acad Sci U S A.* 2006;103(25):9649-54.
105. de Jorge EG, Macor P, Paixão-Cavalcante D, Rose KL, Tedesco F, Cook HT, et al. The development of atypical hemolytic uremic syndrome depends on complement C5. *J Am Soc Nephrol.* 2011;22(1):137-45.
106. Vernon KA, Ruseva MM, Cook HT, Botto M, Malik TH, Pickering MC. Partial Complement Factor H Deficiency Associates with C3 Glomerulopathy and Thrombotic Microangiopathy. *J Am Soc Nephrol.* 2016;27(5):1334-42.
107. Peter J. Coffey* CG, Caroline J. McDermott†, Peter Lundh‡, Matthew C. Pickering§, Charanjit Sethi†, Alan Bird*¶, Fred W. Fitzke‡, Annelie Maass†, Li Li Chen*, Graham E. Holder¶, Philip J. Luthert†, Thomas E. Salt‡, Stephen E. Moss‡, and John Greenwood. Complement factor H deficiency in aged mice causes retinal abnormalities and visual dysfunction. *PNAS.* 2007;107(42):16651–6.
108. Hoh Kam J, Lenassi E, Malik TH, Pickering MC, Jeffery G. Complement component C3 plays a critical role in protecting the aging retina in a murine model of age-related macular degeneration. *Am J Pathol.* 2013;183(2):480-92.
109. Williams JA, Greenwood J, Moss SE. Retinal changes precede visual dysfunction in the complement factor H knockout mouse. *PLoS One.* 2013;8(7):e68616.
110. Sivapathasuntharam C, Hayes MJ, Shinhmar H, Kam JH, Sivaprasad S, Jeffery G. Complement factor H regulates retinal development and its absence may establish a footprint for age related macular degeneration. *Sci Rep.* 2019;9(1):1082.
111. Kasanmoentalib ES, Valls Seron M, Engelen-Lee JY, Tanck MW, Pouw RB, van Mierlo G, et al. Complement factor H contributes to mortality in humans and mice with bacterial meningitis. *J Neuroinflammation.* 2019;16(1):279.
112. Martin M, Leffler J, Smolağ KI, Mytych J, Björk A, Chaves LD, et al. Factor H uptake regulates intracellular C3 activation during apoptosis and decreases the inflammatory potential of nucleosomes. *Cell Death Differ.* 2016;23(5):903-11.
113. Smith SA, Travers RJ, Morrissey JH. How it all starts: Initiation of the clotting cascade. *Crit Rev Biochem Mol Biol.* 2015;50(4):326-36.
114. Adams RL, Bird RJ. Review article: Coagulation cascade and therapeutics update: relevance to nephrology. Part 1: Overview of coagulation, thrombophilias and history of anticoagulants. *Nephrology (Carlton).* 2009;14(5):462-70.
115. Earl W. Davie, Kazuo Fujikawa aWK. The Coagulation Cascade: Initiation, Maintenance, and Regulation. *Biochemistry.* 1991;30(43):10363-70.
116. Mackman N, Tilley RE, Key NS. Role of the extrinsic pathway of blood coagulation in hemostasis and thrombosis. *Arterioscler Thromb Vasc Biol.* 2007;27(8):1687-93.
117. Pilli VS. Understanding the Clotting Cascade, Regulators, and Clinical Modulators of Coagulation. *Hematology - Latest Research and Clinical Advances*2018.

118. Adams TE, Huntington JA. Structural transitions during prothrombin activation: On the importance of fragment 2. *Biochimie*. 2016;122:235-42.
119. Krishnaswamy S. The transition of prothrombin to thrombin. *J Thromb Haemost*. 2013;11 Suppl 1:265-76.
120. Gallwitz M, Enoksson M, Thorpe M, Hellman L. The extended cleavage specificity of human thrombin. *PLoS One*. 2012;7(2):e31756.
121. Bruce Furie MD, and Barbara C. Furie, Ph.D. Mechanisms of Thrombus Formation. *New England Journal of Medicine*. 2008;359:938-49.
122. Grover SP, Mackman N. Intrinsic Pathway of Coagulation and Thrombosis. *Arterioscler Thromb Vasc Biol*. 2019;39(3):331-8.
123. Dahlback B. Blood coagulation and its regulation by anticoagulant pathways: genetic pathogenesis of bleeding and thrombotic diseases. *Journal of Internal Medicine*. 2005;257:209-23.
124. Cera ED. Thrombin. *Mol Aspects Med*. 2008;29.
125. Cera ED. Thrombin as procoagulant and anticoagulant. *Journal of Thrombosis and Haemostasis*. 2007;5.
126. G. A. ALLEN ASW, J. A. OLIVER, M. HOFFMAN, H. R. ROBERTS and D. M. MONROE. Impact of procoagulant concentration on rate, peak and total thrombin generation in a model system. *Journal of Thrombosis and Haemostasis*. 2004;2:402-13.
127. Ignjatovic V, Greenway A, Summerhayes R, Monagle P. Thrombin generation: the functional role of alpha-2-macroglobulin and influence of developmental haemostasis. *Br J Haematol*. 2007;138(3):366-8.
128. J. T. B. CRAWLEY SZ, C. K . N. K . CHION and D. A. LANE. The central role of thrombin in hemostasis. *Journal of Thrombosis and Haemostasis*. 2007;5.
129. K. G. MANN KBaSB. What is all that thrombin for? *Journal of Thrombosis and Haemostasis*. 2003;1:1504-14.
130. Licari LG, Kovacic JP. Thrombin physiology and pathophysiology. *J Vet Emerg Crit Care (San Antonio)*. 2009;19(1):11-22.
131. Walker CP, Royston D. Thrombin generation and its inhibition: a review of the scientific basis and mechanism of action of anticoagulant therapies. *Br J Anaesth*. 2002;88(6):848-63.
132. Wolberg AS, Campbell RA. Thrombin generation, fibrin clot formation and hemostasis. *Transfus Apher Sci*. 2008;38(1):15-23.
133. Xiao J, Melvin RL, Salisbury FR. Mechanistic insights into thrombin's switch between "slow" and "fast" forms. *Phys Chem Chem Phys*. 2017;19(36):24522-33.
134. Adams TE, Huntington JA. Thrombin-cofactor interactions: structural insights into regulatory mechanisms. *Arterioscler Thromb Vasc Biol*. 2006;26(8):1738-45.
135. Doolittle RF. The conversion of fibrinogen to fibrin: A brief history of some key events. *Matrix Biol*. 2017;60-61:5-7.
136. Walton BL, Byrnes JR, Wolberg AS. Fibrinogen, red blood cells, and factor XIII in venous thrombosis. *J Thromb Haemost*. 2015;13 Suppl 1:S208-15.
137. Bouma BN, Mosnier LO. Thrombin activatable fibrinolysis inhibitor (TAFI)--how does thrombin regulate fibrinolysis? *Ann Med*. 2006;38(6):378-88.
138. Laszlo Bajzar JM, and Michael Nesheim. TAFI, or Plasma Procarboxypeptidase B, Couples the Coagulation and Fibrinolytic Cascades through the Thrombin-Thrombomodulin Complex*. *The Journal of Biological Chemistry*. 1996;271(28):16603-8.
139. Longstaff C. Measuring fibrinolysis: from research to routine diagnostic assays. *J Thromb Haemost*. 2018;16(4):652-62.
140. Coughlin SR. Thrombin signalling and protease-activated receptors. *Nature*. 2000;407.
141. Bruce Furie DHB, Richard J. Feldmann', David J. Robison", John P. BurnieraJ, and Barbara C. Furi. Computer-generated Models of Blood Coagulation Factor Xa, Factor IXa, and Thrombin Based upon Structural Homology with Other Serine Proteases*. *The Journal of Biological Chemistry*. 1983;257(7).

142. Huntington JA. Thrombin inhibition by the serpins. *J Thromb Haemost.* 2013;11 Suppl 1:254-64.
143. Fuglestad B, Gasper PM, Tonelli M, McCammon JA, Markwick PR, Komives EA. The dynamic structure of thrombin in solution. *Biophys J.* 2012;103(1):79-88.
144. Malovichko MV, Sabo TM, Maurer MC. Ligand Binding to Anion-binding Exosites Regulates Conformational Properties of Thrombin. *Journal of Biological Chemistry.* 2013;288(12):8667-78.
145. Billur R, Ban D, Sabo TM, Maurer MC. Deciphering Conformational Changes Associated with the Maturation of Thrombin Anion Binding Exosite I. *Biochemistry.* 2017;56(48):6343-54.
146. HUNTINGTON JA. Molecular recognition mechanisms of thrombin. *Journal of Thrombosis and Haemostasis.* 2005;3:1861-72.
147. P. E. BOCK PP, and I. M. A. VERHAMME. Exosites in the substrate specificity of blood coagulation reactions. *Journal of Thrombosis and Haemostasis.* 2007;5.
148. James C. Fredenburgh ARS, and Jeffrey I. Weitz†. Evidence for Allosteric Linkage between Exosites 1 and 2 of Thrombin*. *The Journal of Biological Chemistry.* 1997;272(41).
149. Lane DA, Philippou H, Huntington JA. Directing thrombin. *Blood.* 2005;106(8):2605-12.
150. Ming-Tain Lai‡§ EDC, and Jules A. Shafer. Kinetic Pathway for the Slow to Fast Transition of Thrombin EVIDENCE OF LINKED LIGAND BINDING AT STRUCTURALLY DISTINCT DOMAINS*. *The Journal of Biological Chemistry.* 1997;272(48).
151. Duval C, Allan P, Connell SD, Ridger VC, Philippou H, Ariens RA. Roles of fibrin alpha- and gamma-chain specific cross-linking by FXIIIa in fibrin structure and function. *Thromb Haemost.* 2014;111(5):842-50.
152. Robert A. S. Arieˆns HP, Chandrasekaran Nagaswami, John W. Weisel, David A. Lane, and Peter J. Grant. The factor XIII V34L polymorphism accelerates thrombin activation of factor XIII and affects cross-linked fibrin structure. *Blood.* 2000;96(3).
153. Balendran CA, Lovgren A, Hansson KM, Nelander K, Olsson M, Johansson KJ, et al. Prothrombin time is predictive of low plasma prothrombin concentration and clinical outcome in patients with trauma hemorrhage: analyses of prospective observational cohort studies. *Scand J Trauma Resusc Emerg Med.* 2017;25(1):30.
154. Campbell RA, Overmyer KA, Bagnell CR, Wolberg AS. Cellular procoagulant activity dictates clot structure and stability as a function of distance from the cell surface. *Arterioscler Thromb Vasc Biol.* 2008;28(12):2247-54.
155. Weisel JW, Litvinov RI. Mechanisms of fibrin polymerization and clinical implications. *Blood.* 2013;121(10):1712-9.
156. BJORK ADal. Properties of antithrombin-thrombin complex formed in the presence and in the absence of heparin. *Biochem J.* 1983;213:345-53.
157. Chuang ST0aY-J. Heparin Activates Antithrombin Anticoagulant Function by Generating New Interaction Sites (Exosites) for Blood Clotting Proteinases. *TCM.* 2002;12(8):331-8.
158. Lee CJ, Ansell JE. Direct thrombin inhibitors. *Br J Clin Pharmacol.* 2011;72(4):581-92.
159. Li W, Johnson DJ, Esmon CT, Huntington JA. Structure of the antithrombin-thrombin-heparin ternary complex reveals the antithrombotic mechanism of heparin. *Nat Struct Mol Biol.* 2004;11(9):857-62.
160. Weisel JW, Litvinov RI. Fibrin Formation, Structure and Properties. *Subcell Biochem.* 2017;82:405-56.
161. Scheraga HA. The thrombin-fibrinogen interaction. *Biophys Chem.* 2004;112(2-3):117-30.
162. Litvinov RI, Weisel JW. What Is the Biological and Clinical Relevance of Fibrin? *Semin Thromb Hemost.* 2016;42(4):333-43.
163. Chiu CL, Hecht V, Duong H, Wu B, Tawil B. Permeability of three-dimensional fibrin constructs corresponds to fibrinogen and thrombin concentrations. *Biores Open Access.* 2012;1(1):34-40.
164. Rose T, Di Cera E. Three-dimensional modeling of thrombin-fibrinogen interaction. *J Biol Chem.* 2002;277(21):18875-80.

165. Chernysh IN, Nagaswami C, Purohit PK, Weisel JW. Fibrin clots are equilibrium polymers that can be remodeled without proteolytic digestion. *Sci Rep.* 2012;2:879.
166. Davalos D, Akassoglou K. Fibrinogen as a key regulator of inflammation in disease. *Semin Immunopathol.* 2012;34(1):43-62.
167. Mihalyi E. Review of some unusual effects of calcium binding to fibrinogen. *Biophys Chem.* 2004;112(2-3):131-40.
168. Mullin JL, Gorkun OV, Binnie CG, Lord ST. Recombinant fibrinogen studies reveal that thrombin specificity dictates order of fibrinopeptide release. *J Biol Chem.* 2000;275(33):25239-46.
169. Riedel T, Suttner J, Brynda E, Houska M, Medved L, Dyr JE. Fibrinopeptides A and B release in the process of surface fibrin formation. *Blood.* 2011;117(5):1700-6.
170. Pechik I, Yakovlev S, Mosesson MW, Gilliland GL, Medved L. Structural basis for sequential cleavage of fibrinopeptides upon fibrin assembly. *Biochemistry.* 2006;45(11):3588-97.
171. Weisel JW. FIBRIN ASSEMBLY Lateral Aggregation and the Role of the Two Pairs of Fibrinopeptides. *Biophysical Journal.* 1986;50.
172. Gersh KC, Nagaswami C, Weisel JW. Fibrin network structure and clot mechanical properties are altered by incorporation of erythrocytes. *Thromb Haemost.* 2009;102(6):1169-75.
173. David A. Meh \ddot{u} s KRS, and Michael W. Mosesson. Identification and Characterization of the Thrombin Binding Sites on Fibrin. *the Journal of Biological Chemistry.* 1996;271(38).
174. Michael Muller HLaWB. Fibrinogen - fibrin transformation:
2. Influence of temperature, pH and of various enzymes on the intermediate structures. *Int J Biol Macromol.* 1981;3.
175. Li W, Sigley J, Baker SR, Helms CC, Kinney MT, Pieters M, et al. Nonuniform Internal Structure of Fibrin Fibers: Protein Density and Bond Density Strongly Decrease with Increasing Diameter. *Biomed Res Int.* 2017;2017:6385628.
176. Li W, Sigley J, Pieters M, Helms CC, Nagaswami C, Weisel JW, et al. Fibrin Fiber Stiffness Is Strongly Affected by Fiber Diameter, but Not by Fibrinogen Glycation. *Biophys J.* 2016;110(6):1400-10.
177. Chernysh IN, Weisel JW. Dynamic imaging of fibrin network formation correlated with other measures of polymerization. *Blood.* 2008;111(10):4854-61.
178. Piechocka IK, Kurniawan NA, Grimbergen J, Koopman J, Koenderink GH. Recombinant fibrinogen reveals the differential roles of alpha- and gamma-chain cross-linking and molecular heterogeneity in fibrin clot strain-stiffening. *J Thromb Haemost.* 2017;15(5):938-49.
179. Wolberg AS, Gabriel DA, Hoffman M. Analyzing fibrin clot structure using a microplate reader. *Blood Coagul Fibrinolysis.* 2002;13(6):533-9.
180. Zubairova LD, Nabiullina RM, Nagaswami C, Zuev YF, Mustafin IG, Litvinov RI, et al. Circulating Microparticles Alter Formation, Structure, and Properties of Fibrin Clots. *Sci Rep.* 2015;5:17611.
181. Weigandt KM, White N, Chung D, Ellingson E, Wang Y, Fu X, et al. Fibrin clot structure and mechanics associated with specific oxidation of methionine residues in fibrinogen. *Biophys J.* 2012;103(11):2399-407.
182. Beth A. Bouchard PaPBT, PhD. Platelets, leukocytes, and coagulation. *Curr Opin Hematol.* 2001;8:263-9.
183. Li X, Sim MMS, Wood JP. Recent Insights Into the Regulation of Coagulation and Thrombosis. *Arterioscler Thromb Vasc Biol.* 2020;40(5):e119-e25.
184. Griffin JH, Zlokovic BV, Mosnier LO. Activated protein C: biased for translation. *Blood.* 2015;125(19):2898-907.
185. Lu G, Chhum S, Krishnaswamy S. The affinity of protein C for the thrombin-thrombomodulin complex is determined in a primary way by active site-dependent interactions. *J Biol Chem.* 2005;280(15):15471-8.
186. Dahlback B, Villoutreix BO. The anticoagulant protein C pathway. *FEBS Lett.* 2005;579(15):3310-6.

187. Van de Wouwer M, Collen D, Conway EM. Thrombomodulin-protein C-EPCR system: integrated to regulate coagulation and inflammation. *Arterioscler Thromb Vasc Biol.* 2004;24(8):1374-83.
188. Barranco-Medina S, Murphy M, Pelc L, Chen Z, Di Cera E, Pozzi N. Rational Design of Protein C Activators. *Sci Rep.* 2017;7:44596.
189. Esmon CT. Protein C anticoagulant pathway and its role in controlling microvascular thrombosis and inflammation. *Crit Care Med.* 2001;29:48-52.
190. Mosnier LO, Zlokovic BV, Griffin JH. The cytoprotective protein C pathway. *Blood.* 2007;109(8):3161-72.
191. Handley LD, Treuheit NA, Venkatesh VJ, Komives EA. Thrombomodulin Binding Selects the Catalytically Active Form of Thrombin. *Biochemistry.* 2015;54(43):6650-8.
192. Rezaie AR. Regulation of the Protein C Anticoagulant and Antiinflammatory Pathways. *Curr Med Chem.* 2010;17.
193. Likui Yang CM, and Alireza R. Rezaie. Activation of protein C by the thrombin–thrombomodulin complex: Cooperative roles of Arg-35 of thrombin and Arg-67 of protein C. *PNAS.* 2005;103(4):879-84.
194. Bae JS, Yang L, Manithody C, Rezaie AR. Engineering a disulfide bond to stabilize the calcium-binding loop of activated protein C eliminates its anticoagulant but not its protective signaling properties. *J Biol Chem.* 2007;282(12):9251-9.
195. Carnemolla R, Patel KR, Zaitsev S, Cines DB, Esmon CT, Muzykantov VR. Quantitative analysis of thrombomodulin-mediated conversion of protein C to APC: translation from in vitro to in vivo. *J Immunol Methods.* 2012;384(1-2):21-4.
196. Julia R. Koeppel AS, Timothy Mather, and Elizabeth A. Komives. Thrombomodulin Tightens the Thrombin Active Site Loops To Promote Protein C Activation. *Biochemistry.* 2005;44.
197. Likui Yang CM, and Alireza R. Rezaie. Activation of protein C by the thrombin–thrombomodulin complex: Cooperative roles of Arg-35 of thrombin and Arg-67 of protein C. *PNAS.* 2006;103.
198. Pozzi N, Barranco-Medina S, Chen Z, Di Cera E. Exposure of R169 controls protein C activation and autoactivation. *Blood.* 2012;120(3):664-70.
199. Esmon ARRaCT. The Function of Calcium in Protein C Activation by Thrombin and the Thrombin-Thrombomodulin Complex Can Be Distinguished by Mutational Analysis of Protein C Derivatives*. *J Biol Chem.* 1992;267(36):26104-9.
200. Martin FA, Murphy RP, Cummins PM. Thrombomodulin and the vascular endothelium: insights into functional, regulatory, and therapeutic aspects. *Am J Physiol Heart Circ Physiol.* 2013;304(12):H1585-97.
201. Conway EM. Thrombomodulin and its role in inflammation. *Semin Immunopathol.* 2012;34(1):107-25.
202. A.-K. OHLIN KLaMH. Soluble thrombomodulin activity and soluble thrombomodulin antigen in plasma. *Journal of Thrombosis and Haemostasis.* 2005;3:976–82.
203. Bao YS, Jia XB, Wang D, Liu RC, Zou CB, Na SP. Characterization of soluble thrombomodulin levels in patients with stage 3-5 chronic kidney disease. *Biomarkers.* 2014;19(4):275-80.
204. Hayakawa M. Management of disseminated intravascular coagulation: current insights on antithrombin and thrombomodulin treatments. *Open Access Emerg Med.* 2018;10:25-9.
205. Katayama S, Nunomiya S, Koyama K, Wada M, Koinuma T, Goto Y, et al. Markers of acute kidney injury in patients with sepsis: the role of soluble thrombomodulin. *Crit Care.* 2017;21(1):229.
206. Laszlo Bajzar MN, John Morser, and Paula B. Tracy. Both Cellular and Soluble Forms of Thrombomodulin Inhibit Fibrinolysis by Potentiating the Activation of Thrombin-activable Fibrinolysis Inhibitor*. *The Journal of Biological Chemistry.* 1998;273(5):2792–8.
207. M. LEVI TVDP. Thrombomodulin in sepsis. *Minerva Anesthesiol.* 2013;79:294-8.
208. Majerus HlaPW. Thrombomodulin Is Present in Human Plasma and Urine. *J Clin Invest.* 1985;76:2178-81.

209. Sano T, Terai Y, Daimon A, Nunode M, Nagayasu Y, Okamoto A, et al. Recombinant human soluble thrombomodulin as an anticoagulation therapy improves recurrent miscarriage and fetal growth restriction due to placental insufficiency - The leading cause of preeclampsia. *Placenta*. 2018;65:1-6.
210. Abel Baerga-Ortiz ARRaEAK. Electrostatic Dependence of the ThrombinThrombomodulin Interaction. *J Mol Biol*. 2000;296:651-8.
211. Jan HOFSTEENGE HTaSRs. Effect of thrombomodulin on the kinetics of the interaction of thrombin with substrates and inhibitors. *Biochem J*. 1986;237:243-51.
212. Junji Nishioka HT, and Koji Suzuki. Estimation of the Possible Recognition Sites for Thrombomodulin, Procoagulant, and Anticoagulant Proteins around the Active Center of alpha-Thrombin. *J Biochem*. 1993;14.
213. David R. Light¹ CBG, Melissa Betts², Eric Blasko², Elizabeth Campbell³, Jeffrey H. Clarke², Michael McCaman³, Kirk McLean¹, Mariko Nagashima¹, John F. Parkinson⁴, Galina Rumennik¹, Tish Young² and John Morser¹. The interaction of thrombomodulin with Ca²⁺. *Eur J Biochem* 1999;262:522-33
214. Koeppe JR, Beach MA, Baerga-Ortiz A, Kerns SJ, Komives EA. Mutations in the fourth EGF-like domain affect thrombomodulin-induced changes in the active site of thrombin. *Biochemistry*. 2008;47(41):10933-9.
215. Michitaka Zushi KG, Shuji Yamamoto, Ikuro MaruyamaS, Tatsuya Hayashis, and Koji Suzuki. The Last Three Consecutive Epidermal Growth Factor-like Structures of Human Thrombomodulin Comprise the Minimum Functional Domain for Protein C-activating Cofactor Activity and Anticoagulant Activity*. *The Journal of Biological Chemistry*. 1989;264(18):10351-3.
216. Akio Kishida MN, Ikuro Maruyama, Nobuyuki Sakamoto, and Mitsuru Akashi, Takeshi Serizawa. Study on Complex Formation Between Recombinant Human Thrombomodulin Fragment and Thrombin Using Surface Plasmon Resonance. *American Journal of Hematology*. 2000;63:136-40.
217. Pablo Fuentes-Prior* YI, Robert Huber*, Rene Pagila², Galina Rumennik², Marian Seto², John Morser², David R. Light² & Wolfram Bode*. Structural basis for the anticoagulant activity of the thrombin± thrombomodulin complex. *Nature*. 2000;404.
218. Pablo Fuentes-Prior* YI, Robert Huber*, Rene Pagila², Galina Rumennik², Marian Seto², John Morser², David R. Light² & Wolfram Bode*. Structural basis for the anticoagulant activity of the thrombin± thrombomodulin complex. *Letters to Nature*. 2000;404:518-24.
219. Cheng TL, Lai CH, Shieh SJ, Jou YB, Yeh JL, Yang AL, et al. Myeloid thrombomodulin lectin-like domain inhibits osteoclastogenesis and inflammatory bone loss. *Sci Rep*. 2016;6:28340.
220. Conway EM, Van de Wouwer M, Pollefeyt S, Jurk K, Van Aken H, De Vriese A, et al. The lectin-like domain of thrombomodulin confers protection from neutrophil-mediated tissue damage by suppressing adhesion molecule expression via nuclear factor kappaB and mitogen-activated protein kinase pathways. *J Exp Med*. 2002;196(5):565-77.
221. Edward M. Conway SP, Desire´ Collen, and Marta Steiner-Mosonyi. The Amino Terminal Lectin-Like Domain of Thrombomodulin Is Required for Constitutive Endocytosis. *Blood*. 1997;89(2):652-61.
222. Huang HC, Shi GY, Jiang SJ, Shi CS, Wu CM, Yang HY, et al. Thrombomodulin-mediated cell adhesion: involvement of its lectin-like domain. *J Biol Chem*. 2003;278(47):46750-9.
223. Kuo CH, Chen PK, Chang BI, Sung MC, Shi CS, Lee JS, et al. The recombinant lectin-like domain of thrombomodulin inhibits angiogenesis through interaction with Lewis Y antigen. *Blood*. 2012;119(5):1302-13.
224. Lattenist L, Teske G, Claessen N, Florquin S, Conway EM, Roelofs JJ. The lectin like domain of thrombomodulin is involved in the defence against pyelonephritis. *Thromb Res*. 2015;136(6):1325-31.
225. Lin WL, Chang CF, Shi CS, Shi GY, Wu HL. Recombinant lectin-like domain of thrombomodulin suppresses vascular inflammation by reducing leukocyte recruitment via interacting with Lewis Y on endothelial cells. *Arterioscler Thromb Vasc Biol*. 2013;33(10):2366-73.

226. M. VAN DE WOUWER SP, * A. DE VRIESE,* E. WAELKENS,à D. COLLEN,* J . PERSSON,§M.R.DAHA– and E. M. CONWAY*. The lectin-like domain of thrombomodulin interferes with complement activation and protects against arthritis. *Journal of Thrombosis and Haemostasis*. 2006;4:1813-24.
227. Shi CS, Shi GY, Hsiao HM, Kao YC, Kuo KL, Ma CY, et al. Lectin-like domain of thrombomodulin binds to its specific ligand Lewis Y antigen and neutralizes lipopolysaccharide-induced inflammatory response. *Blood*. 2008;112(9):3661-70.
228. Yi-Heng Li C-HK, Guey-Yueh Shi, and Hua-Lin Wu. The role of thrombomodulin lectin-like domain in inflammation. *Journal of Biomedical Science*. 2012;19(34):1-8.
229. Conway HLaEM. Exploring traditional and nontraditional roles for thrombomodulin. *Blood*. 2018;132(2):148-58.
230. Xu H, Bush LA, Pineda AO, Caccia S, Di Cera E. Thrombomodulin changes the molecular surface of interaction and the rate of complex formation between thrombin and protein C. *J Biol Chem*. 2005;280(9):7956-61.
231. Demeulenaere M, Devreese K, Vanbelleghem H, De Zaeytijd J, Vande Walle J, Van Biesen W, et al. Thrombomodulin and Endothelial Dysfunction: A Disease-Modifier Shared between Malignant Hypertension and Atypical Hemolytic Uremic Syndrome. *Nephron*. 2018;140(1):63-73.
232. Lin WL, Chen CC, Shi GY, Ma CY, Chang CF, Wu HL. Monocytic thrombomodulin promotes cell adhesion through interacting with its ligand, Lewis(y). *Immunol Cell Biol*. 2017;95(4):372-9.
233. Mieke Delvaeye PD, Marina Noris, Ph.D., Astrid De Vriese, M.Sc., Charles T. Esmon, Ph.D., Naomi L. Esmon, Ph.D., Gary Ferrell, M.Sc., Jurgen Del-Favero, Ph.D., Stephane Plaisance, Ph.D., Bart Claes, M.Sc., Diether Lambrechts, Ph.D., Carla Zoja, Ph.D., Giuseppe Remuzzi, M.D., and Edward M. Conway, M.D., Ph.D. Thrombomodulin Mutations in Atypical Hemolytic–Uremic Syndrome. *New England Journal of Medicine*. 2009;361:345-57.
234. Ali Nayer AA. Atypical Hemolytic-Uremic Syndrome The Interplay Between Complements and the Coagulation System. *Iranian Journal of Kidney Diseases*. 2013;7.
235. Markiewski MM, Nilsson B, Ekdahl KN, Mollnes TE, Lambris JD. Complement and coagulation: strangers or partners in crime? *Trends Immunol*. 2007;28(4):184-92.
236. Shats-Tseytlina EA NC, Dhall DP. Complement activation: a new participant in the modulation of fibrin gel characteristics and the progression of atherosclerosis? *Blood*. 1994;5(4).
237. K A Schutt SM, K Lysaja, M Berger, S Ruetten, P Boor, N Marx. Complement activation leads to C3 and C5 dependent prothrombotic alterations of fibrin clots. 2019.
238. Subramaniam S, Jurk K, Hobohm L, Jackel S, Saffarzadeh M, Schwierczek K, et al. Distinct contributions of complement factors to platelet activation and fibrin formation in venous thrombus development. *Blood*. 2017;129(16):2291-302.
239. Amadio P, Porro B, Sandrini L, Fiorelli S, Bonomi A, Cavalca V, et al. Patho- physiological role of BDNF in fibrin clotting. *Sci Rep*. 2019;9(1):389.
240. Howes JM, Richardson VR, Smith KA, Schroeder V, Somani R, Shore A, et al. Complement C3 is a novel plasma clot component with anti-fibrinolytic properties. *Diab Vasc Dis Res*. 2012;9(3):216-25.
241. Scott EM, Ariens RA, Grant PJ. Genetic and environmental determinants of fibrin structure and function: relevance to clinical disease. *Arterioscler Thromb Vasc Biol*. 2004;24(9):1558-66.
242. Stachowicz A, Zabczyk M, Natarska J, Suski M, Olszanecki R, Korbut R, et al. Differences in plasma fibrin clot composition in patients with thrombotic antiphospholipid syndrome compared with venous thromboembolism. *Sci Rep*. 2018;8(1):17301.
243. Suski M, Siudut J, Zabczyk M, Korbut R, Olszanecki R, Undas A. Shotgun analysis of plasma fibrin clot-bound proteins in patients with acute myocardial infarction. *Thromb Res*. 2015;135(4):754-9.
244. Talens S, Leebeek FW, Demmers JA, Rijken DC. Identification of fibrin clot-bound plasma proteins. *PLoS One*. 2012;7(8):e41966.

245. Michael H. Kroll AIS. Biochemical Mechanisms of Platelet Activation. *Blood*. 1989;74(4):1181-95.
246. Leung LL, Myles T, Nishimura T, Song JJ, Robinson WH. Regulation of tissue inflammation by thrombin-activatable carboxypeptidase B (or TAFI). *Mol Immunol*. 2008;45(16):4080-3.
247. Bhole D, Stahl GL. Molecular basis for complement component 6 (C6) deficiency in rats and mice. *Immunobiology*. 2004;209(7):559-68.
248. Mizuno T, Yoshioka K, Mizuno M, Shimizu M, Nagano F, Okuda T, et al. Complement component 5 promotes lethal thrombosis. *Sci Rep*. 2017;7:42714.
249. Buono C, Come CE, Witztum JL, Maguire GF, Connelly PW, Carroll M, et al. Influence of C3 deficiency on atherosclerosis. *Circulation*. 2002;105(25):3025-31.
250. Gushiken FC, Han H, Li J, Rumbaut RE, Afshar-Kharghan V. Abnormal platelet function in C3-deficient mice. *J Thromb Haemost*. 2009;7(5):865-70.
251. K.A. Hess ZK, N. Oxley, F. Phoenix, N. Marx, R. King, R.F. Storey, P.J. Grant, R.A. Ajjan. <Modulation of complement C3 levels and fibrin clot structure the role of aspirin dose. 2013.
252. King RJ, Schuett K, Tiede C, Jankowski V, John V, Trehan A, et al. Fibrinogen interaction with complement C3: a potential therapeutic target to reduce thrombosis risk. *Haematologica*. 2020.
253. Carter AM. Complement activation: an emerging player in the pathogenesis of cardiovascular disease. *Scientifica (Cairo)*. 2012;2012:402783.
254. Muller-Calleja N, Ritter S, Hollerbach A, Falter T, Lackner KJ, Ruf W. Complement C5 but not C3 is expendable for tissue factor activation by cofactor-independent antiphospholipid antibodies. *Blood Adv*. 2018;2(9):979-86.
255. Buckingham SC, Ramos TN, Barnum SR. Complement C5-deficient mice are protected from seizures in experimental cerebral malaria. *Epilepsia*. 2014;55(12):e139-42.
256. THEODORE S. ZIMMERMAN MD, CARLOS M. ARROYAVE, M.D., AND HANS J. MULLER-EBERHARD, M.D. A BLOOD COAGULATION ABNORMALITY IN RABBITS DEFICIENT IN THE SIXTH COMPONENT OF COMPLEMENT (C6) AND ITS CORRECTION BY PURIFIED C6. *the Journal of Experimental Medicine*. 1971;134:1591-600.
257. Barthel D, Schindler S, Zipfel PF. Plasminogen is a complement inhibitor. *J Biol Chem*. 2012;287(22):18831-42.
258. Foley JH, Walton BL, Aleman MM, O'Byrne AM, Lei V, Harrasser M, et al. Complement Activation in Arterial and Venous Thrombosis is Mediated by Plasmin. *EBioMedicine*. 2016;5:175-82.
259. Keshari RS, Silasi R, Lupu C, Taylor FB, Jr., Lupu F. In vivo-generated thrombin and plasmin do not activate the complement system in baboons. *Blood*. 2017;130(24):2678-81.
260. Irmscher S, Doring N, Halder LD, Jo EAH, Kopka I, Dunker C, et al. Kallikrein Cleaves C3 and Activates Complement. *J Innate Immun*. 2018;10(2):94-105.
261. DeHelian D, Holt T, Fritzinger N, Koeppe JR. Investigating Interactions between the Lectin-Like Domain of Thrombomodulin and Complement Component 3. *Biophysical Journal*. 2015;108(2):513a-4a.
262. Koeppe JR, Ellis G, Joannides N, Wiltsie V. Investigating the Role of Thrombomodulin in the Activation of Complement. *Biophysical Journal*. 2018;114(3).
263. Palowitch G, Gambone C, Koeppe JR. Interactions between Thrombomodulin and Complement Component C3 Studied by Fluorescence Resonance Energy Transfer. *Biophysical Journal*. 2015;108(2).
264. Wang H, Vinnikov I, Shahzad K, Bock F, Ranjan S, Wolter J, et al. The lectin-like domain of thrombomodulin ameliorates diabetic glomerulopathy via complement inhibition. *Thromb Haemost*. 2012;108(6):1141-53.
265. M. VAN DE WOUWER SP, * A. DE VRIESE,* E. WAELKENS,à D. COLLEN,* J . PERSSON,§M.R.DAHA– and E. M. CONWAY* The lectin-like domain of thrombomodulin interferes with complement activation and protects against arthritis. *Journal of Thrombosis and Haemostasis*. 2006;4:1813–24.
266. Diamond SL. Systems biology of coagulation. *J Thromb Haemost*. 2013;11 Suppl 1:224-32.

267. Ruggeri ZM. Perspectives Series: Cell Adhesion in Vascular Biology
von Willebrand Factor. *J Clin Invest.* 1997;99(4):559–64.
268. Peyvandi F, Garagiola I, Baronciani L. Role of von Willebrand factor in the haemostasis. *Blood Transfus.* 2011;9 Suppl 2:s3-8.
269. Feng S, Liang X, Kroll MH, Chung DW, Afshar-Kharghan V. von Willebrand factor is a cofactor in complement regulation. *Blood.* 2015;125(6):1034-7.
270. Noone DG, Riedl M, Pluthero FG, Bowman ML, Liszewski MK, Lu L, et al. Von Willebrand factor regulates complement on endothelial cells. *Kidney Int.* 2016;90(1):123-34.
271. Bettoni S, Galbusera M, Gastoldi S, Donadelli R, Tentori C, Sparta G, et al. Interaction between Multimeric von Willebrand Factor and Complement: A Fresh Look to the Pathophysiology of Microvascular Thrombosis. *J Immunol.* 2017;199(3):1021-40.
272. Honda KI, Asada R, Kageyama K, Fukuda T, Terada H, Yasui T, et al. Protein Complex of Fibrinogen Gamma Chain and Complement Factor H in Ovarian Cancer Patient Plasma. *Anticancer Res.* 2017;37(6):2861-6.
273. Walter H.A. Kahr FGP, Christoph Licht. Complement Factor H in Human Platelets: Implications for Atypical HUS. *Blood.* 2008;112(11).
274. Blatt AZ, Saggiu G, Kulkarni KV, Cortes C, Thurman JM, Ricklin D, et al. Properdin-Mediated C5a Production Enhances Stable Binding of Platelets to Granulocytes in Human Whole Blood. *J Immunol.* 2016;196(11):4671-80.
275. Saggiu G, Cortes C, Emch HN, Ramirez G, Worth RG, Ferreira VP. Identification of a novel mode of complement activation on stimulated platelets mediated by properdin and C3(H₂O). *J Immunol.* 2013;190(12):6457-67.
276. Venselaar H, Joosten RP, Vroliing B, Baakman CA, Hekkelman ML, Krieger E, et al. Homology modelling and spectroscopy, a never-ending love story. *Eur Biophys J.* 2010;39(4):551-63.
277. Waterhouse A, Bertoni M, Bienert S, Studer G, Tauriello G, Gumienny R, et al. SWISS-MODEL: homology modelling of protein structures and complexes. *Nucleic Acids Res.* 2018;46(W1):W296-W303.
278. Pearson WR. An introduction to sequence similarity ("homology") searching. *Curr Protoc Bioinformatics.* 2013;Chapter 3:Unit3 1.
279. Using BLAST. *Bioinformatics Activity.*
280. Stephen F. Altschul TLM, Alejandro A. Schäffer, Jinghui Zhang, Zheng Zhang, Webb Miller and David J. Lipman. Gapped BLAST and PSI-BLAST: a new generation of protein database search programs. *Nucleic Acids Res.* 1997;25(17).
281. Xiang Z. Advances in Homology Protein Structure Modeling. *Curr Protein Pept Sci.* 2006;7(3).
282. Wallner B, Elofsson A. All are not equal: a benchmark of different homology modeling programs. *Protein Sci.* 2005;14(5):1315-27.
283. Kufareva I, Abagyan R. Methods of protein structure comparison. *Methods Mol Biol.* 2012;857:231-57.
284. Wu D, Wu Z. Superimposition of protein structures with dynamically weighted RMSD. *J Mol Model.* 2010;16(2):211-22.
285. Okemefuna AI, Nan R, Gor J, Perkins SJ. Electrostatic interactions contribute to the folded-back conformation of wild type human factor H. *J Mol Biol.* 2009;391(1):98-118.
286. MANFRED M. MAYER AGO, OTTO O. BIER, MICHAEL HEIDELBERGER. THE ACTIVATING EFFECT OF MAGNESIUM AND OTHER CATIONS ON THE HEMOLYTIC FUNCTION OF COMPLEMENT. *J Exp Med.* 1946.
287. Pangburn MK. Cutting edge: localization of the host recognition functions of complement factor H at the carboxyl-terminal: implications for hemolytic uremic syndrome. *J Immunol.* 2002;169(9):4702-6.
288. Dumoulin EN, Fiers L, Devreese KM. Investigation of sensitivity for coagulation factor deficiency in APTT and PT: how to perform it? *Clin Chem Lab Med.* 2016;54(5):e169-72.

289. Johnstone IB. The Activated Partial Thromboplastin Time of Diluted Plasma: Variability due to the Method of Fibrin Detection. *Can J Comp Med.* 1984;48:198-201.
290. Kim SY, Kim JE, Kim HK, Kim I, Yoon SS, Park S. Influence of coagulation and anticoagulant factors on global coagulation assays in healthy adults. *Am J Clin Pathol.* 2013;139(3):370-9.
291. Winter WE, Flax SD, Harris NS. Coagulation Testing in the Core Laboratory. *Lab Med.* 2017;48(4):295-313.
292. Negrier C, Shima M, Hoffman M. The central role of thrombin in bleeding disorders. *Blood Rev.* 2019;38:100582.
293. Marcus E, Carr J, and Jan Hermans. Size and Density of Fibrin Fibers from Turbidity. *Macromolecules.* 1977;11(1):46-50.
294. Nagaswami JWWaC. Computer modeling of fibrin polymerization kinetics correlated with electron microscope and turbidity observations: clot structure and assembly are kinetically controlled. *Biophys J.* 1992;63:111-28.
295. Zeng Z, Fagnon M, Nallan Chakravarthula T, Alves NJ. Fibrin clot formation under diverse clotting conditions: Comparing turbidimetry and thromboelastography. *Thromb Res.* 2020;187:48-55.
296. Sommeijer DW, van Oerle R, Reitsma PH, Timmerman JJ, Meijers JC, Spronk HM, et al. Analysis of blood coagulation in mice: pre-analytical conditions and evaluation of a home-made assay for thrombin-antithrombin complexes. *Thromb J.* 2005;3:12.
297. Jacek Borawski MM. Soluble thrombomodulin: a marker of endothelial injury, an antithrombotic agent, or both? *Med Sci Monit.* 2001;7.
298. Zhang L, Dai Y, Huang P, Saunders TL, Fox DA, Xu J, et al. Absence of complement component 3 does not prevent classical pathway-mediated hemolysis. *Blood Adv.* 2019;3(12):1808-14.
299. Turner NA, Moake J. Assembly and activation of alternative complement components on endothelial cell-anchored ultra-large von Willebrand factor links complement and hemostasis-thrombosis. *PLoS One.* 2013;8(3):e59372.
300. MARIE-CLAUDE BOURIN* M-CB, INGEMAR BJORKt, AND ULF LINDAHLt. Functional domains of rabbit thrombomodulin. *Proc Natl Acad Sci U S A.* 1986;83:5924-8.
301. Marie-Claude Bourinl A-KO, David A. Lanen, Johan Stenfloe, and Ulf LindahlS. Relationship between Anticoagulant Activities and Polyanionic Properties of Rabbit Thrombomodulin. *The Journal of Biological Chemistry.* 1988;263(17):8044-52.
302. Maruyama I, Salem HH, Ishii H, Majerus PW. Human thrombomodulin is not an efficient inhibitor of the procoagulant activity of thrombin. *J Clin Invest.* 1985;75(3):987-91.
303. Haque A, Cortes C, Alam MN, Sreedhar M, Ferreira VP, Pangburn MK. Characterization of Binding Properties of Individual Functional Sites of Human Complement Factor H. *Front Immunol.* 2020;11:1728.
304. McCluskey G DG, Velounias R, Hughes TR, Morgan BP, Preston R, Collins PW, Jenkins PV, Heurich M. Complement Regulator Factor H is a Cofactor for Thrombin in both Pro- and Anticoagulant Roles [abstract]. *Res Pract Thromb Haemost.* 2020.
305. Shogo Takano SK, Shinichi Ohdama, and Nobuo Aoki. Plasma Thrombomodulin in Health and Diseases. *Blood.* 1990;76(10):2024-9.
306. . W. J. BOEHME YD, * U. RAETH, A. BIERHAUS,* R. ZIEGLER,* W. STREMMEL &, NAWROTH PP. Release of thrombomodulin from endothelial cells by concerted action of TNF-a and neutrophils: in vivo and in vitro studies. *Immunology.* 1996;87:134-40.
307. Ito T, Thachil J, Asakura H, Levy JH, Iba T. Thrombomodulin in disseminated intravascular coagulation and other critical conditions-a multi-faceted anticoagulant protein with therapeutic potential. *Crit Care.* 2019;23(1):280.
308. Drozd D, Latka M, Drozd T, Sztéfko K, Kwinta P. Thrombomodulin as a New Marker of Endothelial Dysfunction in Chronic Kidney Disease in Children. *Oxid Med Cell Longev.* 2018;2018:1619293.
309. Rijken F, Bruijnzeel PL. The pathogenesis of photoaging: the role of neutrophils and neutrophil-derived enzymes. *J Investig Dermatol Symp Proc.* 2009;14(1):67-72.

310. Alexander JJ, Hack BK, Jacob A, Chang A, Haas M, Finberg RW, et al. Abnormal immune complex processing and spontaneous glomerulonephritis in complement factor H-deficient mice with human complement receptor 1 on erythrocytes. *J Immunol*. 2010;185(6):3759-67.
311. Smith RJ, Alexander J, Barlow PN, Botto M, Cassavant TL, Cook HT, et al. New approaches to the treatment of dense deposit disease. *J Am Soc Nephrol*. 2007;18(9):2447-56.
312. Kaartinen K, Safa A, Kotha S, Ratti G, Meri S. Complement dysregulation in glomerulonephritis. *Semin Immunol*. 2019;45:101331.
313. Alchi B, Jayne D. Membranoproliferative glomerulonephritis. *Pediatr Nephrol*. 2010;25(8):1409-18.
314. Ewa Stępień¹ DP, Agnieszka Branicka¹, Elżbieta Stankiewicz¹, Maria Śnieżek-Maciejewska AP, Izabela Górkiewicz¹, Bogusław Kapelak², Jerzy Sadowski². Factors influencing thrombin generation measured as thrombin-antithrombin complex and calibrated automated thrombogram method in patients with advanced coronary artery disease. *POLSKIE ARCHIWUM MEDYCYNY WEWNĘTRZNEJ*. 2007;117(7).
315. Satyam A, Graef ER, Lapchak PH, Tsokos MG, Dalle Lucca JJ, Tsokos GC. Complement and coagulation cascades in trauma. *Acute Med Surg*. 2019;6(4):329-35.
316. Yau JW, Teoh H, Verma S. Endothelial cell control of thrombosis. *BMC Cardiovasc Disord*. 2015;15:130.
317. Boral BM, Williams DJ, Boral LI. Disseminated Intravascular Coagulation. *Am J Clin Pathol*. 2016;146(6):670-80.
318. Liu Y, Jennings NL, Dart AM, Du XJ. Standardizing a simpler, more sensitive and accurate tail bleeding assay in mice. *World J Exp Med*. 2012;2(2):30-6.
319. Licht C, Pluthero FG, Li L, Christensen H, Habbig S, Hoppe B, et al. Platelet-associated complement factor H in healthy persons and patients with atypical HUS. *Blood*. 2009;114(20):4538-45.
320. Borkowska S, Suszynska M, Wysoczynski M, Ratajczak MZ. Mobilization studies in C3-deficient mice unravel the involvement of a novel crosstalk between the coagulation and complement cascades in mobilization of hematopoietic stem/progenitor cells. *Leukemia*. 2013;27(9):1928-30.
321. Huber-Lang M, Sarma JV, Zetoune FS, Rittirsch D, Neff TA, McGuire SR, et al. Generation of C5a in the absence of C3: a new complement activation pathway. *Nat Med*. 2006;12(6):682-7.
322. Eriksson O, Mohlin C, Nilsson B, Ekdahl KN. The Human Platelet as an Innate Immune Cell: Interactions Between Activated Platelets and the Complement System. *Front Immunol*. 2019;10:1590.
323. Sauter RJ, Sauter M, Reis ES, Emschermann FN, Nording H, Ebenhoch S, et al. Functional Relevance of the Anaphylatoxin Receptor C3aR for Platelet Function and Arterial Thrombus Formation Marks an Intersection Point Between Innate Immunity and Thrombosis. *Circulation*. 2018;138(16):1720-35.
324. Morigi M, Galbusera M, Gastoldi S, Locatelli M, Buelli S, Pezzotta A, et al. Alternative pathway activation of complement by Shiga toxin promotes exuberant C3a formation that triggers microvascular thrombosis. *J Immunol*. 2011;187(1):172-80.
325. Papageorgiou C, Synetos A, Tampakis K, Anninos H, Kontogiannis C, Kapelouzou A, et al. Activated Clotting Time as a Marker of Inflammation in Hospitalized Patients. *Clin Appl Thromb Hemost*. 2020;26:1076029620929090.
326. Kamal AH, Tefferi A, Pruthi RK. How to interpret and pursue an abnormal prothrombin time, activated partial thromboplastin time, and bleeding time in adults. *Mayo Clin Proc*. 2007;82(7):864-73.
327. Bezuidenhout JA, Venter C, Roberts T, Tarr G, Kell DB, Pretorius E. 2020.
328. Blondon M, Biver E, Braillard O, Righini M, Fontana P, Casini A. Thrombin generation and fibrin clot structure after vitamin D supplementation. *Endocr Connect*. 2019;8(11):1447-54.
329. Cheng T MK, Abrams-Ogg A, Wood D. The link between inflammation and coagulation: influence on the interpretation of diagnostic laboratory tests. *Compend Contin Educ Vet*. 2011.

330. Konings J, Govers-Riemslog JW, Philippou H, Mutch NJ, Borissoff JJ, Allan P, et al. Factor XIIIa regulates the structure of the fibrin clot independently of thrombin generation through direct interaction with fibrin. *Blood*. 2011;118(14):3942-51.
331. Thangaraj SS, Christiansen SH, Graversen JH, Sidelmann JJ, Hansen SWK, Bygum A, et al. Contact activation-induced complex formation between complement factor H and coagulation factor XIIIa. *Journal of Thrombosis and Haemostasis*. 2020;18(4):876-84.
332. Niederdockl J, Dempfle CE, Schonherr HR, Bartsch A, Miles G, Laggner A, et al. Point-of-care PT and aPTT in patients with suspected deficiencies of coagulation factors. *Int J Lab Hematol*. 2016;38(4):426-34.
333. Litvinov RI, Weisel JW. Role of red blood cells in haemostasis and thrombosis. *ISBT Sci Ser*. 2017;12(1):176-83.
334. Hess K, Alzahrani SH, Mathai M, Schroeder V, Carter AM, Howell G, et al. A novel mechanism for hypofibrinolysis in diabetes: the role of complement C3. *Diabetologia*. 2012;55(4):1103-13.
335. Wufsus AR, Macera NE, Neeves KB. The hydraulic permeability of blood clots as a function of fibrin and platelet density. *Biophys J*. 2013;104(8):1812-23.
336. Mohan Rao LV, Esmon CT, Pendurthi UR. Endothelial cell protein C receptor: a multiliganded and multifunctional receptor. *Blood*. 2014;124(10):1553-62.
337. Slungaard A, Fernandez JA, Griffin JH, Key NS, Long JR, Piegors DJ, et al. Platelet factor 4 enhances generation of activated protein C in vitro and in vivo. *Blood*. 2003;102(1):146-51.
338. Carter WJ, Cama E, Huntington JA. Crystal structure of thrombin bound to heparin. *J Biol Chem*. 2005;280(4):2745-9.
339. Chahal G, Thorpe M, Hellman L. The Importance of Exosite Interactions for Substrate Cleavage by Human Thrombin. *PLoS One*. 2015;10(6):e0129511.
340. Ott I. Inhibitors of the initiation of coagulation. *Br J Clin Pharmacol*. 2011;72(4):547-52.
341. Bu F, Zhang Y, Wang K, Borsa NG, Jones MB, Taylor AO, et al. Genetic Analysis of 400 Patients Refines Understanding and Implicates a New Gene in Atypical Hemolytic Uremic Syndrome. *J Am Soc Nephrol*. 2018;29(12):2809-19.
342. Goicoechea de Jorge E, Tortajada A, Garcia SP, Gastoldi S, Merinero HM, Garcia-Fernandez J, et al. Factor H Competitor Generated by Gene Conversion Events Associates with Atypical Hemolytic Uremic Syndrome. *J Am Soc Nephrol*. 2018;29(1):240-9.
343. Jokiranta TS, Jaakola VP, Lehtinen MJ, Parepalo M, Meri S, Goldman A. Structure of complement factor H carboxyl-terminus reveals molecular basis of atypical haemolytic uremic syndrome. *EMBO J*. 2006;25(8):1784-94.
344. Pouw RB, Brouwer MC, de Gast M, van Beek AE, van den Heuvel LP, Schmidt CQ, et al. Potentiation of complement regulator factor H protects human endothelial cells from complement attack in aHUS sera. *Blood Adv*. 2019;3(4):621-32.
345. Stahl AL, Vaziri-Sani F, Heinen S, Kristoffersson AC, Gydell KH, Raafat R, et al. Factor H dysfunction in patients with atypical hemolytic uremic syndrome contributes to complement deposition on platelets and their activation. *Blood*. 2008;111(11):5307-15.
346. Chen Q, Wiesener M, Eberhardt HU, Hartmann A, Uzonyi B, Kirschfink M, et al. Complement factor H-related hybrid protein deregulates complement in dense deposit disease. *J Clin Invest*. 2014;124(1):145-55.
347. Sethi S, Fervenza FC. Pathology of renal diseases associated with dysfunction of the alternative pathway of complement: C3 glomerulopathy and atypical hemolytic uremic syndrome (aHUS). *Semin Thromb Hemost*. 2014;40(4):416-21.
348. Master Sankar Raj V, Gordillo R, Chand DH. Overview of C3 Glomerulopathy. *Front Pediatr*. 2016;4:45.
349. Nichols EM, Barbour TD, Pappworth IY, Wong EK, Palmer JM, Sheerin NS, et al. An extended mini-complement factor H molecule ameliorates experimental C3 glomerulopathy. *Kidney Int*. 2015;88(6):1314-22.

350. Yang Y, Denton H, Davies OR, Smith-Jackson K, Kerr H, Herbert AP, et al. An Engineered Complement Factor H Construct for Treatment of C3 Glomerulopathy. *J Am Soc Nephrol*. 2018;29(6):1649-61.
351. Brocklebank V, Johnson S, Sheerin TP, Marks SD, Gilbert RD, Tyerman K, et al. Factor H autoantibody is associated with atypical hemolytic uremic syndrome in children in the United Kingdom and Ireland. *Kidney Int*. 2017;92(5):1261-71.
352. McDonnell T, Wincup C, Buchholz I, Pericleous C, Giles I, Ripoll V, et al. The role of beta-2-glycoprotein I in health and disease associating structure with function: More than just APS. *Blood Rev*. 2020;39:100610.
353. Nakamura H, Oku K, Ogata Y, Ohmura K, Yoshida Y, Kitano E, et al. Alternative pathway activation due to low level of complement factor H in primary antiphospholipid syndrome. *Thromb Res*. 2018;164:63-8.
354. Savelli SL, Roubey RAS, Kitzmiller KJ, Zhou D, Nagaraja HN, Mulvihill E, et al. Opposite Profiles of Complement in Antiphospholipid Syndrome (APS) and Systemic Lupus Erythematosus (SLE) Among Patients With Antiphospholipid Antibodies (aPL). *Front Immunol*. 2019;10:885.
355. Wada H, Matsumoto T, Suzuki K, Imai H, Katayama N, Iba T, et al. Differences and similarities between disseminated intravascular coagulation and thrombotic microangiopathy. *Thromb J*. 2018;16:14.
356. Zhang K, Lu Y, Harley KT, Tran MH. Atypical Hemolytic Uremic Syndrome: A Brief Review. *Hematol Rep*. 2017;9(2):7053.
357. Kurosawa S, Stearns-Kurosawa DJ. Complement, thrombotic microangiopathy and disseminated intravascular coagulation. *J Intensive Care*. 2014;2(1):65.
358. Ruggenti P, Noris M, Remuzzi G. Thrombotic microangiopathy, hemolytic uremic syndrome, and thrombotic thrombocytopenic purpura. *Kidney Int*. 2001;60(3):831-46.
359. Cserhalmi M, Uzonyi B, Merle NS, Csuka D, Meusburger E, Lhotta K, et al. Functional Characterization of the Disease-Associated N-Terminal Complement Factor H Mutation W198R. *Front Immunol*. 2017;8:1800.
360. Herbert AP, Kavanagh D, Johansson C, Morgan HP, Blaum BS, Hannan JP, et al. Structural and functional characterization of the product of disease-related factor H gene conversion. *Biochemistry*. 2012;51(9):1874-84.
361. JOHN A. HEIT TMP, WHYTE G. OWEN, JAMES P . BURKE, MARIZA DE ANDRADE and L. JOSEPH MELTON Thrombomodulin gene polymorphisms or haplotypes as potential risk factors for venous thromboembolism: a population-based case-control study. *Journal of Thrombosis and Haemostasis*. 2005;3:710-7.
362. Ueda Y, Mohammed I, Song D, Gullipalli D, Zhou L, Sato S, et al. Murine systemic thrombophilia and hemolytic uremic syndrome from a factor H point mutation. *Blood*. 2017;129(9):1184-96.
363. Sakurai S, Kato H, Yoshida Y, Sugawara Y, Fujisawa M, Yasumoto A, et al. Profiles of Coagulation and Fibrinolysis Activation-Associated Molecular Markers of Atypical Hemolytic Uremic Syndrome in the Acute Phase. *J Atheroscler Thromb*. 2020;27(4):353-62.
364. Smith-Jackson K, Yang Y, Denton H, Pappworth IY, Cooke K, Barlow PN, et al. Hyperfunctional complement C3 promotes C5-dependent atypical hemolytic uremic syndrome in mice. *J Clin Invest*. 2019;129(3):1061-75.

Appendices

Appendix chapter 2

Appendix 2.1. Factor H constructs information before and after dialysis.

Factor H construct	Aa sequence	Molecular weight (kDa)	Extinction coefficient	A (0.1%)	Absorbance A280nm	Volume (µl)	Concentration (g/l)	Amount protein (µg)	Concentration (µM)
1-4 (1) - 20µM	1-264	29.843	53495	1.792	0.39	252	0.22	55.44	7.4
1-5 (2) - 62µM	1-322	36.333	65205	1.795	1.2	380	0.67	254.6	18
1-6 (2) - 60µM	1-386	43.844	88375	2.016	2.7	140	1.34	187.6	31
6-8 (1) - 20µM	324-507	20.844	48080	2.307	0.11	140	0.048	6.72	2.3
6-8 (2) - 980µM	324-507	20.844	48080	2.307	0.32	250	0.14	35	6.7
8-15 (1) - 20µM	446-928	54.399	89780	1.650	0.84	205	0.51	104.55	9.4
15-18 (1) - 20µM	868-1104	26.395	43860	1.662	0.69	105	0.41	43.05	15
18-20 (1) - 20µM	1046-1230	21.113	39140	1.818	0.13	235	0.071	16.7	3.4
18-20 (2) - 175µM	1046-1230	21.113	39140	1.818	0.23	265	0.13	34.45	6.2

All factor H constructs had been expressed in *Pichia Pastoris*.

Factor H constructs dialysed into HEPES 10mM/NaCl 150mM (2h on ice, buffer changed after 1h)

- (1) Is the first batch of factor H that was sent
- (2) Second batch of factor H constructs sent

Concentrations of factor H constructs indicated in “Factor H construct” section, before dialysis (was in PBS)

Appendix 2.2. Full sequences for soluble thrombomodulin recombinant proteins full length, lectin like domain and EGF456-S/T domain.

The sequences for each recombinant thrombomodulin construct are shown as follows, based on the sequences in Uniprot (P07204):

Full length soluble thrombomodulin (sTM, aa20-515):

	20	30	40	50
	P	AEPQPGGSQC	VEHDCFALYP	GPATFLNASQ
60	70	80	90	100
ICDGLRGHLM	TVRSSVAADV	ISLLLNGDGG	VGRRRLWIGL	QLPPGCGDPK
110	120	130	140	150
RLGPLRGFQW	VTGDNNTSYS	RWARLDLNGA	PLCGPLCVAV	SAAEATVPSE
160	170	180	190	200
PIWEEQQCEV	KADGFLCEF	FPATCRPLAV	EPGAAAAVS	ITYGTPFAAR
210	220	230	240	250
GADFQALPVG	SSAAVAPLGL	QLMCTAPPGA	VQGHWAREAP	GAWDCSVENG
260	270	280	290	300
GCEHACNAIP	GAPRCQCPAG	AALQADGRSC	TASATQSCND	LCEHFVCPNP
310	320	330	340	350
DQPGSYSCMC	ETGYRLAADQ	HRCEDVDDCI	LEPSPCPQRC	VNTQGGFECH
360	370	380	390	400
CYPNYDLVDG	ECVEPVDPCF	RANCEYQCQP	LNQTSYLCVC	AEGFAPIPHE
410	420	430	440	450
PHRCQMFCNQ	TACPADCDPN	TQASCECPEG	YILDDGFICT	DIDECENGGF
460	470	480	490	500
CSGVCHNLPG	TFECICGPDS	ALARHIGTDC	DSGKVDGGDS	GSGEPPPSPT
510				
PGSTLTTPPAV	GLVHS			

Lectin-like domain thrombomodulin (sLLD, aa20-169):

	20	30	40	50
	P	AEPQPGGSQC	VEHDCFALYP	GPATFLNASQ
60	70	80	90	100
ICDGLRGHLM	TVRSSVAADV	ISLLLNGDGG	VGRRRLWIGL	QLPPGCGDPK
110	120	130	140	150
RLGPLRGFQW	VTGDNNTSYS	RWARLDLNGA	PLCGPLCVAV	SAAEATVPSE
160				
PIWEEQQCEV	KADGFLCEF			

EGF-like 4,5,6 + serine/threonine rich domain thrombomodulin (sEGF456-S/T, aa365-515):

	370	380	390	400
	VDPCF	RANCEYQCQP	LNQTSYLCVC	AEGFAPIPHE
410	420	430	440	450
PHRCQMFCNQ	TACPADCDPN	TQASCECPEG	YILDDGFICT	DIDECENGGF
460	470	480	490	500
CSGVCHNLPG	TFECICGPDS	ALARHIGTDC	DSGKVDGGDS	GSGEPPPSPT
510				
PGSTLTPPAV	GLVHS			

The endogenous signal peptide was used for each, so from Met1 to Ala19 of thrombomodulin, sourced from Uniprot:

Thrombomodulin signal peptide (aa1-19):

10
MLGVLVLGAL ALAGLGFP

Appendix chapter 3

Appendix 3.1. Tail bleeding and haemolysis in *CFH*^{-/-} mice

To further understand the impact of factor H on clotting in an *in vivo* setting, the coagulation profiles of *CFH*^{-/-} mice were studied. For this bleeding time and haemolysis (results obtained before my PhD) (Figure A5.18), coagulation biomarkers (soluble thrombomodulin, thrombin-antithrombin complex, and activated protein C) were measured (Figure A5.19). The same parameters were measured in *C3*^{-/-} mice. When factor H is deleted, complement is overactivated and all the C3 is cleaved and consumed. Absence of C3 presents a similar profile, in that no C3 is present. The key difference between *CFH*^{-/-} and *C3*^{-/-} mice is the generation of C3b.

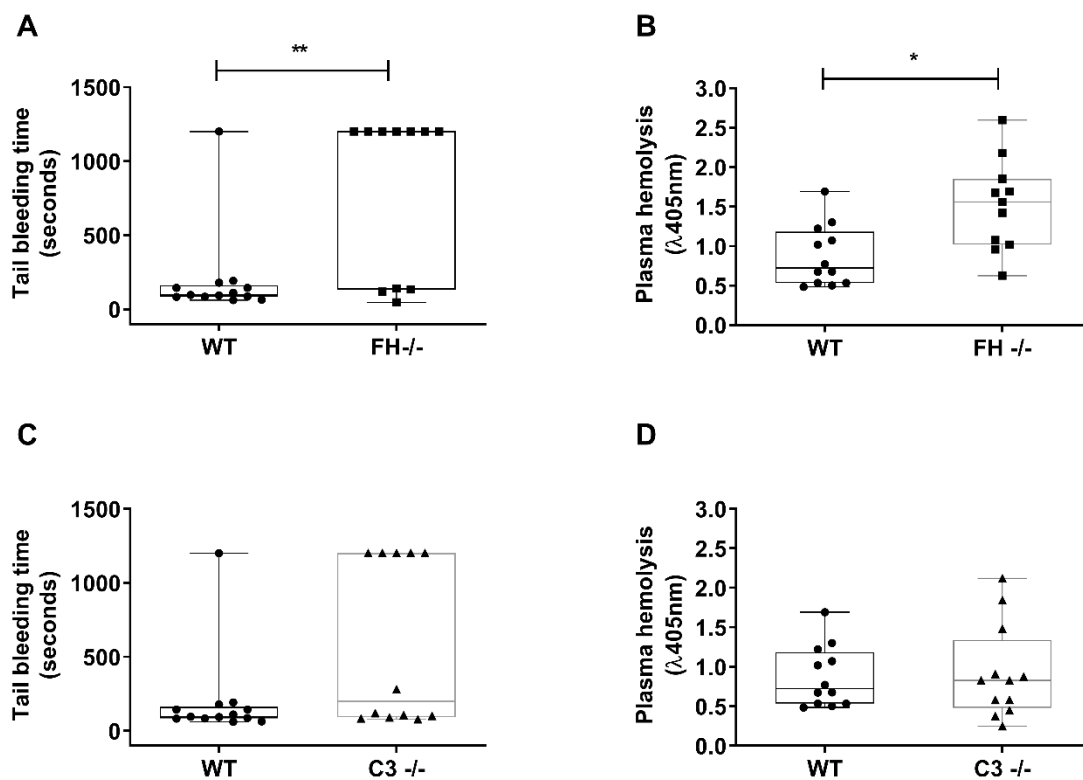


Figure A3.1. *CFH*^{-/-} mice have a significantly increased bleeding time compared to wild type. Tests were performed blind to genotype, in male mice, age 20 weeks. Tail bleeding time, tail bleed hemoglobin and plasma haemolysis was measured in *CFH*^{-/-} (■) or *C3*^{-/-} (▲) mice and compared to wild-type (WT) (●). Tail bleeding assay was performed by 3mm-tail tip amputation, immersing the tail in PBS at 37°C and monitoring time (seconds) until cessation of bleeding. (A) *CFH*^{-/-} mice showed prolonged total bleeding time (*CFH*^{-/-} mice: 804±550 seconds, n=11, vs WT: 196±305 seconds, n=13, p-value 0.017) and recurrent bleeding in 7 out of 11 *CFH*^{-/-} mice. (B) Plasma haemolysis was significantly increased in *CFH*^{-/-} compared to WT mice (p-value 0.009). (C) *C3*^{-/-} mice showed prolonged total bleeding time (*C3*^{-/-} mice: 571±557 seconds, n=11, vs WT: 196±305 seconds, n=13, p-value 0.13) and recurrent bleeding in 5 out of 12 *C3*^{-/-} mice. (E) No significant difference in (D) plasma haemolysis in *C3*^{-/-} vs wild-type mice. P values calculated by non-parametric Mann-Whitney test.

It is important to note that mouse models often have dual phenotypes, explaining the two populations of mice present in the tail bleeding assay measurements.

Bleeding time (Figure A3.1A and C) and haemolysis (Figure A3.18B and D) were measured in *CFH*^{-/-} (Figure A3.1A and B) and *C3*^{-/-} (Figure A3.1C and D) mice. *CFH*^{-/-} mice showed a significantly increased bleeding time (Figure A3.1A) compared to their wild type counterparts. Haemolysis in the *CFH*^{-/-} mice (Figure A3.1B) was also increased significantly. In the *C3*^{-/-} mice, there was an increase in bleeding time (Figure A3.1C), however not as significant as the *CFH*^{-/-} mice. Haemolysis levels in the *C3*^{-/-} mice were also not significantly altered (Figure A3.1D). Overall, the absence of factor H significantly increases bleeding time and haemolysis in mice.

Appendix chapter 5

Appendix 5.1. Impact of factor H on active protein C

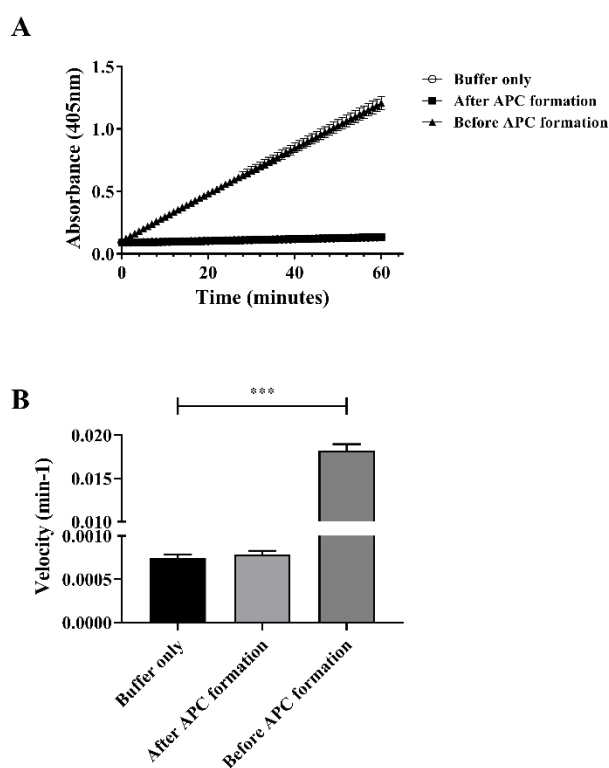


Figure A5.1. Factor H has no effect on substrate cleavage by activated protein C. 100nM Factor H was incubated before and after protein C activation, with 1.75nM thrombin and 100nM protein C, and compared to buffer only (no factor H). There was no increase in absorbance when factor H was added after formation of active protein C. Activation of protein C was monitored at 405nm over time (A) and the velocity (B) was measured using the slope. Velocity was 0.00065min⁻¹ for buffer only condition, 0.00065min⁻¹ for after APC formation and 0.017min⁻¹ for before APC formation. Results show mean +/-SD (n=3, p-value 0.0006). Unpaired parametric Welch's t-test was performed. Illustration representative of one independent experiment.

Factor H shows no significant impact on activated protein C cleavage of substrate, compared to the negative buffer control.

Factor H significantly increased protein C activation when incubated before APC formation, however no significant impact was seen after APC formation. The rate of activation after APC formation was not significantly different to the buffer control whereas there was a significant increase when factor H was added before APC formation. These results indicate that factor H enhances protein C activation via interaction and binding with thrombin alone, in the absence of thrombomodulin, and exerts no evident effect on active protein C and its catalytic activity.

Appendix 5.2. Verification of protein expression and excretion into the media from HEK293 cells pre-purification

The plasmids were transiently transfected into HEK293 cells, and a HIS-tag purification of recombinant thrombomodulin was performed using HisPur purification columns. To verify the presence of the transfected constructs thrombomodulin full length (sTM), lectin-like domain (LLD) and EGF-like 456-Ser/Thr domain (EGF456S/T), a dot blot was performed after 48h and 72h post transfection before purification of the samples. Soluble thrombomodulin from R&D Systems was used as a control.

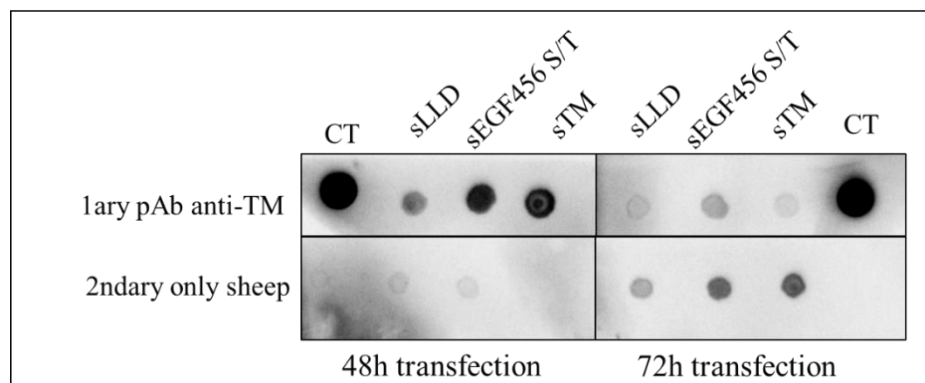


Figure A5.2. Recombinant thrombomodulin LLD and EGF456S/T constructs expression confirmed by dot blot before purification. Concentrated cell culture media was dotted on a nitrocellulose membrane and incubated with a polyclonal anti-sheep anti-thrombomodulin antibody to confirm the presence of the protein constructs at 48 and 72 hours post transfection. Control was secondary anti-sheep antibody only. Thrombomodulin was detected at 48h transfection and showed very little non-specific binding in the control. The 72h transfection showed less protein expressed and there were more impurities based on the higher signal in the control condition.

At 48h transfection, the sheep polyclonal anti-thrombomodulin detected fragments for each transfection, with little non-specific binding from the secondary anti-sheep antibody (Figure A5.2). At 72h transfection, the signal was not as strong, indicating that the expression of the recombinant proteins was not as successful. Non-specific binding was observed with the secondary antibody only control after 72 hours transfection (Figure A5.2). It was likely that after 72h the cells stopped expressing the transfected plasmids, and therefore 48h transfection was a suitable time for plasmid uptake and subsequent protein expression.

The media was then put through a HisPur Nickel column to purify the recombinant proteins via the His-tag and eluted using increasing concentration of imidazole. Protein concentration for each construct was determined at 280nm. Table A5.1 contains all information relevant to each thrombomodulin construct.

Table A5.1. Values of absorbance, volume, molecular weight, extinction coefficient and deduced volumes for western blot for each recombinant thrombomodulin construct.

Thrombomodulin construct	Wash 1 (A280)	Eluate 1 (A280)	Volume (µl) approx. Eluate 1	Molecular weight (kDa)	Extinction coefficient and A(0.1%) 280nm	Concentration (mg/ml)	Total amount in eluate (µg)	ng/µl	µl to load for ~200ng/ lane
sLLD	0.62	0.12	120	16.08	• 25480 • 1.585	0.0757	9	7.5	26
sTM	0.86	0.19	30	52.09	• 50775 • 0.975	0.195	5.85	195	1.02
s456-S/T	0.54	0.09	120	15.08	• 5595 • 0.354	0.254	30.5	254	0.8

Based on absorbance values, the volume collected from eluates, molecular weight, and extinction coefficient for each thrombomodulin construct, concentration of each preparation was calculated (Table A5.1), and from that the volume of protein needed to load 200ng onto the gel for western blotting.

Polyclonal and monoclonal antibodies were used to detect the recombinant thrombomodulin constructs, which would verify that there was expression of the corresponding regions of thrombomodulin.

First the anti-sheep polyclonal antibody was tested, to detect as much protein as possible for each construct (Figure A5.3).

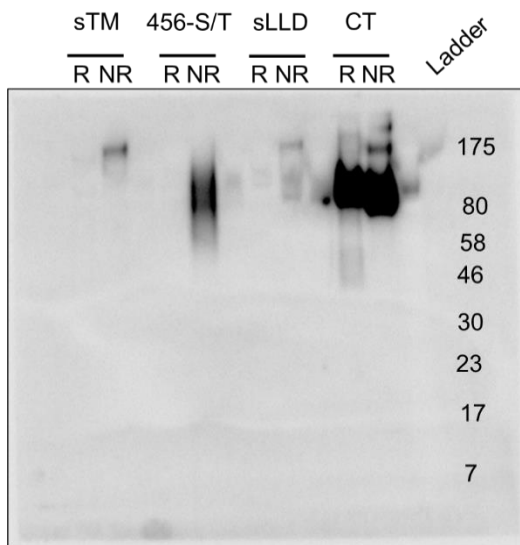


Figure A5.3. Each thrombomodulin construct is detectable in non-reduced conditions. On the gel 1 μ g of recombinant proteins were loaded in non-reduced and reduced (added 4 μ l of DTT) conditions. Samples were heated for 10min at 70 $^{\circ}$ C before loading onto the gel. Migration was done for 50min, first at 100V for 15min, then 130V until the end. The proteins were transferred onto a nitrocellulose membrane for 1h at 90V. The membrane was blocked in PBST-milk 5% for 4h at room temperature. Polyclonal sheep anti-thrombomodulin antibody was used at 1/2000 and left to incubate overnight at 4 $^{\circ}$ C. Anti-sheep secondary antibody at 1/5000 was added for 1h at room temperature. The membrane was washed after each antibody incubation in PBST. ECL substrate was added for 2min before exposure. The control condition was the recombinant soluble thrombomodulin from R&D Systems.

The control condition, which was commercial soluble full-length thrombomodulin, was detected in reduced (R) and non-reduced conditions (NR), confirming that the antibody was functional. The data sheet for commercial thrombomodulin informed that the protein was detected between 80 and 105kDa on SDS-PAGE, which was the case. For each thrombomodulin construct, bands were only detected in the non-reduced conditions. More protein was present in the EGF456-S/T preparation. Recombinant soluble thrombomodulin was detected at the correct molecular weight (Figure A5.3). However, the expected molecular weights were 16kDa for the lectin-like domain (sLLD) and 15kDa for the EGF456-Ser/Thr region. The bands corresponding to these protein preparations were around 80 and 175kDa. It was possible that these shorter constructs formed oligomers, and in reduced conditions were decomposed and fell to lower molecular weights and were non-detectable. This could be

because the gel was run for too long, or else the antibody was not able to detect the smaller fragments.

To check that the correct regions of thrombomodulin were expressed, monoclonal antibodies were used against the lectin like domain to probe the membrane for the soluble lectin like domain (Figure A5.4). Control was the commercial thrombomodulin from R&D Systems.

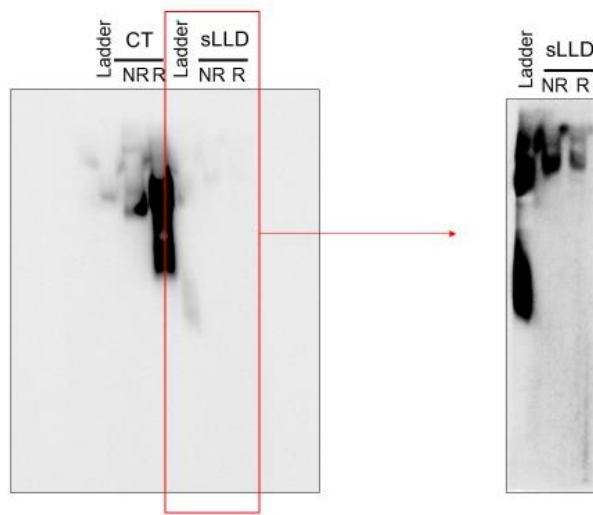


Figure A5.4. Monoclonal antibody against the Lectin-like domain detects the correct respective region. On the gel 1ug of recombinant proteins were loaded in non-reduced and reduced (added 4ul of DTT) conditions. Samples were heated for 10min at 70 °C before loading onto the gel. Migration was done for 1h, first at 100V for 15min, then 110V until the end. The proteins were transferred onto a nitrocellulose membrane for 1h at 90V. The membrane was blocked in PBST-milk 5% for 1h at room temperature. Monoclonal mouse anti-lectin like domain (thrombomodulin) antibody was used at 1/500 and left to incubate overnight at 4 °C. Anti-mouse secondary antibody at 1/5000 was added for 1h at room temperature. The membrane was washed after each antibody incubation in PBST. ECL substrate was added for 2min before exposure. The control condition was the recombinant soluble thrombomodulin from R&D Systems.

The control condition, commercial thrombomodulin, was strongly detected by the lectin like antibody, specifically in the reduced conditions (Figure A5.4). Therefore, the section of the membrane containing the lanes with the recombinant sLLD construct was cut off and re-exposed due to the high signal from the control. A high signal was detected in the ladder, likely overflow from the control reduced condition. However, bands were detectable in reduced and

non-reduced conditions, although the bands were brighter in the non-reduced condition (Figure A5.4). However, the bands were detected at a higher molecular weight, between 80kDa and 125kDa, in both conditions. Overall, although it seemed that the correct region was expressed due to the antibody detection, it is at the wrong molecular weight. It would be interesting to run the protein samples through mass spectroscopy to determine the amino acid sequence of the recombinant construct expressed.

To determine whether the EGF456-Ser/Thr had been expressed correctly, a monoclonal antibody against EGF5 was used to detect the recombinant thrombomodulin construct (Figure A5.5). Control was soluble thrombomodulin expressed in house.

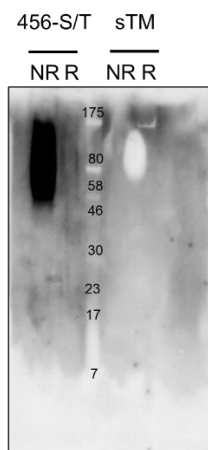


Figure A5.5. Monoclonal antibody against EGF5 detects the EGF⁵⁶-S/T construct. On the gel 1ug of recombinant proteins were loaded in non-reduced and reduced (added 4µl of DTT) conditions. Samples were heated for 10min at 70 °C before loading onto the gel. Migration was done for 50min, first at 100V for 15min, then 110V until the end. The proteins were transferred onto a nitrocellulose membrane for 1h at 90V. The membrane was blocked in PBST-milk 5% for 1h at room temperature. Monoclonal anti-EGF5 (thrombomodulin) antibody was used at 1/500 and left to incubate overnight at 4 °C. Anti-mouse secondary antibody at 1/5000 was added for 1h at room temperature. The membrane was washed after each antibody incubation in PBST. ECL substrate was added for 2min before exposure. The control condition was the recombinant soluble thrombomodulin from R&D Systems.

Bands were not correctly detected (Figure A5.5) in the control condition, therefore it was difficult to conclude whether the antibody was functional. In the non-reduced condition of the EGF456-Ser/Thr construct, a smear was detected between about 50kDa and 170kDa. Nothing was seen in the reduced condition, as when the western blot was performed with the polyclonal

anti-thrombomodulin antibody. Based on the sequence, the molecular weight of EGF456-Ser/Thr construct is 15kDa. Therefore, the EGF5 antibody detects the EGF456-Ser/Thr construct, indicating that part of the protein was expressed correctly, however the molecular weight does not correspond. Performing mass spectroscopy and determining the amino acid sequence would give information on the expression profile of the thrombomodulin construct.

Appendix chapter 6

Appendix 6.1. Verification of the thrombomodulin antibodies

It was key to verify the binding of thrombomodulin to its different antibodies, to eliminate any false positive results. For this, monoclonal antibodies against specific regions of thrombomodulin were attached to the surface of the well via passive adhesion, and thrombomodulin was added and detected using a sheep polyclonal antibody anti-thrombomodulin (Figure A6.1).

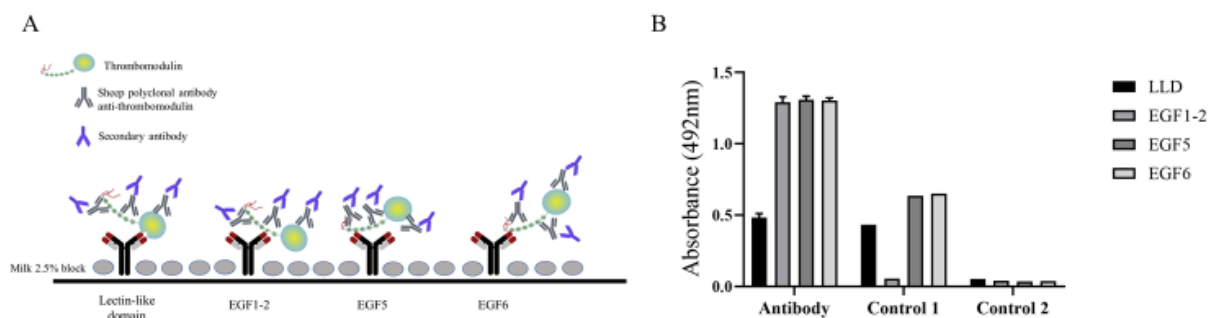


Figure A6.1. Lectin-like antibody does not efficiently bind thrombomodulin compared to EGF1-2, EGF5 and EGF6. (A) ELISA set up with thrombomodulin 2.5 μ g/ml captured by monoclonal antibodies 10 μ g/ml against the lectin-like domain (LLD), EGF1-2, EGF5 or EGF6 and detected using sheep polyclonal anti-thrombomodulin 10 μ g/ml. (B) Control 1 was without thrombomodulin and without the primary detecting sheep anti-thrombomodulin antibody (controlling non-specific binding of the secondary HRP-conjugated antibody to the capture antibody). Control 2 was without the capture antibody, thrombomodulin and the primary detecting sheep anti-thrombomodulin antibody (controlling non-specific binding of the secondary HRP-conjugated antibody to the blocking buffer). Absorbance at 492nm was measured with HRP-conjugated secondary anti-sheep antibody 1/5000 (or 0.3 μ g/ml). Results represented as mean \pm SD (triplicate), n=1.

Thrombomodulin was detected when captured with the antibodies EGF1-2, EGF5 and EGF6 (absorbance 1.29, 1.31 and 1.30 respectively) (Figure A6.1A), however the signal was a lot lower with the antibody against the lectin-like domain (LLD, 0.48). Control 2 showed that there

was no non-specific binding of the HRP-conjugated, sheep secondary antibody to the blocking buffer (Figure A6.1B). However, control 1 showed that there was some non-specific binding of the HRP-conjugated sheep secondary antibody to the capture antibodies lectin-like domain (LLD), EGF5 and EGF6. No cross-reaction between the capture antibody (mouse) on the surface and the secondary detection antibody (sheep) was expected, as they were not from the same species. Results demonstrated that the most specific antibody was anti-EGF1-2 as there was no cross-reaction of the secondary, and thrombomodulin bound with high affinity. Antibodies EGF5 and EGF6 bind thrombomodulin significantly, however there was some cross-reactivity between the sheep secondary antibody and the capture antibodies in question. The LLD antibody against the lectin-like domain bound very weakly to thrombomodulin, as well as showing binding of the sheep secondary. Absorbance values for control 1 and the antibody test for the lectin-like domain were also not significantly different control 1 being 0.43. Therefore, the lectin-like domain (LLD) antibody was not reliable to study the interaction between thrombomodulin and factor H. EGF5 and EGF6 antibodies were selected to analyse binding of factor H to thrombomodulin, as they are against key regulatory regions of thrombomodulin.

Appendix 6.2. Verification of the homology models for SCR14 and SCR17

The Ramachandran plot was done for the SCR14 homology model (Figure A6.2)

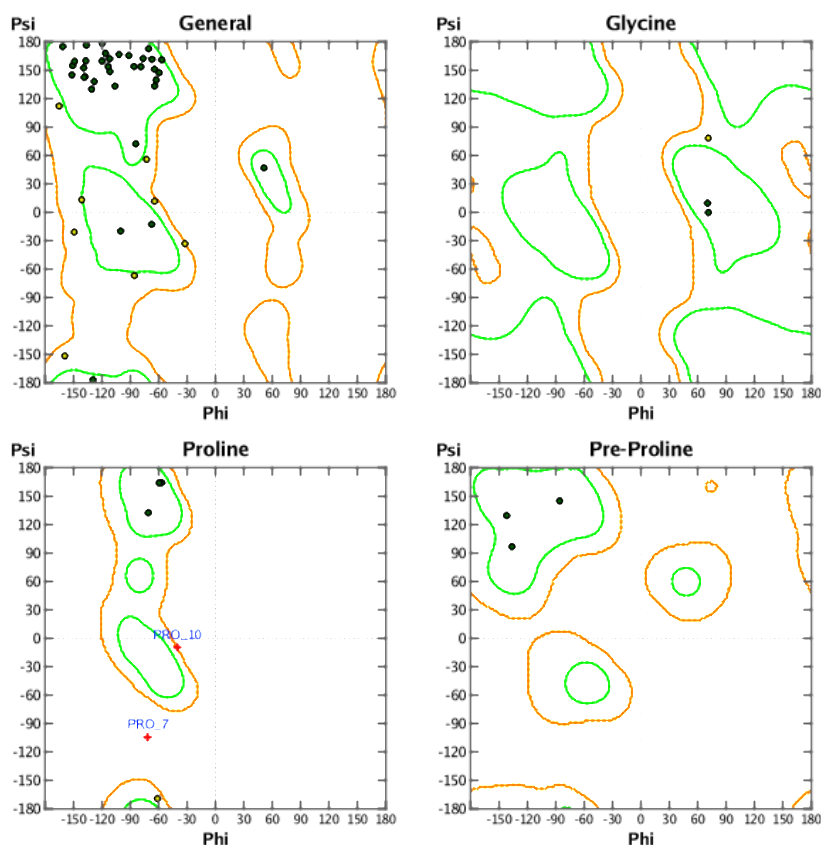


Figure A6.2. Ramachandran plot of SCR14. The torsional angles Phi (x axis) and Psi (y axis) are plotted for each residue, in a General plot (all residues), only Glycine, Proline or Pre-Proline. Based on the General plot, the majority of residues are in the top left of the plot, corresponding to beta strands. Two outliers were detected as seen in the Proline plot, proline 7 and proline 10.

The green delineated regions correspond to no steric clashes between atoms at those phi-psi coordinates, the areas delineated in orange are coordinates where shorter Van Der Waals calculations are used, therefore some atoms come close, and the areas around are the disallowed regions, where clashes occur between atoms and there is steric hindrance. Based on the Ramachandran plot, the predominant secondary structures of SCR14 are beta strands, as the Phi-Psi coordinates for most residues are located in the upper left region of the plot. Two outliers were noted, proline 5 and proline 10 of the homology model.

To verify the accuracy of the model built, the Ramachandran plot was performed for the structure of SCR17 (Figure A6.3).

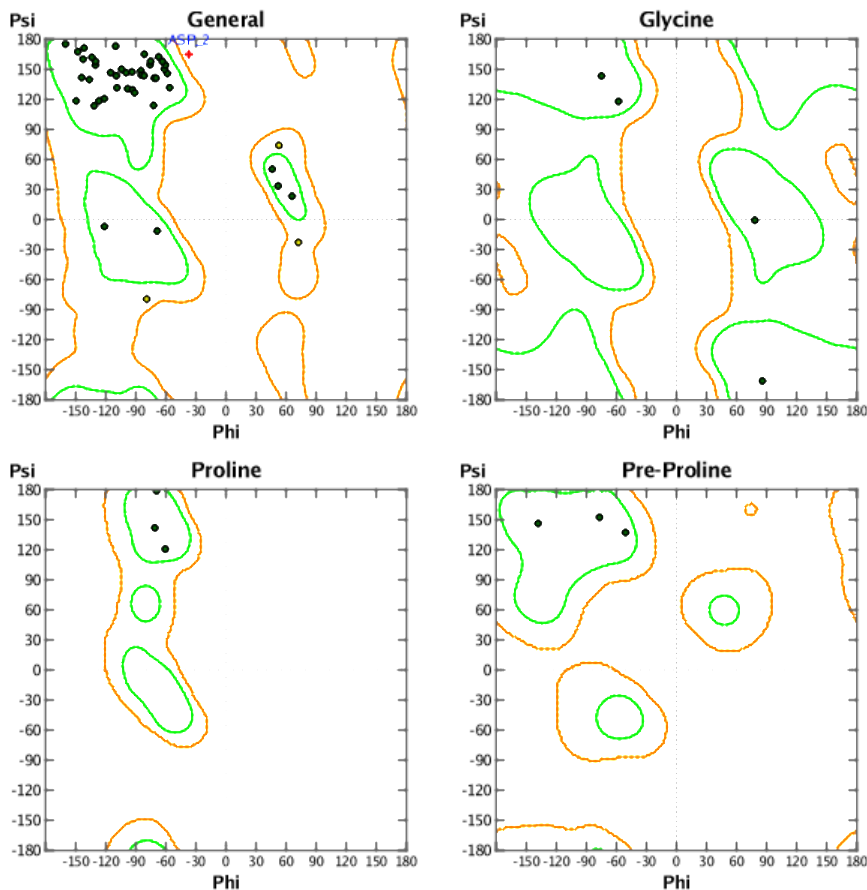


Figure A6.3. Ramachandran plot of SCR17. The torsional angles Phi (x axis) and Psi (y axis) are plotted for each residue, in a General plot (all residues), only Glycine, Proline or Pre-Proline. Based on the General plot, the majority of residues are in the top left of the plot, corresponding to beta strands. One outlier was detected as seen in the General plot, Aspartate 2.

Based on the Ramachandran plot, the predominant secondary structures of SCR17 are beta strands, as the Phi-Psi coordinates for most residues are located in the upper left region of the plot. One outlier was noted, aspartate 2, of the homology model.

Appendix 6.3. Competitive binding between factor H and heparin, and factor H and hirudin with thrombin

Heparin is a glycosaminoglycan that binds both thrombin and factor H. Thrombin-heparin binding occurs to enhance the specificity of antithrombin for thrombin's inactivation (19,20),

and factor H binds cell surfaces via heparin (21,22). Heparin binds thrombin in exosite II (23) and binds factor H in SCR 6-8 and 19-20 (13). A competitive binding assay was developed to determine whether the heparin binding sites on thrombin and factor H overlapped (Figure A6.4).

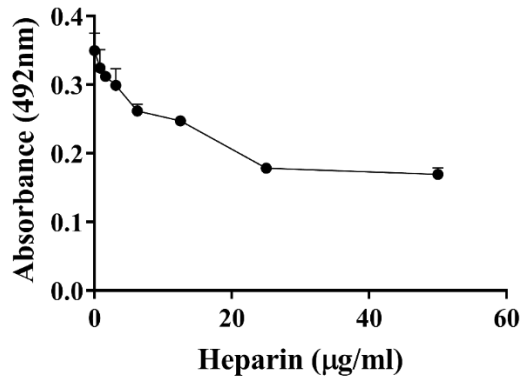


Figure A6.4. Thrombin binding to factor H is reduced in presence of increasing concentrations of heparin.

In the set-up, 2.5µg/ml factor H was bound to the surface of the well via 5µg/ml of monoclonal antibody anti-10-15, before addition of 5µg/ml thrombin preincubated with heparin at different concentrations (0.8-50µg/ml). Thrombin was detected using 5µg/ml polyclonal sheep anti-thrombin antibody, and HRP labelled anti-sheep secondary antibody to detect binding at 492nm. Thrombin detection decreased proportionally to heparin concentration (r value -1, p-value <0.0001). Binding of thrombin to factor H decreases as heparin concentrations increase. Correlation was calculated using nonparametric Spearman correlation. Results represented as mean +/- SD (triplicate), n=2.

Factor H was bound via the 10-15 antibody-capture to the surface of a microtitre plate, before addition of the mix thrombin preincubated with heparin at different concentrations. A polyclonal antibody against thrombin was used to detect binding. The results showed that as the concentration of heparin increased, the detection of thrombin decreased, indicating that thrombin and factor H were unable to interact because of heparin. Detection of thrombin was significantly correlated to the concentration of heparin (r value -1, p-value <0.0001). Heparin bound increasingly to factor H, blocking the binding site of thrombin to factor H. If heparin did not share the same binding site on factor H as thrombin, thrombin would still be detectable despite heparin, as different binding sites would be involved. Therefore, it is likely that factor H binds thrombin in the same site as heparin binding, in exosite II.

Hirudin, a thrombin inhibitor that binds exosite I, was also tested in a competitive binding assay to determine whether factor H interacted with exosite I (Figure A6.5). There is no reported interaction between factor H and hirudin.

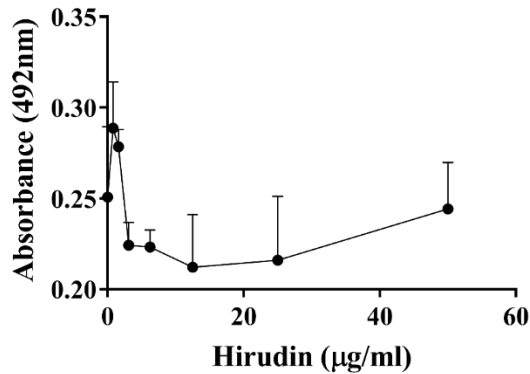


Figure A6.5. Hirudin does not block the factor H-thrombin interaction. Factor H (2.5µg/ml) was bound to the surface of the well via the monoclonal antibody anti-10-15 (5µg/ml). Thrombin (5µg/ml) was preincubated with hirudin at different concentrations (titrated 0.8-50µg/ml) and added to the well. Thrombin was detected using a polyclonal sheep anti-thrombin antibody (5µg/ml), before addition of HRP labelled anti-sheep secondary antibody to detect binding at 492nm. No correlation was seen between thrombin detection and hirudin concentration (r value -0.6667, p-value non-significant), therefore there was no effect of hirudin on thrombin/factor H binding. Results represented as mean +/-SD (triplicate), n=2.

Results demonstrated that there was no consistent effect on the factor H-thrombin interaction in the presence of hirudin, nor was there a dose-dependent effect (Figure A6.5). However, there is no evident binding between factor H and thrombin. Therefore, these results remain inconclusive.